

396
IV-10-80
JULY

Dr. 1962

RHO-BWI-ST-8

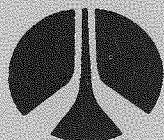
MASTER

Near-Surface Test Facility Phase I Geologic Site Characterization Report

MASTER

D. J. Moak
T. M. Wintczak

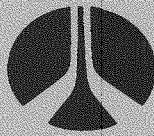
Prepared for the United States
Department of Energy
Under Contract DE-AC06-77RL01030



Rockwell International

Rockwell Hanford Operations
Energy Systems Group
Richland, WA 99352

DISTRIBUTION OF THIS DOCUMENT IS UNLIMITED



Rockwell International

Rockwell Hanford Operations
Energy Systems Group
Richland, WA 99352

DISCLAIMER

This report was prepared as an account of work sponsored by an agency of the United States Government. Neither the United States Government nor any agency thereof, nor any of their employees, makes any warranty, express or implied, or assumes any legal liability or responsibility for the accuracy, completeness, or usefulness of any information, apparatus, product, or process disclosed, or represents that its use would not infringe privately owned rights. Reference herein to any specific commercial product, process, or service by trade name, trademark, manufacturer, or otherwise, does not necessarily constitute or imply its endorsement, recommendation, or favoring by the United States Government or any agency thereof. The views and opinions of authors expressed herein do not necessarily state or reflect those of the United States Government or any agency thereof.

AVAILABLE FROM THE
NATIONAL TECHNICAL INFORMATION SERVICE
SPRINGFIELD, VA. 22161

PRICE: MICROFICHE: \$3.00
PAPER COPY: \$9.50

DISCLAIMER

This report was prepared as an account of work sponsored by an agency of the United States Government. Neither the United States Government nor any agency Thereof, nor any of their employees, makes any warranty, express or implied, or assumes any legal liability or responsibility for the accuracy, completeness, or usefulness of any information, apparatus, product, or process disclosed, or represents that its use would not infringe privately owned rights. Reference herein to any specific commercial product, process, or service by trade name, trademark, manufacturer, or otherwise does not necessarily constitute or imply its endorsement, recommendation, or favoring by the United States Government or any agency thereof. The views and opinions of authors expressed herein do not necessarily state or reflect those of the United States Government or any agency thereof.

DISCLAIMER

Portions of this document may be illegible in electronic image products. Images are produced from the best available original document.

RHO-BWI-ST-8
Distribution Category
UC-11, 70, and 85

NEAR-SURFACE TEST FACILITY
PHASE I GEOLOGIC SITE
CHARACTERIZATION REPORT

D. J. Moak
T. M. Wintczak
Engineering Testing
Near-Surface Test Facility
Basalt Waste Isolation Project

August 1980

DISCLAIMER

This book was prepared as an account of work sponsored by an agency of the United States Government. Neither the United States Government nor any agency thereof, nor any of their employees, makes any warranty, express or implied, or assumes any legal liability or responsibility for the accuracy, completeness, or usefulness of any information, apparatus, product, or process disclosed, or represents that its use would not infringe privately owned rights. Reference herein to any specific commercial product, process, or service by trade name, trademark, manufacturer, or otherwise, does not necessarily constitute or imply its endorsement, recommendation, or favoring by the United States Government or any agency thereof. The views and opinions of authors expressed herein do not necessarily state or reflect those of the United States Government or any agency thereof.

Rockwell International
Rockwell Hanford Operations
Energy Systems Group
Richland, Washington 99352

DISTRIBUTION OF THIS DOCUMENT IS UNLIMITED

DISTRIBUTION

This report has been distributed according to the category "Environmental Control Technology and Earth Sciences," UC-11, "Nuclear Waste Management," UC-70, and "Spent Fuel Storage," UC-85, as given in the Standard Distribution for Unclassified Scientific and Technical Reports, TID-4500.

ABSTRACT

The report is a description of the geology and characterization of the rock mass of the area in which the Phase I qualification tests at the Near-Surface Test Facility (NSTF) are being performed. The NSTF is located on Gable Mountain within the Hanford Site near Richland, Washington. It is located in the entablature of the Pomona Member, an upper flow in the Columbia River Basalt Group, and is approximately 150 feet (47.5 meters) below the surface.

Core logging from the instrument boreholes coupled with joint mapping, statistics, and other test data provided the basis for a detailed characterization of the 16-foot x 20-foot x 28-foot (5-meter x 6-meter x 9-meter) rock masses surrounding Full-Scale Heater Tests #1 and #2.

The Pomona entablature contains three joint sets delineated by their degree of dip, each with apertures averaging 0.25 millimeter and having no preferred strike orientation. Although joint frequencies in the study area exceed 4 joints per foot (13 per meter), the rock-mass classification rating is "good."

CONTENTS

1.0	Introduction	1-1
1.1	Purpose of the Near-Surface Test Facility	1-1
1.2	Scope of Geologic Site Characterization	1-1
1.3	Site	1-2
1.3.1	Location	1-2
1.3.2	Layout of the Near-Surface Test Facility	1-4
1.4	Phase I Tests	1-4
2.0	Geology of Gable Mountain	2-1
2.1	Stratigraphy	2-1
2.1.1	Description of Rock Units	2-1
2.2	Structure	2-6
2.2.1	Geomorphology	2-7
3.0	Geology of the Near-Surface Test Facility	3-1
3.1	Elephant Mountain Flow	3-1
3.2	Rattlesnake Ridge Interbed	3-1
3.3	Pomona Flow	3-5
3.4	Summary of Geologic Observations	3-7
3.4.1	East Access Tunnel	3-7
3.4.2	West Access Tunnel	3-13
3.4.3	Heater Test Room	3-18
3.5	Investigative Drill Holes	3-19
3.6	Construction Methods	3-20
3.6.1	Tunnels	3-20
3.6.2	Core Drilling the Instrument Boreholes	3-24
4.0	Baseline Data for Phase I Full-Scale Heater Tests	4-1
4.1	Detailed Site Characterization	4-1
4.1.1	Geologic Maps	4-1
4.1.2	Photographs	4-2
4.1.3	Detailed Line Mapping	4-3
4.1.4	Instrument Borehole Core Logs	4-4
4.1.5	Geomechanical Core Logs	4-5
4.1.6	Impression Packer Testing	4-7
4.1.7	Geophysical Testing	4-13
4.1.8	Petrography	4-16
4.1.9	Borescope Investigations	4-22
4.1.10	In Situ Stress	4-22
4.2	Joint Analysis	4-28
4.2.1	Determination of Joint Sets	4-28
4.2.2	Rock-Mass Classification	4-55
5.0	Summary	5-1
6.0	Acknowledgments	6-1

Appendix A--Data-Gathering Procedures	A-1
Appendix B--Photographs of Instrument Borehole Core	B-1
Appendix C--Graphs and Tables of Joint Characteristics	C-1
References	C-91

FIGURES:

1. Near-Surface Test Facility Site Location Map	1-3
2. Layout of Near-Surface Test Facility Tunnels	1-5
3. Schematic Layout of Near-Surface Test Facility Tests	1-6
4. Plan View of Holes Drilled from Heater Test Room, Full-Scale Heater Test #1	1-7
5. Plan View of Holes Drilled from Heater Test Room, Full-Scale Heater Test #2	1-8
6. Schematic View of Typical Instrumentation Location in Full-Scale Heater Test #2	1-10
7. Aerial Photograph of the Western End of Gable Mountain . .	2-2
8. Pasco Basin Stratigraphic Nomenclature	2-3
9. Geology of Gable Mountain	2-8
10. Geology of the East Access Tunnel	3-2
11. Geology of the West Access Tunnel	3-3
12. Idealized Section of Rattlesnake Ridge Interbed at the Near-Surface Test Facility	3-4
13. Geology of the Heater Test Room	3-6
14. Conceptual Sketch, Near-Surface Test Facility Geology . .	3-21
15. Conceptual Sketch, Near-Surface Test Facility Support Systems	3-22
16. Equal Angle Stereonet Plot of Lineation Dip Directions . .	4-8
17. Retrieving Impression Packer from Full-Scale Heater Test #2 Main Heater Hole	4-11
18. Impression Sleeve from Full-Scale Heater Test #2 Main Heater Hole	4-12
19. Test Hole Location Plan for Acoustic Survey	4-17
20. Acoustic Survey Data 2E-4 to 2E-3	4-18
21. Plagioclase Phenocryst, Hole 2M-16	4-21
22. Scattered Microphenocrysts, Hole 1M-5	4-21
23. Pyroxenes, Hole 1M-5	4-22
24. Location and Orientation of Overcore Holes	4-27
25. Holes and Block Locations for Full-Scale Heater Test #1 . .	4-29
26. Holes and Block Locations for Full-Scale Heater Test #2 . .	4-30
27. Holes and Block Locations for Extensometer Room	4-31
28. Holes and Block Locations for Full-Scale Heater Test #2 . .	4-32
29. Holes and Block Locations for Full-Scale Heater Test #1 . .	4-33
30. Core Hole 1E-8, Joint Aperture Frequency	4-34
31. Core Hole 1E-19, Joint Aperture Frequency	4-35
32. Core Hole 2M-4, Joint Aperture Frequency	4-36
33. Core Hole 2E-24, Joint Aperture Frequency	4-37
34. Core Hole 1E-9, Joint Dip Frequency	4-39
35. Core Hole 1E-12, Joint Dip Frequency	4-40
36. Joint Dip Frequency, Holes 1M-3 and 1E-20	4-41

Figures (continued)

37. Joint Dip Frequency, Holes 2M-12 and 2E-23.	4-42
38. Joint Strike Frequency for Dip Range 0 to 37 Degrees, Holes 1M-4, 1M-5, 1E-3, 1M-7, 1E-21, 1E-16, and 1E-12 . . .	4-43
39. Joint Strike Frequency for Dip Range 38 to 65 Degrees, Holes 1M-4, 1M-5, 1E-3, 1M-7, 1E-21, 1E-16, and 1E-12 . . .	4-44
40. Joint Strike Frequency for Dip Range 66 to 90 Degrees, Holes 1M-4, 1M-5, 1E-3, 1M-7, 1E-21, 1E-16, and 1E-12 . . .	4-45
41. Joint Strike Frequency for Dip Range 0 to 37 Degrees, Holes 2E-1, 2M-3, 2E-9, 2M-4, 2E-25, 2E-20, and 2E-15 . . .	4-46
42. Joint Strike Frequency for Dip Range 38 to 65 Degrees, Holes 2E-1, 2M-3, 2E-9, 2M-4, 2E-25, 2E-20, and 2E-15 . . .	4-47
43. Joint Strike Frequency for Dip Range 66 to 90 Degrees, Holes 2E-1, 2M-3, 2E-9, 2M-4, 2E-25, 2E-20, and 2E-15 . . .	4-48
44. Joint Strike Frequency for Dip Range 66 to 90 Degrees, Holes 2E-27, 2E-28, 2E-29, and 2M-16	4-49
45. Joint Strike Frequency for Dip Range 66 to 90 Degrees, Holes 1E-16, 1E-17, and 1M-8	4-50
46. Joint Strike Frequency for Dip Range 66 to 90 Degrees, Holes 2E-1, 2E-9, 2M-3, 2M-4, 2M-7, 2M-12, and 2M-13 . . .	4-51
47. Joint Strike Frequency, North Wall, Heater Test Room	4-52
48. Detail Line Map of Joints in Area of Full-Scale Heater Test #1 Test Array	4-53
49. Idealized Basalt Column with a Southerly Dip	4-53
50. Core Hole 1E-17, Fracture Top Frequency	4-58
51. Core Hole 1E-13, Fracture Top Frequency	4-59
A-1 Geomechanical Core Log	A-3
A-2 Data Sheet for Detail Line Mapping	A-12
A-3 Distance Measurements	A-13
A-4 Joint Terminations	A-13
C-1 Stereonet Plot of Joints in Full-Scale Heater Test #1 . . .	C-88
C-2 Stereonet Plot of Joints in Full-Scale Heater Test #2 . . .	C-89

TABLES:

1. Summary of Instrumentation and Heater Holes for Each Test	1-9
2. Summary of Features Used to Identify Basalt Units in the Gable Mountain-Gable Butte Area	2-4
3. Radiogenic Ages of Selected Columbia River Basalt Flows	2-4
4. Geomechanical Borehole Logs	4-6
5. Impression Packer Mapping	4-10
6. Location of Thin Sections	4-19
7. Point Counts in Transmitted and Reflected Light	4-20
8. In Situ Stress--DC-11	4-24

Tables (continued)

9.	Hydrofracturing Pressures--DC-11	4-25
10.	Geomechanical Borehole Logs	4-54
11.	Summary of Rock-Mass Classifications for Blocks in Full-Scale Heater Tests #1 and #2	4-56
12.	Rock-Mass Classification Values	4-60
C-1	Joint Density of Block 1-1	C-27
C-2	Joint Density of Block 1-2	C-28
C-3	Joint Density of Block 1-3	C-29
C-4	Joint Density of Block 1-4	C-30
C-5	Joint Density of Block 2-1	C-31
C-6	Joint Density of Block 2-2	C-32
C-7	Joint Density of Block 2-3	C-33
C-8	Joint Density of Block 2-4	C-34
C-9	Rock-Quality Designation Values of Block 1-1	C-35
C-10	Rock-Quality Designation Values of Block 1-2	C-36
C-11	Rock-Quality Designation Values of Block 1-3	C-37
C-12	Rock-Quality Designation Values of Block 1-4	C-38
C-13	Rock-Quality Designation Values of Block 2-1	C-39
C-14	Rock-Quality Designation Values of Block 2-2	C-40
C-15	Rock-Quality Designation Values of Block 2-3	C-41
C-16	Rock-Quality Designation Values of Block 2-4	C-42
C-17	Joint Set Characteristics	C-87

1.0 INTRODUCTION

1.1 PURPOSE OF THE NEAR-SURFACE TEST FACILITY

Work was undertaken from 1968 to 1972 at Hanford to examine the feasibility of using the underlying Columbia Plateau basalts for the permanent disposal of nuclear waste. In February 1976, the U.S. Energy Research and Development Administration, now the U.S. Department of Energy (DOE), established the National Waste Terminal Storage Program with a mission to provide multiple storage facilities for commercial nuclear waste in various geologic formations within the United States.

As part of the logical development needed to establish feasibility of geologic storage in basalt, literature surveys, laboratory experiments, drilling studies, technology development, demonstration projects, and repository design must be undertaken.

A Near-Surface Test Facility (NSTF) was selected for the initial in situ testing program because basalt sites at depth were not available. A NSTF could be constructed relatively quickly in a thick basaltic flow to provide space for a number of thermomechanical tests.

In mid-1978, a contract was let to construct the NSTF including both Phase I and Phase II test rooms. Phase I included the heater test area and Phase II included the spent-fuel test area.

The design of Phase I was adopted from the full-scale heater tests proposed by Lawrence Berkeley Laboratory and initiated at the Stripa mine in Sweden. A test plan was prepared by Rockwell Hanford Operations (Rockwell), and construction and hole drilling were performed on the basis of that plan. The Phase II test program was proposed in late 1977 and construction has not proceeded beyond the test room and access tunnels. The Phase I test plan was revised and reissued during 1979 with minor modifications, including the addition of a jointed block test.

As a result of continuing review, the test plans were restructured to conform to two distinct testing programs; one to qualify basalt as a storage medium (Phase I) and the other for demonstration tests (Phase II) that would provide validation and additional design information.

1.2 SCOPE OF GEOLOGIC SITE CHARACTERIZATION

Geologic characterization is required to describe the structural and mineralogical composition of the rock mass before testing begins. This report will serve as baseline data to permit identification of changes resulting from the qualification tests. These data will also provide the geologic input for predictive analysis and computer modeling. The characterization includes geologic maps, borehole core logs, detailed studies of joint characteristics, and impression packer testing.

1.3 SITE

1.3.1 Location

The NSTF is located in the northern side of Gable Mountain, a tholeiitic basalt outcrop. The outcrop is in the north-central part of the Hanford Site, approximately 35 miles (56 kilometers) northwest of Richland, Washington (Figure 1). The site was selected to meet the following criteria (Sharpe, 1979):

1. It must be in a basalt flow which is similar in chemical and physical properties to those basalt flows found at depth being considered as repository candidates.
2. The basalt flow must be at least 100 feet (30 meters) thick so that the experimental tests are not influenced by interbeds, weathered zones, etc.
3. The flow should be under approximately 100 feet (30 meters) of cover so as not to be influenced by weathering effects on basalt.
4. The basalt flow must be strong enough so that suitable openings may be safely maintained.
5. The basalt should be dry.
6. The specific location within the basalt flow must be typical of the central portion (entablature) of the flow as a whole and not significantly influenced by folding, faulting, alterations, or anomalies in jointing patterns and other intraflow structural features.
7. The site must be secure from public intrusion and vandalism.
8. The location is to have sufficient lateral extent to develop a storage site and have a 100-foot (30-meter) buffer zone of undisturbed rock on all sides.
9. The site is to be located in a low seismic activity area so as not to pose a threat to safe operation of the test facility.

The Pomona flow, exposed on Gable Mountain, was selected as the site for the NSTF. This site generally meets all of the criteria, except the stress field is low because of the relief offered by the ridge. The Pomona flow dips at approximately 9 degrees to the north and is overlain by approximately 150 feet (47.5 meters) of basalt and interbedded sediments.

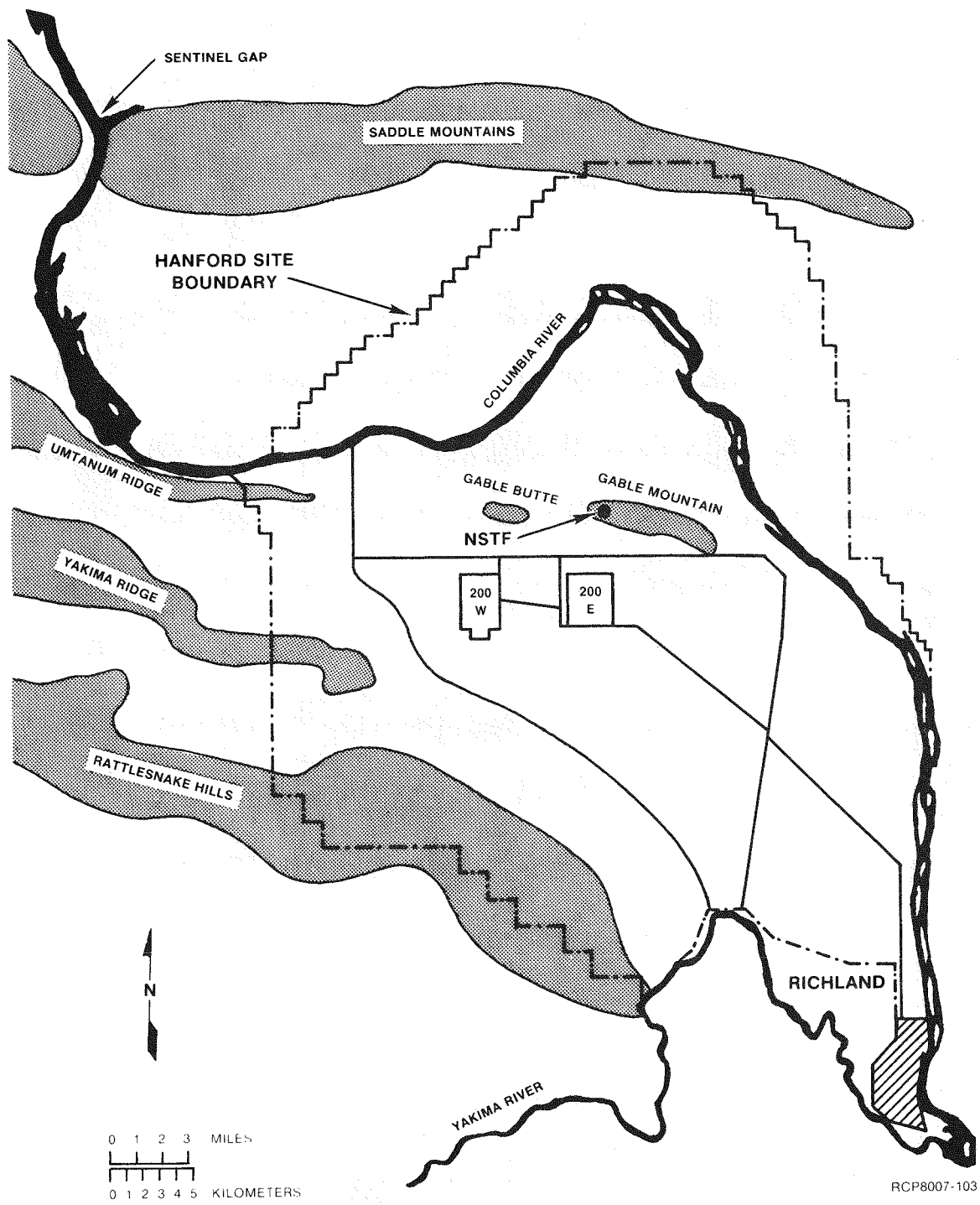


FIGURE 1. Near-Surface Test Facility Site Location Map.

1.3.2 Layout of the Near-Surface Test Facility

The NSTF, located in the Pomona flow entablature, consists primarily of three entrance tunnels 640 to 730 feet (195 to 223 meters) in length (Figure 2). The tunnels are connected at their ends by two test rooms: a Heater Test Room, 350 feet (107 meters) long, and a Spent-Fuel Test Room, 400 feet (122 meters) long (Figure 3). This report deals only with the eastern and central tunnels, called Tunnel #3 and Tunnel #2 (the East Access Tunnel and West Access Tunnel, respectively) and their associated test rooms. The section of Tunnel #2 beyond its intersection with the Heater Test Room is not discussed in this report. Parallel to the Heater Test Room, which connects Tunnels #2 and #3, is the Extensometer Room located approximately 26 feet (8 meters) below the surface and 40 feet (12 meters) to the north.

The East Access Tunnel has an as-built dimension of 10 feet x 10 feet (3.1 meters x 3.1 meters). The tunnel is 640 feet (195 meters) long and is at a -10.1% grade to the south. Preceding the tunnel is an open box cut 190 feet (58 meters) long and 16 feet (5 meters) wide with a -1% grade to the north.

The West Access Tunnel has an open box cut 350 feet (107 meters) long and 27 feet (8 meters) wide that trends slightly northeast. The tunnel is approximately 15 feet wide x 15 feet high (5 meters wide x 5 meters high) and 610 feet (186 meters) long and grades approximately 4% to the south. The two access tunnels are 350 feet (107 meters) apart, centerline to centerline, and are connected at right angles by the Heater Test Room. The test room grades approximately -1% to the west. The room changes in dimension from 23 feet wide x 23 feet high (7 meters wide x 7 meters high) at its western end to 17 feet wide x 17 feet high (5.2 meters wide x 5.2 meters high) 200 feet (64 meters) to the east. This area extends approximately 150 feet (46 meters) to where the Heater Test Room is connected to the East Access Tunnel by a 6-foot (1.8-meter) diameter raise. This eastern area of the Heater Test Room is the location of Full-Scale Heater Tests #1 and #2.

Six hundred feet (182.9 meters) into the East Access Tunnel is the Extensometer Room, which extends 164 feet (50 meters) toward the west at a right angle to the East Access Tunnel and parallel to the Heater Test Room. The Extensometer Room has dimensions of approximately 14 feet wide x 21 feet high (4.3 meters wide x 6.4 meters high).

1.4 PHASE I TESTS

The rock mass surrounding two of the Phase I tests to be run in the Heater Test Room will be characterized in this report (Figure 3). Two isolated, full-scale, electric heater tests are scheduled to start in June 1980. These tests will use an electric heater placed in the floor of the Heater Test Room with instrumentation in the surrounding vertical boreholes and in the three planes of horizontal boreholes from the Extensometer Room. The two tests are designed to:

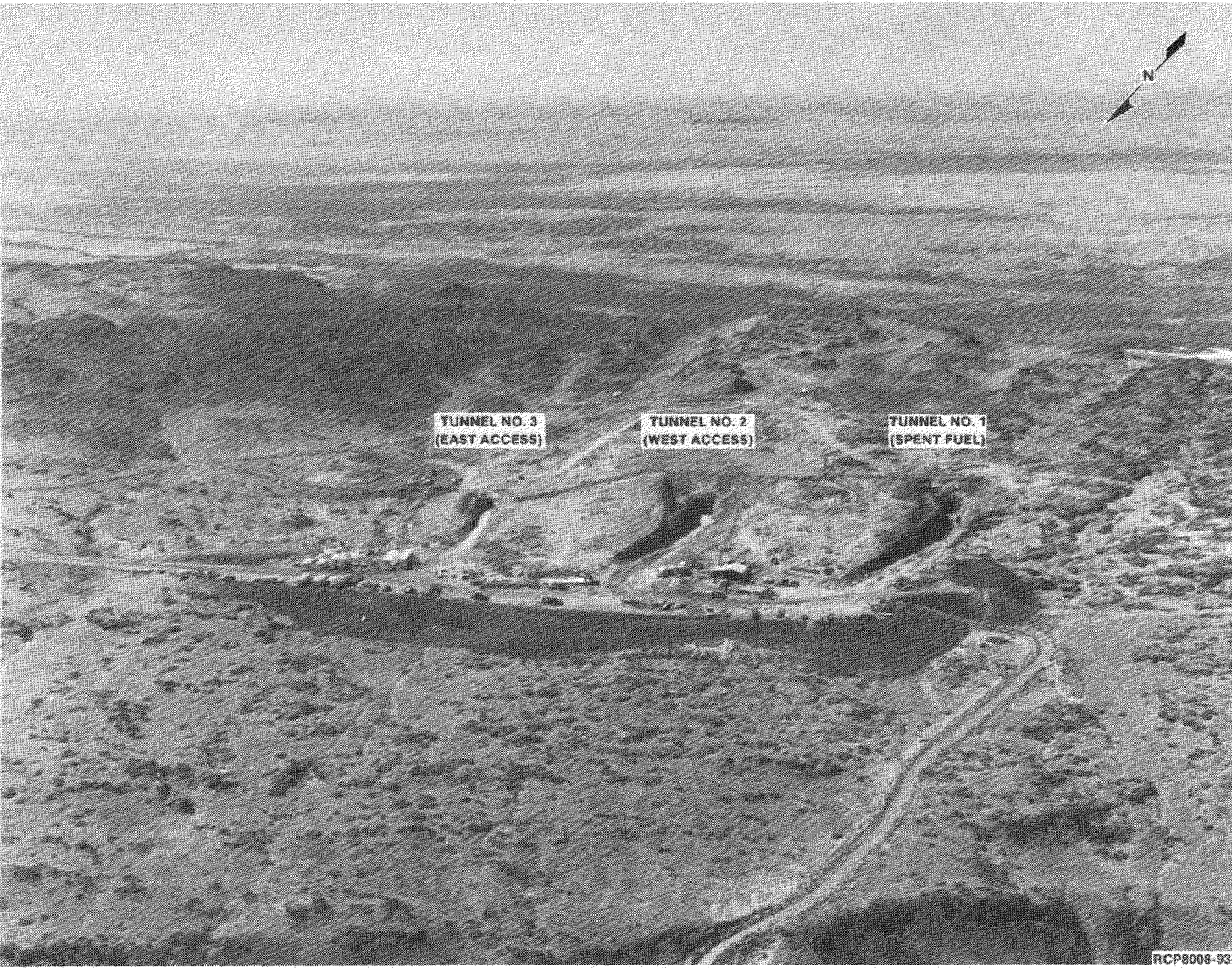


FIGURE 2. Layout of Near-Surface Test Facility Tunnels.

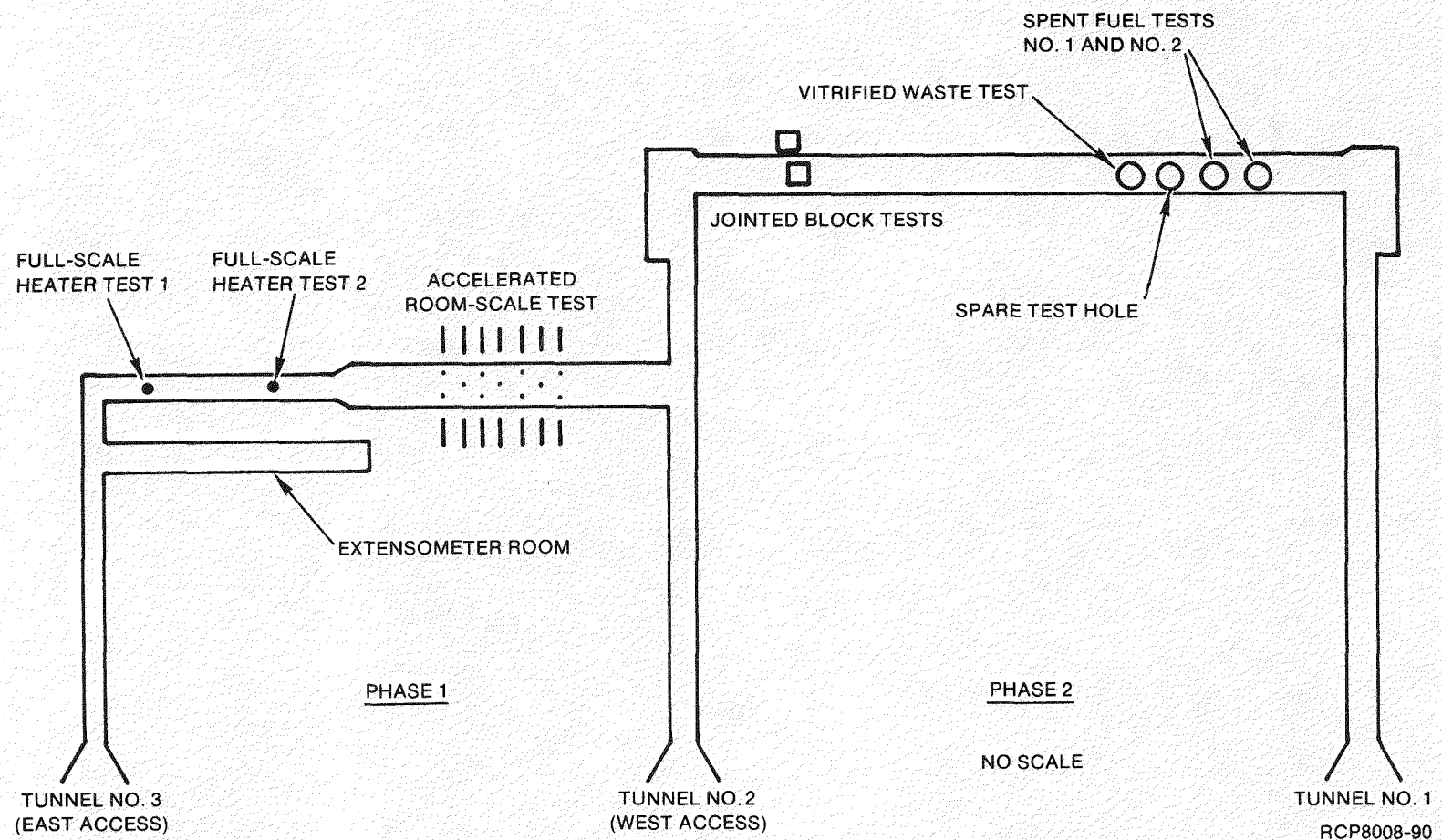


FIGURE 3. Schematic Layout of Near-Surface Test Facility Tests.

1. Simulate nominal canister operating conditions in the repository with a thermal loading of approximately 1 kilowatt
2. Induce borehole decrepitation with a thermal loading of approximately 5 kilowatts to determine the upper limit of thermal loading.

The first test (Full-Scale Heater Test #1) (Figure 4), with eight peripheral heaters, is intended to simulate a variety of operating conditions near a canister borehole. The second test (Full-Scale Heater Test #2) (Figure 5) is an overload test in which heater power will be increased above nominal operating conditions expected in a repository. Summarized in Table 1 are the number and type of instrument holes drilled for the tests shown in Figures 4 and 5. Figure 6 shows the typical location of the instrument holes in relation to a central heater. The total footage of these cored boreholes is 3,802 feet (1,159 meters) and this represents a major portion of the rock mass used for this characterization.

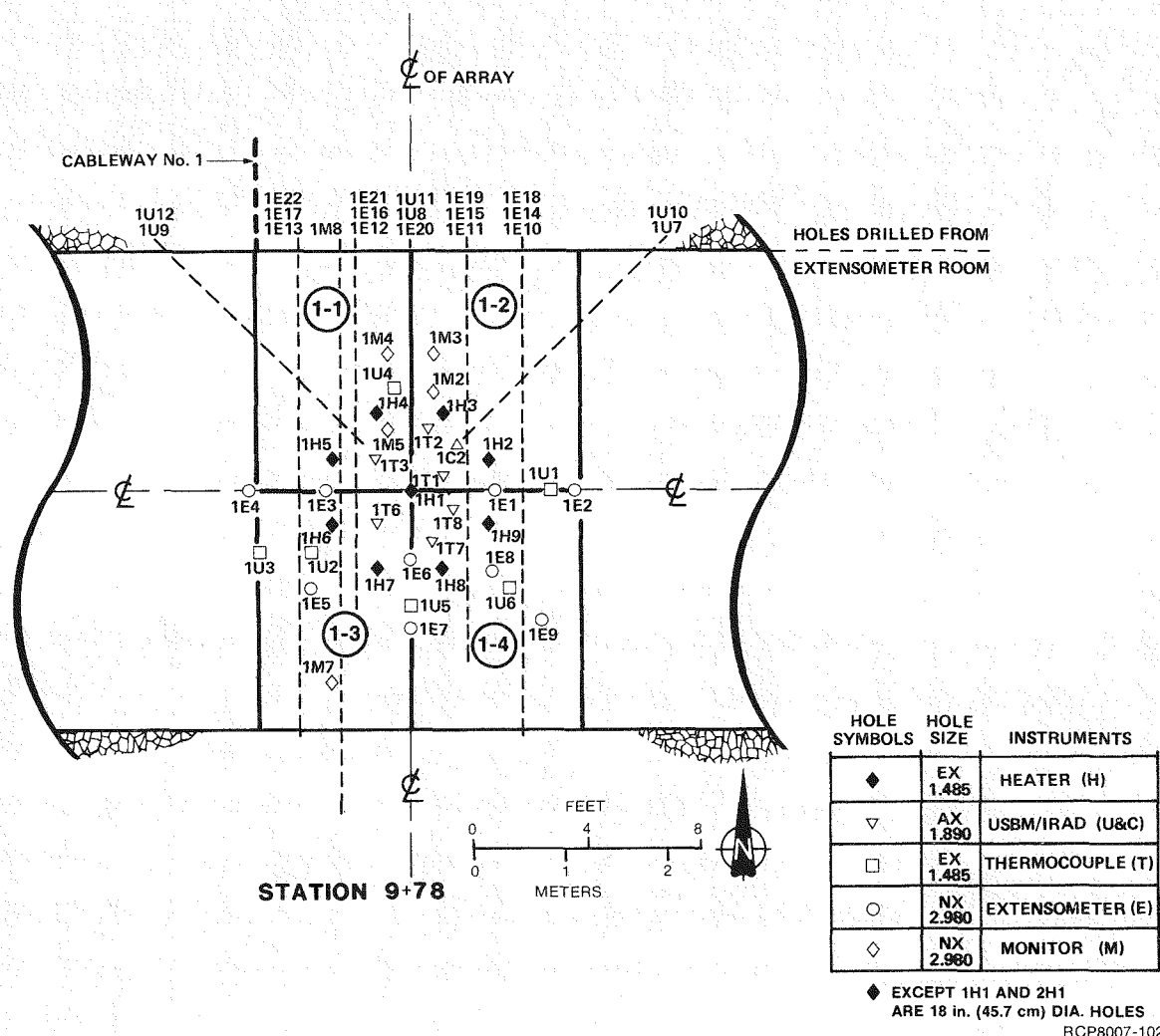


FIGURE 4. Plan View of Holes Drilled from Heater Test Room, Full-Scale Heater Test #1.

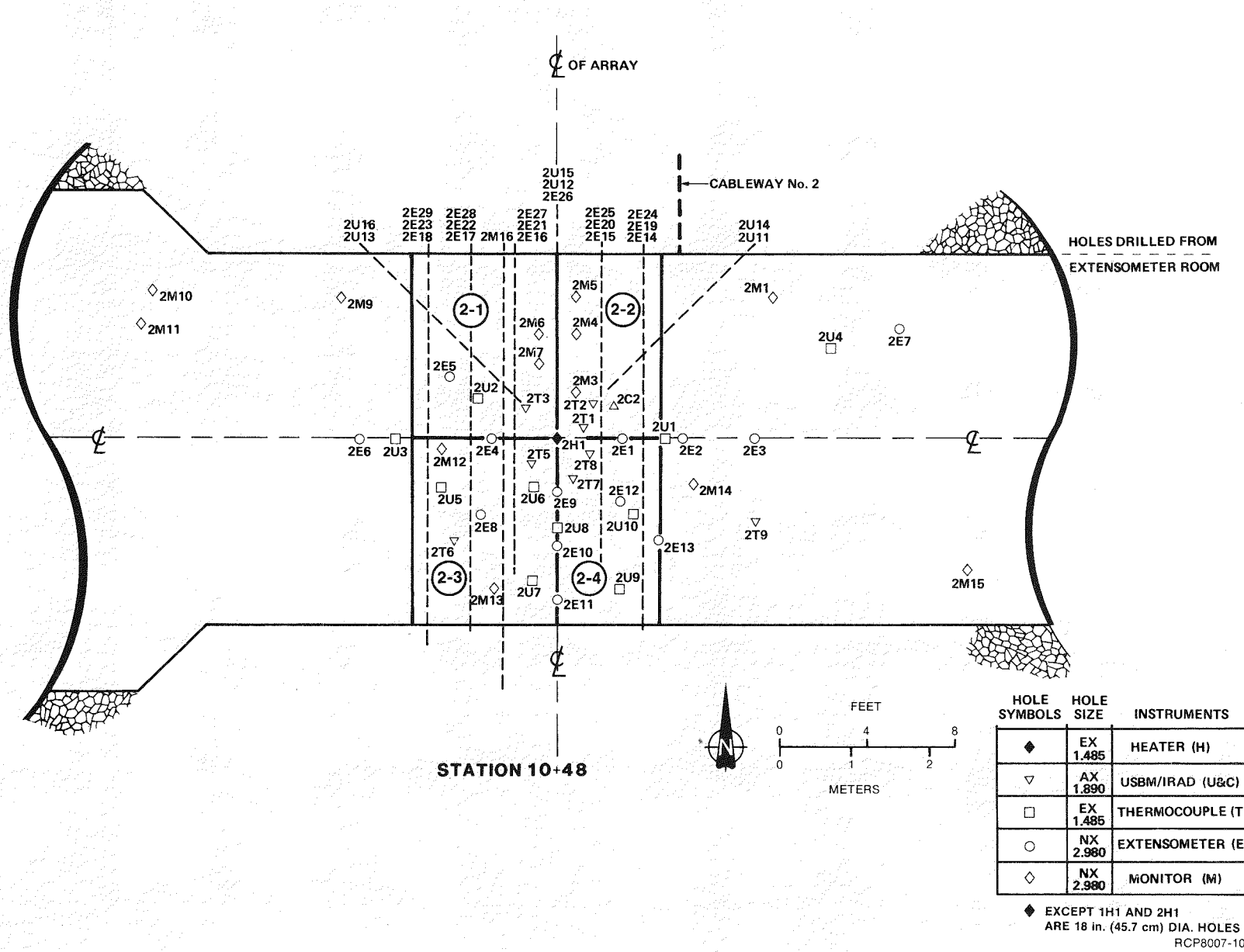


FIGURE 5. Plan View of Holes Drilled from Heater Test Room, Full-Scale Heater Test #2.

TABLE 1. Summary of Instrumentation and Heater Holes for Each Test.

Test Description	Number of Holes						Total Number of Holes
	Extensometer ⁰	Borehole Deformation*	Thermo-couples ⁺	Monitoring	Full-Scale Heater	Peripheral Heaters	
Full-Scale Heater Test #1	21	12	8	6	1	8	56
Full-Scale Heater Test #2	29	17	8	14	1	-	69

NOTE: Extensometer and borehole deformation holes all contain thermocouples.

0 - 4 Anchor-point extensometers

* - 2 Gauges per hole

+ - 5 Thermocouples per hole

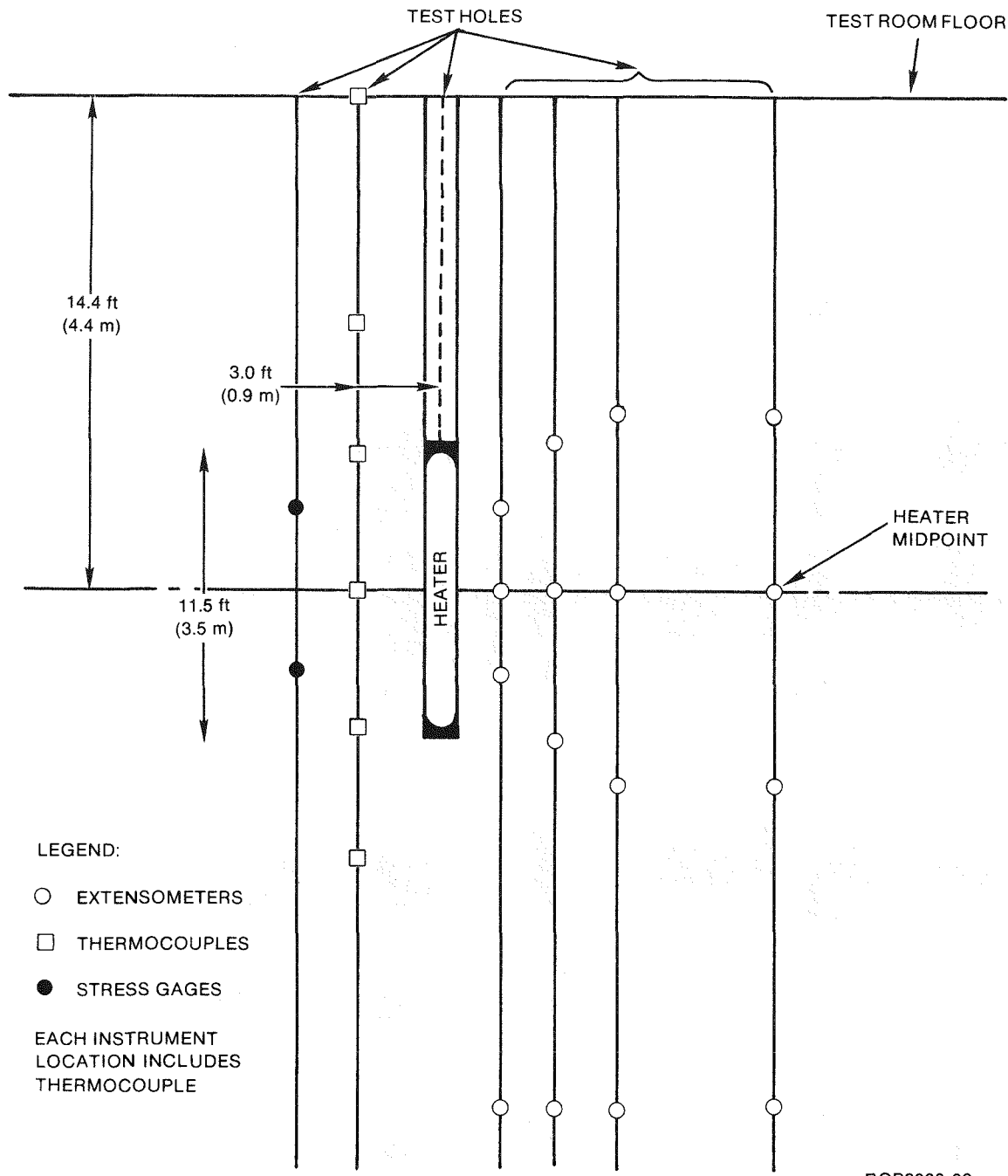


FIGURE 6. Schematic View of Typical Instrumentation Location in Full-Scale Heater Test #2.

1-12

2.0 GEOLOGY OF GABLE MOUNTAIN

Gable Mountain is located in the north-central part of the Hanford Site approximately 35 miles (56 kilometers) northwest of Richland, Washington. It is an anticlinal ridge of basalt and interbedded sediments standing as one of the few extensive bedrock outcrops exposed within the central portion of the Pasco Basin.

2.1 STRATIGRAPHY

Basalt flows from the Asotin, Esquatzel, Pomona, and Elephant Mountain Members of the Saddle Mountains Basalt and two interbedded sedimentary units (Selah and Rattlesnake Ridge) of the Ellensburg Formation are exposed on Gable Mountain (Fecht, 1978a) (Figure 7). The Ringold Formation, the glaciofluvial sands and gravels (Hanford formation), and a veneer of eolian loess cover parts of the flanks of Gable Mountain and the surrounding plain. These rock units constitute the upper part of the Pasco Basin stratigraphic section (Figure 8).

2.1.1 Description of Rock Units

Features used to distinguish various basalt units in Gable Mountain and the NSTF are summarized in Table 2. The radiogenic ages of the flows are given in Table 3.

Asotin Member. The oldest basalt flow exposed on Gable Mountain is the Huntzinger flow, which represents the Asotin Member of the Saddle Mountains Basalt. Exposures of this flow are limited to small outcrops on the southern flank of the western Gable Mountain anticline along the southern Gable Mountain escarpment.

Esquatzel Member. The Gable Mountain flow of the Esquatzel Member of the Saddle Mountains Basalt directly overlies the Huntzinger flow. The Gable Mountain flow is about 69 feet (21 meters) thick near the crest of Gable Mountain and thickens to about 102 feet (31 meters) on the lower flanks of Gable Mountain.

Selah Interbed. The Selah interbed of the Ellensburg Formation overlies the Gable Mountain flow of the Saddle Mountains Basalt. No good exposures of the Selah interbed are found on Gable Mountain, except for a few prominent benches partially covered with talus.

Core hole DC-11, located high on the northern flank of the western Gable Mountain anticline (Figure 7) penetrated about 20 feet (6.1 meters) of the Selah interbed. There, it is an orange to brown, fine-grained vitric tuff.

2-2

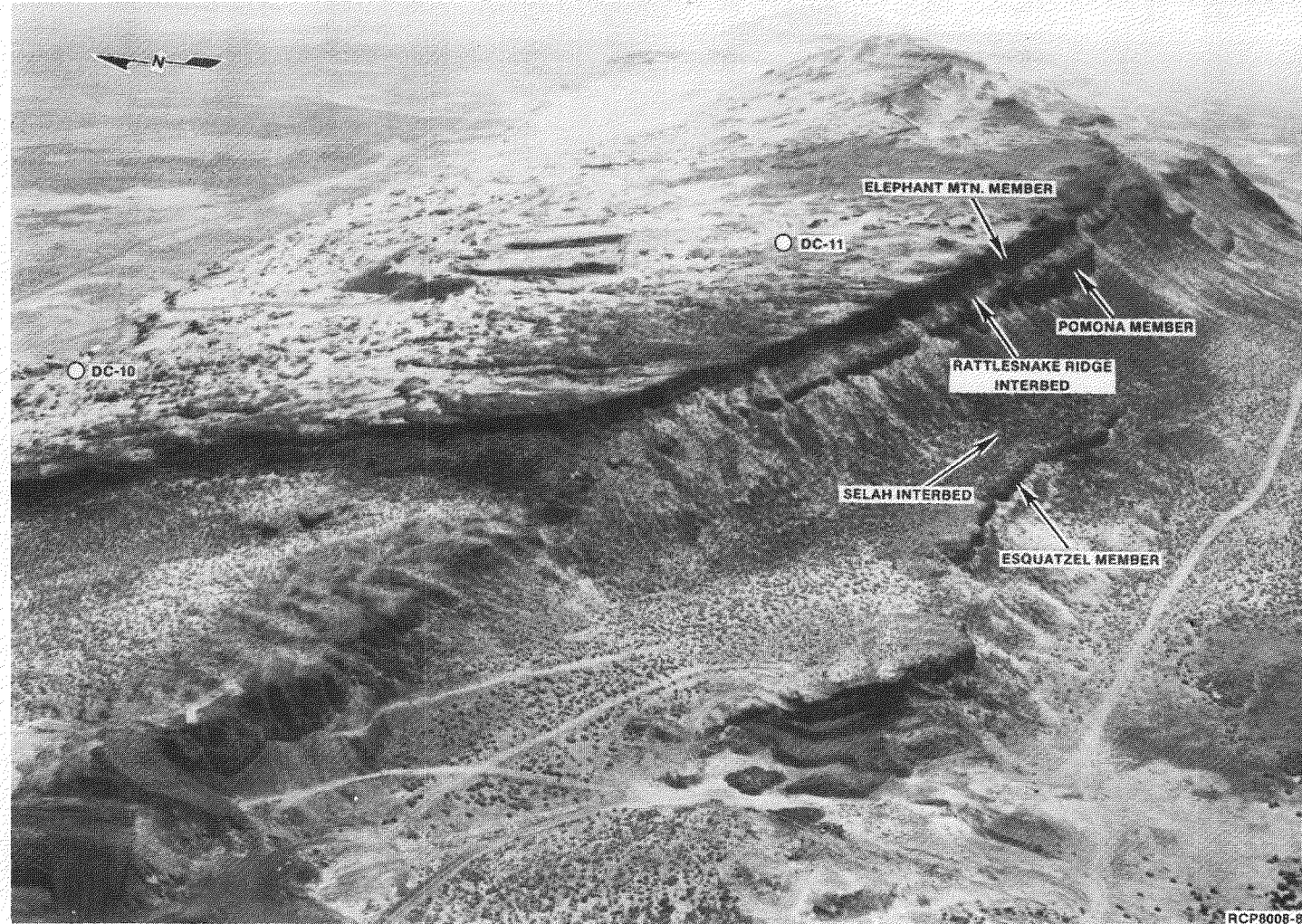


FIGURE 7. Aerial Photograph of the Western End of Gable Mountain.

RHO-BMI-ST-8

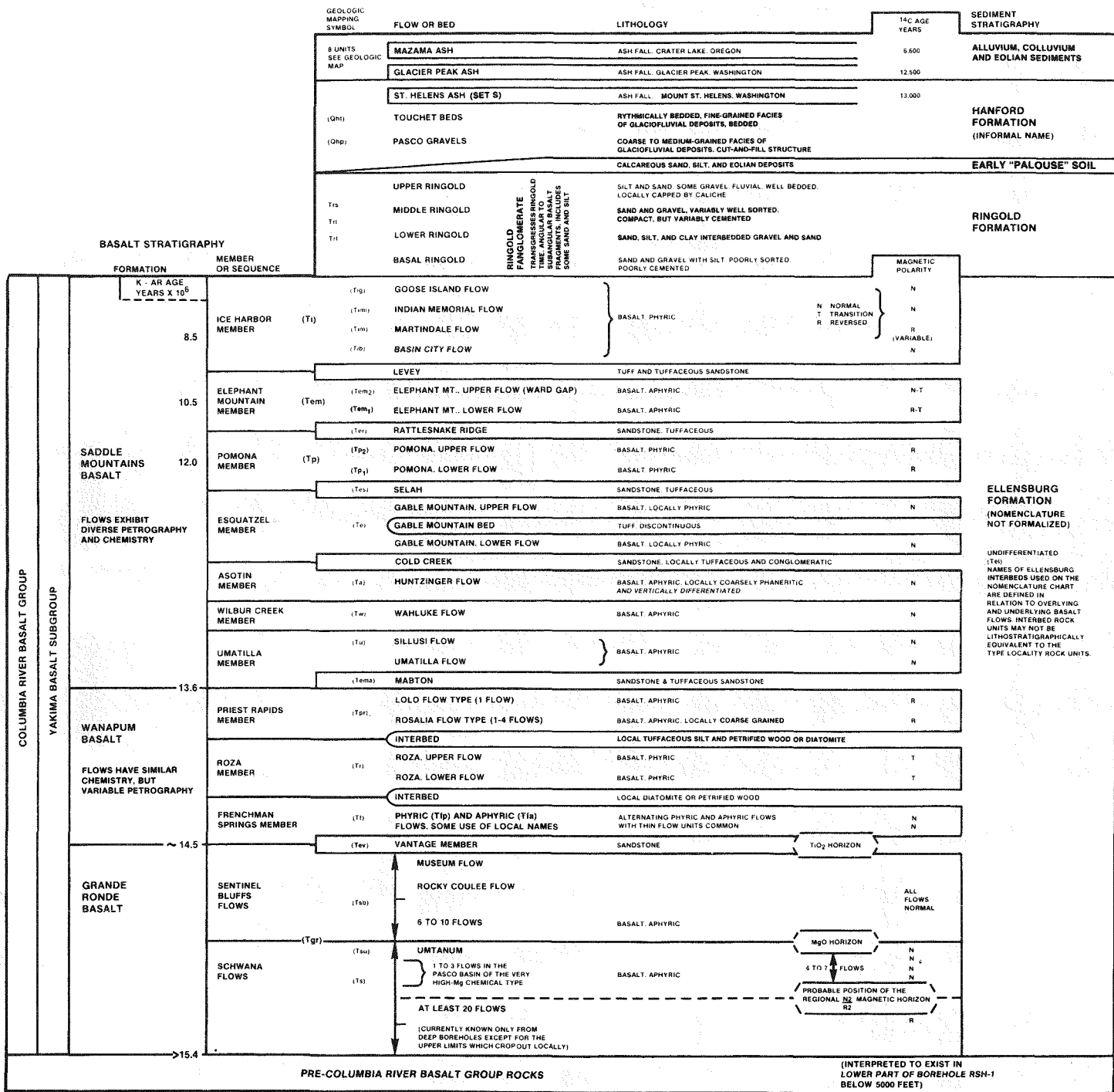


FIGURE 8. Pasco Basin Stratigraphic Nomenclature.

TABLE 2. Summary of Features Used to Identify Basalt Units in the Gable Mountain-Gable Butte Area.
(After Fecht, 1978a.)

Basalt Unit	Relative CaO/TiO ₂	Magnetic Polarity	Microscopic and Megascopic Features
Elephant Mountain Member	Low	Normal--transitional	Coarse to medium texture, sparsely plagioclase phryic
Pomona Member	High	Pomona II reversed; Pomona I not known	Sparsely plagioclase phryic
Esquatzel Member	Low	Normal	Sparsely plagioclase phryic; slightly diktytaxitic
Asotin Member	High	Normal	Diabasic; gray, ophitic pyroxene, black groundmass

TABLE 3. Radiogenic Ages of Selected Columbia River Basalt Flows.

Stratigraphic Unit	Range of Dates in Millions of Years	Probable Date
Ice Harbor I Flow	7.9 - 11.3	8.5
Elephant Mountain Member	8.1 - 12.0	9.5
Pomona Member	7.7 - 13.3	10.5
Gable Mountain Flow	10.3 - 12.9	
Huntzinger Flow	10.8 - 12.9	
Wahluke Flow	12.7	12.7
Umatilla Member	12.0 - 15.0	14.1
Priest Rapids IV Flow	13.1 - 16.2	14.9
Priest Rapids I, II, and III Flows	11.9 - 15.5	
Roza Member	12.5 - 16.3	

In core hole DC-10 (located on the lower northern flank of the western Gable Mountain anticline) (Figure 7), the Selah interbed is about 35 feet (11 meters) thick. The upper 20 feet (6 meters) are similar to core hole DC-11 and the lower 18 feet (6 meters) are fine- to medium-grained arkosic sand.

Pomona Member. The Pomona Member of the Saddle Mountains Basalt, generally thought to be a single flow throughout the region, consists of two basalt flows (or flow units) on Gable Mountain. These flows are informally named Pomona I (lower) and Pomona II (upper) and are locally separated by a tuffaceous interbed about 2 inches (6 centimeters) thick. The Pomona I overlies the Selah interbed and is known only from core holes DC-10 and DC-11; elsewhere, it is covered. The Pomona I is 26 feet (8 meters) and 38 feet (12 meters) thick in core holes DC-10 and DC-11, respectively, and exhibits medium-grained texture with plagioclase phenocrysts. The flow top and flow bottom are vesicular and glassy. The central portion of the flow is dense with few vesicles and exhibits moderate vertical jointing and cross-jointing. The major-element chemistry of the Pomona I and Pomona II is similar.

The Pomona II unit of the Saddle Mountains Basalt found at the NSTF locally overlies a thin, tuffaceous interbed separating it from the underlying Pomona I unit. The Pomona II is about 144 feet (44 meters) thick on the western Gable Mountain anticline and has four intraflow zones: basal colonnade, entablature, upper colonnade, and flow top.

The basal colonnade of the Pomona II consists of large, blocky, well-developed columns 0.75 to 2.0 feet (0.3 to 0.6 meter) in diameter. Above the basal colonnade is the entablature, which constitutes nearly two-thirds of the Pomona flow and consists generally of long, undulating, well-developed, slender columns and displays hackly jointing formed by the intersection of the vertical columnar joints and numerous cross-joints. Locally, there are anomalous zones in the entablature outcrops, where the columns have a radial fanning pattern.

The entablature grades abruptly upward into the upper colonnade, which constitutes less than one-quarter of the flow. The upper colonnade consists of long, undulating columns, 1 to 3 feet (0.5 to 1.0 meter) in diameter, with many cross-joints and scattered vesicles.

Locally, within the upper colonnade, are zones of glassy, vesicular basalt with a "frothy" appearance that stand in sharp contrast to the surrounding, massive columns. These anomalous zones can extend the full length of the upper colonnade, protruding into the top of the entablature which shows fan jointing adjacent to these zones and extending to the flow top (Schmincke, 1964). The extent and development of these anomalous zones in the Pomona II unit on the northern flank of the western Gable Mountain anticline were factors in the site evaluation process for the NSTF (Fecht, 1978b).

The flow top of the Pomona II unit consists of a highly vesicular, glassy basalt grading downward into the more dense basalt of the upper colonnade.

For purposes of this report, the term "Pomona" is used to define the flow where the NSTF test rooms are located.

Rattlesnake Ridge Interbed. The Rattlesnake Ridge interbed of the Ellensburg Formation is positioned between the underlying Pomona II unit and the overlying Elephant Mountain flow. Exposures of the Rattlesnake Ridge interbed are limited to those along the southern Gable Mountain escarpment on the western Gable Mountain anticline, in the trenches in the saddle of Gable Mountain, and at the crest of the eastern major Gable Mountain anticline. At these localities, the Rattlesnake Ridge interbed varies in thickness from 5 to 18 feet (1.5 to 5.4 meters). On the northern flank of the western Gable Mountain anticline, the interbed thickens toward the north from 20 feet (6 meters) in core hole DC-11 to 61 feet (8.5 meters) in core hole DC-10.

The Rattlesnake Ridge interbed, in outcrop, consists of an orange to tan, medium-grained, locally cross-bedded, arkosic sand overlain by a light gray, silty, vitric tuff. At its upper contact, the interbed is baked and locally welded by heat from the overriding Elephant Mountain flow.

Elephant Mountain Member. The youngest basalt flow in the Gable Mountain-Gable Butte vicinity is the Elephant Mountain flow of the Saddle Mountains Basalt. The Elephant Mountain flow overlies the Rattlesnake Ridge interbed of the Ellensburg Formation.

The Elephant Mountain flow is about 90 feet (24 meters) thick and is divided into three zones: colonnade, entablature, and flow top. The colonnade forms the lower one-third of the flow. To the colonnade, the flow top and entablature of the Elephant Mountain flow have been largely eroded at the NSTF area by proglacial floodwaters.

Sediments. Fanglomerate rock of the Ringold Formation, coarse sand and gravel from the ice-age deposits called the Hanford formation (informal name), and loess deposits cover the basalts in scattered areas on Gable Mountain.

2.2 STRUCTURE

Gable Mountain was formed by a complex series of anticlinal ridges composed of basalt and interbedded sediments representing the only extensive exposure of bedrock in the central portion of the Pasco Basin. These ridges are up to 1,109 feet (338 meters) in elevation and are surrounded by a plain of fluvial sediments, which varies in elevation from 420 to 700 feet (128 to 213 meters).

The structure of Gable Mountain is characterized by a complex series of doubly plunging, en echelon anticlines and synclines situated within the closure of a larger, asymmetrical fold; the eastern extension of Umtanum Ridge (Fecht, 1978a).

The parasitic folds resemble one another geometrically. The fold axes of the parasitic folds are curvilinear and trend easterly and southeasterly under the fluvial plain. The termini of the hinge lines of the parasitic folds are generally doubly plunging, but are often subdued by surrounding folds with higher amplitudes and greater wavelengths. In cross section, the parasitic folds are asymmetrical. The two major Gable Mountain anticlines have opposite directions of asymmetry; the angles subtended by the two flanks (inter-limb angle) and the fold closures of the hinge lines of the parasitic folds range from closed to gentle and angular to rounded depending on the amplitude and wavelength of a given fold.

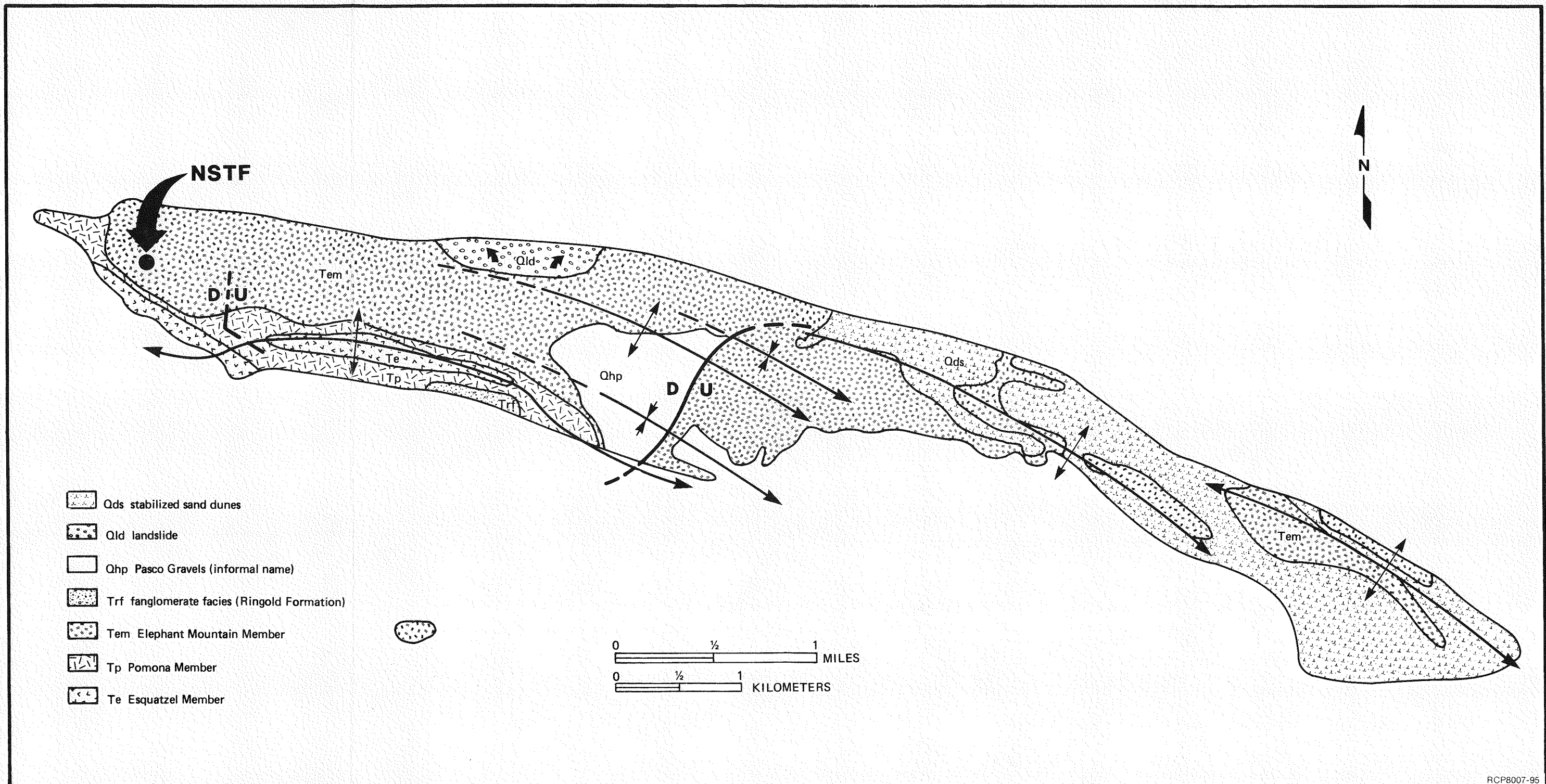
The westerly trending, asymmetrical, major fold which extends over most of Gable Mountain has been mapped from surface exposures and geophysical and well data. The southern flank of the major fold has a gentle southerly dip (about 2 degrees). The uppermost flow, extending over most of the southern flank and associated parasitic folds, is the Elephant Mountain flow. There are, however, areas between and immediately adjacent to Gable Mountain in which stratigraphically lower flows are the uppermost flow, but these areas are the result of extensive erosion by ancestral river systems and glaciofluvial flooding. The north flank of the major fold has a steep northerly dip. The basalt surface 0.5 mile (0.8 kilometer) north of Gable Mountain lies at an elevation of 115 feet (35 meters) below sea level or 1,227 feet (374 meters) below the crest of the western Gable Mountain anticline.

2.2.1 Geomorphology

The geomorphology of the Gable Mountain vicinity is dominated by topographic features resulting from uplift of the Gable Mountain-Gable Butte ridge and proglacial flooding of the Pasco Basin. Only minor changes in the topography have occurred in the last 13,000 years (Fecht, 1978a).

Late Pleistocene flooding from Glacial Lake Missoula and from other comparable ice-margin lakes has formed both erosional and depositional features within the Gable Mountain area. Erosional landforms include scabland features, breached pre-flood structures, and anastomosing channels. Depositional landforms include gravel bars, giant current ripples, and ice-rafted erratics.

Faults. Few faults have been identified and mapped on Gable Mountain (Newcomb and Others, 1972; Bingham and Others, 1970; Fecht, 1978a), but their surface expression is generally obscured by overlying sediments (Figure 9). One fault has been mapped on the western end of Gable



Mountain, but is at least 2,000 feet (610 meters) east and south of the NSTF. This is a northerly trending fault near the west end of the western Gable Mountain anticline along the southern Gable Mountain escarpment. Stratigraphic offset of approximately 35 feet (11 meters) can be seen near the ridge crest where the Pomona II is in juxtaposition with the Elephant Mountain flow. The fault plane, which is totally obscured by talus debris, is estimated to dip at 30 degrees to the east (Bingham and Others, 1970). The stratigraphic relationships and dip of the fault plane indicate the fault to be a low-angle reverse fault with about 80 feet (24 meters) of offset. No evidence of shearing or brecciation in the basalt was noted north of where the fault is last exposed. There was no evidence of this fault in the NSTF.

Another fault has been mapped in the central portion of Gable Mountain following extensive trenching to expose the fault planes (Bingham and Others, 1970; Fecht, 1978a). These faults are at least 2.5 miles (4 kilometers) east of the NSTF and have no bearing on the integrity of the site.

3.0 GEOLOGY OF THE NEAR-SURFACE TEST FACILITY

The following lithologic descriptions are a compilation of the daily observations made during the excavation of the NSTF.

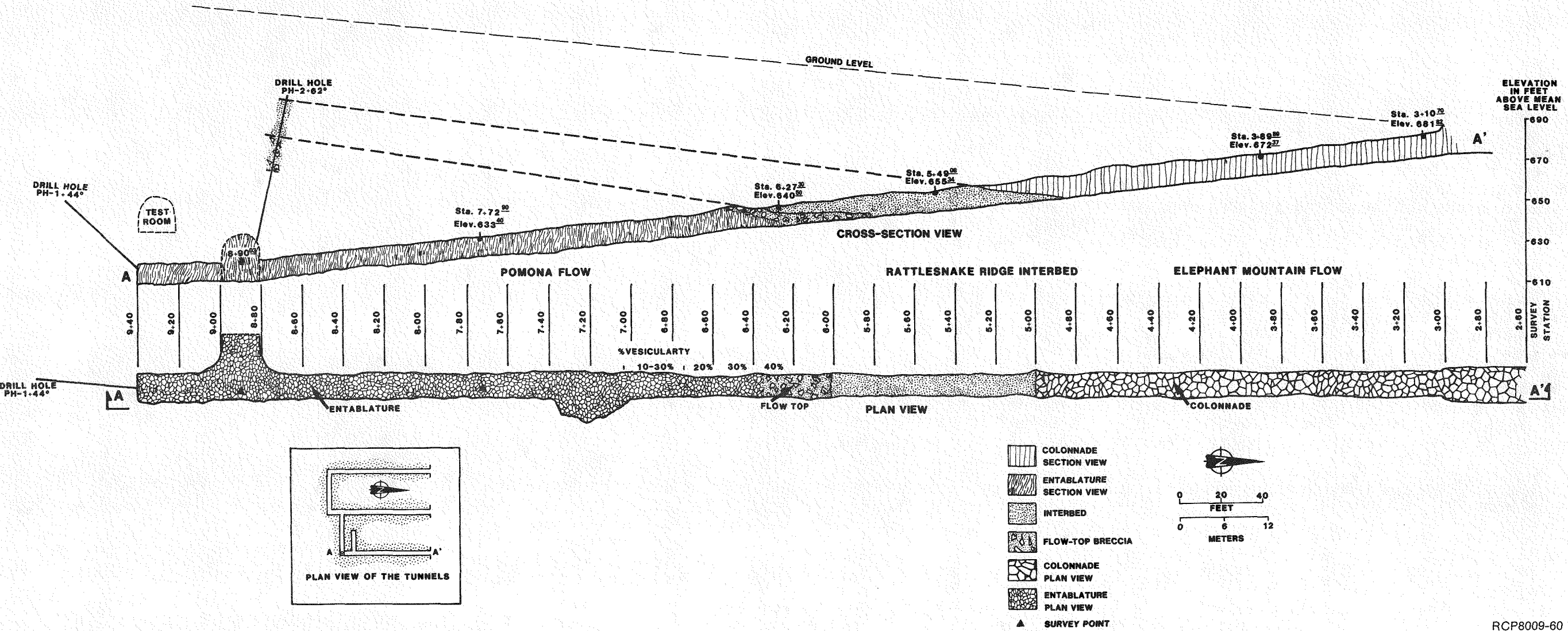
3.1 ELEPHANT MOUNTAIN FLOW

The Elephant Mountain flow at the NSTF is approximately 70 feet (21 meters) thick and consists of the basal colonnade and a thin flow bottom. The entablature and flow top have been removed by proglacial floodwaters. The basal colonnade consists of large, irregular 5- to 12-foot (1.5- to 3.5-meter) diameter columns. These large columns are dissected by numerous 2- to 4-foot (0.6- to 0.9-meter) diameter wavy columns and abundant cross-joints which develop 2- to 3-foot (0.6- to 0.9-meter) sub-rectangular blocks. Due to the proximity of the flow to the surface, most of the joints have developed yellow-brown oxidation rinds of 1 to 10 millimeters. The joint filling normally consists of yellow-brown clay 0.1 to 5.0 millimeters. Very scattered vesicles ranging up to 5 millimeters in diameter were observed throughout the colonnade. The flow bottom is 15 to 30 centimeters of basalt breccia with a yellow-brown clay matrix.

Two sub-parallel shears were observed in the open cut of the West Access Tunnel. Their strike is approximately 270 degrees with a 5- to 10-degree dip to the north. Although there is no apparent offset, the shears have a 1- to 6-centimeter infilling of yellow-brown clay and basalt fragments. Another shear was observed in the West Access Tunnel from Station 18+78 to Station 18+50. The shear was wavy, with an average strike of 160 degrees and a dip of 82 degrees west. The material on the shear was highly weathered, dark brown clay and basalt fragments, and ranged in thickness from 5 millimeters to 45 centimeters.

3.2 RATTLESNAKE RIDGE INTERBED

The Rattlesnake Ridge interbed is approximately 20 feet (6 meters) thick at the NSTF. In the West Access Tunnel, the interbed was from Station 17+47 to Station 16+52; in the East Access Tunnel, it was from Station 4+84 to Station 5+83 (Figures 10 and 11). The interbed can be divided into seven individual sections which were traceable between the exposures in the tunnels (Figure 12). There were minor variations in lithology and thickness of the individual sections, so the following descriptions and thicknesses are generalizations. Immediately below the Elephant Mountain flow bottom are 2.5 feet (0.8 meter) of gray, tuffaceous siltstone which has a 2- to 4-inch (5- to 10-centimeter) baked zone at the top. The next 1.5 feet (0.5 meter) is a brown and gray tuffaceous siltstone with irregular white and pink clay stringers. This overlies 1 foot (0.3 meter) of dark brown and gray tuffaceous siltstone with parallel stringers of white clay. This is underlain by 6 inches



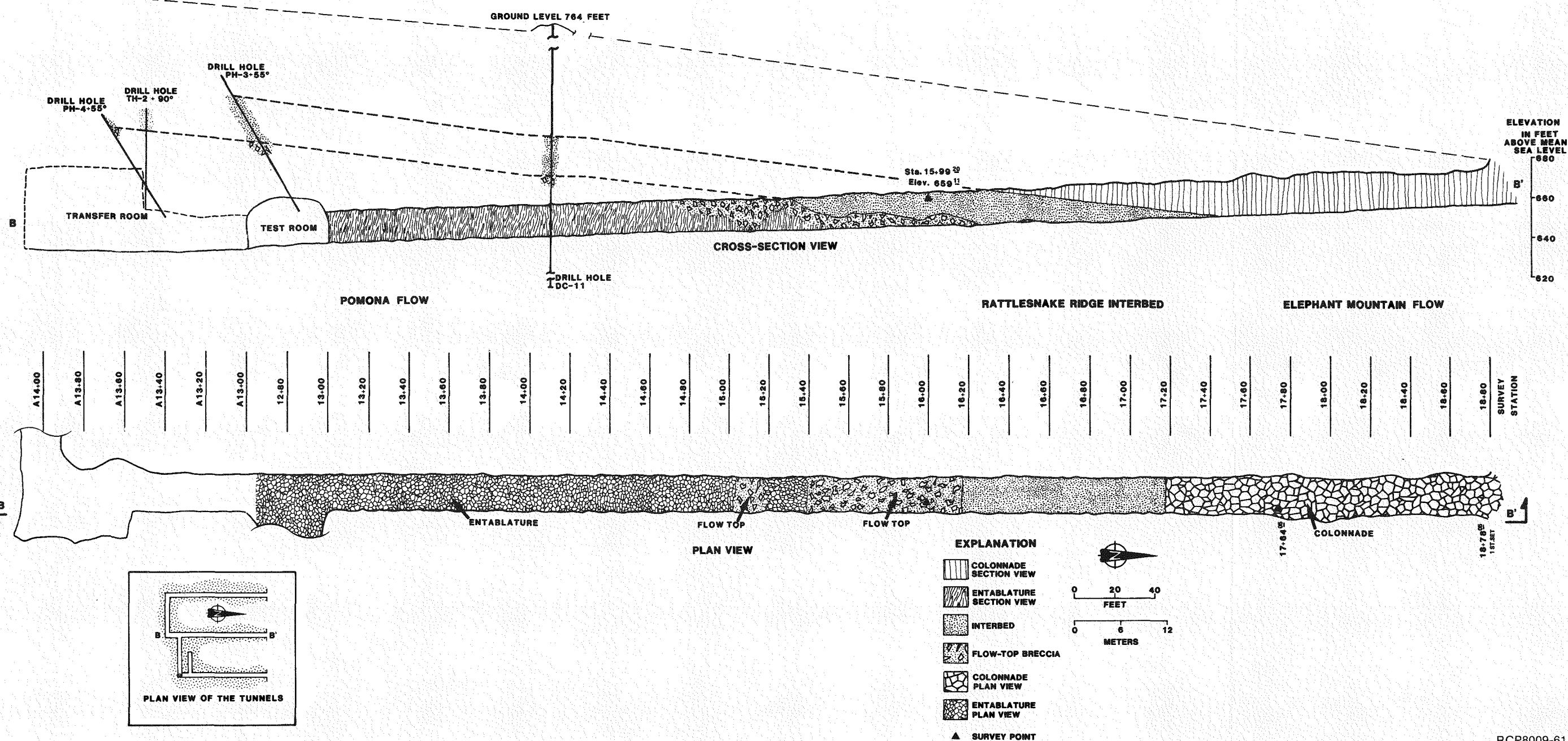
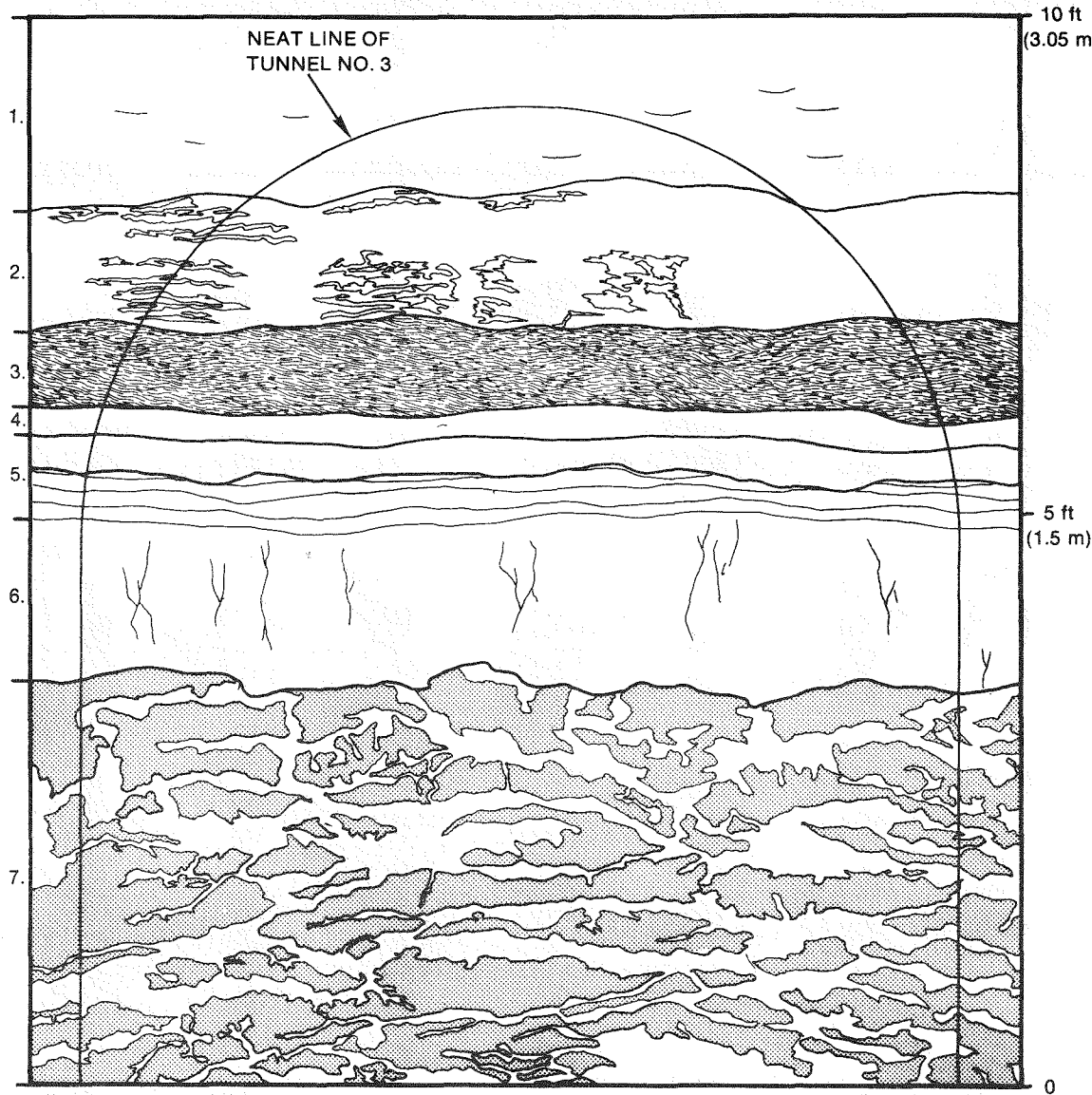


FIGURE 11. Geology of the West Access Tunnel.



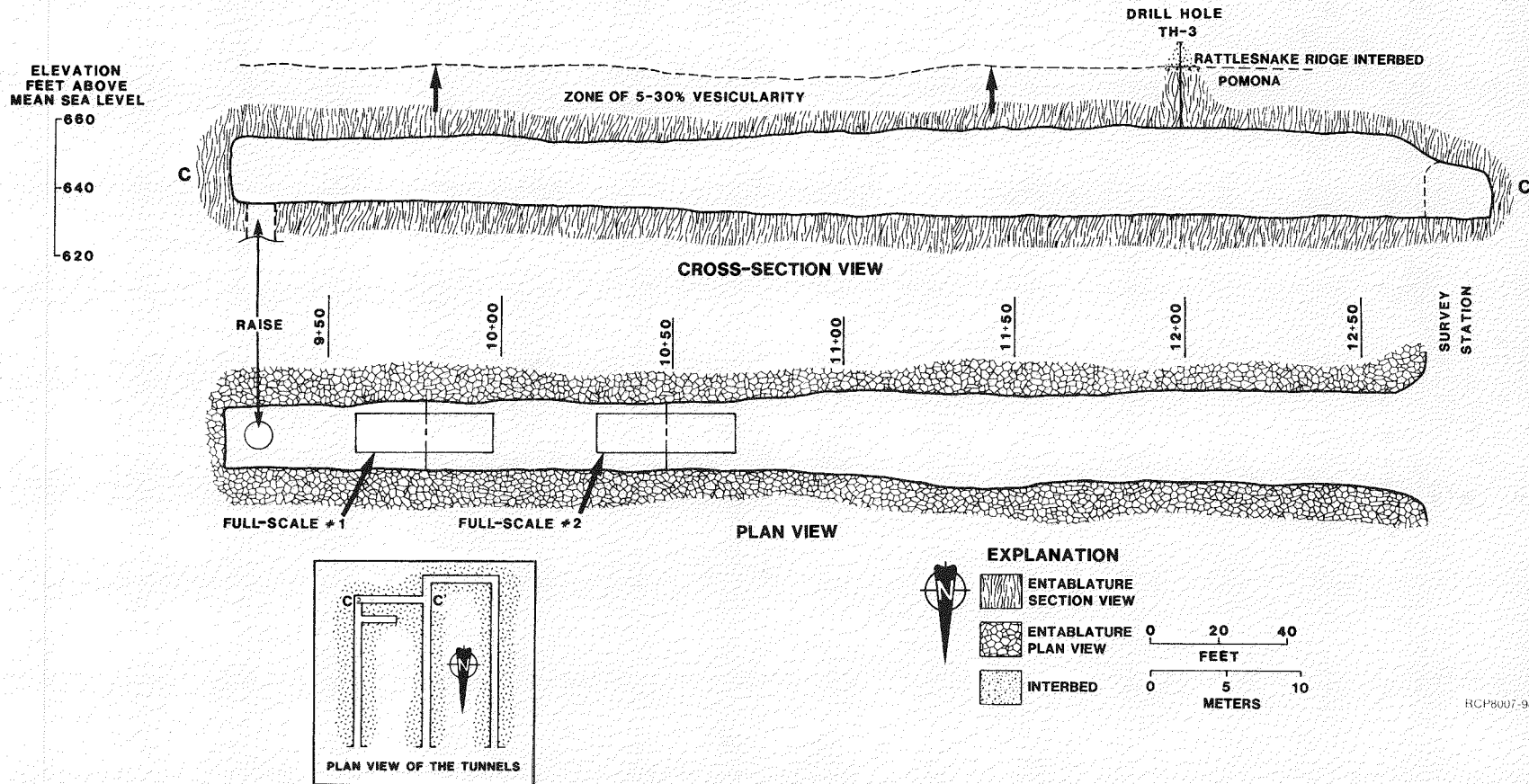
RCP8008-82

FIGURE 12. Idealized Section of Rattlesnake Ridge Interbed at the Near-Surface Test Facility.

6 inches (15 centimeters) of reddish-brown, tuffaceous siltstone. The next 1 foot (0.3 meter) is a dark-brown to brown, tuffaceous siltstone. This is underlain by 1.5 feet (0.5 meter) of gray, tuffaceous siltstone similar to the material immediately below the Elephant Mountain flow. The major constituent of the tuffaceous siltstones mentioned above is siliceous glass, with the clay being a smectite. There were traces of α -cristobalite in the upper two sections of the interbed. Further analysis of the clay is being undertaken. The lower 12 feet (3.6 meters) of interbed are an arkosic sand with irregular, yellow-brown clay stringers up to 3 inches (8 centimeters) thick.

3.3 POMONA FLOW

The Pomona flow was first observed at Station 16+52 in the West Access Tunnel and Station 5+90 in the East Access Tunnel (Figures 10 and 11). The flow-top breccia in the East Access Tunnel was approximately 4 to 8 feet (1 to 2 meters) thick consisting of 1- to 3-foot (0.3- to 0.9-meter) rectangular blocks of highly vesicular (30 to 40% vesicles) basalt with a matrix of sand and clay. In the West Access Tunnel, the flow-top breccia ranged from 8 to 16 feet (2 to 5 meters) thick consisting of 1-inch to 5-foot (2.5-centimeter to 1.5-meter), highly vesicular, basalt breccia clasts. A channel in the flow top of the Pomona, striking 280 degrees, was observed from Station 15+18 to Station 15+04. This channel accounted for the thickest portions of the flow-top breccia. The upper colonnade is 10 to 15 feet (3.1 to 4.6 meters) thick with poorly defined 3- to 6-foot (0.9- to 1.8-meter) diameter columns; it was observed in both the West and East Access Tunnels, but the column diameter appeared consistently smaller in the East Access Tunnel. The joints were mainly vertical with 0.5- to 10.0-millimeter yellow-brown clay filling. The basalt is dark gray and dense with plagioclase laths to 3 millimeters. The upper colonnade grades from 30 to 40% vesicles at the top to 5 to 10% vesicles where it is gradually dissected by smaller columns defining the top of the entablature (Figure 13). The remainder of the tunnels and test rooms are located in the entablature. This section of the flow consists of dark gray, dense basalt with plagioclase laths to 3 millimeters. The top 10 feet (3 meters) of the entablature grade downward from 15% vesicles to 2% or less. The remainder of the entablature has very scattered and localized zones of up to 5% vesicularity. Scattered amygdules were observed throughout the entablature; most were filled with a blue-green clay and were 0.3 inch (8 millimeters) or less in diameter. The columns are regular, but sinuous, ranging from 0.6 to 1.2 feet (0.2 to 0.4 meter) in diameter. Except for some very localized fanning, the columns dip from 70 to 90 degrees. The column faces are continuous for 5 to 8 feet (1.5 to 2.5 meters), but the columns are dissected by numerous, low-angle, discontinuous cross-joints.



3.4 SUMMARY OF GEOLOGIC OBSERVATIONS

As the tunnels advanced, geologic observations were made on a daily basis. These observations included photographs and a description of lithology and structure. The following are selected daily observations and the station locations can be referenced on Figures 10 and 11. The sketches are cross-section and plan views of selected mining faces.

3.4.1 East Access Tunnel

Open Cut (Elephant Mountain)

Moderately fractured, slightly wavy columns, 0.2 to 5.0 millimeters yellow and brown clay, column faces are 1.8 to 2.7 meters per side in width.

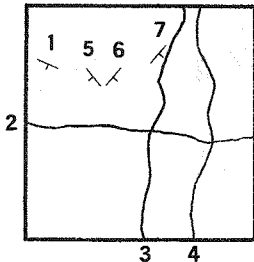
3+00 to 3+11.5

Slightly fractured; 0.2- to 4.0-millimeter brown clay, some with oxidation; medium to finely phaneritic colonnade; high-angle joints appear to be terminated by the low horizontal ones filled with 5 millimeters brown clay; high-angle fractures are slightly wavy, low-lying ones are flatter.

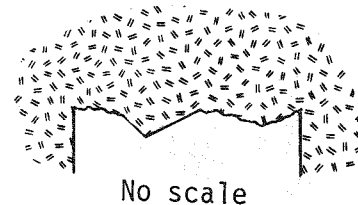
3+21

Finely phaneritic with abundant plagioclase phenocrysts ≤ 1 millimeter; moderately fractured.

3+21



- 1 = 86/85N
- 2 = 235/5W
- 3 = 245/78E
- 4 = Irregular
- 5 = 316/78E
- 6 = 245/88W
- 7 = 281/81W



Scale: 1" = 3 m

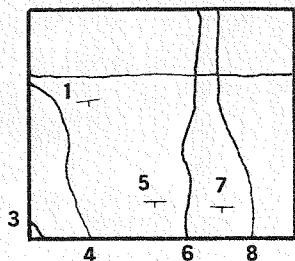
3+24.5

No noticeable low-angle joints; high-angle joints are slightly curved, contain ≤ 3 millimeters brown clay; little to no oxidation; better developed columns.

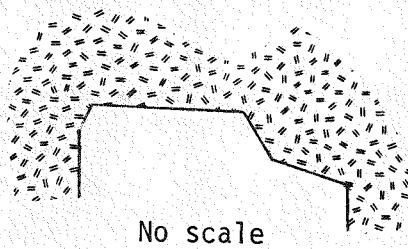
3+33 to 3+46

Dark brown mineraloid filling, shiny but not polished; 2.0 millimeters filling; joints are rough and continuous, mostly high angle, north or south dip; some joints have a light-colored, banded, orange-red oxidation coating.

3+33

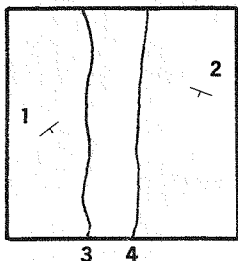


1 = 92/88N
 2 = 94/6N
 3 = 97/78W
 4 = 22/74W
 5 = 124/88N
 6 = 152/87N
 7 = 109/88N
 8 = 107/82W

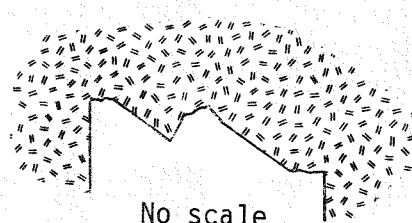


Scale: 1" = 3 m

3+46



1 = 127/87N
 2 = 308/90
 3 = 208/88W
 4 = 138/82N



Scale: 1" = 3 m

3+51.5 to 3+63.6

Medium to coarse phaneritic, very columnar; main column faces up to 2.4 meters in length, curved and wavy; \leq 4.0-millimeter brown clay and oxidation, rough surfaces.

4+21

Column faces aligned more parallel to tunnel than before; three to four main joints at 4+21; joints \leq 9.0 millimeters with dark-brown clay.

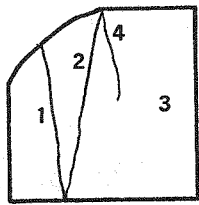
4+00 to 4+21

Three types of clay infilling: (1) sticky and pliable; (2) sandy; and, (3) hard, dark brown with weathered spalling basalt \leq 7 millimeters due to groundwater movement (metasomatic condition).

4+28

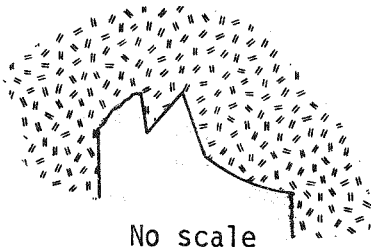
Random joint planes with oxidation \leq 6.0 millimeters thick; 60-centimeter diameter rock fall at 4+00; ball and socket joint; clay has dried and shrunk causing rock fall.

4+35



Scale: 1" = 3 m

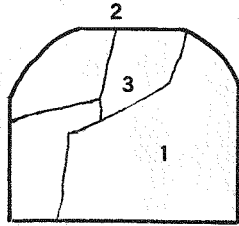
1 = 173/90
 2 = 43/88W
 3 = 122/88S with
 8-mm black
 clay and 10-
 15-mm spall-
 ing, weathered
 rock
 4 = 163/90



No scale

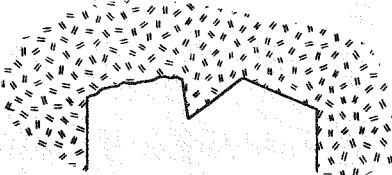
4+42

Joints show much oxidation, orange-brown clay, and some altered spalling rock; blocky ground, but dominant, large joint faces.



Scale: 1" = 3 m.

1 = 109/77N;
 5-mm clay
 2 = 172/90
 3 = 53/84S



No scale

4+56

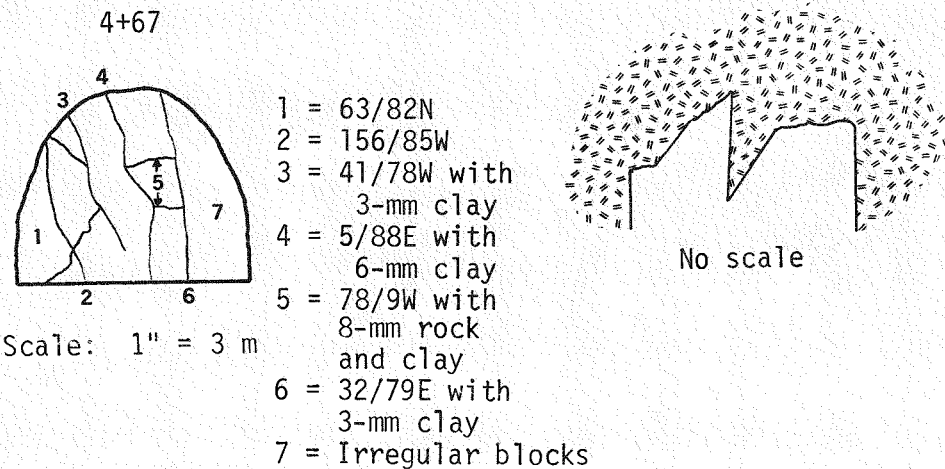
One or two principal joints, remainder is secondary blocky jointing; one joint has \leq 1.2-centimeter spalling weathered rock with 2 millimeters of clay.

4+61

Longhole drilled 1.4 meters above floor at +5 degrees; drilling rates, chips, and return water were monitored; Rattlesnake Ridge interbed at 14.5 meters, stopped hole.

4+67

Fairly tight but few joints \leq 6 millimeters thick with brown clay; few alteration rinds from groundwater movement.



4+72 to 4+77

Finely phaneritic, no signs of vesicularity.

4+89

Interbed (Rattlesnake Ridge) exposed at 4+84 in east rib and rapidly attains a height of 0.5 meter; at 4+89, interbed is 0.8 meter high, but only 0.2 meter high in west corner of face; composed of some weathered, rubbly breccia with clasts \leq 10 centimeters and breccia zone is 20 centimeters thick (flow base of Elephant Mountain); clasts are subrounded with irregular and elongated vesicles; cementation is by a yellow-brown clay; below the breccia is an irregular zone of the yellow-brown material. The thickness of it varies and it interfingers the material below which is a gray, well-indurated ash or tuff; the ash deposit has pink, irregular stringers (calcite-like).

4+94

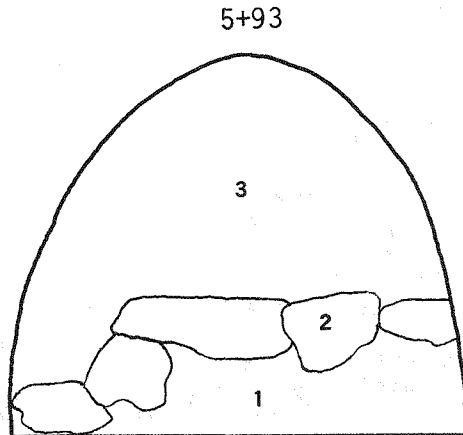
Interbed is 1.1 to 1.2 meters high on the face, tapering to 60 centimeters high in the west corner; interbed first appeared at 4+79 in east rib, but was mostly weathered rock and baked ash-tuff; 4+83 in the west wall was the first appearance; at 4+94, interbed is 90 centimeters high in east wall and 80 centimeters on right.

5+36

Strike of interbed is east-west with 6 degrees north dip.

5+93

Pomona flow top 30 centimeters up on east side, 60 centimeters up on west side; first seen at 5+85 right and 5+81 left; flow top is 30 to 50% vesicles \leq 6 millimeters; not very brecciated.



- 1 = Light-brown-yellow sandy clay
- 2 = Flow top; blocks to 0.9 m x 0.3, subangular; 30-50% vesicles; vesicles \leq 8-mm coated with dark green, light-blue, or brown mineraloid
- 3 = Brown, sandy clay; soft; few small bedding planes

Scale: 1" = 1.5 m

6+20

Flow top is lower 80 centimeters of face with 30 to 40% vesicles.

6+25

Flow top is 1.7 meters up on face with some minor clay in mosaic breccia, vesicular zone below; 20% vesicles at bottom 30 to 60 centimeters.

Surveyed elevations:

Contact of Elephant Mountain interbed/Rattlesnake Ridge interbed is 198.7 meters; contact of Rattlesnake Ridge interbed/Pomona is 195.7 meters.

6+37

Breccia in upper 1.2 meters of face; lower 1.2 meters are vesicular with clay-filled joints.

6+43

Top 80 centimeters of face are breccia with yellow-brown clay matrix; bottom 1.8 meters are blocky and vesicular (\leq 40%).

6+57

Full face of Pomona.

6+64

Finely phaneritic with \leq 2% vesicles; vesicles are irregular shaped, 2 to 12 millimeters in diameter, and lined with blue or green clay.

6+72

Scattered vugs \leq 12 millimeters in diameter; 20 centimeters of breccia in arch, with up to 50% vesicles; basalt is finely phaneritic and joints are from tenths to 2 millimeters.

6+99

Basalt is very tight, but hackly joints with \leq 2 millimeters dark-green or yellow-brown clay; random vesicles \leq 10%; six or eight vugs 15 to 25 centimeters in diameter in face.

7+22

Hackly entablature, small (0.2 to 0.3 meter) column faces.

7+58

Entablature with hackly jointing and moderately sinuous columns with 0.3- to 0.6-meter faces.

7+82

Regular columns with faces 0.1 to 0.2 meter; vugs 1 to 4 centimeters; some moisture dripping from back.

8+29

Basalt is finely phaneritic with numerous plagioclase laths; jointing is hackly with moderately sinuous columns with 0.2- to 0.3-meter faces; 1 to 3 millimeters dark-green clay along many of the primary joints; 25- x 36-centimeter vug in middle of face with 5 to 25 millimeters of dark-green, sandy clay lining.

8+45

Dark-gray, phaneritic with plagioclase laths \leq 2 millimeters; 1% of rock is amygdules \leq 8 millimeters diameter; pyrite coating on numerous joints.

8+94

Columns with 0.2- to 0.3-meter sides; minimal horizontal joints; 0.1- to 0.2-millimeter dark-green and black along joints; finely phaneritic with amygdules \leq 10 millimeters.

9+43

Longhole drilled at +45 degrees (south 2 degrees west); also hole drilled at intersection of Extensometer Room +60 degrees (north 66 degrees west) (see drill logs). The Extensometer Room is measured from the centerline (C_L) of Tunnel #3.

C_L+41 feet

Extensometer Room top heading; columns are 0.3 meter per side and \leq 1.5 meters long.

C_L+56 feet

No noted vugs or amygdules.

C_L+100 feet

193.4-meter elevation at back; 1.1-meter-wide oxidized zone at face; wet, dripping goes up into back and then 2.1 meters along arch; brown, wet clay in joints very oxidized, up to 10 millimeters wide of clay and weathered zone at joints; abrupt contact at edge of oxidized area.

CL+112 feet

Egg-shaped vug in face 40 centimeters deep x 30 to 35 centimeters wide; joints are abundant with slick, shiny green to black rippled glass 1.5 millimeters thick; scattered vugs \leq 5 millimeters, but \leq 1% with slight green infilling.

CL+148 feet

\leq 0.5 millimeter clay, blue and green, on joints.

CL+164 feet

Finely phaneritic with column lengths of 1.8 to 3.6 meters per side; scattered vugs to 100-millimeter diameter with light-blue lining.

BENCH @ CL+55 feet

CL+55 feet

\leq 0.5 millimeter clay on joints, light blue; columns \leq 0.9 meter long with 0.1- to 0.2-meter faces.

CL+65 feet

Left rib oxidized; scattered amygdules.

CL+114 feet

North rib oxidized from CL+110 to CL+114, rind of 5.1 centimeters with 3-millimeter yellow-brown, sandy clay along joints.

3.4.2 West Access Tunnel

Open Cut (Elephant Mountain Member)

6-millimeter brown clay on joints near portal face; severely to moderately weathered; columnar, jointed, and blocky; columns are sinusoidal with faces of 0.3 to 1.8 meters; low-angle shear across top of portal with estimated 20-millimeter thickness.

18+63

Large shear visible near back, 40 millimeters thick; clay is damp and contains small breccia fragments within the clay, strike is approximately 172 degrees; dip 87 degrees west.

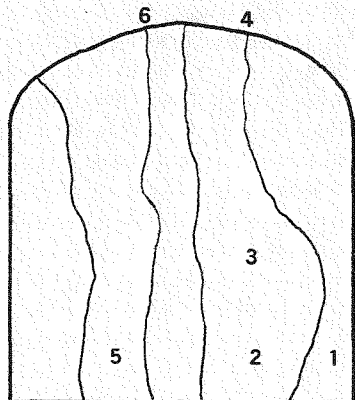
18+78 to 18+60

6- to 8-millimeter dark-brown clay and weathered rock on joints; columns are sinusoidal and very blocky; weathering/alteration rinds around joints are dark black and \leq 10.0 millimeters wide; many oxidized zones, some with onion skin-like texture, orange and orange-brown color; horizontal joints \leq 150 centimeters in length, strike 155 degrees; dip 8 degrees east average.

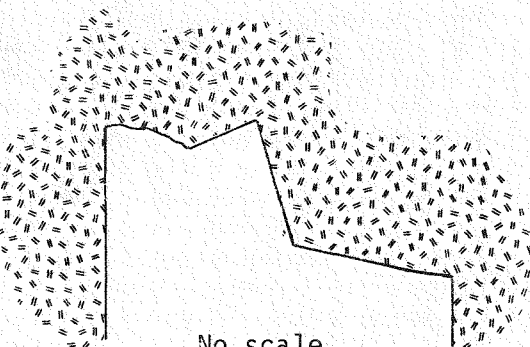
18+57

Large joint 50 millimeters wide in east side, strike 161 degrees; dip 75 degrees west, with weathered rock, slightly gougy, wavy strike; conduit to the surface. Mostly blocky in the east side, blocks 30 to 60 centimeters in size. Horizontal planes up to 4 millimeters with brown oxidized clay, averages 143 degrees strike/dip 13 degrees east.

18+57



- 1 = 99/81S curved
- 2 = 93/
- 3 = 102/80-90
- 4 = 11/88
- 5 = 71-86/90
- 6 = 163/87W



Scale: 1" = 3 m

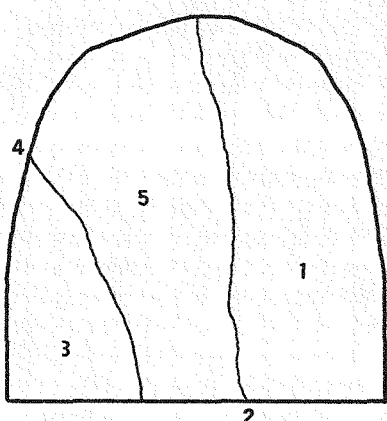
18+51

Large shear on the east side visible high above the springline; appears to be disappearing at face; strike 145 degrees/dip 90 degrees at face; slightly damp, contains wet clay with weathered rock; shear zone is a maximum of 40 centimeters wide at face.

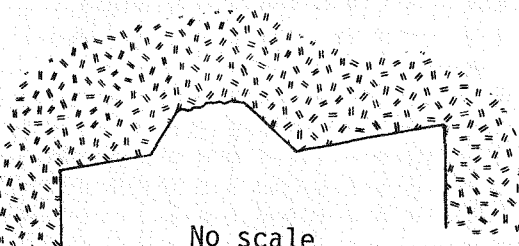
18+38

Large column faces; orange oxidation, clays and spalling of weathered rock on main joints.

18+38



- 1 = 81/82N
- 2 = 133/88E
- 3 = 82/90
- 4 = 32/87W Curved
- 5 = Blocky; blast shatter



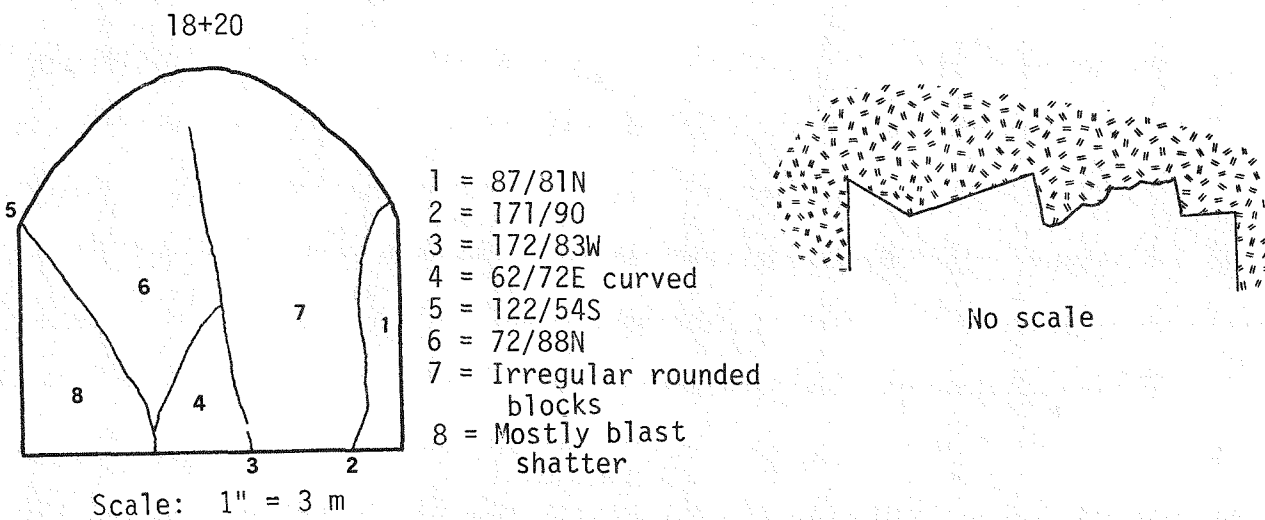
Scale: 1" = 3 m

18+28

Blocky, but columnar; secondary joints and cooling joints break the columns into 0.6- to 0.9-centimeter slightly subrounded rectangles; black alteration rims to 4.0 centimeters around most joints; some orange-brown iron oxide stains and spalling basalt rinds to 8 millimeters.

18+35 to 18+20

Blocky with cooling joints from 5 to 40 degrees with average strike of 43 degrees; moderately tight with ≤ 3 millimeters brown sandy clay on the primary joints and usually orange-brown staining on the secondary joints; some primary joints have ≤ 8 millimeters of weathered basalt rind peeling off; rock is finely phaneritic, smooth joints; blue-green clay ≤ 0.5 millimeter thick on some joints.



18+12

Blocky columns with dominant vertical jointing, ≤ 2.5 millimeters of brown clay; irregular blocks up to 0.9 meter; vesicles $\leq 1\%$, but ≤ 6 millimeters in length--mostly oval shaped.

17+46.5

Banded iron staining and light-blue clay on secondary joints; ≤ 3 -millimeter brown clay on primary vertical joints; absence of horizontal joints; very few vesicles, ≤ 6 millimeters long and partially filled with light-blue clay. Interbed at floor at 17+47, strikes north 86 degrees west.

17+36

Interbed is 30 centimeters off the floor; Elephant Mountain is very blocky with blocks to 1.2 meters per side; column faces are not well developed.

17+20

Interbed extends 1.4 meters up on face.

16+91

Blocky irregular jointing of Elephant Mountain; interbed is 2.7 meters high at face, top 0.8 meter is breccia, clay, and tuff; 0.8 to 1.5 meters light-brown clay, black varve-like organic deposits, 1.5 to 2.7 meters brown sand and brown-yellow clay.

16+81

Interbed dipping 8 to 9 degrees and is 3.1 meters up on face.

Surveyed elevations: Elephant Mountain/Rattlesnake Ridge interbed contact at 198-meter elevation at 16+27, Rattlesnake Ridge interbed/Pomona at 197 meters at 16+52.5.

16+72

Interbed is 3.8 meters up on face; invert to 1.4 meters of sand and clay, 1.4 to 1.8 meters of tuff and siltstone, 1.8 to 1.9 meters of dark-brown to black siltstone, 1.9 to 2.4 meters of pink, white, and gray varve-like, 1.9 to 2.9 meters gray-brown tuff siltstone with pink clay stringer, 2.9 to 3.7 meters gray tuff siltstone, 3.7 to 3.6 meters flow bottom of Elephant Mountain.

16+56

Interbed 0 to 4.3 meters up face; sand and clay lenses 0 to 2.2 meters.

16+52.5

Vesicular flow-top breccia in east side 0.3 meter up.

16+45

Flow top of Pomona extends across the face 0.3 meter up; clasts are scoriaceous to highly vesicular.

16+15.5

Breccia is 1.8 meters up on face; clasts to 0.9 meter in size.

16+06

Breccia is up 1.5 meters on east and 1.2 meters on west; vesicles in clasts to 12 millimeters with light-blue coating; breccia matrix is yellow-brown clay.

15+89

Pomona breccia is 1.4 meters high on face and clasts \leq 0.5 meter.

15+85

Flow-top breccia is 1.5 meters high on west corner and 2.3 meters high on east side, upper part of face is sand and clay.

15+67

Flow-top breccia is 2.4 meters high on east corner and 1.5 meters high on west; breccia contains clasts with interconnecting vugs to 90 millimeters with dark-green clay lining, 20- to 25-millimeter vugs with white SiO_2 lining.

15+60

Flow top is 2.4 meters high on east and 1.5 meters high on west.

15+31

Entablature is 2.4 to 3.1 meters high on face; rest is breccia; entablature is blocky with 40% vesicles \leq 10 millimeters in diameter.

15+11

Pomona breccia 0.6 to 0.9 meter above the invert to the back; a channel was observed from 15+18 to 15+04, accounting for this sudden change.

15+04

Bottom 1.2 meters of face appear to be top of Pomona, upper part of face is breccia; a large 45- x 25-centimeter vug partially filled was in the Pomona.

14+82

Upper colonnade(?) faces are 0.6 meter; larger columns than what were seen in Tunnel #3; vesicular basalt with blue-green coating and fillings.

14+74

0.3 to 0.6 meter of flow-top breccia in top of face; semi-regular columns with faces 0.3 to 0.6 meter; \leq 20% vesicles; two joints in face at 90-degree strike/dip of 75 degrees south at 14+79 to 14+81 with 2 millimeters yellow-brown clay.

14+69

Full face Pomona entablature.

14+34

5% vesicles with zones to 15%; vesicles \leq 12 millimeters diameter with black and dark green lining.

14+24

Bottom 1.8 meters of face are massive with \leq 1% vesicles; upper 3.1 meters have 10 to 20% vesicles \leq 15 millimeters; joints \leq 0.4 millimeter, columns 0.3 to 0.5 meter per side.

13+89

Zones of vesicles to 30%, mostly \leq 20 millimeters light-blue coating; dark-green and white vesicle fillings (30% of vesicles are filled); columns with 0.3- to 0.6-meter faces; dark-green and yellow-brown joint filling \leq 2 millimeters; some oxidation.

13+42

Finely phaneritic with \leq 5% vesicles; scattered vugs to 15 centimeters with dark-green and blue coatings; light-blue coating along joint surfaces.

13+35

Vugs to 30 millimeters; scattered zones of 20% vesicles; wet, drippy area at 13+41 in arch.

12+76

1.2-meter zone of highly oxidized joints on left rib at turnout to Heater Test Room with \leq 13 millimeters of highly weathered rind, 8 to 10 millimeters thick of brown, moist, sandy, silty clay; basalt is finely phaneritic with light blue on joints; no vesicles, but few amygdules \leq 5 millimeters; scattered vugs to 10 millimeters lined with light-blue-green clay; oxidation zone, 4.3 meters from face on east rib, 6 meters from face on left rib (1.1-meter-wide zone).

3.4.3 Heater Test Room

12+33

Columns with 0.2- to 0.4-meter faces; some tilting in middle of face (~70 degrees south); oxidation zone 60 centimeters in from left corner, 1.2-meter-wide zone with rinds 10 to 40 centimeters; 11+97 20.5- x 20.5- x 20.5-centimeter vug.

11+93

Finely phaneritic; columns 0.2 to 0.4 meter dipping 60 degrees west at bottom of face; joints \leq 0.5 millimeter with light-blue, dark-green clay; 1.2-meter oxidized zone in middle of face with \leq 1-millimeter yellow-brown clay; vesicles \leq 20 millimeters with blue-green clay lining; vug 20 x 10 x 10 centimeters at 11+99 (south wall); 12+15, 2.4 meters above invert, vug 35 x 45 x 60 centimeters with 15 centimeters clay in bottom.

11+73

Oxidized zone 2.1 meters wide on south side of face with rinds to 5 centimeters; columns 0.2 to 0.4 meter, faces dipping 69 degrees south on north side of face; scattered vugs and amygdules, vugs to 15 centimeters.

11+55

1-centimeter wide minor oxidation zone along vertical joints 2.1 meters from south corner in face; brown sandy clay \leq 2 millimeters on few joints; \leq 0.2 millimeter on 60% of joints; 20-centimeter diameter vug in south corner of face; 11+62 north wall is 20-centimeter vug; no vesicles or amygdules.

11+28

Horizontal shear, 0.5-meter-wide band on south rib and 1.2 meters down from back, rock here is moderately altered with vesicular zones to 20%; columns are hackly and irregular; 11+40 to 11+46 dripping from back on south side.

10+67

All joints $<$ 1 millimeter; dark-green clay and calcite; irregular columns, scattered zones of vesicles \leq 4 millimeters in diameter.

11+85 Bench Heading

Finely phaneritic, tight jointing; oxidized zone 0.9 meter wide at 11+91 right rib with 5-centimeter oxidized rind, joints with \leq 10-millimeter sandy clay in this zone.

11+42 Bench Heading

Oxidized zone on south rib at 11+62; joints \leq 0.3 millimeter, scattered pyrite; scattered amygdules; 11+52 10-centimeter vug north rib; 11+56 20-centimeter vug in north rib.

11+34 Bench Heading

Joints \leq 0.3 millimeter with light-blue clay and calcite; scattered vugs to 10 centimeters.

10+69 (Full Face 5.2 x 5.2 meters)

10+37

Finely phaneritic, sinuous columns with 0.2- to 0.3-meter faces; dark-green filling \leq 0.3 millimeter; joints wavy and rough; scattered vugs to 13 centimeters, scattered amygdules \leq 6 millimeters with light-blue filling; 10+42 25-centimeter vug 2.1 meters up from floor.

9+36

Tight joints \leq 0.3 millimeter with dark-green clay; scattered pyrite and calcite on joints; 0.2- to 0.4-meter column faces; frequent (\leq 1%) vugs to 5 centimeters; scattered vesicles (\leq 2%).

3.5 INVESTIGATIVE DRILL HOLES

Prior to siting the NSTF, two core holes were drilled on Gable Mountain for preliminary assessment of the rock conditions and for stratigraphic depth determination. DC-10 was drilled at the base of the north flank of Gable Mountain north and west of the existing tunnels (Figure 7). The hole was drilled 30 degrees from the vertical, due south, to a depth of 456 feet (139 meters). DC-11 was a vertical hole drilled near the top of Gable Mountain approximately 25 feet (7.6 meters) west of where the West Access Tunnel is now located (Figure 7). This hole, also NX oversize (3.032 inches [77 millimeters]), diamond drilled, was completed at 385 feet (117.3 meters).

As the tunnels were being advanced, several investigative holes were drilled to maintain a good knowledge of the local stratigraphy and to assess the rock quality. The first hole to be drilled was a percussion-drilled hole in the East Access Tunnel at the mining face at Station 4+62. This hole was drilled at 5 degrees above horizontal in an attempt to locate the Rattlesnake Ridge interbed. Penetration rates and the drill cuttings were carefully monitored and it was estimated that the interbed was 47.5 feet (14.5 meters) from the hole collar.

PH-1 and PH-2 were two percussion-drilled holes near the end of the East Access Tunnel. Their purpose was to give an indication of the rock quality above the arch prior to mining the Extensometer Room and the Heater Test Room (see Figure 10). Again, the penetration rates and water returns were monitored, and cuttings samples were collected.

Boreholes PH-3 and PH-4 were drilled in the arch of the West Access Tunnel at Stations 12+83 and A13+40, respectively (see Figure 11). The holes were drilled approximately 55 degrees up from horizontal. PH-3, near the intersection of the Heater Test Room and the West Access Tunnel, was drilled to determine the amount of Pomona basalt from the tunnel arch to the Rattlesnake Ridge interbed. PH-4 also was for this purpose and to determine whether there was sufficient, competent rock overhead to mine the high Transfer Room #2 at the end of the West Access Tunnel.

A diamond-drilled hole, TH-2, was cored at Station A13+51 to allow visual examination of the rock above the tunnel arch and for stratigraphic confirmation. The hole confirmed the stratigraphic interpretations from boreholes PH-3, PH-4, DC-11, and observations in the tunnel.

3.6 CONSTRUCTION METHODS

3.6.1 Tunnels

The East Access Tunnel was advanced full face using jack-leg drills and a Joy ACM-II two-boom jumbo. A Gardner-Denver three-boom jumbo was used in the West Access Tunnel and the Heater Test Room. The Extensometer Room and the first 211 feet (64 meters) of the Heater Test Room were mined by the top heading and bench method.

Neither smooth-wall blasting nor pre-splitting were used in mining the facility. Inconsistently drilled and loaded rounds resulted in overblasting and severe rock breakage in some areas. Some blast-induced fractures, primarily around the excavation, resulted from these methods, which also resulted in opening small-aperture, tightly healed joints. This increased the permeability of the rock mass and decreased its overall quality. This was a contributing factor in allowing the drill water to communicate between boreholes in the core drilling program. The zones of blast damage are visible in the photographs of the borehole core and in the joint frequency histograms in Section 4.2.2.

In the East Access Tunnel, the initial tunnel support for the first 30 feet (9.2 meters) of the Elephant Mountain basalt was steel sets (Figures 14 and 15). Rock bolts of number 10 rebar, fully encapsulated in polyester resin, were contemplated for use to support the remaining basalt portions of the excavation. Rock bolts and mesh were used for a distance of 70 feet (21.4 meters). This area was later covered with

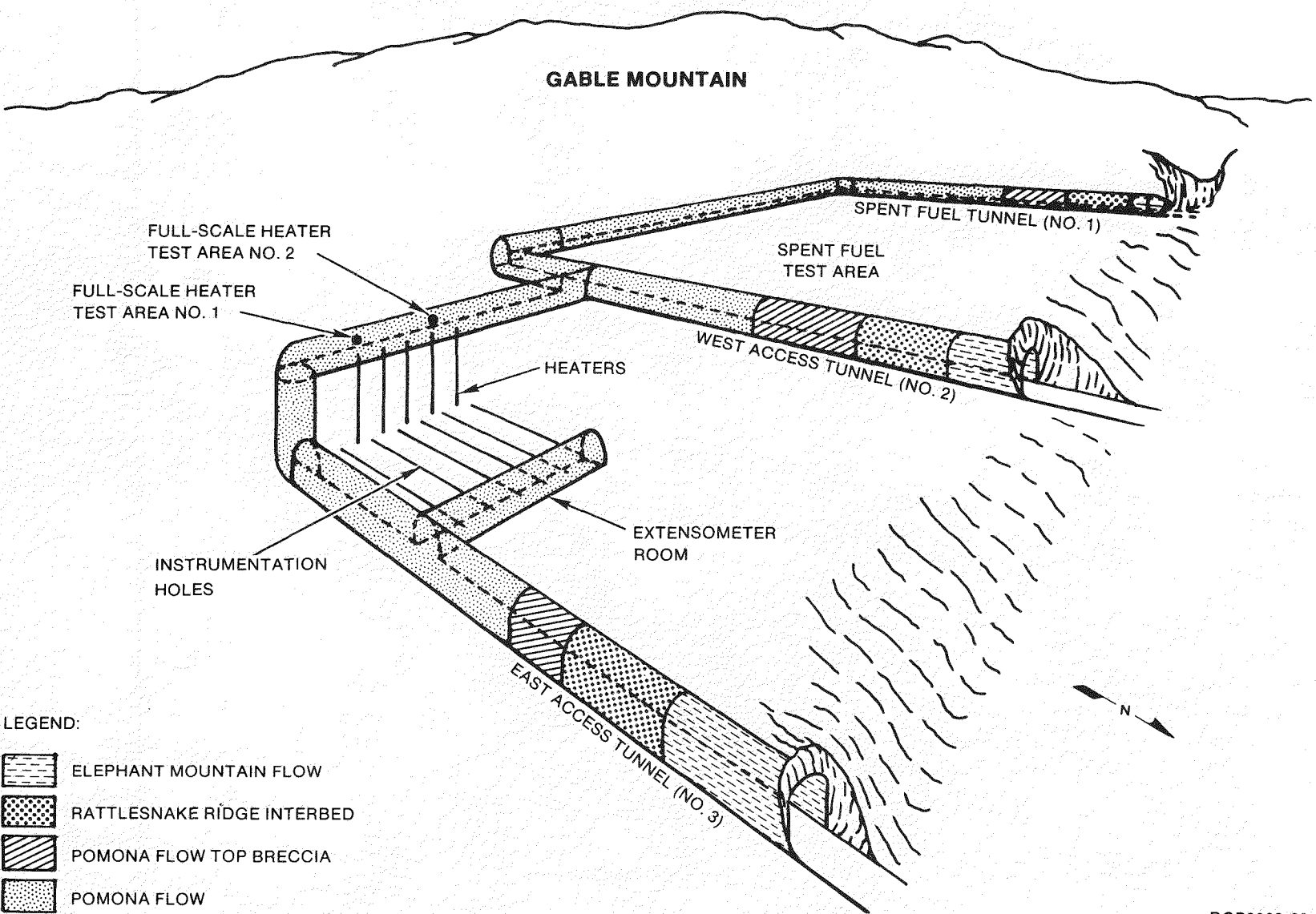
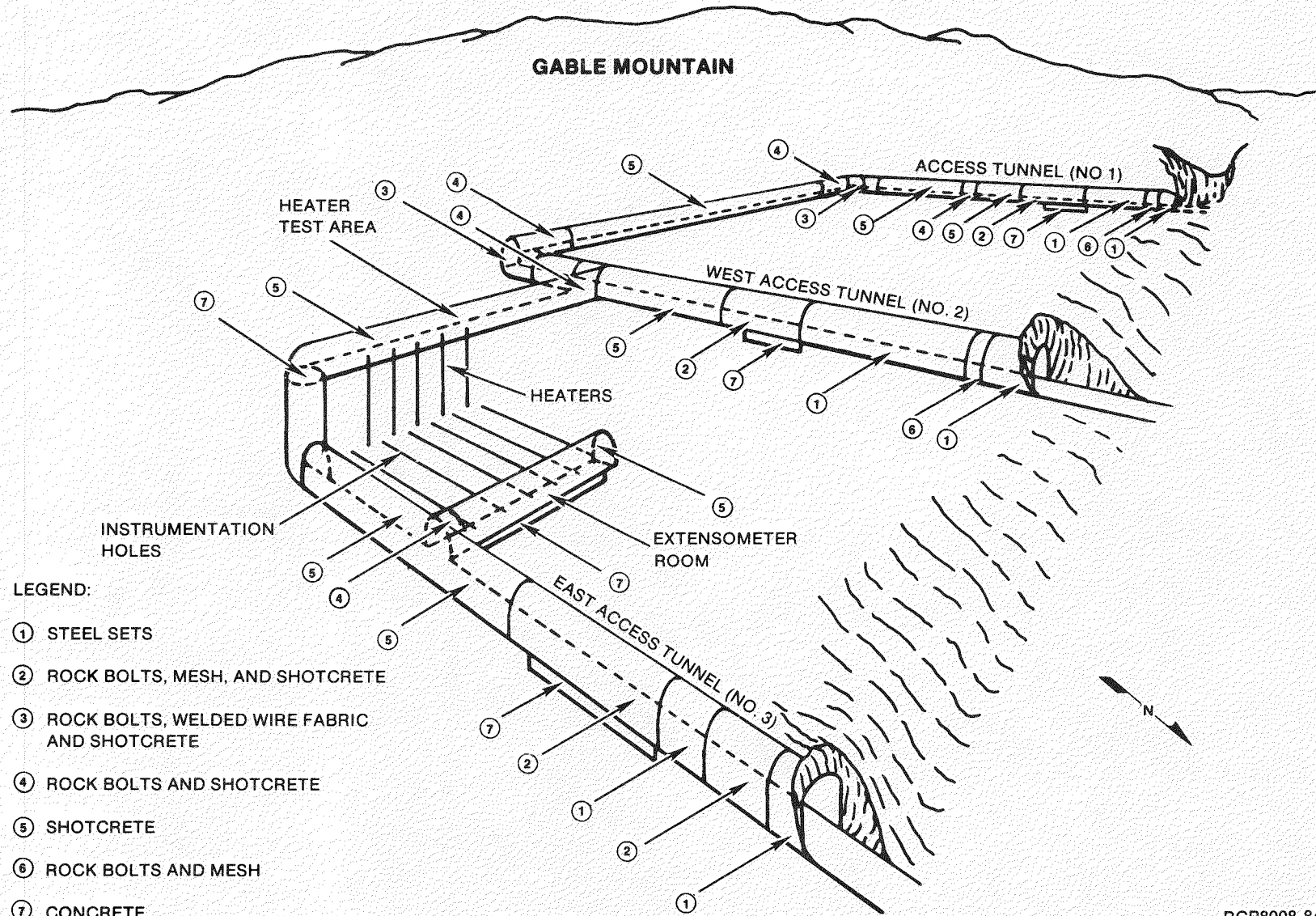


FIGURE 14. Conceptual Sketch, Near-Surface Test Facility Geology.



RCP8008-84

FIGURE 15. Conceptual Sketch, Near-Surface Test Facility Support Systems.

shotcrete when all excavation was completed. Two small rock falls occurred when the contractor was following the excavation by as much as 28 feet (8.5 meters) with the rock bolt and mesh support. After the rock fall, steel sets were installed for support for about 50 feet (15.3 meters). The remainder of the Elephant Mountain basalt was supported with rock bolts, mesh, shotcrete, and, in special cases, rock spiles. The rock spiles pre-support rock before the rock is mined out and were used to control overbreak in the Elephant Mountain basalt. The Rattlesnake Ridge interbed is supported by a combination of rock spiles, split sets, mesh, and, finally, shotcrete. Because of various difficulties with the shotcrete, it was not applied until the interbed had been penetrated by the tunnel. Eventually, the invert (floor) in the interbed area was covered with concrete and drain holes were drilled in the ribs. Support in the Pomona basalt is primarily by shotcrete, except where augmented by rock bolts at the intersection with the Extensometer Room.

A ramp was driven up from the East Access Tunnel as steeply as possible until the arch of the Extensometer Room was reached. Then a top heading was driven the full 164-foot (50-meter) length of the room, followed by bench removal using horizontal blast holes to reach the final cross section of 14 x 21 feet (4.3 x 6.4 meters).

Initial support for the West Access Tunnel was 45 feet (14 meters) of steel sets followed by 25 feet (7.6 meters) supported with rock bolts and mesh. The next 210 feet (64 meters) through the remainder of the Elephant Mountain basalt and into the upper portion of the Rattlesnake Ridge interbed are supported by steel sets augmented with rock spiles and shotcrete. The remainder of the interbed is primarily supported with shotcrete in combination with rock spiles, split sets, mesh, and concrete on the invert. Support in the Pomona basalt is primarily by shotcrete, except where augmented by rock bolts at the intersection with the Heater Test Room.

Rock support for the Heater Test Room was primarily provided by shotcrete, except where augmented with rock bolts for the first 45 feet (13.7 meters) from the intersection with the West Access Tunnel.

The area supported solely by rock bolts and mesh provided ample opportunity for geologic mapping and interpretation. However, the decision to use shotcrete as the primary means of ground support severely limited the amount of time available for rock characterization. The shotcrete was applied immediately after blasting each round and this only provided time for photographs of the face and a generalized geologic description.

Shotcrete was applied to the tunnel ribs (walls) after the blasted rock was removed. Again, time was of the essence and attempts were made to protect the lower portions of the tunnel ribs from shotcrete overspray; this was successful in some locations.

The construction group and contractor were provided daily geologic and geotechnical input during construction of the tunnels and the borehole drilling program.

Geologic surveillance was continually made in all areas, but detailed investigations were severely restricted due to the immediate application of the shotcrete. Photographs and field notes provided the bulk of geologic information prior to the instrument borehole core drilling.

3.6.2 Core Drilling the Instrument Boreholes

One hundred and twenty-five holes, varying in diameter from 1.50 to 18.0 inches (38 to 450 millimeters) were drilled in the Extensometer Room and Heater Test Room to accommodate the heaters and instruments. All of the holes were cored using either CP-65, CP-55B, CP-8, or CP-15 air-powered, diamond drills. The core from the NX (2.98-inch [76-millimeter]) holes was obtained using a Longyear Triple Tube Core Barrel to preserve the core in a near-in situ condition. The core was removed from the split inner tube by overlaying a split cardboard tube and then removing the inner tube. The core and cardboard tube were then placed in 5-foot (1.5-meter) wooden core boxes. Due to the fractured nature of the basalt and mishandling of some core, not all of the core was preserved in an ideal state. An attempt was made to obtain oriented core in at least 60 NX holes, both horizontal and vertical. The remanent magnetism in the rock precluded the use of a downhole compass. The contractor attempted to use a set of oriented rods with a punch on the end to orient the top of each run. This system was not adequate and a fluxgate magnetometer was later used to orient the core to the "north" in the vertical holes and in the "up" position for the horizontal holes.

An attempt was made to core the 18-inch (457-millimeter) Full-Scale Heater Tests #1 and #2 main heater holes. The fractured nature of the rock was not compatible with the drilling equipment being used and recovering core from the holes was difficult. Most of the recovered rock was rubbly and disoriented; hence, no detailed characterization could be made of the core.

Concrete pads were poured over the borehole arrays in the Heater Test Room to facilitate leveling and anchoring the drills. The thickness of the concrete was included in the total measured depth of the boreholes. The same holds true for the holes drilled from the Extensometer Room, where the initial few inches (centimeters) were drilled in shotcrete.

4.0 BASELINE DATA FOR PHASE I FULL-SCALE HEATER TESTS

4.1 DETAILED SITE CHARACTERIZATION

4.1.1 Geologic Maps

As construction of the NSTF progressed, the mapping procedures for the site characterization that were originally stated in the test plan were modified. The test plan provided the following:

"Geologic maps will be constructed of the NSTF open cuts, tunnels, and rooms. Maps will be constructed on a scale of 1:20 for the open cuts and tunnels, and a scale of 1:10 for the test room. The geologic maps to describe the rock mass mineralogy, fabric, and structure will include:

"A detailed mineralogical description of the intact rock composition, fracture location, and attitude. Maps will be developed for the test room floor, roof, and walls. All major discontinuities and discernible joint sets will be noted. Fracture characteristics, including fracture-filling materials, aperture, persistence, roughness, tortuosity, and termination or continuity of fracturing. If possible, differentiation will be made between naturally occurring fractures and those induced by mining. All rooms and tunnels will be photographed for record purposes. Rock surfaces will be surveyed and marked in order to provide a scale on the photographs (Staff, 1979)."

These criteria were followed during excavation of the open cuts and into the Elephant Mountain portions of the tunnels. The mapping procedures were modified, however, when the support system was changed to include shotcrete as the tunnels were advanced into the Rattlesnake Ridge interbed and the Pomona Member. The shotcrete was applied, immediately after blasting, to the upper ribs and face, and again immediately after the broken rock was removed. This procedure, which allowed no time for detailed mapping, in conjunction with the high joint density of the entablature, resulted in the use of daily photography and a concise, written description for geologic characterization.

Since the arch and upper portions of the ribs were shotcreted, the 1:10-scale maps of the arch and ribs were replaced by several detailed line maps along the lower portions of the rib. To facilitate the drilling program, concrete pads were installed over the areas for Full-Scale Heater Tests #1 and #2. At the completion of drilling, the pads were to be removed and maps on a scale of 1:1 were to be drawn of the test areas. Due to the lack of controlled-blasting techniques during excavation, the floor under the concrete pads had been severely damaged; therefore, the concrete pads were left to preserve the upper portion of the boreholes. This eliminated the floor maps, but since no through-going joints had been observed and many of the joints on the floor had been modified by blasting, no pertinent information was lost.

The final mapping process that evolved included detailed line mapping, daily photography, and daily written descriptions. These, in conjunction with the information obtained from the boreholes, constitute a major part of the data base for inclusion in the Site Characterization Report.

4.1.2 Photographs

Tunnels. A large volume of color-print photographs was collected since the initial construction of the NSTF. These photographs document both geologic and construction activities that took place at the NSTF.

The photographs were taken with a 35-millimeter camera using either a 28- or 50-millimeter lens. Initial attempts were made to produce a photomosaic of the open cuts, ribs, and back of the tunnels and test rooms. Overlapping photographs were taken starting at one rib by the invert and photographing up to the centerline in the back, then down the opposite rib. Each series of photographs contained a 6-foot ruler for scale and a sign noting the date and survey location by convention; the sign was always positioned on the side of the rule nearest the mining face, thus making it easy to identify which rib was being photographed. Photographs were also taken, with date and survey station noted, of many of the mining faces.

The photographic coverage was carried out through most of the Elephant Mountain flow, although steel sets and lagging obscured some of the rock. When the use of shotcrete became the principal means of support, it was not possible to continue producing a complete photomosaic. Frequent photographs of the mining faces were continued, although many were partially obscured by muck (freshly blasted rock) or by shotcrete overspray.

The Extensometer Room and the first 211 feet (64 meters) of the Heater Test Room were mined by the top heading and bench method. Shotcrete was only applied during the excavation of the top heading; hence, the lower portions of the ribs were clean. Complete photo-documentation was made of both ribs of the Extensometer Room from the invert to approximately 8 feet (2.4 meters) above the invert. Likewise, the north wall of the Heater Test Room was photographed, although portions were covered with shotcrete overspray.

Close-up photographs were taken of specially noted geologic features in the Heater Test Room such as the large vugs and their clay in-filling. Also, close-ups were taken of features in the interbed and the Pomona flow-top breccia.

The original site characterization plans (patterned after the Stripa, Sweden project) (Thorpe, 1979) included a photomosaic of the Heater Test Room invert. This project was deleted from this report for a number of reasons:

1. No continuous joints or features were readily seen in the core that could be projected upward to the invert.
2. Excavation by extensive blasting had loosened much of the rock (up to 4 feet [1.2 meters]) below the invert, making much of it irregular and disturbed.
3. The large number of joints seen on the invert rendered a photomosaic meaningless for mapping or comparison purposes; it would have only served as photo-documentation.
4. A large volume of joint data had been gathered from the horizontal holes and detail line maps, so no joint distribution bias would be lost by not having a photomosaic or map of the floor.
5. Concrete pads, separated from the rock by visqueen, were poured over the borehole array areas to facilitate drilling the holes. These were left in place (to facilitate instrument installation) as a result of the above-listed information.

Borehole. Upon completion of the instrument boreholes, the core was transported to the core repository. Each hole, except the main heater holes, was photographed. Because of the poor quality and bulk of the rock from the main heater holes, the core was transported to a warehouse for storage and was photographed there.

Photo-documentation of the walls of the two 18-inch (45.7-centimeter) heater holes was done prior to heater installation. This consisted of lowering a 35-millimeter camera with a 25-millimeter lens, motor drive, cable release, and high-intensity light source into the borehole. Color photographs were taken at 10-inch (25-centimeter) intervals in vertical strips from the borehole bottom to just below the collar. The photograph strips were taken beginning at the north, then at 90-degree intervals around the hole; this provided almost complete coverage of the borehole walls. Particular emphasis was on the lower 9 feet (2.7 meters) of the hole at the 90-degree quadrants. This will be the location of the viewing ports within the main heater, where borescope monitoring will take place during the test. These photographs document the initial characteristics of the borehole wall and serve as baseline data. Additional photographs will be made through the borescope viewpiece until the tests are completed and the heaters removed from the holes. A complete photo-documentation process (such as the one just described) will then be repeated. Photographs were also taken of the core from the overcoring test and other cored investigation holes.

4.1.3 Detailed Line Mapping

Detailed line mapping is a systematic sampling technique for characterization of fracture systems developed by Call and Others (1976). Originally presented as a method for analyzing slope stability,

it can be adapted to numerous other problems. Detailed line mapping was used at the NSTF to characterize the jointing in the Pomona flow, particularly in areas of close proximity to the areas for Full-Scale Heater Tests #1 and #2 and the Extensometer Room.

At each mapping site, a tape is stretched along the wall as a reference line. A zone 1.5 feet (0.46 meter) above and 1.5 feet (0.46 meter) below the reference line, in which the mapping will be done, is marked out. The length of the line is determined by the amount of rock exposed and the quantity of data desired. For each joint longer than 0.5 feet (15 centimeters) occurring within the mapping zone, the following data were recorded: distance along the line; rock type; geologic structure type; strike and dip; waviness; length of joint; overlap; termination of structure; roughness; joint thickness; joint-filling material; and water conditions.

The results of the mapping are presented in Section 4.2.

4.1.4 Instrument Borehole Core Logs

One hundred and twenty-five holes varying in diameter from 1.50 to 18.0 inches (38 millimeters to 45.7 centimeters) were drilled in the Extensometer Room and Heater Test Room to accommodate the heaters and instruments. Core was recovered and logged in all holes.

The core was labeled and boxed in accordance with a Rockwell-developed procedure (see Appendix B), which is common to all core holes on the Hanford Site. The labeled and boxed core was transported to the surface by the drilling contractor.

Detailed lithologic and structure logs were prepared shortly after completion of the hole. This was done expediently so any large joints, shears, or unusual features could be wrapped and preserved to prevent dessication of the clays and in-filling material; however, no features such as these were seen and, consequently, only a few examples of the in-filling material were wrapped and sealed.

A geologic core log (see Appendix A) was prepared especially for the NSTF site characterization. It contains a compilation of much of the data recorded on geologic engineering logs and geologic descriptions pertinent to basalt.

All holes were logged by the authors and should provide a consistent usage of terms and descriptions throughout the logs.

The locations of the boreholes were obtained from survey records provided by the drilling contractor's survey crew. Hole angle and bearing were generally rounded off to the nearest one-half degree for these logs. The hole elevation and starting point are the top of the concrete or shotcrete pad.

The log contains six distinct lithologic divisions:

1. Rock name
2. Weathering/alteration state
3. Structure
4. Color
5. Texture
6. Strength.

These are further subdivided into more categories, many of which are not applicable to the rock in the area of Full-Scale Heater Tests #1 and #2. The nomenclature and abbreviations used are contained in Appendix A.

4.1.5 Geomechanical Core Logs

The Basalt Core Geomechanical Data Log was prepared by Rockwell for the recording of individual joints in the core from the deep basalt boreholes. This log was slightly modified for use at the NSTF to log individual joints from selected horizontal and vertical NX holes drilled with a triple tube core barrel.

The NX core was to have been oriented by the drilling contractor. However, the method of orientation was not fully reliable, so all NX core was oriented by the authors with a fluxgate magnetometer. An orientation mark to true north was made on the core. Also, the horizontal core was oriented in an "up" position by comparing magnetometer readings with in situ rock. The magnetometer was also used to check whether the core was properly placed in the box and to correct the core often placed upside down in the box. Photographs of the NX core that do not have magnetometer orientation marks may contain runs or portions of runs that are upside down; however, prior to detailed logging of the joints, all NX core was correctly aligned.

All horizontally drilled NX holes and selected vertical NX holes were logged on the geomechanical data log. Table 4 is a listing of the holes that were logged in this format. The vertical holes chosen give a representative sampling of the joints in a plane perpendicular to the axis of the horizontal holes. Due to the apparent lack of horizontal continuity of the joints, projection of the joints to more than 2 feet (0.6 meter) away would be inaccurate. For this reason, only vertical holes that were within this distance of the horizontal holes were logged on the geomechanical core logs.

All of the geomechanical core logs prepared for this report were done by the authors. Use of the terms "planar," "smooth," "rough," etc. should be consistent and relative throughout the report.

TABLE 4. Geomechanical Borehole Logs.

Full-Scale Heater Test #1	Full-Scale Heater Test #2
Horizontal Holes	
1E-10	2E-14
1E-11	2E-15
1E-12	2E-16
1E-13	2E-17
1E-15	2E-18
1E-16	2E-19
1E-17	2E-20
1E-18	2E-21
1E-19	2E-22
1E-20	2E-23
1E-21	2E-24
1E-22	2E-25
1M-8	2E-26
	2E-27
	2E-28
	2E-29
	2M-16
Vertical Holes	
1E-1	2E-1
1E-3	2E-9
1E-8	2M-3
1E-9	2M-4
1M-3	2M-7
1M-4	2M-12
1M-5	2M-13
1M-7	

The measured strike is always referenced to true north. The strike recorded, by convention, is 90 degrees counter-clockwise to the dip when the core is oriented to true north.

Due to the tortuosity of many high-angle joints, it was obvious that an individual joint could exist along the core for at least 3 feet (1 meter), but have a highly variable strike. The average strike for a section of the joint was recorded and another strike recorded for an obvious change in the strike direction.

Most of the joints were broken along the in-filling material. The "width" of the joint was measured or closely estimated as the summation of the amount of in-filling material on both halves of the joint. With the exception of joints induced by a drilling or hammer break across solid rock, all joints appeared to be totally filled with clay or other material. The measurement of the in-filling material appears to be a

valid, or at least consistent, way to measure the joint aperture. The greater the joint in-filling, the more accurate the recorded measurement. The greatest measured in-filling thickness was approximately 5 millimeters of slightly oxidized clay and was on a columnar joint. Only selected NX core was logged in this detail. The smaller diameter holes were drilled using a rigid core barrel and often times considerable force was used to remove the core. This resulted in careless handling and excessive breakage of the core. Lithologic and structural logs were prepared for the smaller holes and major joints were described in these logs.

Copies of the geomechanical data logs are on file in the Basalt Waste Isolation Project Library. These data and similar joint data were used to produce the computer plots and analyses and are summarized in Section 4.2 as follows:

1. Contoured stereonets
2. Histograms of number of joints versus distance
3. Histograms of joint frequency versus joint dip
4. Histograms of joint frequency versus in-filling material
5. Histograms of joint frequency versus aperture
6. Histograms of joint frequency versus waviness.

The histograms provide hole-to-hole comparisons of the joint geometry and comparisons of selected intervals within the holes.

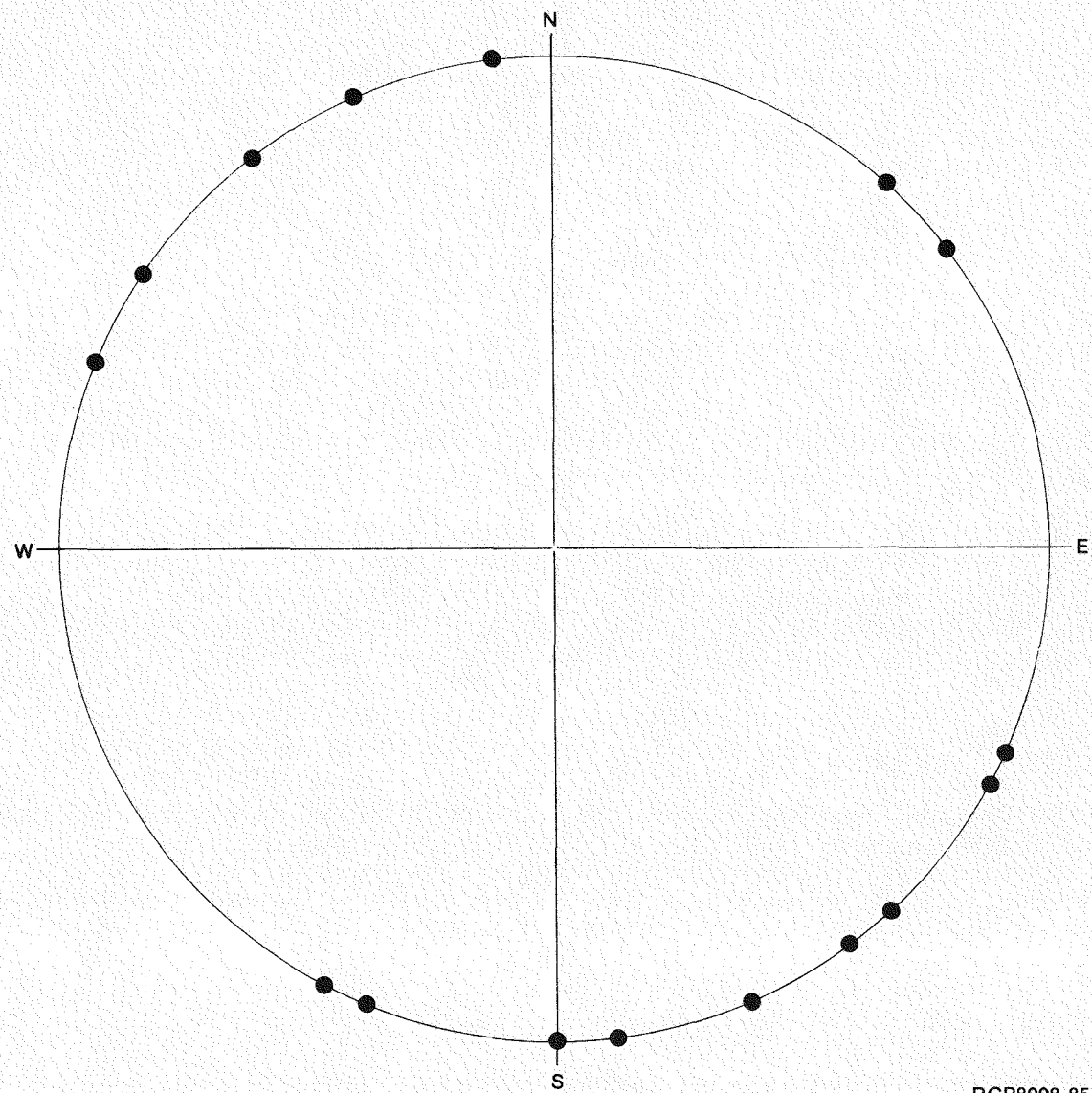
No apparent tectonic fractures or fracture systems were observed in the core. Tectonic fracturing is defined as fractures caused by the formation of the Gable Mountain anticlinal structures or post-deformational faulting. Also, no apparent fault breccia or fault gouge were seen on any of the joints in the instrument boreholes.

However, 17 joints with lineations, assumed to be slickensides, were recorded. This group represents 0.03% of the total joints measured. The lineation directions were determined using an equal-angle stereonet with the downdip direction recorded as direction of lineation. The stereonet (Figure 16) shows no preferred orientation of the lineations. Although these lineations are probably related to the same period or periods of movement, due to the sinusoidal nature of the joints in the entablature, the lineations appear to be randomly oriented.

4.1.6 Impression Packer Testing

Two methods of obtaining baseline data from the borehole walls were evaluated: closed-circuit borehole television and impression packers. These data would primarily be used for a comparison of the borehole wall before the heater testing begins and again after the testing is completed. The impression packers were chosen for a number of reasons:

1. Ease of repeatability within a given area of the borehole
2. Ease of comparison of one 5-foot (1.5-meter) impression sleeve with another



RCP8008-85

FIGURE 16. Equal Angle Stereonet Plot of Lineation Dip Directions
(X = Direction of Lineations).

3. A single frame of the television camera film would only cover a maximum of 2 square inches (13 square centimeters)
4. Less potential for mechanical breakdown
5. Lack of availability and high cost of a borehole television camera needed to completely map a small-diameter borehole
6. Less impact on overall time schedule.

Table 5 is a listing of the holes in which impression packer testing was performed.

Impression packers have been utilized in oil fields for a number of years. They are used to determine casing perforations, casing splits, and geologic features in an open hole such as bedding planes and fossils. Geotechnical applications have been limited because of the cost involved and a lack of need for such a tool.

A contract to perform the testing, which was the largest single project of this type ever attempted, was let to one of the two firms in the United States that provide this type of service. The contractor provided the manpower and all necessary equipment to produce impressions of 445 feet (135.6 meters) of 2.98-inch (76-millimeter) hole, and 38 feet (11.6 meters) of 18-inch (45.7-centimeter) hole.

The holes selected for testing were NX size monitor holes and the main heater holes. The monitor holes were the only NX size holes that would not contain grouted instruments; hence, testing could be concurrent with the operation of Full-Scale Heater Tests #1 and #2. Zones within the monitor holes were chosen for testing that would best represent the total rock mass and zones that would most likely show changes in the joints as the heat output was increased. This was considered to be a zone approximately 5 feet (1.5 meters) on either side of the heater mid-plane. Only 40 feet (12.2 meters) of horizontal impressions were made.

The impressions were made on 5-foot (1.5-meter) natural rubber sleeves providing 360-degree coverage of the borehole wall. The sleeves are wrapped over a cured rubber sleeve and then banded over a hollow steel mandrel. The complete assembly was lowered to the specified depth, oriented to north, and expanded with compressed nitrogen to 100 pounds per square inch (277 grams per cubic centimeter). This was set for 10 minutes to allow the impression packers to conform to the hole configuration. The packers were then deflated and removed from the hole (Figure 17). The sleeves were cured in a curing oven for 2 hours at 200°F (93°C). The impression packer sleeves retained impressions of joints with a minimum aperture of 0.20 millimeter and will retain them for an indefinite period of time (Figure 18).

TABLE 5. Impression Packer Mapping.

Hole Number	Hole Size inches (centimeters)	Impression Footage (meters) Interval
Horizontal Holes		
1M-8	3 (7.6)	25-45
2M-16	3 (7.6)	25-45
Vertical Holes		
1M-3	3 (7.6)	0-35 (0-10.7)
2M-6	3 (7.6)	0-35 (0-10.7)
2M-15	3 (7.6)	0-35 (0-10.7)
2M-1	3 (7.6)	7-22 (2.1-6.7)
2M-3	3 (7.6)	0-30 (0-9.1)
2M-4	3 (7.6)	2-27 (0.6-8.2)
2M-5	3 (7.6)	0-20 (0-6.1)
2M-7	3 (7.6)	0-30 (0-9.1)
2M-9	3 (7.6)	7-22 (2.1-6.7)
2M-11	3 (7.6)	7-22 (2.1-6.7)
2M-12	3 (7.6)	5-25 (1.5-7.6)
2M-13	3 (7.6)	5-25 (1.5-7.6)
2M-14	3 (7.6)	5-25 (1.5-7.6)
1M-2	3 (7.6)	5-30 (1.5-9.1)
1M-4	3 (7.6)	5-30 (1.5-9.1)
1M-5	3 (7.6)	0-30 (0-9.1)
1M-7	3 (7.6)	7-32 (2.1-9.8)
3H-1	4.92 (12.5)	0-35 (0-10.7)
3H-2	4.92 (12.5)	0-35 (0-10.7)
3H-3	4.92 (12.5)	0-35 (0-10.7)
3H-4	4.92 (12.5)	0-35 (0-10.7)
3H-5	4.92 (12.5)	0-35 (0-10.7)
3H-6	4.92 (12.5)	0-35 (0-10.7)
3H-7	4.92 (12.5)	0-35 (0-10.7)
3H-8	4.92 (12.5)	0-35 (0-10.7)
3H-9	4.92 (12.5)	0-35 (0-10.7)
1H-1	18 (45.7)	0-19 (0-5.8)
2H-1	18 (45.7)	0-19 (0-5.8)



FIGURE 17. Retrieving Impression Packer from Full-Scale Heater Test #2 Main Heater Hole.



FIGURE 18. Impression Sleeve from Full-Scale Heater Test #2 Main Heater Hole (approximately 23 inches [59 centimeters] long).

The impression sleeves are stored in sturdy cardboard tubes in a protected environment for post-test characterization comparisons. Preliminary analysis of the sleeves indicates excellent retention of the major joints on the borehole walls. Many joints, though, have a larger aperture than the joints observed in core; apparently this is a result of drill water washing away much of the in-filling material and also as a function of the bit cutting the joint at an oblique angle to its strike. Careful alignment of the core with the impression sleeves shows that some of the tightly healed joints were impervious and did not allow the expanding rubber sleeves to obtain an impression. Also, because of the tortuosity and close spacing of the joints, some do not appear in the borehole wall that are seen in the core. Some terminate or bend in the void left by the drill bit and do not appear on the impression sleeve or else may appear as a scalloped joint.

Impression packer testing appears to have great merit as a comparative testing tool for geotechnical purposes; however, in basalt, it does not indicate the total joint frequency or pattern within a borehole.

4.1.7 Geophysical Testing

Rockwell's Geosciences Group technical personnel reviewed several geophysical and permeability tests for use in characterizing the NSTF rock mass prior to electric heater startup. The geophysical tests evaluated included cross-hole seismic, neutron-thermal, neutron moisture content, and air permeability.

Cross-Hole Seismic Testing. Cross-hole seismic testing is presented here to define the amount of rock deterioration as a function of thermal loading. The major effect of this loading should be the development of rock fractures. It is our opinion that this seismic testing will be unable to effectively detect the rock mass change due to the following.

DC-10 core-testing data show a variation in the modulus of elasticity from 12.9×10^6 pounds per square inch (88.8×10^3 megapascals) to 10.1×10^6 pounds per square inch (69.8×10^3 megapascals) with an average of 11.2×10^6 pounds per square inch (77.1×10^3 megapascals) (Duvall and Others, 1978). By using the corresponding data for Poisson's ratio and density of 0.0071 and 0.1033 pound per cubic inch (0.20 and 2.86 grams per cubic centimeter), 0.0083 and 0.1026 pound per cubic inch (0.229 and 2.84 grams per cubic centimeter), and 0.0066 and 0.1015 pound per cubic inch (0.183 and 2.81 grams per cubic centimeter), respectively, and

$$V_p = \frac{Eg(1 - V)}{p(1 + V)(1 - 2V)} \quad (1)$$

where

E = modulus of elasticity

g = acceleration due to gravity

ρ = density

V = Poisson's ratio,

the primary-wave velocity (V_p) can be determined; that is,

	Modulus of Elasticity		ft/sec	m/sec
	psi	MPa		
High	12.9×10^6	88.8×10^3	19,298	5,882
Low	10.1×10^6	69.8×10^3	17,510	5,337
Average	11.2×10^6	77.1×10^3	18,051	5,502

Using the average values of approximately 18,000 feet per second (5,486 meters per second) and a test hole separation of 6.56 feet (2 meters), a change of +1 inch (2.6 centimeters) in transmission path length causes an increase in measured velocity from 18,000 to 18,300 feet per second (5,486 to 5,578 meters per second). This change represents approximately 25% of the range between the high and average conditions listed above. This 1-inch (2.6-centimeter) change could easily occur by incorrect angular orientation of the two probes in the pair of borings. Further, as a comparison, a change in density from 0.102 pound per cubic inch (2.81 grams per cubic centimeter) to 0.098 pound per cubic inch (2.71 grams per cubic centimeter) will create the same magnitude of change in the measured primary-wave velocity.

Borehole acoustic probes using magnetostrictive or piezoelectric crystals produce specific beam patterns both in transmit and receive mode. Generally, their beam patterns have the half-power points (-3.03 decibels) at between 20 and 30 degrees from beam center. Amplitude measurements then require the exact angular orientation be repeated from test to test. Further, the verticality of the probes must be maintained for the same reasons. Mechanical devices cannot ensure the needed accuracy in clamping the tools in the exact location and orientation as previous tests.

If the orientation changes, then the amplitude of the received energy will vary as a function of orientation.

At 18,000 feet per second (5,486 meters per second), the wave takes 55.6 microseconds to travel 1 foot (0.3 meter) or $55.6 \mu\text{s}/\text{feet}$. This means the wave takes $4.58 \approx 5 \mu\text{s}/\text{inch}$. Therefore, a timing error of 5 μs would result in an error of 1 inch (2.6 centimeters) in determination of

the hole separation or from above will cause the velocity to vary from 18,000 to 18,300 feet per second (5,486 to 5,578 meters per second).

Further, if for example 25 kiloHertz of acoustic energy are used, then the wave period is 40 μ s. The problem here is in the needed time measurement accuracy of 5 μ s by a wave of 40 μ s in length. This is a severe problem if $\frac{1}{2}\lambda$ resolution is argued.

At 200 kiloHertz, the period is 5 μ s. This means that if $\frac{1}{2}\lambda$ resolution is possible, then an accuracy of 2.5 μ s in timing is needed. This is half the effect of the variation from above. However, it should be noted that, in practical application, one wavelength is the best resolution obtainable.

In summary, if an accurate wave-form definition is needed, then experience has shown that between 5 and 8 samples are needed per cycle. This means that timing accuracy of 1 μ s is needed in the instrumentation. From above, 5 μ s are equivalent to 1-inch (2.6-centimeter) travel time. Therefore, 1 μ s is equivalent to 0.2 inch (0.5 centimeter). This 0.2-inch (0.5-centimeter) position accuracy for field tools used at 6-month intervals is extremely difficult at best.

Neutron-Thermal Neutron Testing. Neutron-thermal neutron testing was discussed for the NSTF in support of the thermal loading test. The anticipated moisture content was between 1 and 4% and these data were apparently needed to help in the heat flow equations.

Available data indicate that an accuracy of approximately 1% can be obtained by this technique. This represents 33% of the measurement range. Measurement accuracy of this would probably be of insignificant value considering the cost of obtaining it.

Neutron-thermal neutron testing depends upon diffusion of neutrons through the medium, thermalization by collision, and detection of the thermalized neutrons. This diffusion is very small in the megascopic distance the neutrons travel; therefore, effects of repeatable orientation and location become increasingly important for time-sequencing testing.

Neutron tools are sensitive to temperature variations which will degrade measurement statistics throughout the heater tests.

Based on the above, neutron-thermal neutron tests would not provide quality data to be of use in the NSTF program.

Air Permeability. The air permeability tests were suggested as a means to determine permeability changes in basalt due to heat-induced fractures. However, it was our opinion that this type of testing was inconclusive and would be of no value. The permeability of the basalts is in the range of 25^{-7} to 25^{-9} inches per second (10^{-7} to 10^{-9} centimeters per second). Measurements recorded at or beyond this level are academic.

However, borehole sonic surveys were later conducted at the NSTF to demonstrate and test a borehole-sonic system in three pairs of holes (Figure 19). These tests were designed to measure the acoustic-wave travel time and amplitude between pairs of boreholes so that relative data on the acoustic-wave velocity and amplitudes as a function of borehole pairs could be determined. These data could then provide preliminary information on the spatial variations of acoustic-wave velocity created by acoustic-impedance boundaries located between the borehole pairs.

Typical data from survey 2E-4 to 2E-3 with the transmitter and receiver each 20 feet (6.1 meters) deep in their respective holes are shown on Figure 20. Interpretation of the signal arrival times from the data indicates a primary-wave velocity of 17,943 feet per second (5,469 meters per second) and a shear-wave velocity of 9,673 feet per second (2,948 meters per second).

The observed arrival-time delay (survey 2E-4 to 2E-3) in the interval coinciding with the presence of the 18-inch (450-millimeter) borehole (Figure 19) in the sonic-ray path demonstrates that local changes in the rock medium, whether man-made or naturally occurring, will cause arrival-time changes if the local anomaly is accompanied by a density change. The bottom of hole 2H-1 is at 18 feet (5.5 meters).

Further refinement of this system and the development of sufficient baseline data may prove this tool to be an effective means of detecting variations in other test localities or even a repository. However, it is beyond the resolution of this system to detect the minute variations that may occur within areas for the Full-Scale Heater Tests #1 and #2.

4.1.8 Petrography

Samples for polished thin sections were taken at 5-foot (1.5-meter) intervals from horizontal and vertical boreholes in borehole arrays for Full-Scale Heater Tests #1 and #2 (Table 6). The thin sections were oriented north-south and east-west at 5-foot (1.5-meter) alternate intervals and their relationship to the top of the flow was marked. The sections were examined for vertical or lateral variations in the Pomona flow in the test areas. Two 500-point counts were done on three thin sections which represented the range in composition as determined under low-power microscopic examination. The point counts were done using both transmitted and reflected light. The results are listed in Table 7. The Pomona flow is characterized by three sizes of plagioclase crystals; the largest are sparse phenocrysts (Figure 21) up to 0.12 inch (0.3 millimeter) long. The mid-sized group is composed of scattered microphenocrysts (Figure 22) up to 0.12 inch (0.3 millimeter) long. The third are abundant microlites (Figures 21 and 22) which make up at least 90% of the plagioclase content. The pyroxenes are mostly microlites with very scattered microphenocrysts up to 0.12 inch (0.3 millimeter) long (Figure 23). The plagioclase/pyroxene ratio ranged from 1.1 to 1.4.

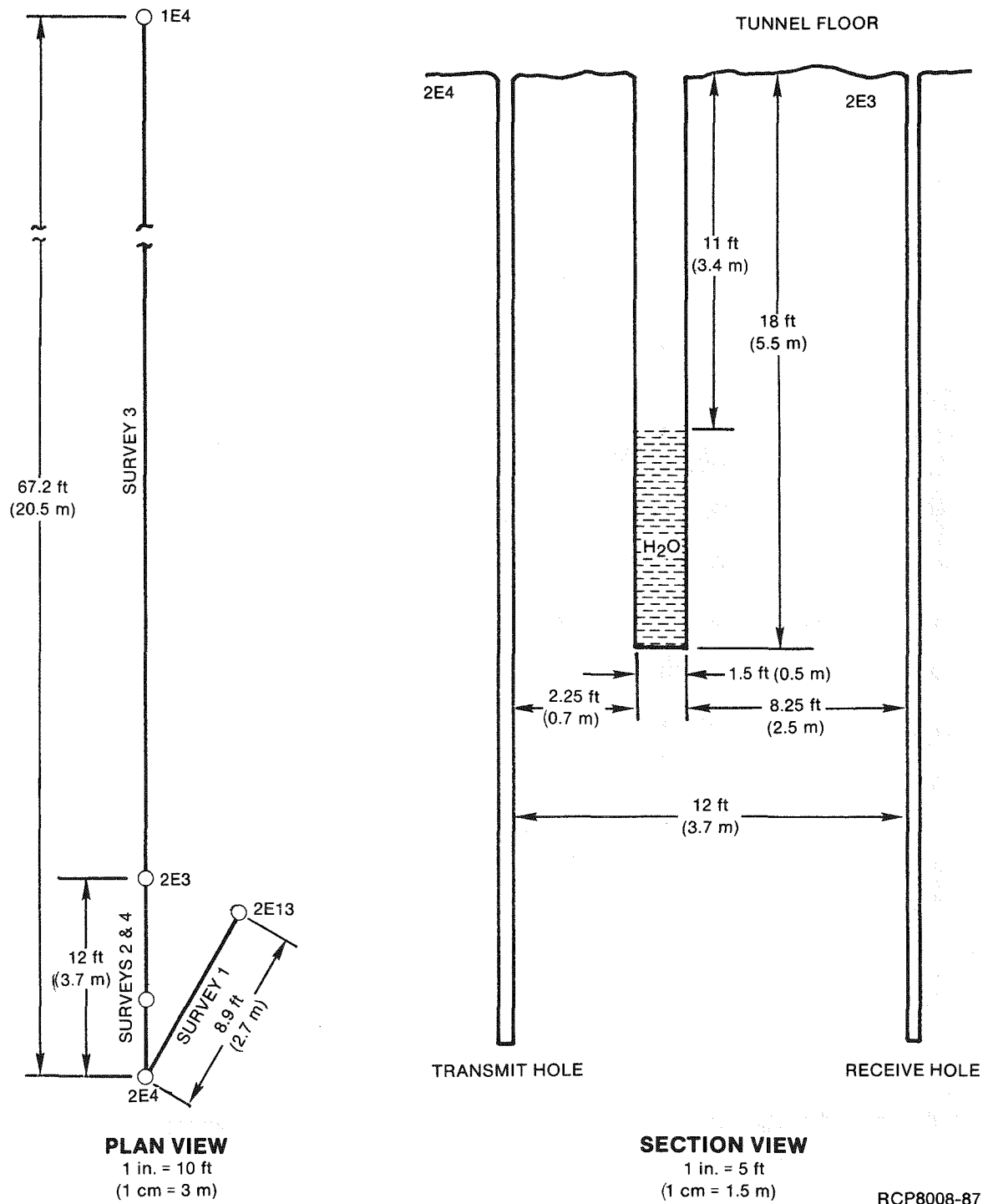
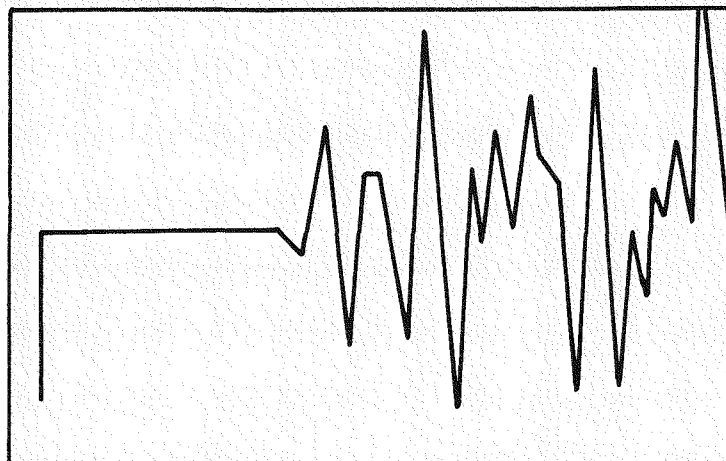
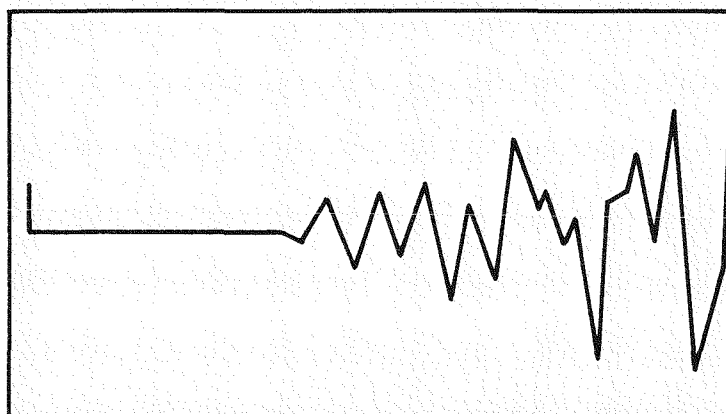


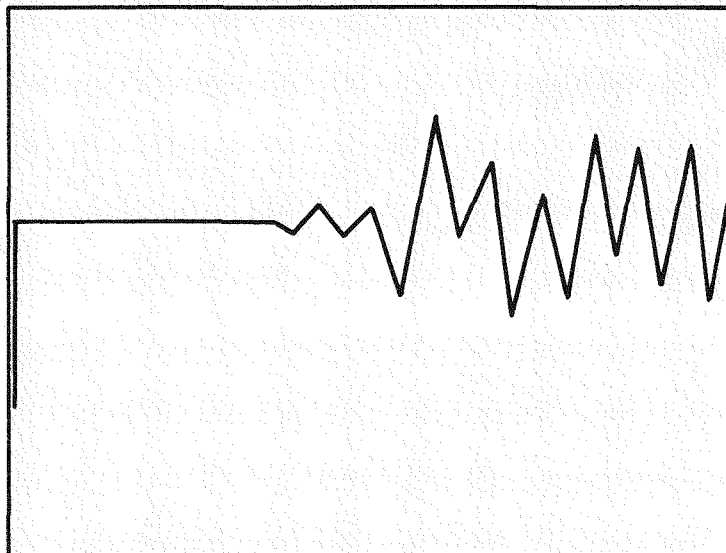
FIGURE 19. Test Hole Location Plan for Acoustic Survey.



DEPTH = 20 ft (6.1 m)



DEPTH = 18 ft (5.5 m)



DEPTH = 16 ft (4.9 m)

RCP8008-86

FIGURE 20. Acoustic Survey Data 2E-4 to 2E-3.

TABLE 6. Location of Thin Sections.

Hole No.	Depth feet (meters)	Orientation
1E-11 ^a	5.0 (1.5)	E-W
1E-11	10.2 (3.1)	N-S
1E-11	15.7 (4.8)	E-W
1E-11	20.0 (6.1)	N-S
1E-11	25.0 (7.6)	E-W
1E-11	31.1 (9.5)	N-S
1E-11	34.4 (10.5)	E-W
2E-16 ^b	5.0 (1.5)	N-S
2E-16	10.0 (3.0)	E-W
2E-16	15.0 (4.6)	N-S
2E-16	20.5 (6.2)	E-W
2E-16	24.8 (7.5)	N-S
2E-16	30.0 (9.1)	E-W
2E-16	35.0 (10.7)	N-S
1M-5 ^c	5.0 (1.5)	N-S
1M-5	10.0 (3.0)	E-W
1M-5	15.0 (4.6)	N-S
1M-5	20.0 (6.1)	E-W
1M-5	25.2 (7.7)	N-S
1M-5	30.2 (9.2)	E-W
2M-3 ^d	5.0 (1.5)	E-W
2M-3	10.3 (3.1)	N-S
2M-3	15.0 (4.6)	E-W
2M-3	20.2 (6.1)	N-S
2M-3	24.8 (7.5)	E-W
2M-3	30.0 (9.1)	N-S

^aHole 1E-11 Location: Extensometer Room;
Orientation: +0 Due South.

^bHole 2E-16 Location: Extensometer Room;
Orientation: +0 Due South.

^cHole 1M-5 Location: Heater Test Room;
Orientation: -90 .

^dHole 2M-3 Location: Heater Test Room;
Orientation: -90 .

TABLE 7. Point Counts in Transmitted and Reflected Light.

Sample	Volume (%)	First 500 Points	Second 500 Points
1E-11 5.0 ft (1.5 m)			
Plagioclase			
Phenocrysts		3	2
Microphenocrysts	39.9	3	2
Microlites		195	193
Pyroxene			
Microphenocrysts	29.1	2	0
Microlites		141	148
Chlorophaeite	11.1	56	55
Tachylyte	17.7	89	88
Opaques	2.2	11	11
1E-11 34.4 ft (10.5 m)			
Plagioclase			
Phenocrysts		0	4
Microphenocrysts	39.0	4	5
Microlites		194	183
Pyroxene			
Microphenocrysts	34.0	6	3
Microlites		166	165
Chlorophaeite	11.3	58	55
Tachylyte	12.2	55	67
Opaques	3.5	17	18
2M-3 30.0 ft (9.1 m)			
Plagioclase			
Phenocrysts		7	4
Microphenocrysts	40.7	9	7
Microlites		189	191
Pyroxene			
Microphenocrysts	37.2	4	2
Microlites		182	184
Chlorophaeite	7.3	32	41
Tachylyte	12.7	67	60
Opaques	2.1	10	11

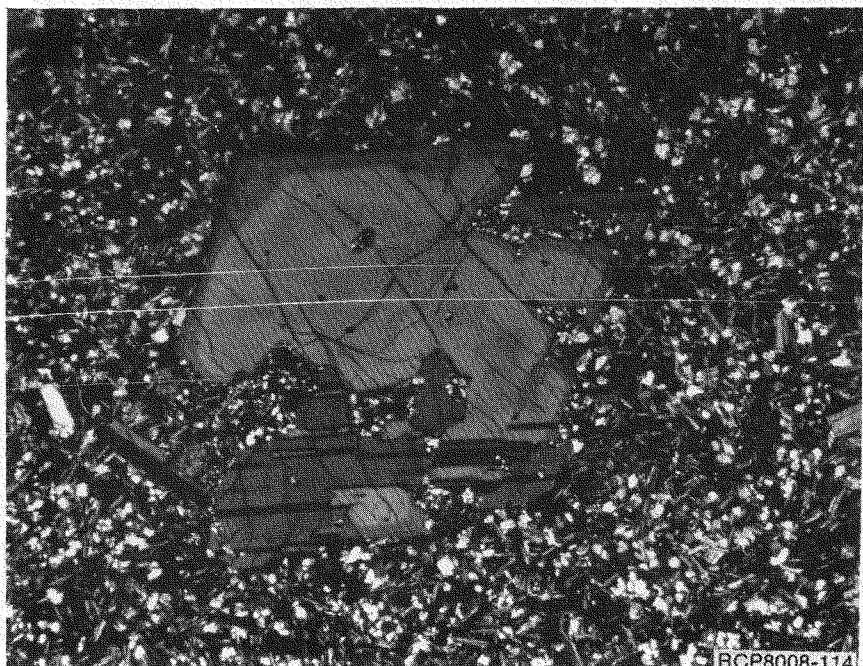


FIGURE 21. Plagioclase Phenocryst (30x), Hole 2M-16.

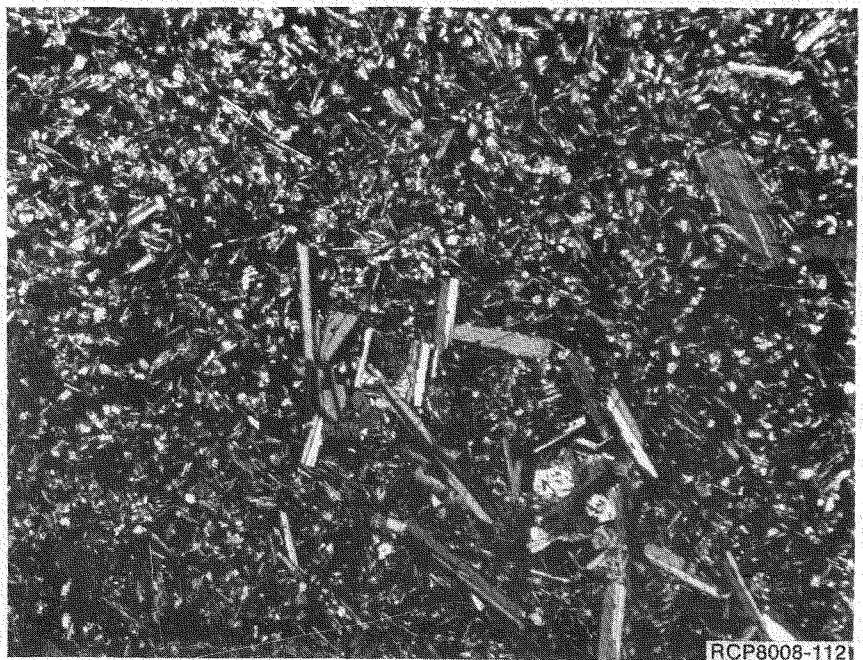


FIGURE 22. Scattered Microphenocrysts (30x), Hole 1M-5.

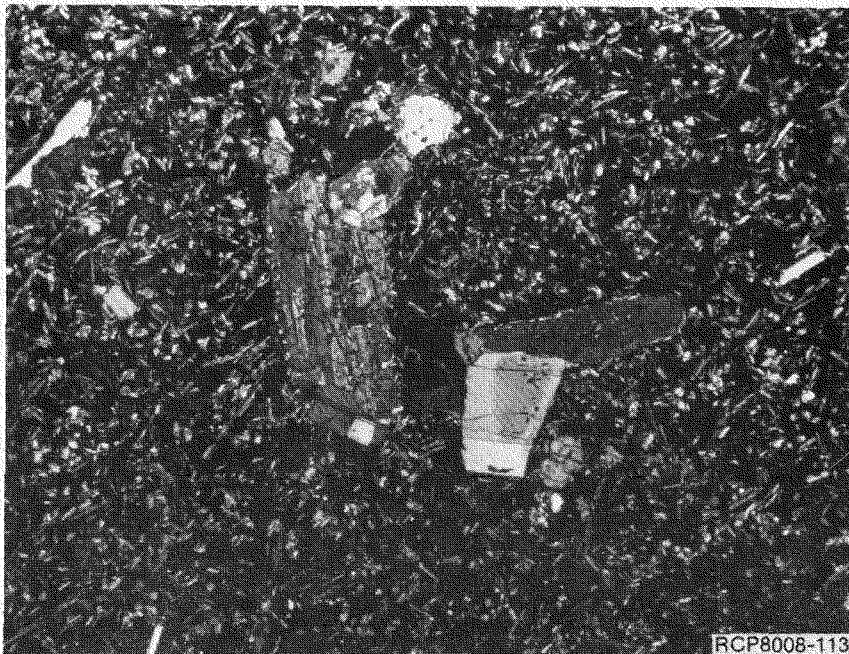


FIGURE 23. Pyroxenes (30x), Hole 1M-5.

4.1.9 Borescope Investigations

A 25-foot x 1.5-inch (7.6-meter x 3.8-centimeter) magnification borescope was used in the boreholes. Due to the low optical quality of the borescope, no detailed logging of boreholes was attempted. The main application of the borescope was for examining sections of the boreholes that showed unusual jointing, rubble, or loss of core. Borescope ports have been provided within the main heaters for Full-Scale Heater Tests #1 and #2. An 18-foot x 0.75-inch (5.5-meter x 1.9-centimeter) borescope will be used to observe deterioration of the borehole walls during Full-Scale Heater Tests #1 and #2.

4.1.10 In Situ Stress

In situ stress tests were conducted at the NSTF twice and utilized two different methods. Six hydrofracturing tests were conducted in core hole DC-11 prior to the excavation of the NSTF. Two core holes were drilled in the Extensometer Room after the excavation was completed and the standard overcoring technique, developed by the U.S. Bureau of Mines, was used to measure the in situ stress.

Hydrofracturing. The hydrofracturing tests took place between the depths of 55 and 227 feet (16.8 and 69.2 meters). All of the pressurization tests were successful and five out of six fracture impressions were traceable. The selected 2.25-foot (0.69-meter) zone was straddled with two 3-foot (0.91-meter) inflatable packers and pressurized until fracturing was induced. The inclination and direction of the induced fracture were obtained using an impression packer and a gyroscopic orienting instrument. All of the hydrofracture impressions (five of six were visible) were approximately vertical and oriented northwest to west-northwest.

The vertical stress magnitude could not be obtained directly from the test results; therefore, it was calculated using the relationship:

$$\sigma_v = \text{depth (ft)} \times \text{rock density (lbs/ft}^3 \times 1/144 (\text{ft}^2/\text{in}^2) \quad (2)$$

The density value of 176.5 pounds per cubic foot (2,875.0 kilograms per cubic meter) was obtained from laboratory measurements. The calculated vertical stresses are given in Table 8.

The least horizontal compressive stress (σ_{Hmin}) and the maximum horizontal stress (σ_{Hmax}) were computed using standard equations and the values obtained from field testing. Hydrofracturing pressures recorded in DC-11 are shown in Table 9.

The results show that all the principal stress magnitudes increase with depth: the vertical stress from 65 pounds per square inch (44.8×10^4 Pascals) at the 55-foot (16.8-meter) depth to 280 pounds per square inch (19.3×10^4 Pascals) at the 227-foot (69.2-meter) depth; the least horizontal stress from 115 pounds per square inch (79.3×10^4 Pascals) to 275 pounds per square inch (19×10^5 Pascals); and the largest horizontal stress from 2,120 pounds per square inch (14.6×10^6 Pascals) to 3,525 pounds per square inch (24.3×10^6 Pascals). The average direction of the latter stress was north 60 degrees west.

The measured stresses appear to be strongly affected by the topographic relief. The direction of the largest horizontal stress is subparallel to the axis of Gable Mountain, in general, and to the strike of the slope in the vicinity of core hole DC-11, in particular. The magnitude of the largest horizontal stress is also considerably higher than both the least horizontal stress and the vertical stress, the directions of which are perpendicular to the neighboring free surfaces.

Test #6 (Table 9) at a depth of 144 feet (43.9 meters) approximates the location of the elevations in the Pomona for Full-Scale Heater Tests #1 and #2. The relatively high 2,195 pounds per square inch (15.1×10^6 Pascals) maximum horizontal stress was not observed nor measured during the excavation of the NSTF. Vertical and horizontal tape extensometers were installed and routinely monitored as excavation progressed and following completion of the tunnels. Observation of the shotcrete and rock mass has not detected any appreciable horizontal stresses.

TABLE 8. In Situ Stress--DC-11.

Test #	Depth/ft (m)	Flow	σ_v psi	Pa (10^5)	σ_{Hmin} psi	Pa (10^5)	σ_{Hmax} psi	Pa (10^5)	σ_{Hmax} Direction*
1	55.0 (16.8)	Elephant Mountain	65	4.5	115	7.9	2,120	146.2	N70°W
6	144.0 (43.9)	Pomona	175	12.1	235	16.2	2,195	151.3	N80°W
2	172.5 (52.6)	Pomona	210	14.5	140	9.7	1,970	135.8	N70°W
3	196.0 (59.7)	Pomona	240	16.6	175	12.1	2,715	187.2	N40°W
5	200.0 (61.0)	Pomona	245	16.9	210	14.5	3,270	225.5	-
4	227.0 (69.2)	Pomona	280	19.3	275	19.0	3,525	243.0	N50°W

*Rounded to the nearest 5 degrees.

TABLE 9. Hydrofracturing Pressures--DC-11.

Test #	Depth/ft (m)	P _o psi	Pa (10 ⁵)	P _H psi	Pa (10 ⁵)	P _c ^s psi	Pa (10 ⁵)	P _s ^s psi	Pa (10 ⁵)
1	55.0 (16.8)	0	0	25	1.7	950	65.5	90	6.2
6	144.0 (43.9)	0	0	60	4.1	750	51.7	175	12.1
2	172.5 (52.6)	0	0	75	5.2	1,175	81.0	65	4.5
3	196.0 (59.7)	0	0	85	5.9	975	67.2	90	6.2
5	200.0 (61.0)	0	0	85	5.9	1,625	112.0	125	8.6
4	227.0 (69.2)	0	0	100	6.9	750	51.7	175	12.1

Vertical stresses calculated and those measured in the tunnel are probably due to the overburden; however, using the equations and figures previously listed would result in very high vertical stresses at depth. Additional stress measurements should be obtained to substantiate these data.

Overcoring. The standard overcoring technique developed by the U.S. Bureau of Mines was not designed for use in highly fractured rock; hence, the validity of the tests done in the jointed basalt at the NSTF is questionable.

The overcore test measures the borehole deformation across three diameters as the surrounding stress field is relieved. The highly jointed nature of the rock reduced the data to only four tests of low quality out of an attempted 16 tests. The tests took place in two holes drilled in the north wall of the Extensometer Room (Figure 24). OC-1 is a hole at a bearing of north 27 degrees west and OC-2 is a 25.5-foot (7.8-meter) hole oriented north 37 degrees west; both holes were inclined 5 degrees upward from horizontal. Due to schedule, cost, and the apparent lack of valid data from OC-1 and OC-2, a third hole was not drilled.

Factors which influenced the quality of the data are the fractured nature of the basalt, incomplete stress relief, and thermal variations in the drill water. The interpretations of the data from the four overcore tests rely heavily on the behavior of the overcore gauge and the readout system.

Several factors which influence the accuracy of the analysis are:

1. The assumption that the rock is elastic and homogeneous
2. The assumption that tests in two separate drill holes describe the same point in the rock mass
3. The orientation of the boreholes
4. The assumed modulus values
5. The testing did not extend beyond the zone of stress concentration around the tunnel
6. Only two holes were drilled.

The principal stress ellipsoid orientation conforms with the major topographic axes of Gable Mountain. The major, principal stress axis is oriented roughly along the axis of Gable Mountain, which is reasonable, since the other principal axes are only short distances to stress-relieved free surfaces of the mountain. Whether the major, principal stress is due to tectonic stress or residual stress from burial is unknown.

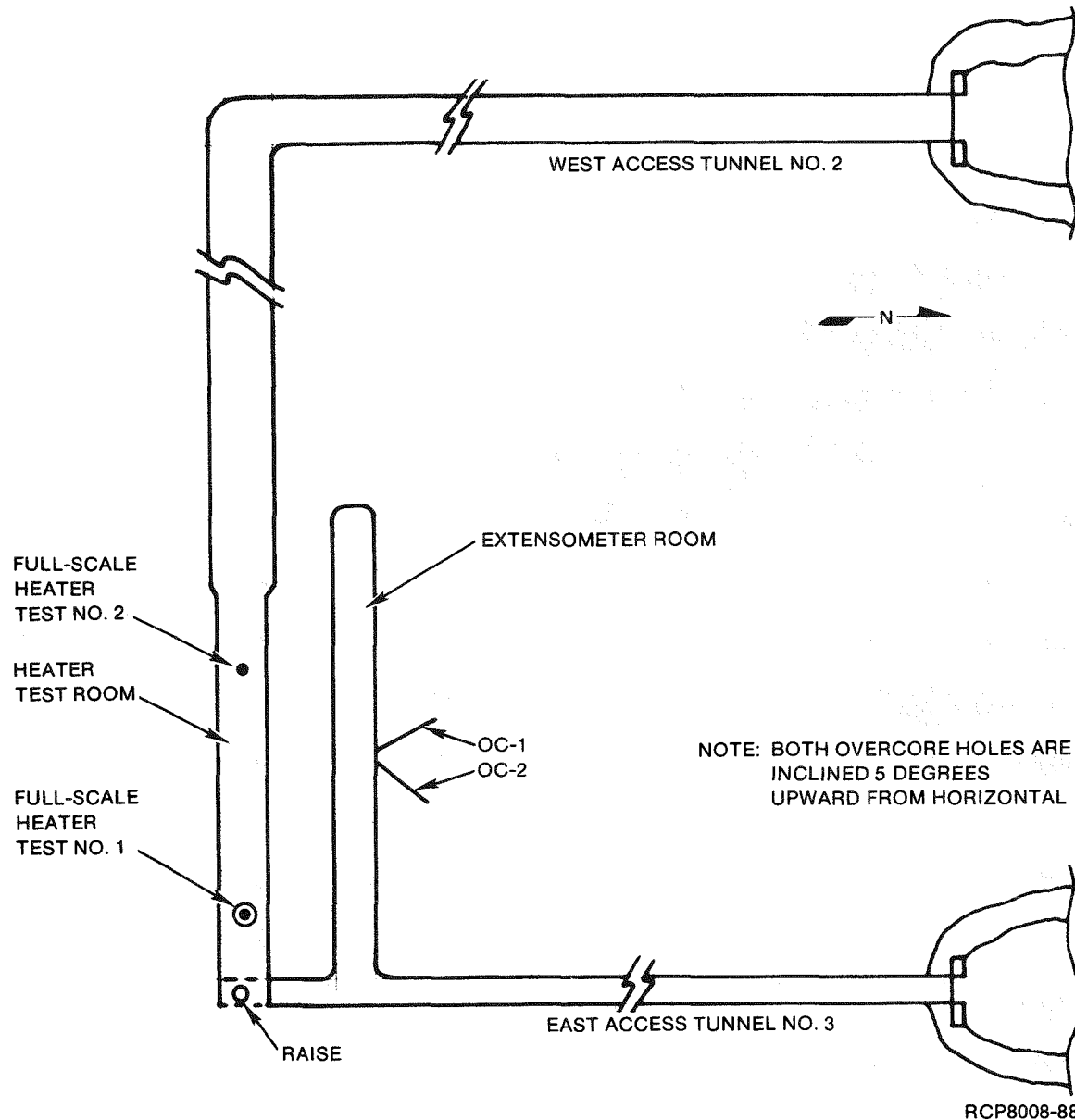


FIGURE 24. Location and Orientation of Overcore Holes.

The minor, principal stress oriented nearly vertically is probably an overburden stress increased by the stress concentration effect of the Extensometer Room excavation.

Discrepancies are apparent in the results of these two in situ stress tests. Both the magnitude and direction are variable to a large degree; therefore, it is believed that these results are not indicative of the true stress fields at the NSTF, nor do they offer any real data for projection of the stresses to depth. It is apparent that further testing and refinement of existing stress-measuring techniques are needed at the Hanford Site to accurately determine the in situ stress levels in basalt.

4.2 JOINT ANALYSIS

4.2.1 Determination of Joint Sets

Characterization of the joint sets in the arrays for Full-Scale Heater Tests #1 and #2 was a process of joint analysis of the geomechanical logs, detail line maps, and core logs. Using this information, joint sets were defined. From the boreholes, both horizontal and vertical, volumes of the rock mass surrounding Full-Scale Heater Tests #1 and #2 were delineated. Twelve blocks (Figures 25 to 29) were outlined for each heater test, and joint orientations, dip groups, and rock-mass classifications were determined. The block boundaries were defined on the basis of the extensometer locations. From this definition, an attempt to provide an equal amount of data from both the vertical and horizontal NX holes was made. The entablature of the Pomona is highly jointed due to the polygonal cooling pattern and numerous low-angle joints. Therefore, several problems were encountered which would not be expected in other rock mediums such as granite or salt. The polygonal columns are continuous, some exceeding 8 feet (2.4 meters) in length, but observations were limited by the dimensions of the tunnel and the shotcrete support system. Over their length, the columns are sinuous or undulating varying in overall dip by 15 to 25 degrees. The number and size of column faces often varied every 2 to 5 feet (0.61 to 1.5 meters) along the length of the column. This, in conjunction with the low-angle joints which were usually continuous only within a single column 6 to 12 inches (15 to 30 centimeters) in diameter, prohibited any type of correlation from the tunnel floor to depth or between boreholes.

The sinusoidal nature of the columns made the waviness measured in the geomechanical logs less meaningful, since the waviness is over several feet of the joint and the core provides only several inches of the joint for analysis. The joint apertures averaged approximately 0.2 millimeter and varied by ± 0.1 millimeter (Figures 30 to 33). With such small average apertures and minor variations, this parameter was not useful in defining joint sets.

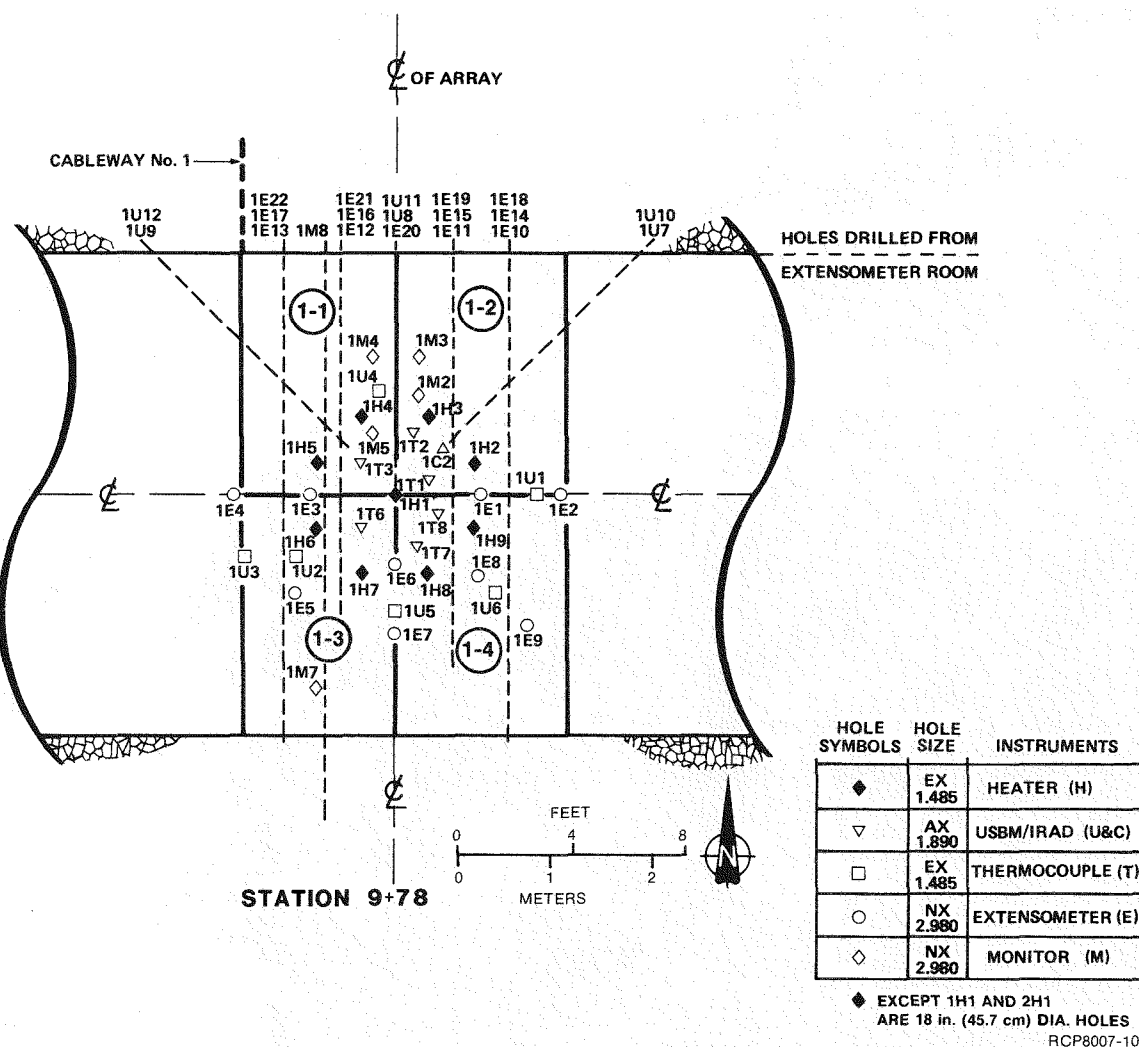


FIGURE 25. Holes and Block Locations for Full-Scale Heater Test #1.

4-30

RHO-BWI-ST-8

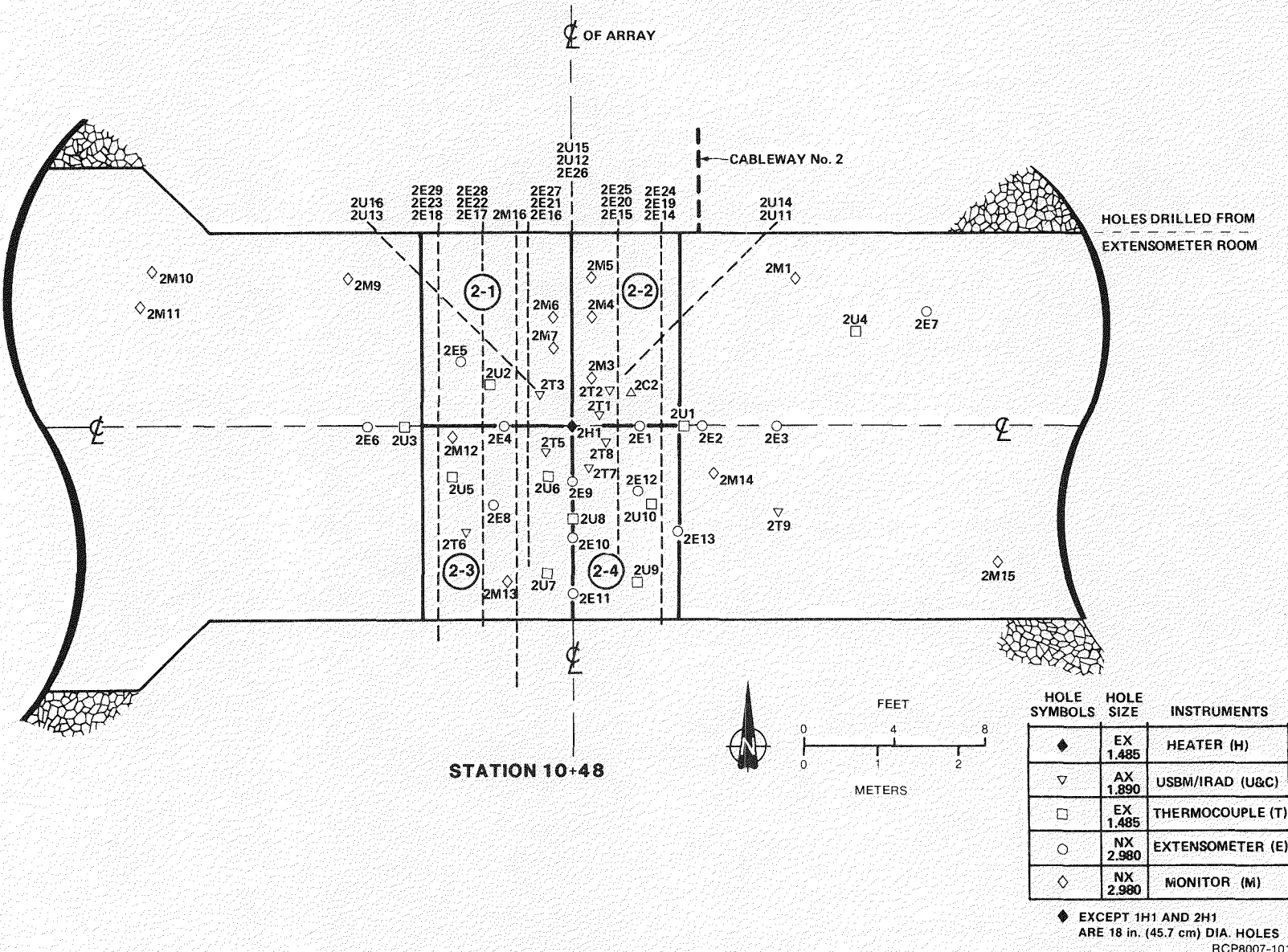


FIGURE 26. Holes and Block Locations for Full-Scale Heater Test #2.

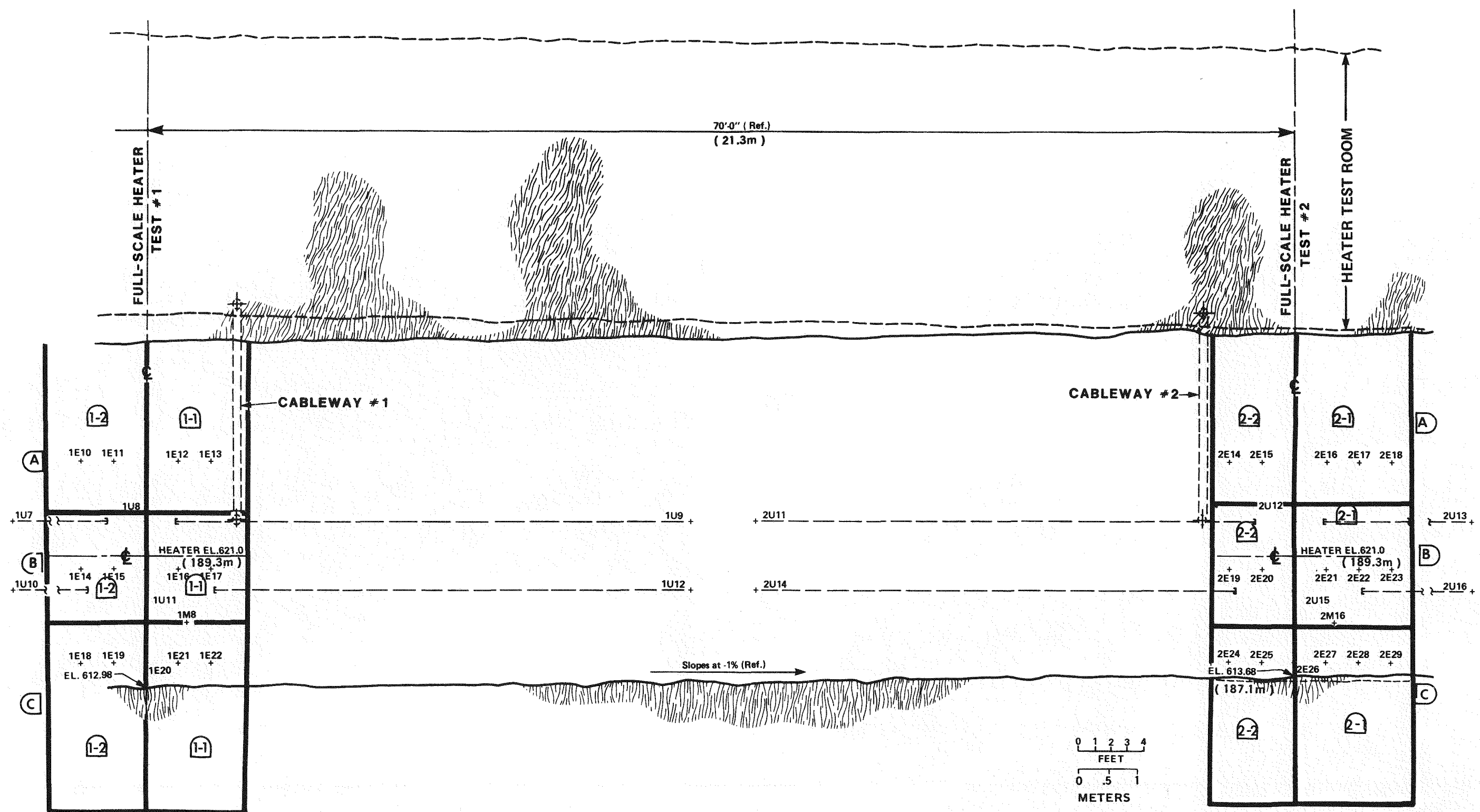


FIGURE 27. Holes and Block Locations for Extensometer Room (Looking South).

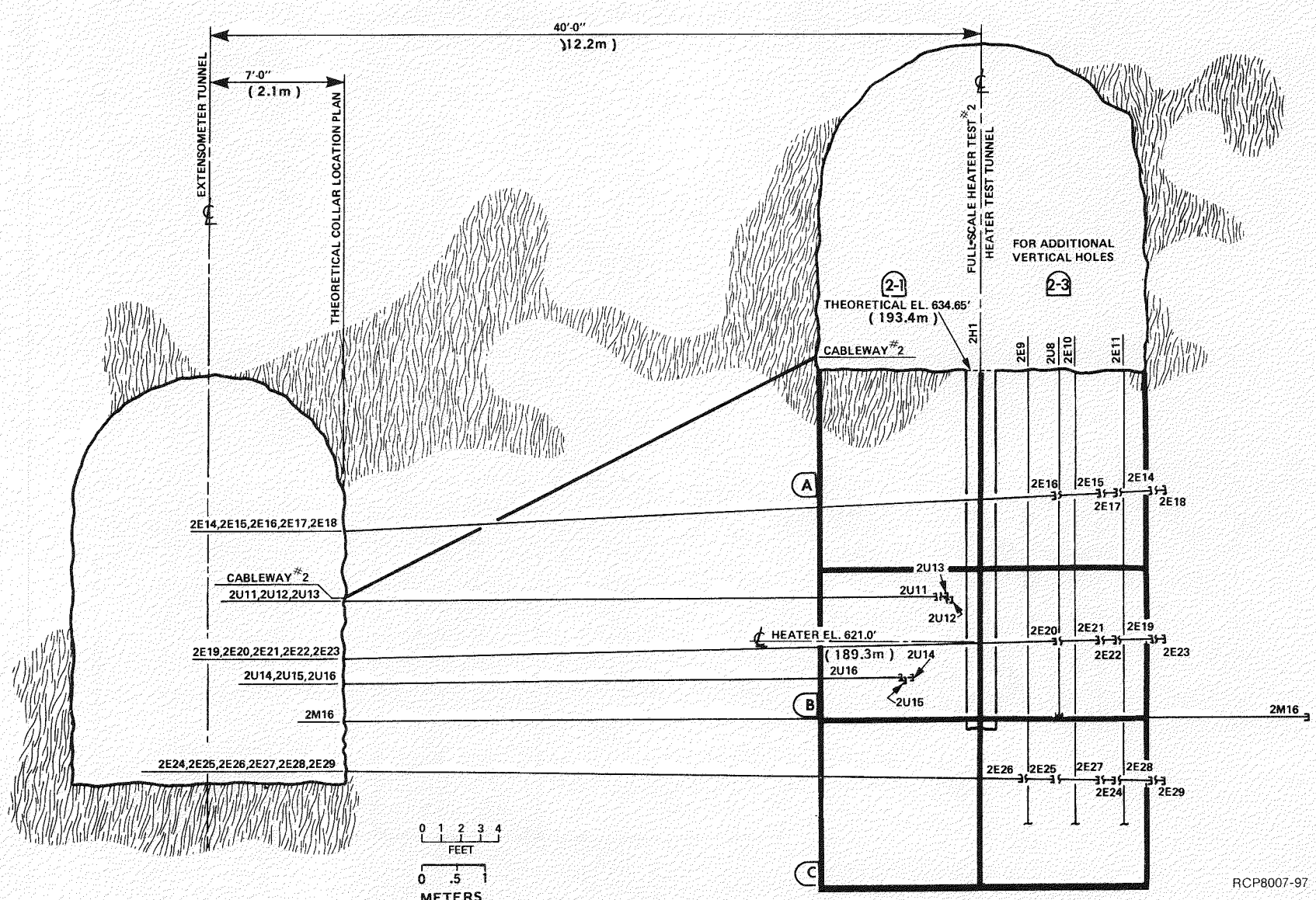


FIGURE 28. Holes and Block Locations for Full-Scale Heater Test #2 (Looking East).

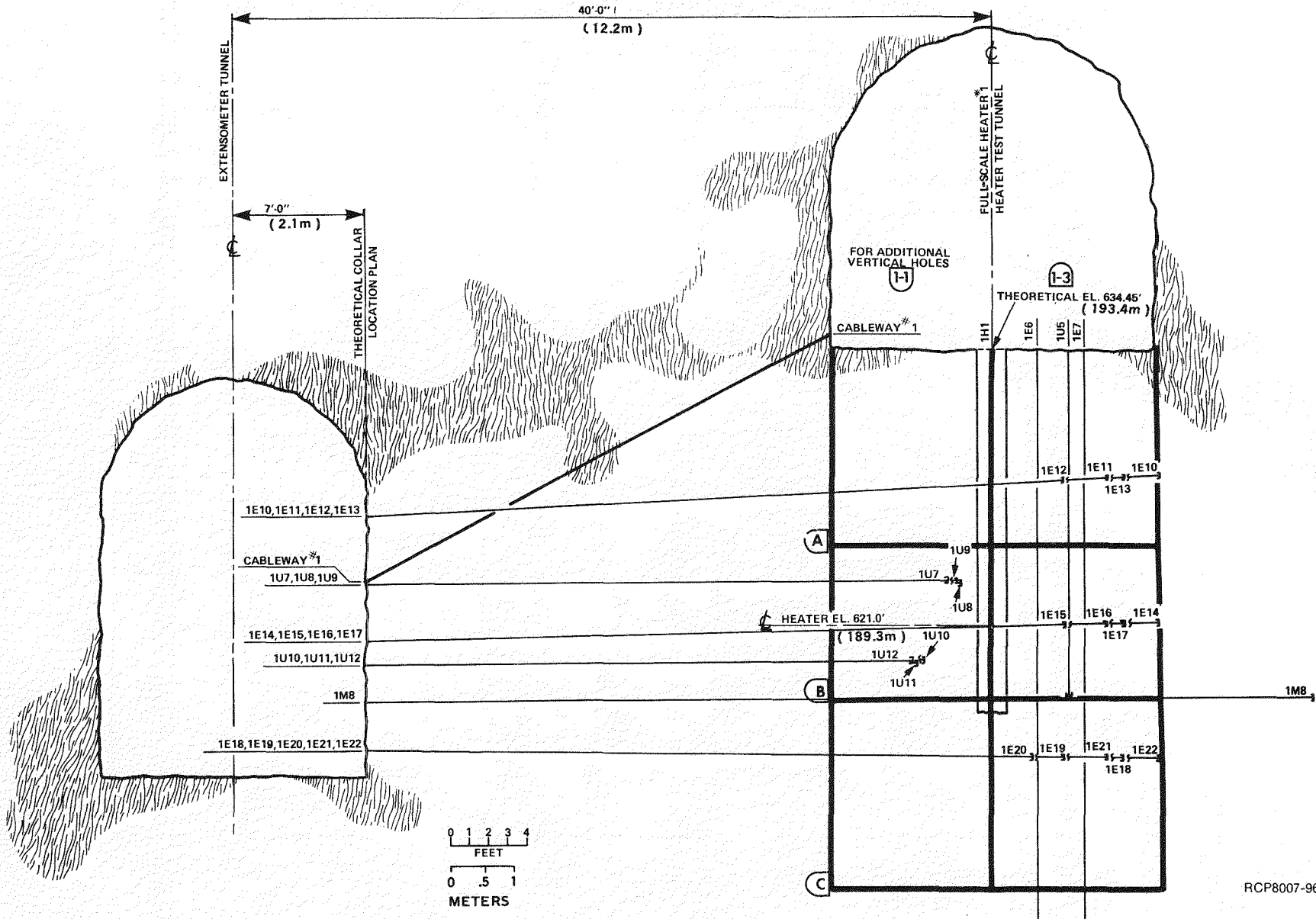


FIGURE 29. Holes and Block Locations for Full-Scale Heater Test #1 (Looking East).

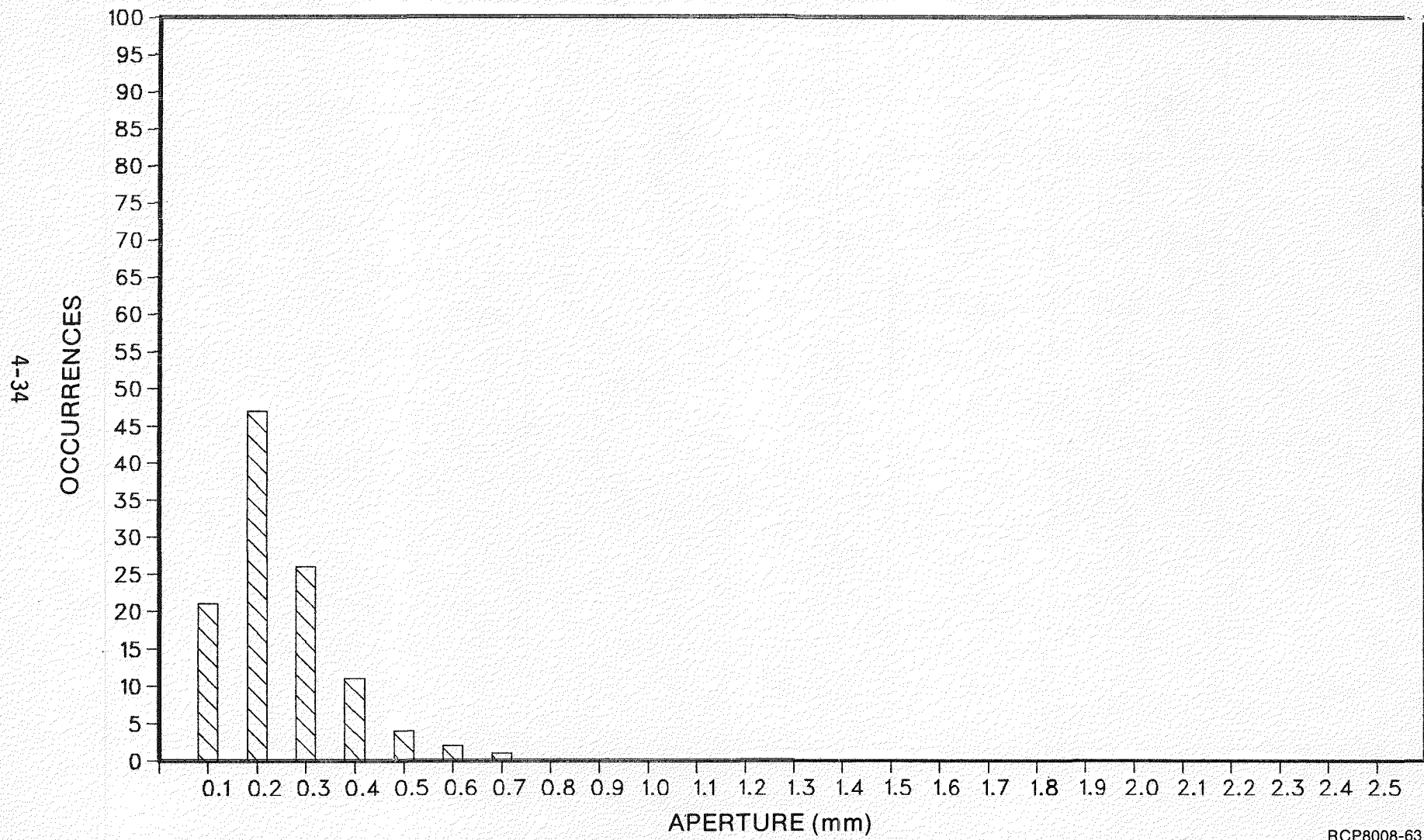


FIGURE 30. Core Hole 1E-8, Joint Aperture Frequency.

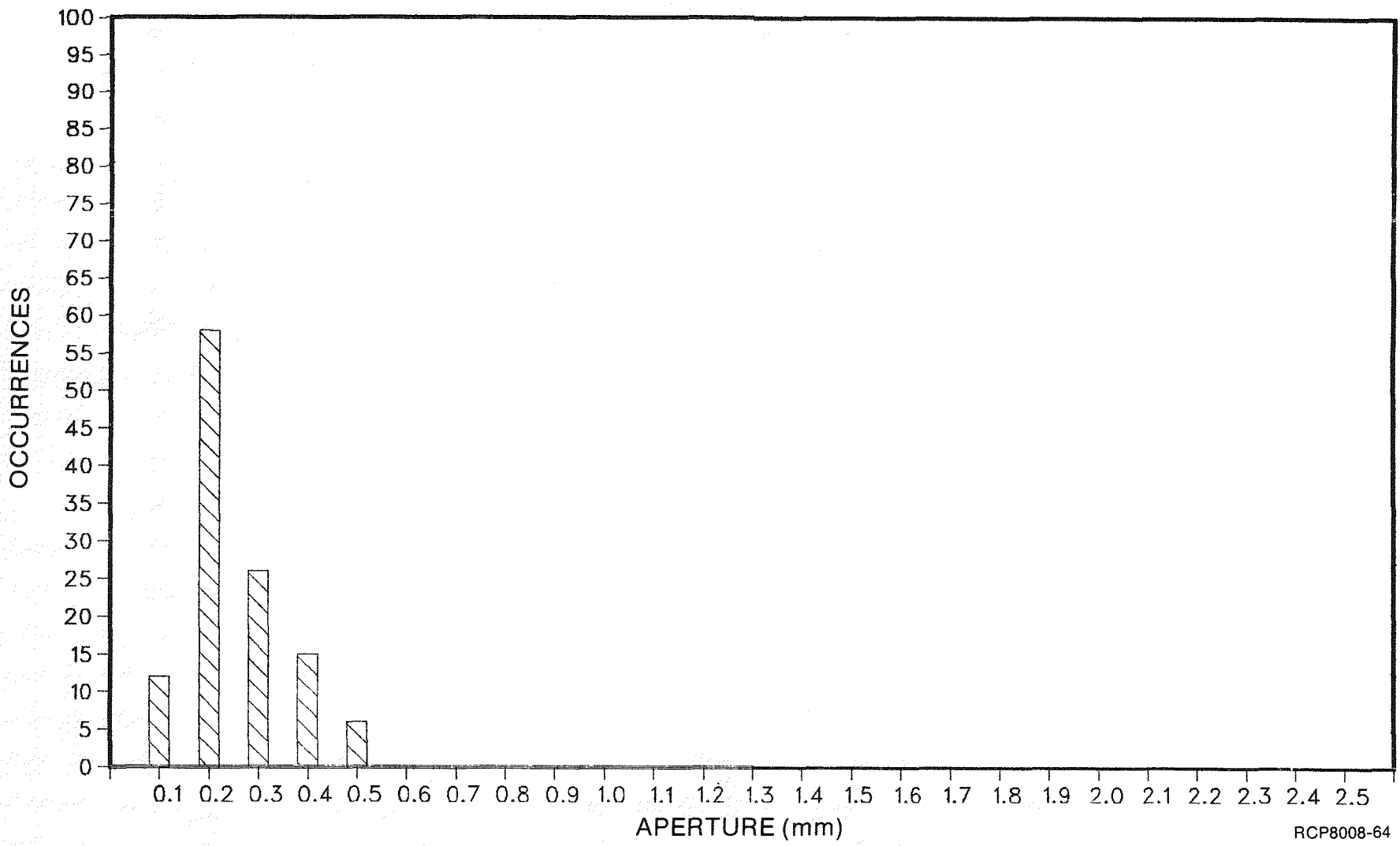
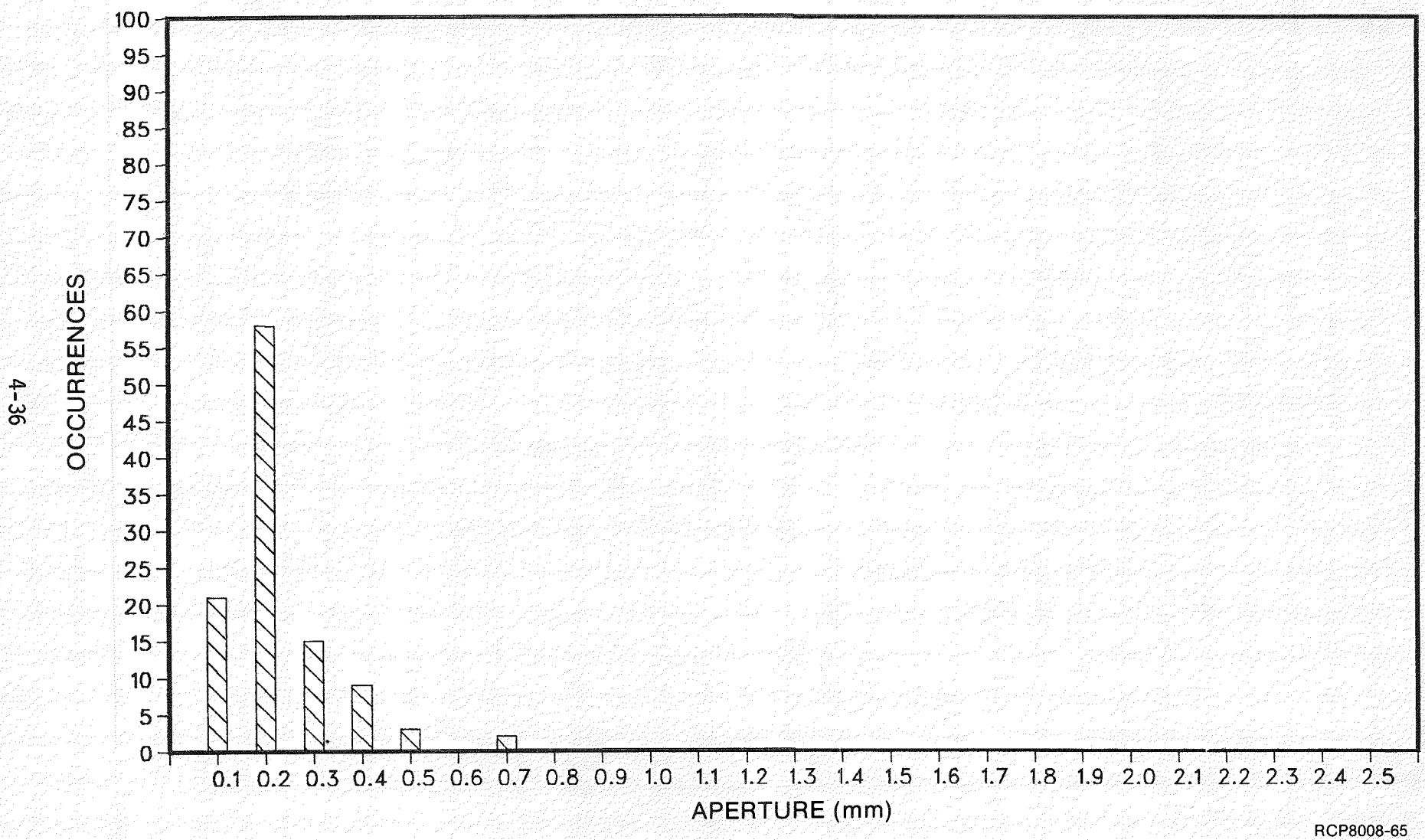


FIGURE 31. Core Hole 1E-19, Joint Aperture Frequency.



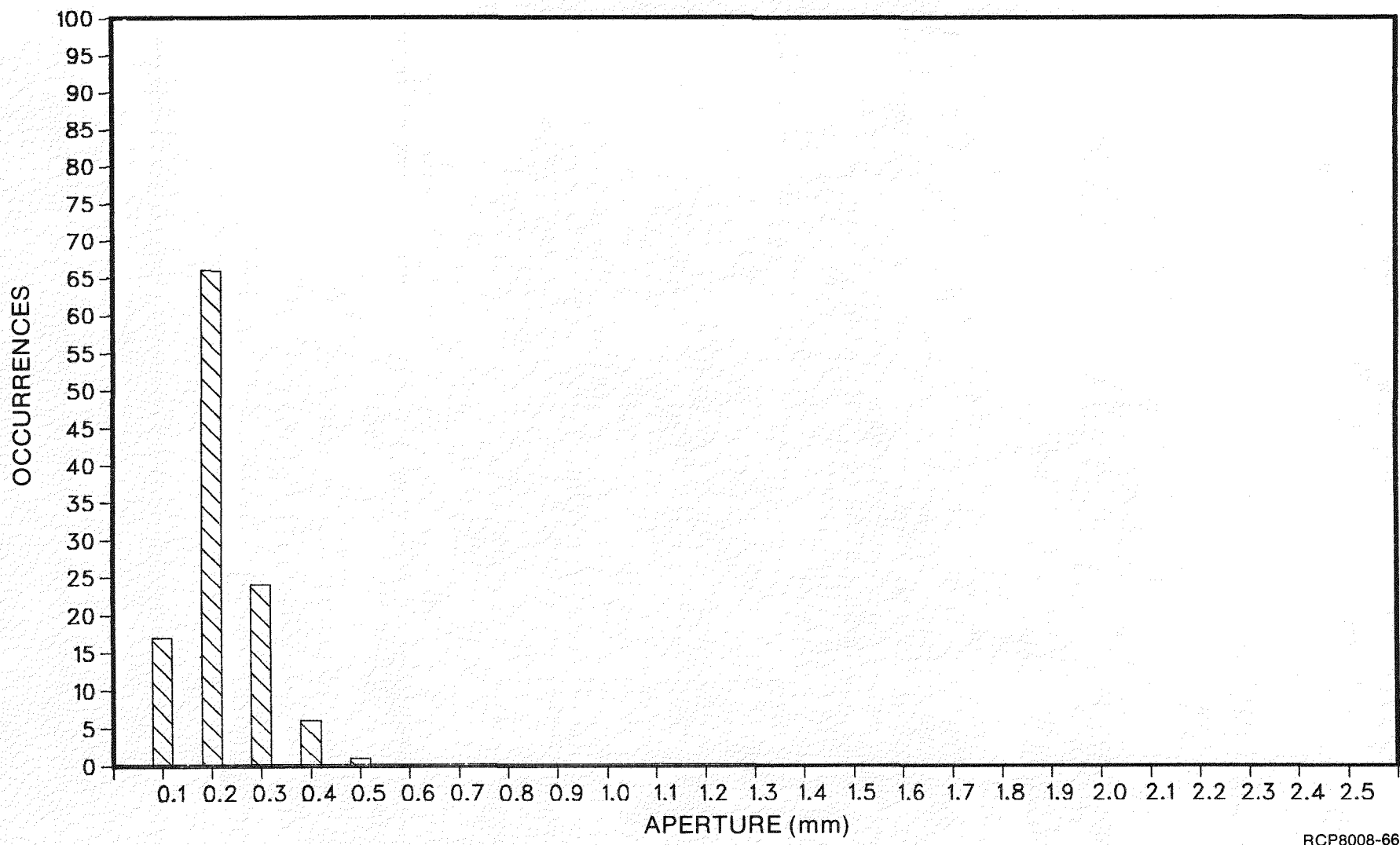


FIGURE 33. Core Hole 2E-24, Joint Aperture Frequency.

The undulating nature of the discontinuities in polygonal columns caused statistical variation in the strike and dip measurements making joint sets difficult to determine and poorly defined. Histograms of dip frequency were plotted for each of the boreholes (Figures 34 and 35). These plots demonstrate the biased sampling of joints by horizontal and vertical boreholes. As expected, the horizontal holes intersected a higher number of high-angle joints, while vertical holes intersected a majority of low-angle joints (Figures 34 and 35). However, by plotting equal numbers of joint dips from horizontal and vertical boreholes, a less biased dip frequency can be obtained (Figures 36 and 37). With these histograms, three groups or sets of joints can be determined: the 66- to 90-degree-dip group comprises 47% of the measured joints; the 0- to 37-degree-dip group comprises 30%; and the 38- to 65-degree-dip group is the remaining 23%.

Using these groupings, histograms of frequency versus strike were plotted (Figures 38 to 43). The 0- to 37-degree and 38- to 65-degree plots show no definable pattern, but the 66- to 90-degree plot has two broad groupings centered around 90 and 270 degrees. These two groups are apparent whenever the 66- to 90-degree-dip group from any of the horizontal holes is plotted (Figures 44 and 45). However, if the 66- to 90-degree-dip group from only the vertical holes is used (Figure 46), there is no definable pattern. This is attributed to the layout of the horizontal holes, which were drilled due south, creating a bias in the orientation of the joints intersected.

When the 66- to 90-degree-dip group from the detailed line maps in the Heater Test Room is plotted (Figure 47) the 90- and 270-degree groups are not apparent, but a group from 40 to 160 degrees is dominant. This group is also due to a directional bias, the east-west direction of the Heater Test Room. The convention for measuring the joint strike, 90 degrees counterclockwise from the joint dip, contributes to the strike location of this biased grouping. These two factors, coupled with the predominantly southerly dip of the high-angle joints (Figure 48) caused by the anticlinal structure, all contribute to the biased dominance of the 40- to 160-degree grouping; this bias is illustrated in Figure 49.

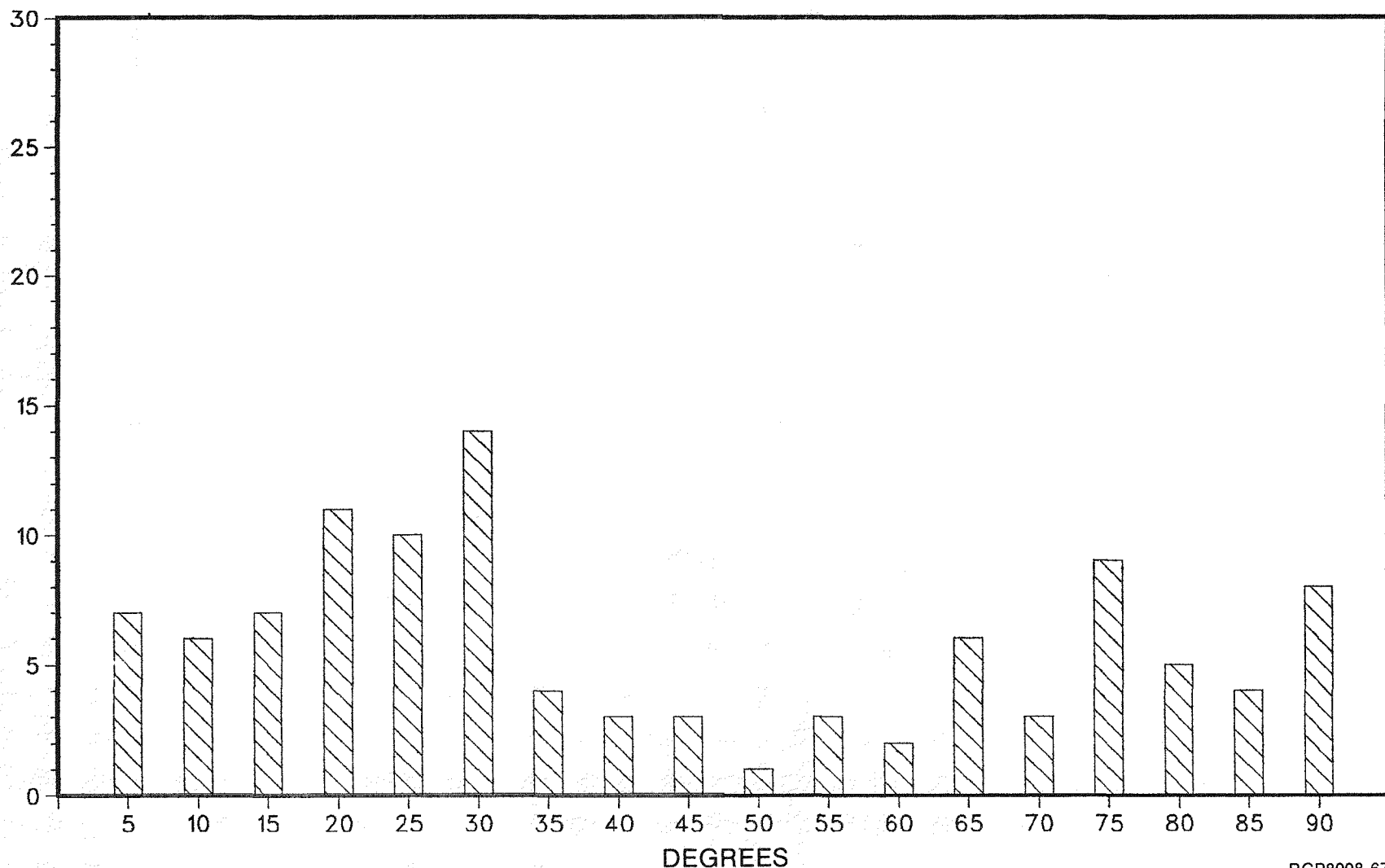
Stereonet plots and histograms from all of the geomechanically logged holes (Table 10) provided the basis for this analysis. The histograms included:

- Joint density/2 feet (0.6 meter)
- Joint density/5 feet (1.5 meters)
- Joint aperture
- Joint dip frequency
- Joint in-filling color
- Joint waviness.

Many of these plots are contained in the appendix of this report and the remainder are located in the Basalt Waste Isolation Project Library.

4-39

OCCURRENCES



RHO-BWI-ST-8

RCP8008-67

FIGURE 34. Core Hole 1E-9, Joint Dip Frequency.

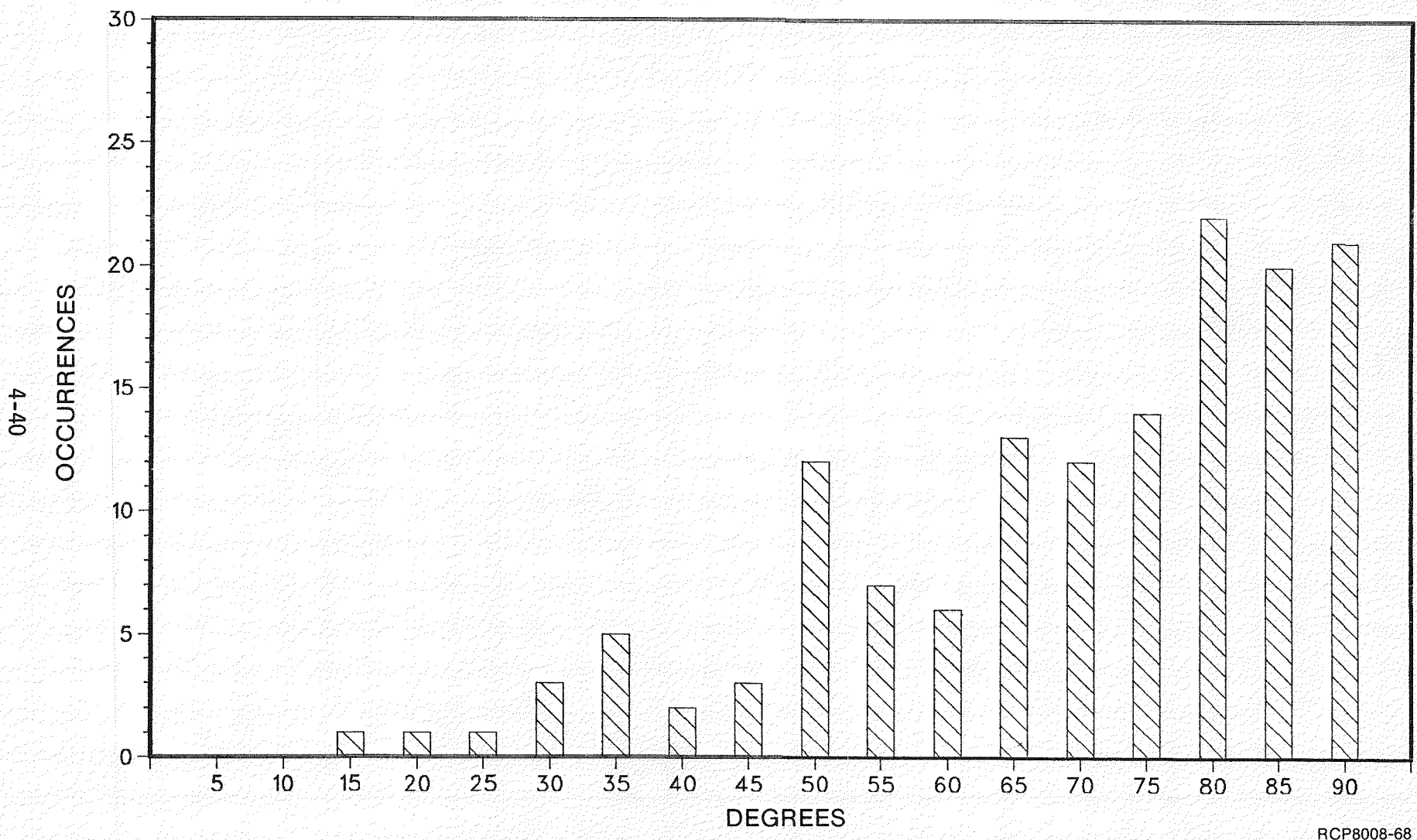


FIGURE 35. Core Hole 1E-12, Joint Dip Frequency.

RHO-BMI-ST-8

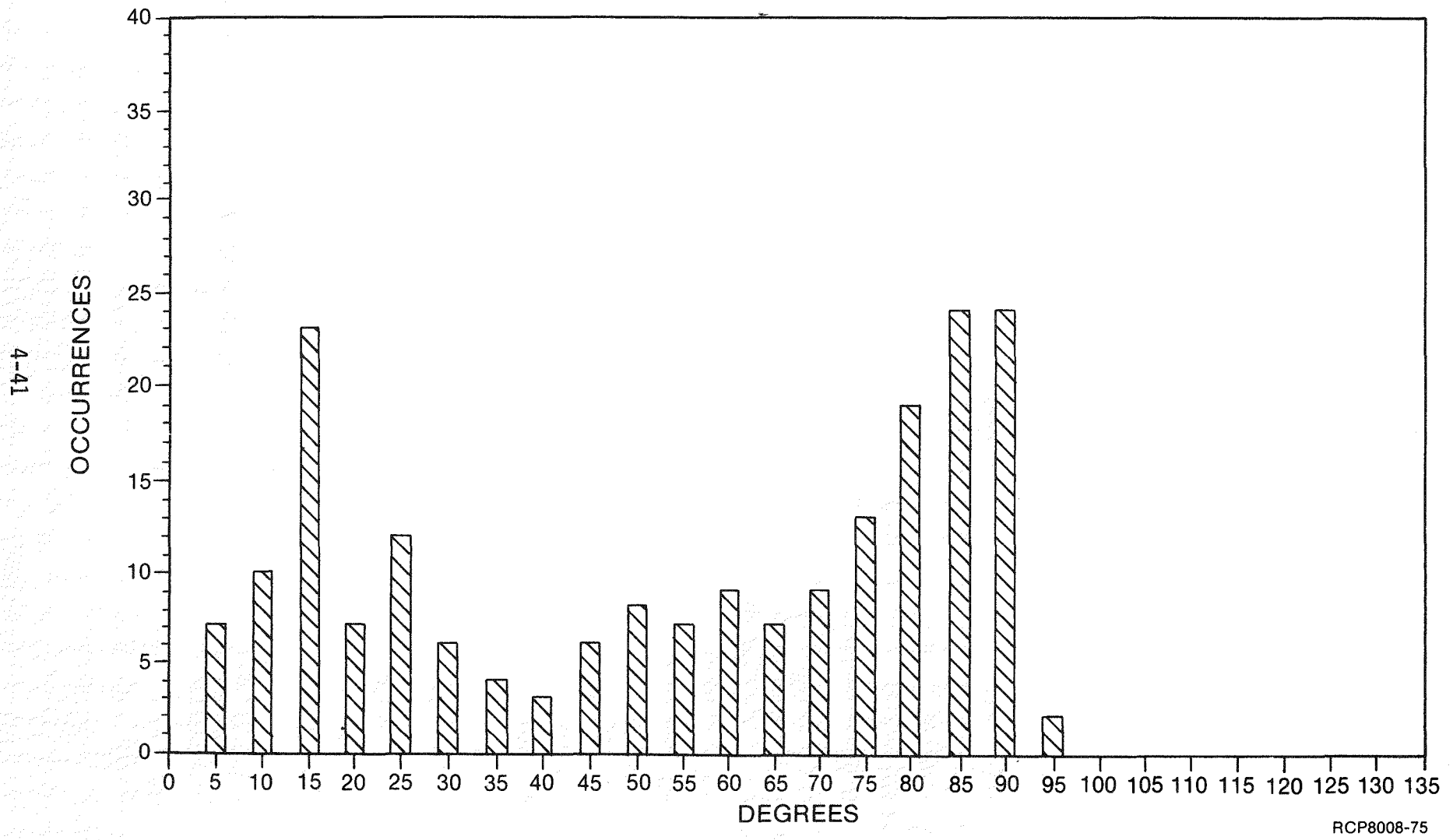
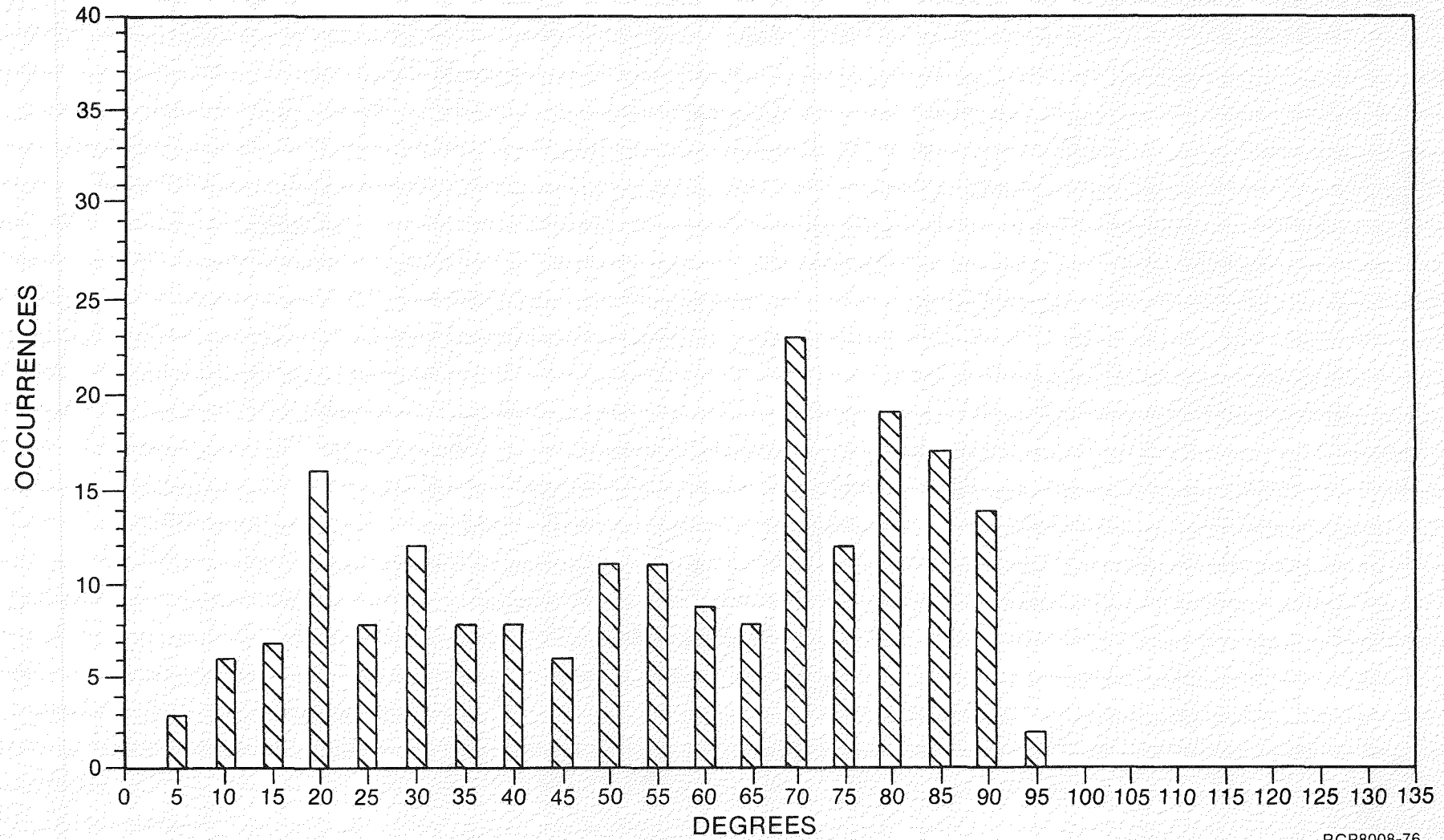


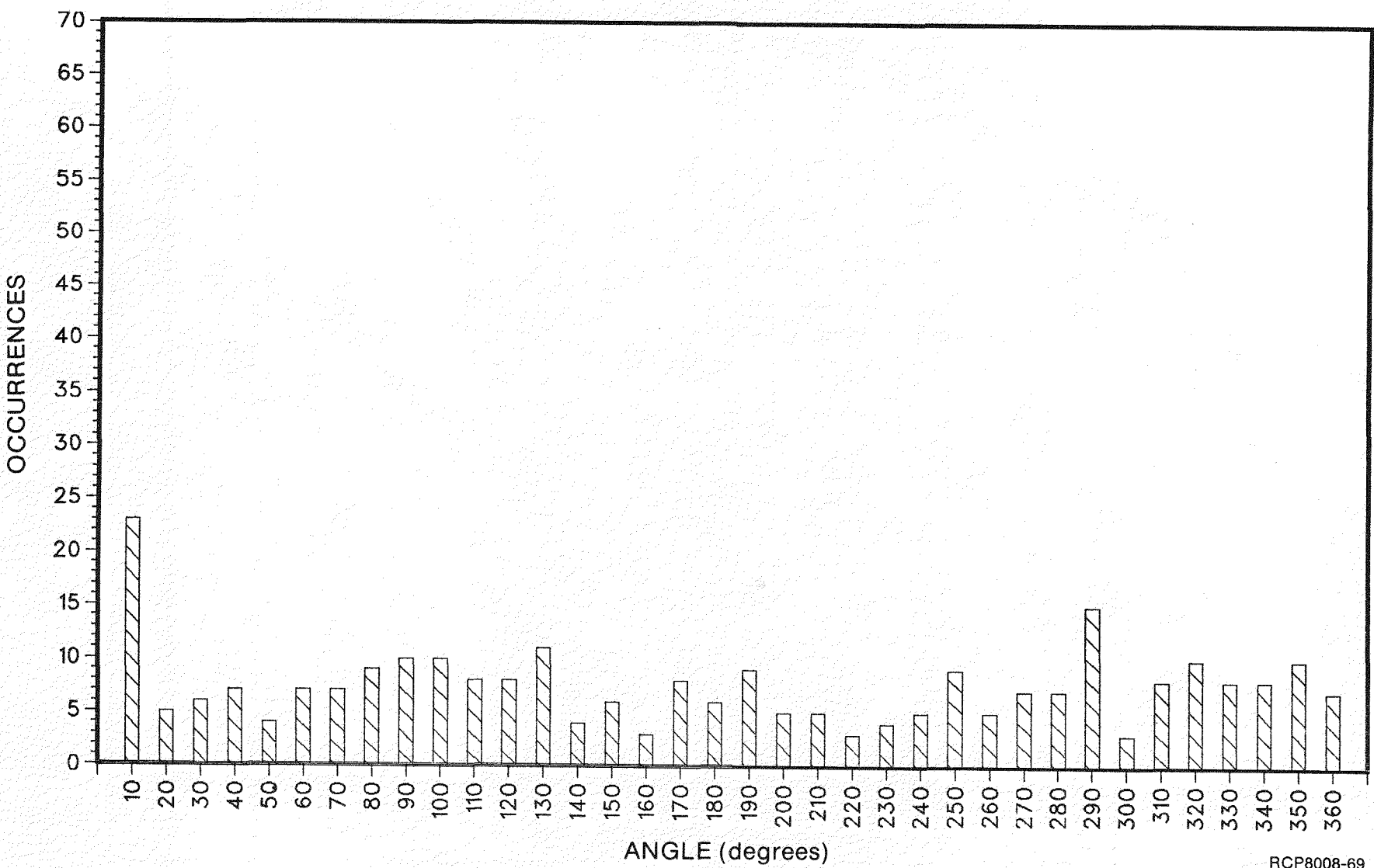
FIGURE 36. Joint Dip Frequency, Holes 1M-3 and 1E-20 (100 Data Points Each).



RHO-BMI-ST-8

RCP8008-76

FIGURE 37. Joint Dip Frequency, Holes 2M-12 and 2E-23 (100 Data Points Each).



RCP8008-69

FIGURE 38. Joint Strike Frequency for Dip Range 0 to 37 Degrees, Holes 1M-4, 1M-5, 1E-3, 1M-7, 1E-21, 1E-16, and 1E-12.

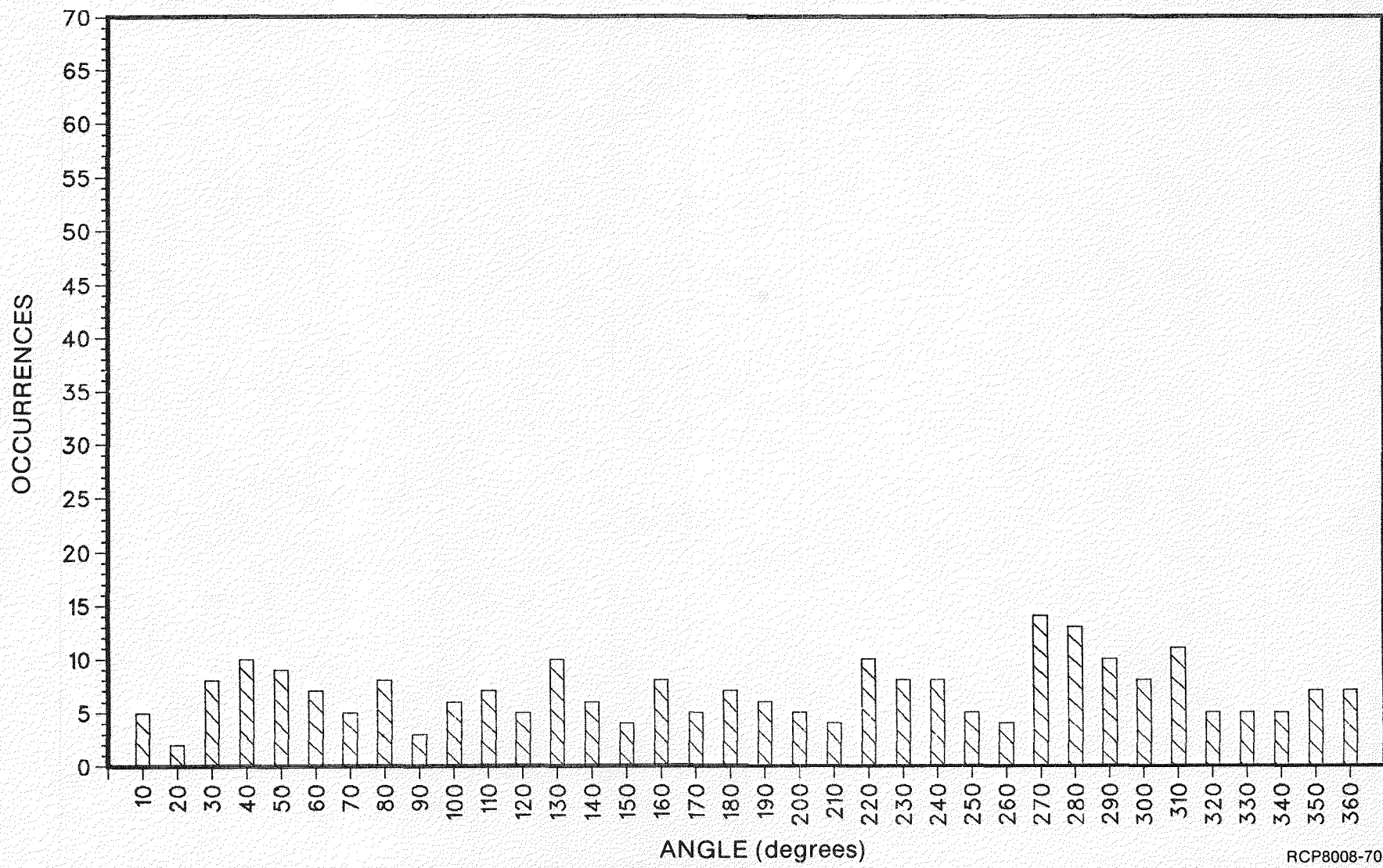
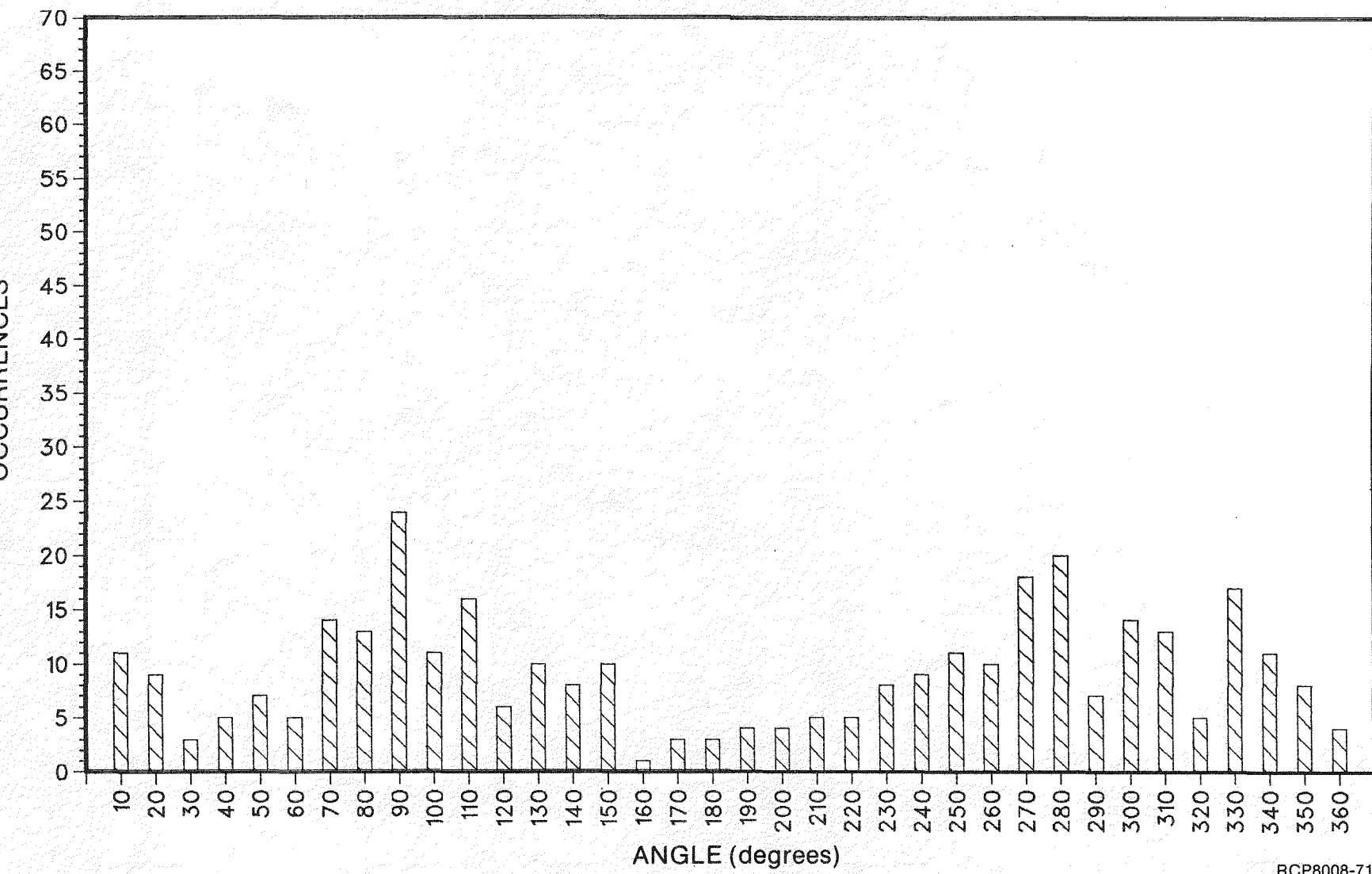


FIGURE 39. Joint Strike Frequency for Dip Range 38 to 65 Degrees, Holes 1M-4, 1M-5, 1E-3, 1M-7, 1E-21, 1E-16, and 1E-12.



RHO-BWI-ST-8

RCP8008-71

FIGURE 40. Joint Strike Frequency for Dip Range 66 to 90 Degrees, Holes 1M-4, 1M-5, 1E-3, 1M-7, 1E-21, 1E-16, and 1E-12.

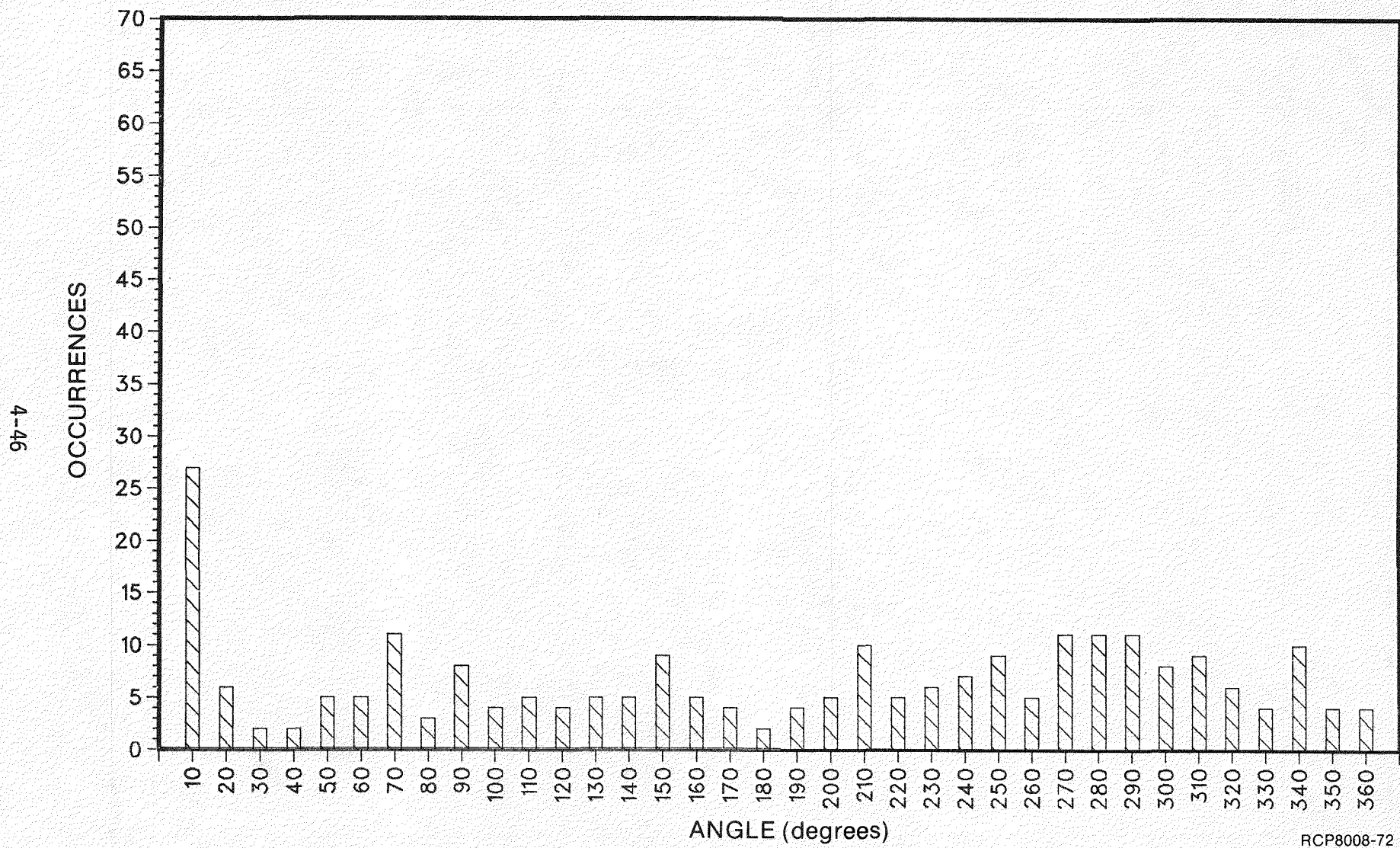


FIGURE 41. Joint Strike Frequency for Dip Range 0 to 37 Degrees, Holes 2E-1, 2M-3, 2E-9, 2M-4, 2E-25, 2E-20, and 2E-15.

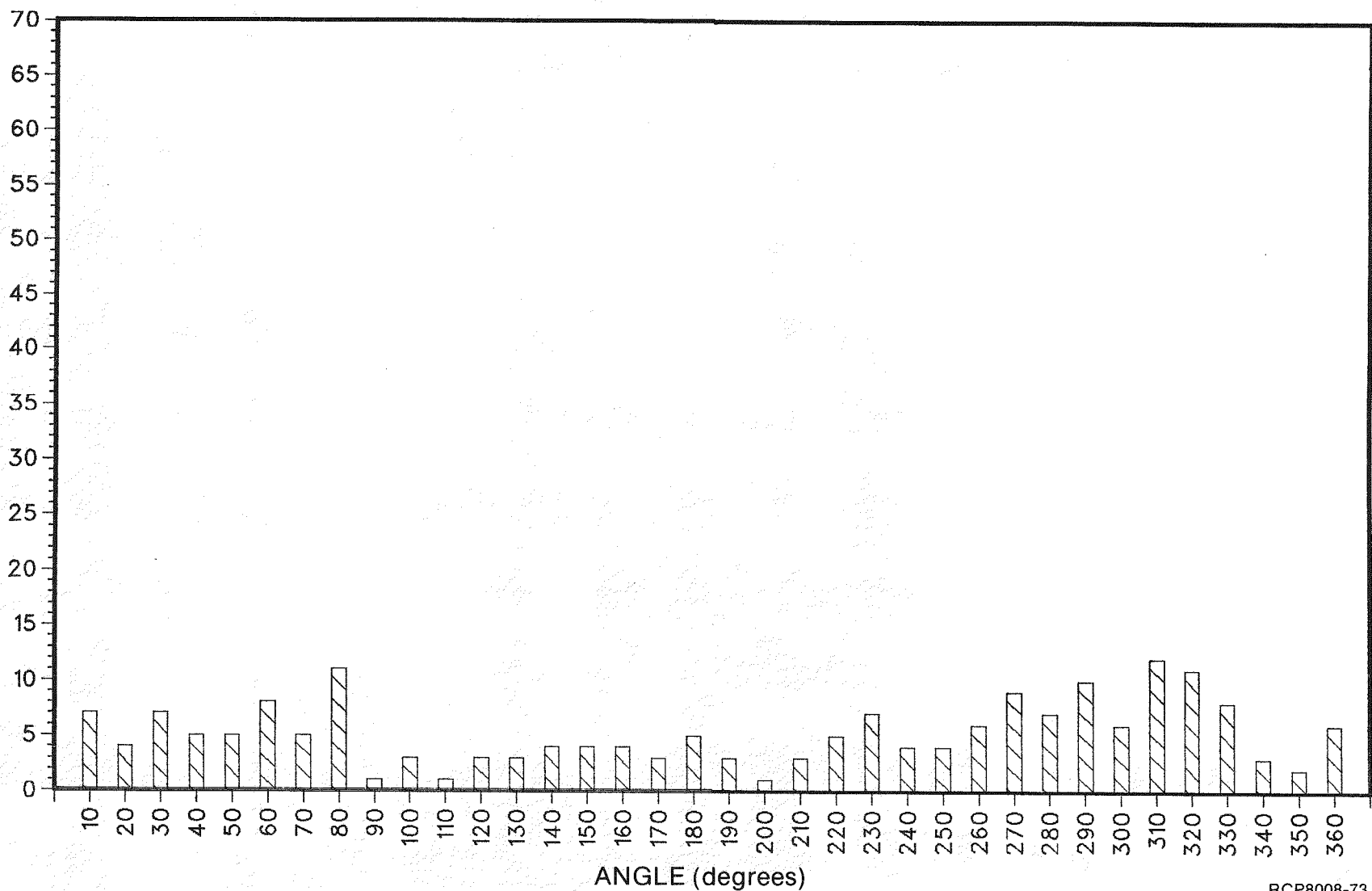
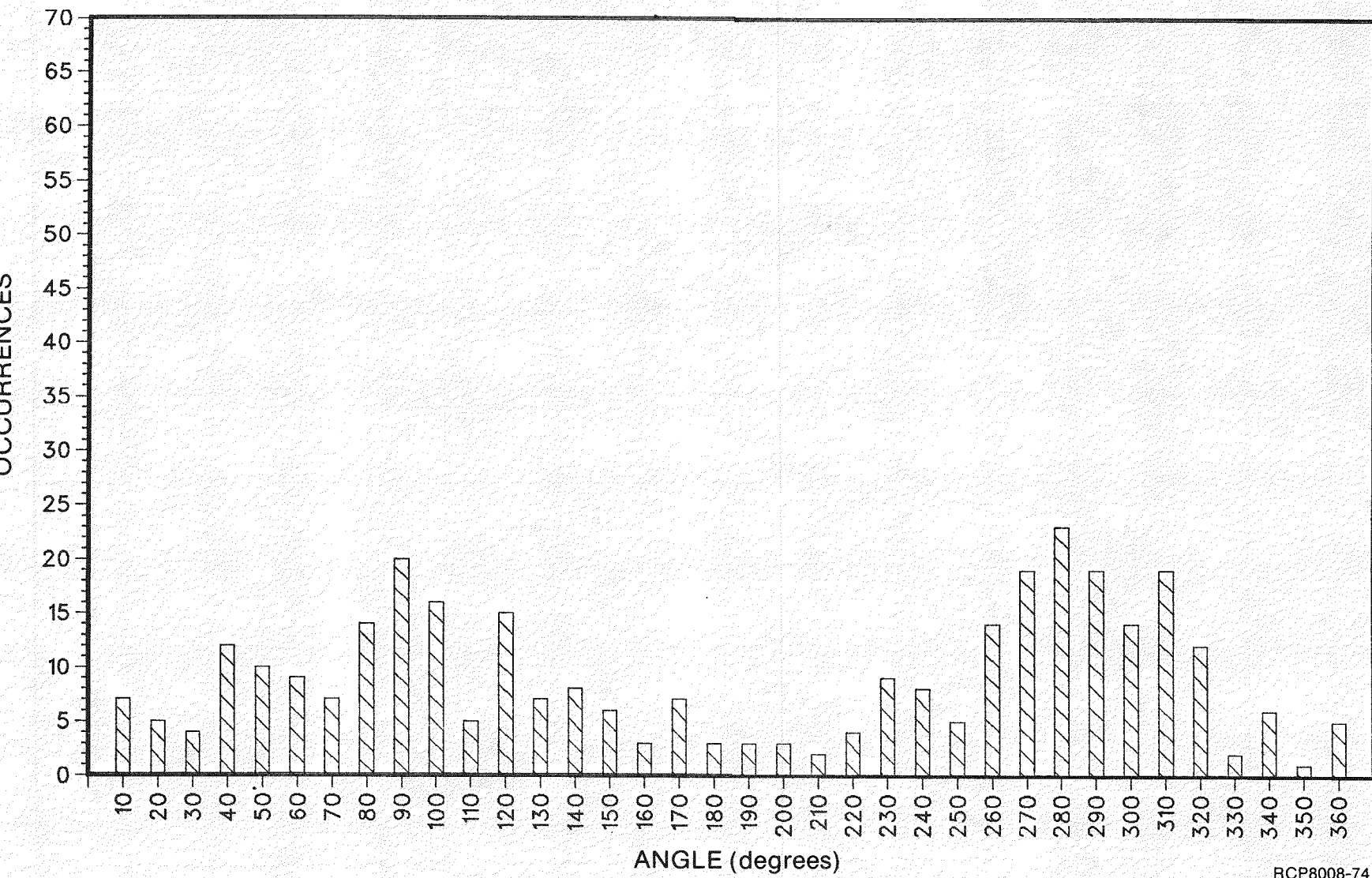


FIGURE 42. Joint Strike Frequency for Dip Range 38 to 65 Degrees, Holes 2E-1, 2M-3, 2E-9, 2M-4, 2E-25, 2E-20, and 2E-15.

4-48

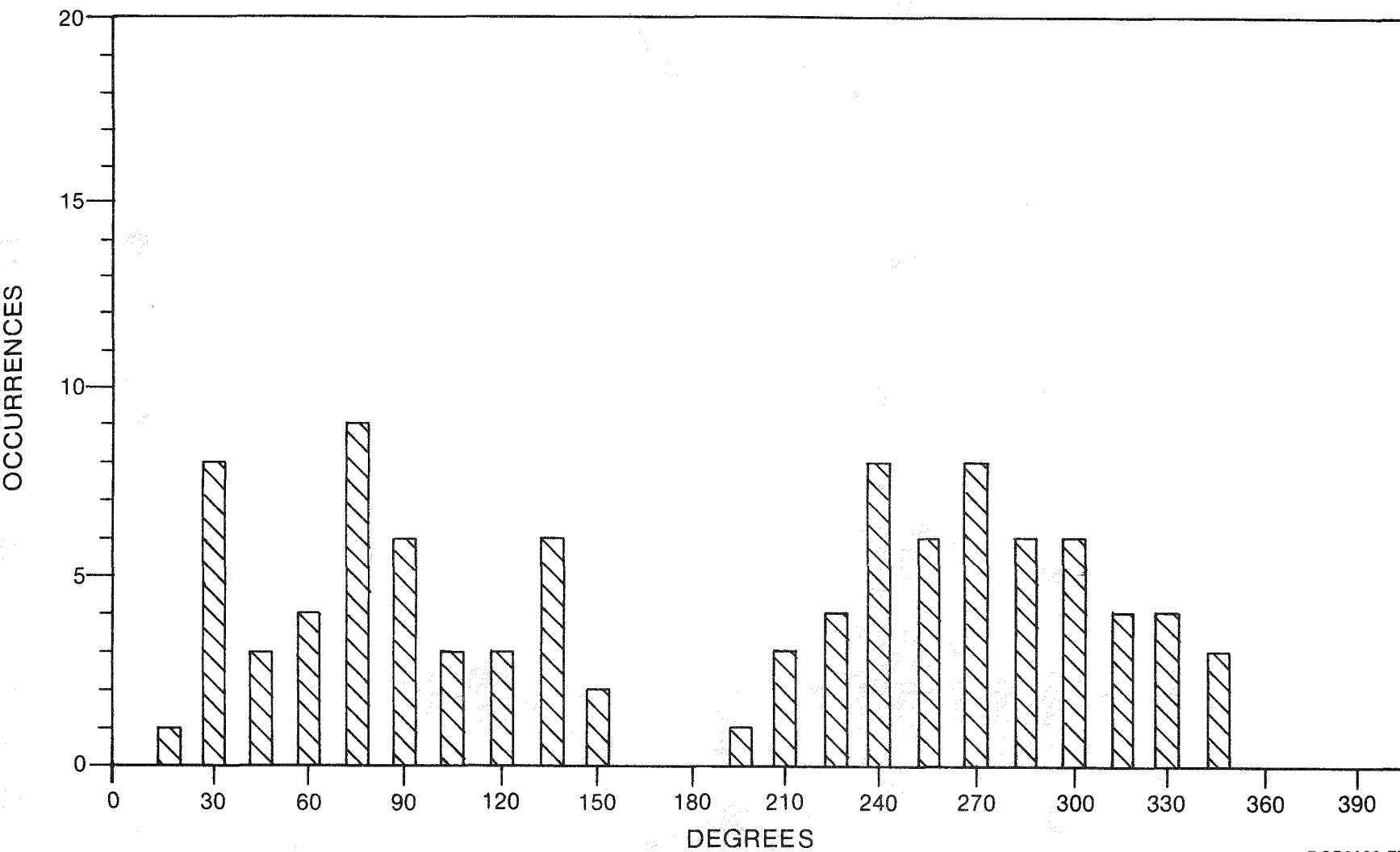


RHO-BMI-ST-8

RCP8008-74

FIGURE 43. Joint Strike Frequency for Dip Range 66 to 90 Degrees, Holes 2E-1, 2M-3, 2E-9, 2M-4, 2E-25, 2E-20, and 2E-15.

4-49



RHO-BWI-ST-8

RCP8008-77

FIGURE 44. Joint Strike Frequency Dip Range, 66 to 90 Degrees, Holes 2E-27, 2E-28, 2E-29, and 2M-16.

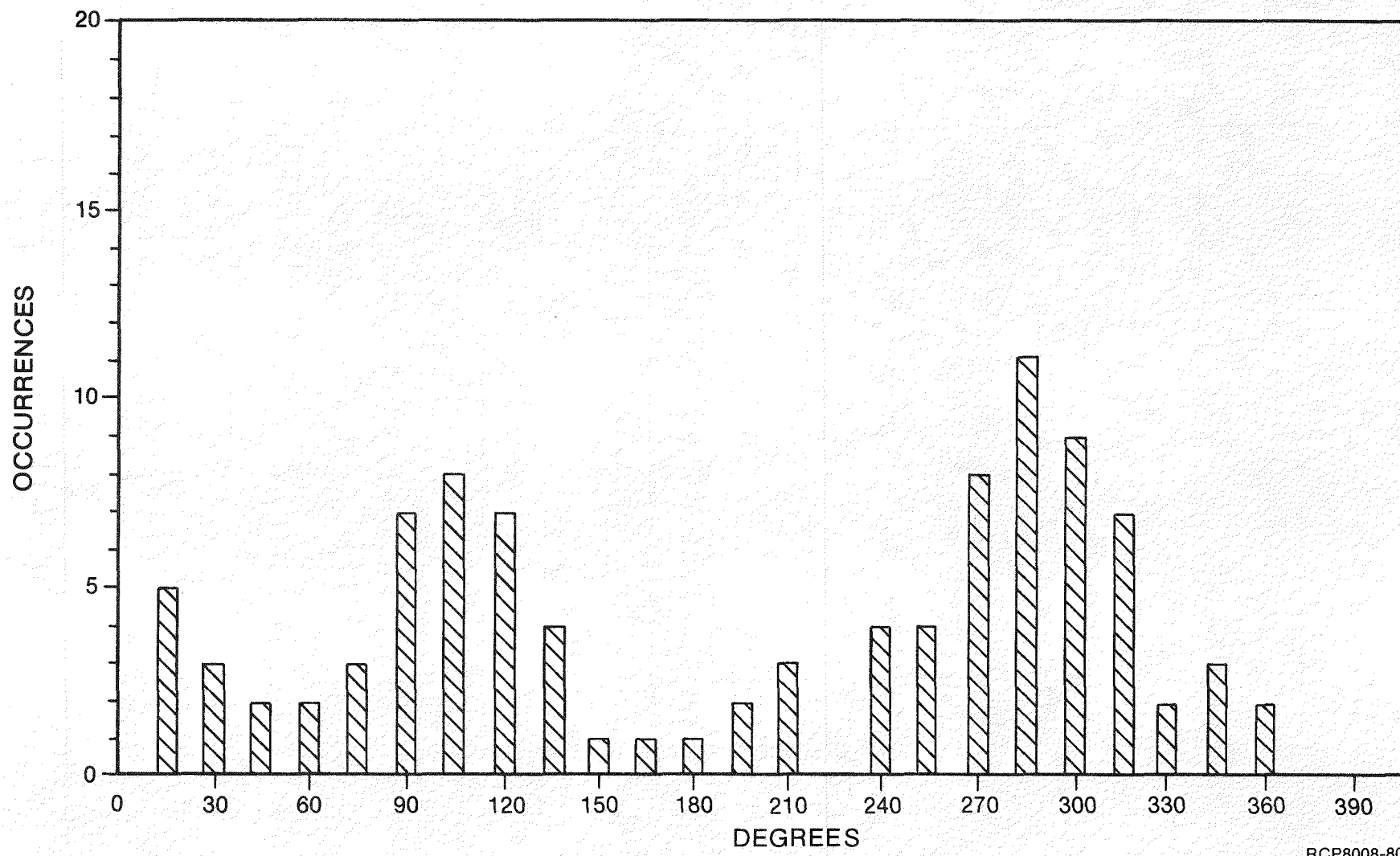
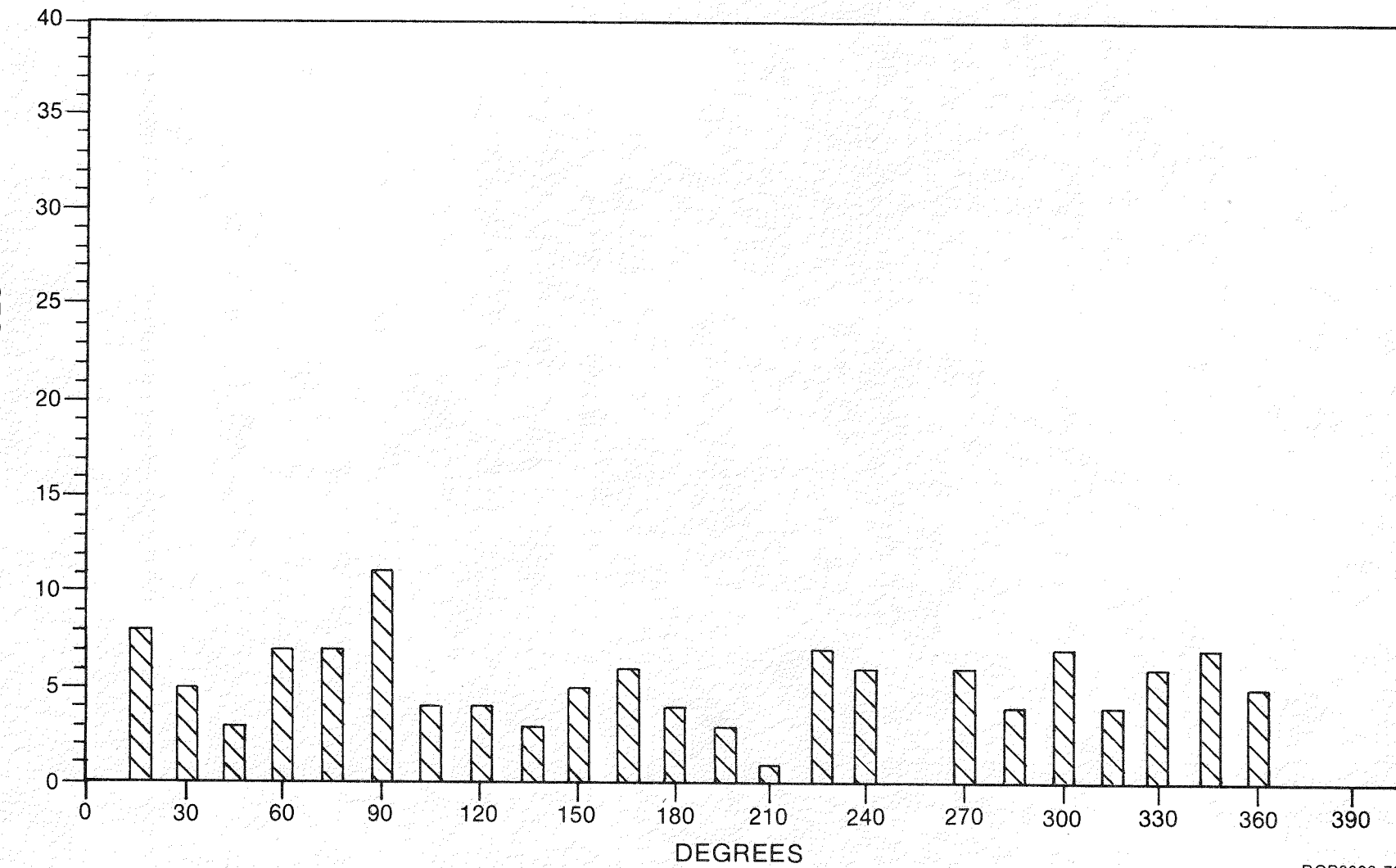
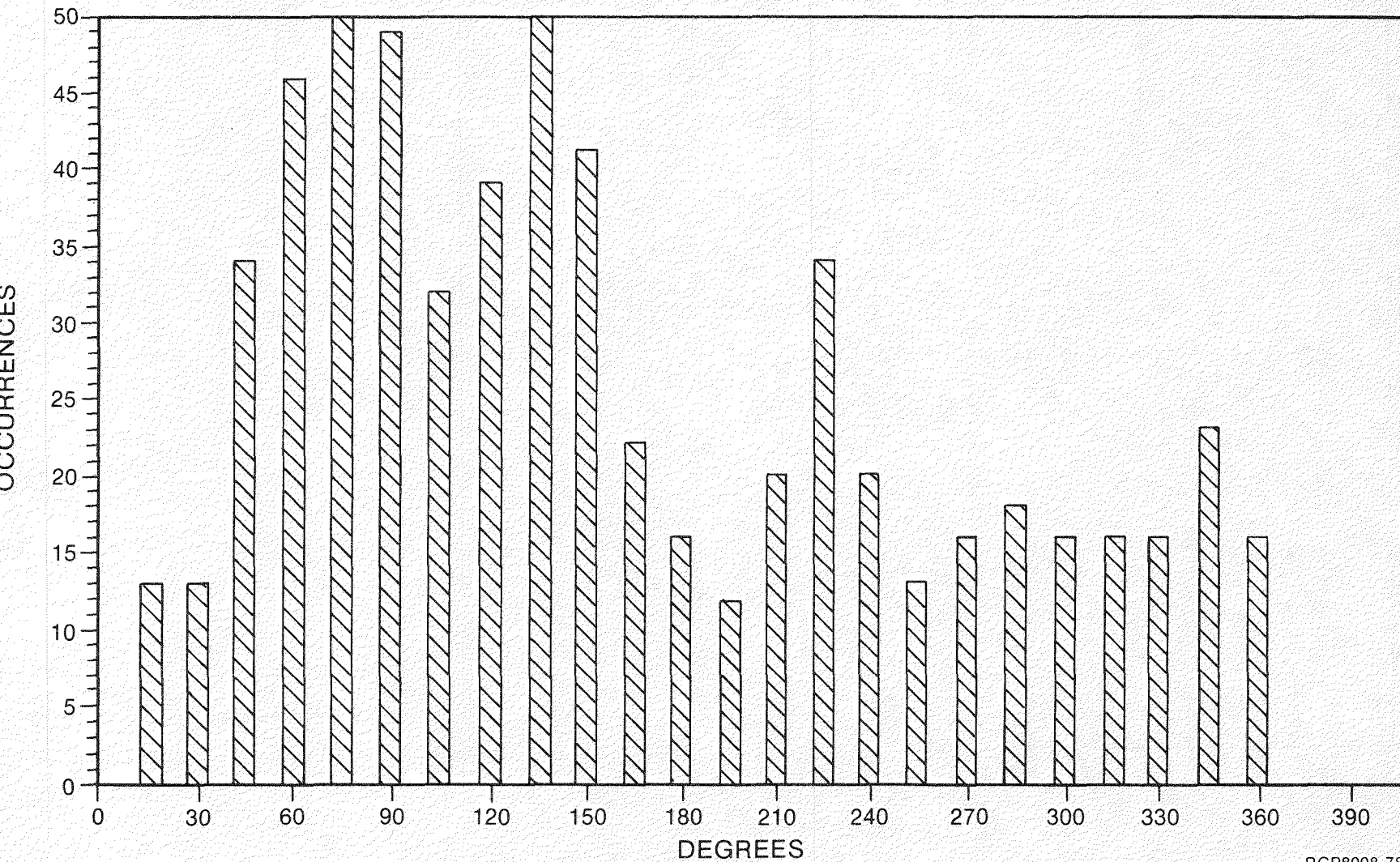


FIGURE 45. Joint Strike Frequency Dip Range, 66 to 90 Degrees, Holes 1E-16, 1E-17, and 1M-8.



RCP8008-79

FIGURE 46. Joint Strike Frequency for Dip Range 66 to 90 Degrees, Holes 2E-1, 2E-9, 2M-3, 2M-4, 2M-7, 2M-12, and 2M-13.



RHO-BWI-ST-8

RCP8008-78

FIGURE 47. Joint Strike Frequency, North Wall, Heater Test Room.

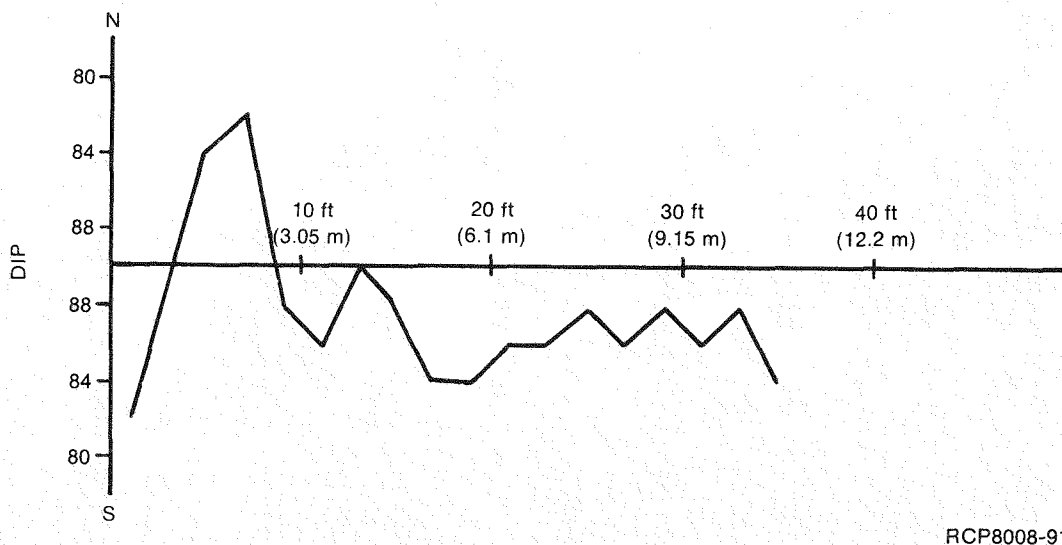


FIGURE 48. Detail Line Map of Joints in Area of Full-Scale Heater Test #1 Test Array.

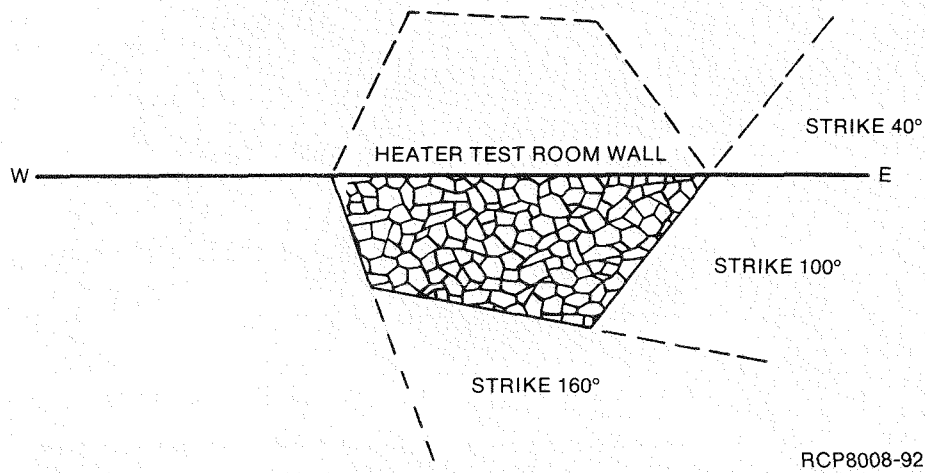


FIGURE 49. Idealized Basalt Column with a Southerly Dip.

TABLE 10. Geomechanical Borehole Logs.

Full-Scale Heater Test #1	Full-Scale Heater Test #2
Horizontal Holes	
1E-10	2E-14
1E-11	2E-15
1E-12	2E-16
1E-13	2E-17
1E-15	2E-18
1E-16	2E-19
1E-17	2E-20
1E-18	2E-21
1E-19	2E-22
1E-20	2E-23
1E-21	2E-24
1E-22	2E-25
1M-8	2E-26
	2E-27
	2E-28
	2E-29
	2M-16
Vertical Holes	
1E-1	2E-1
1E-3	2E-9
1E-8	2M-3
1E-9	2M-4
1M-3	2M-7
1M-4	2M-12
1M-5	2M-13
1M-7	

In summary, the Pomona entablature has been divided into three joint groups or sets defined by the frequency of dip.

- 0 - 37 degrees
- 37 - 66 degrees
- 66 - 90 degrees.

The first two groups represent 53% of the total number of joints measured. The remaining 47% are in the 66- to 90-degree group. The 66- to 90-degree group are undulating and represent faces of the polygonal cooling columns. These joints may be continuous up to 8 feet (2.4 meters) in length. The remaining two groups are discontinuous, seldom crossing the joint boundaries of the 66- to 90-degree group. From the data available, it is not possible to determine preferred orientations of these joint sets. The cooling pattern of the basalt joints are not oriented to a preferred direction, but only in sets delineated by dip frequency.

4.2.2 Rock-Mass Classification

Engineering classifications of the rock mass surrounding Full-Scale Heater Tests #1 and #2 were developed. Three engineering classifications were used: the rock-mass rating (Bieniawski, 1979); the Q-System (Barton and Others, 1974); and the Rock-Quality Designation (RQD) (Deere, 1963). The RQD system is the summation of the lengths of core pieces greater than 4 inches (10 centimeters) in length divided by the percentage of core recovered per run. The rock-mass rating considers six rock-mass parameters:

- Uniaxial compressive strength
- RQD
- Discontinuity spacing
- Condition of discontinuities
- Groundwater conditions
- Joint orientation.

Each of these is assigned a numerical value and the rock-mass rating is calculated from the formula

$$RMR = RQD/5 + UCS + Ds + Dc + G + Jo \quad (3)$$

where

	<u>Value</u>	<u>Designation</u>
RQD is the rock-quality designation	see Table 11	
UCS is uniaxial compressive strength	15	4.5×10^4 psi (313 MPa)
Ds is discontinuity spacing	6	2.8 to 3.5 in. (70 to 90 mm)
Dc is discontinuity condition	27	slightly rough aperture <1 mm no weathering
G is groundwater	13	Inflow <2.64 gal/min (<10 liter/min)
Jo is joint orientation.	-5	Fair

The Q-System by Barton and Others (1974) considers six categories in determining the rock-mass classifications:

- RQD
- Joint set number
- Joint roughness number
- Joint alteration number
- Joint water reduction factor
- Stress reduction factor.

TABLE 11. Summary of Rock-Mass Classifications for Blocks in Full-Scale Heater Tests #1 and #2.

Blocks in Full-Scale Heater Test #1				
Block	Joint Density Per Foot (per meter)	RQD	RMR	Q
1-1-A	4.83 (15.8)	35	63.0	11.67
1-1-B	4.67 (15.3)	42	64.4	14.00
1-1-C	3.94 (12.9)	45	65.0	15.00
1-2-A	4.63 (15.2)	45	65.0	15.00
1-2-B	3.96 (13.0)	46	65.2	15.33
1-2-C	4.33 (14.2)	31	62.2	10.33
1-3-A	4.55 (14.9)	42	64.4	14.00
1-3-B	5.91 (19.4)	39	63.8	13.00
1-3-C	4.98 (16.3)	28	61.6	9.33
1-4-A	4.71 (15.4)	35	63.0	11.66
1-4-B	4.79 (15.7)	36	63.2	12.00
1-4-C	4.19 (13.7)	49	65.8	16.33
Total	4.62 (15.1)	39(poor)	63.9(good)	13.14(good)

Blocks in Full-Scale Heater Test #2				
2-1-A	5.24 (17.2)	44	64.8	14.67
2-1-B	3.93 (12.9)	62	68.4	20.67
2-1-C	3.45 (11.3)	69	69.8	23.00
2-2-A	4.61 (15.1)	40	64.0	13.33
2-2-B	5.09 (16.7)	54	66.8	18.00
2-2-C	3.42 (11.2)	65	69.0	21.67
2-3-A	4.93 (16.2)	39	63.8	13.00
2-3-B	4.24 (13.9)	52	66.4	17.33
2-3-C	3.47 (11.4)	58	67.6	19.33
2-4-A	4.83 (15.8)	39	63.8	13.00
2-4-B	4.31 (14.1)	51	66.2	17.00
2-4-C	3.48 (11.4)	57	67.4	19.00
Total	4.25 (13.9)	53(fair)	66.5(good)	17.50(good)

RQD = Rock-quality designation.

RMR = Rock-mass rating.

Q = Q-system.

These parameters were assigned values based on Barton and Others (1974) classifications and the formula:

$$Q = (RQD/Jn) (Jr/Ja) (Jw/SRF) \quad (4)$$

where

	<u>Value</u>	<u>Designation</u>
RQD is the Rock-Quality Designation	see Table 11	
Jn is the joint set number	7.5	Three joint sets
Jr is the joint roughness number	2.5	Rough-smooth undulating
Ja is the joint alteration number	1.0	Unaltered joint walls
Jw is the joint water reduction factor	1.0	Minor inflow, <1.32 gal/min (<5 liter/min)
SRF is the stress reduction factor	1.0	$\sigma_e/\sigma_i = \sigma_t/\sigma_i = 1.6$

was used to derive Q (Table 11).

To aid in evaluating these formulas and as a comparative tool, histograms of the frequency of joints per 2 feet (0.6 meter) of borehole were plotted and examples are shown in Figures 50 and 51. In many of the boreholes, zones of rubble caused by the drilling technique and/or the intersection of several joints were recorded. These zones were not originally included on the histograms, but were later added using a factor of six joints per foot (20 joints per meter). A line was drawn on these histograms, to denote the number of joints in the rubble zones. Using these histograms, joint densities for each of the 12 blocks in Full-Scale Heater Tests #1 and #2 (see Figures 25 to 29) were calculated (Table 11).

In addition to computing the RQD values for each block, the designations were also calculated for each individual core run. Summary tables are included in the appendix.

The RQD and joint densities are variable with each hole, but limited cross-hole similarities can be seen. Generalities can be made by comparing the RQD of the vertical holes in the blocks to determine possible zones of damage due to the excavation method. The initial 2 to 3 feet (0.8 to 1.0 meter) below the collars of the holes have average RQD values less than 20. The values increase to an average of approximately 40 to 50 to depths of 18 to 20 feet (5.5 to 6.1 meters) below the collar. RQD values vary from 0 to 100 below this point, but give an overall indication of reasonably competent rock.

Values for joint densities, RQD, rock-mass rating, and Q were calculated for each of the 12 blocks in Full-Scale Heater Tests #1 and #2 and are summarized on Table 11. These calculated values indicate that the highly jointed Pomona unit in these blocks can be classified as "good rock" in the Q- and rock-mass rating systems (Table 12). The RQD

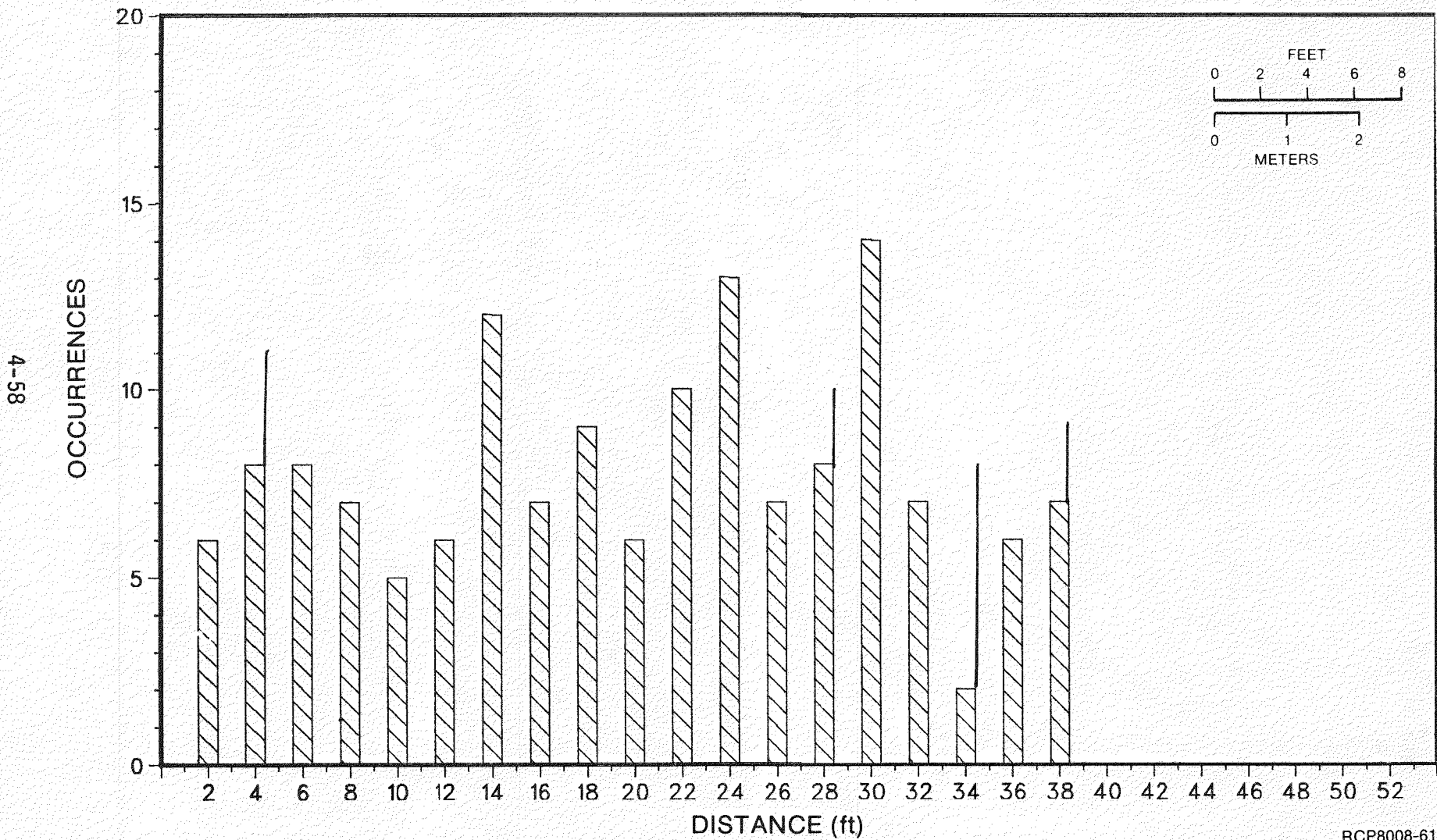


FIGURE 50. Core Hole 1E-17, Fracture Top Frequency.

4-59

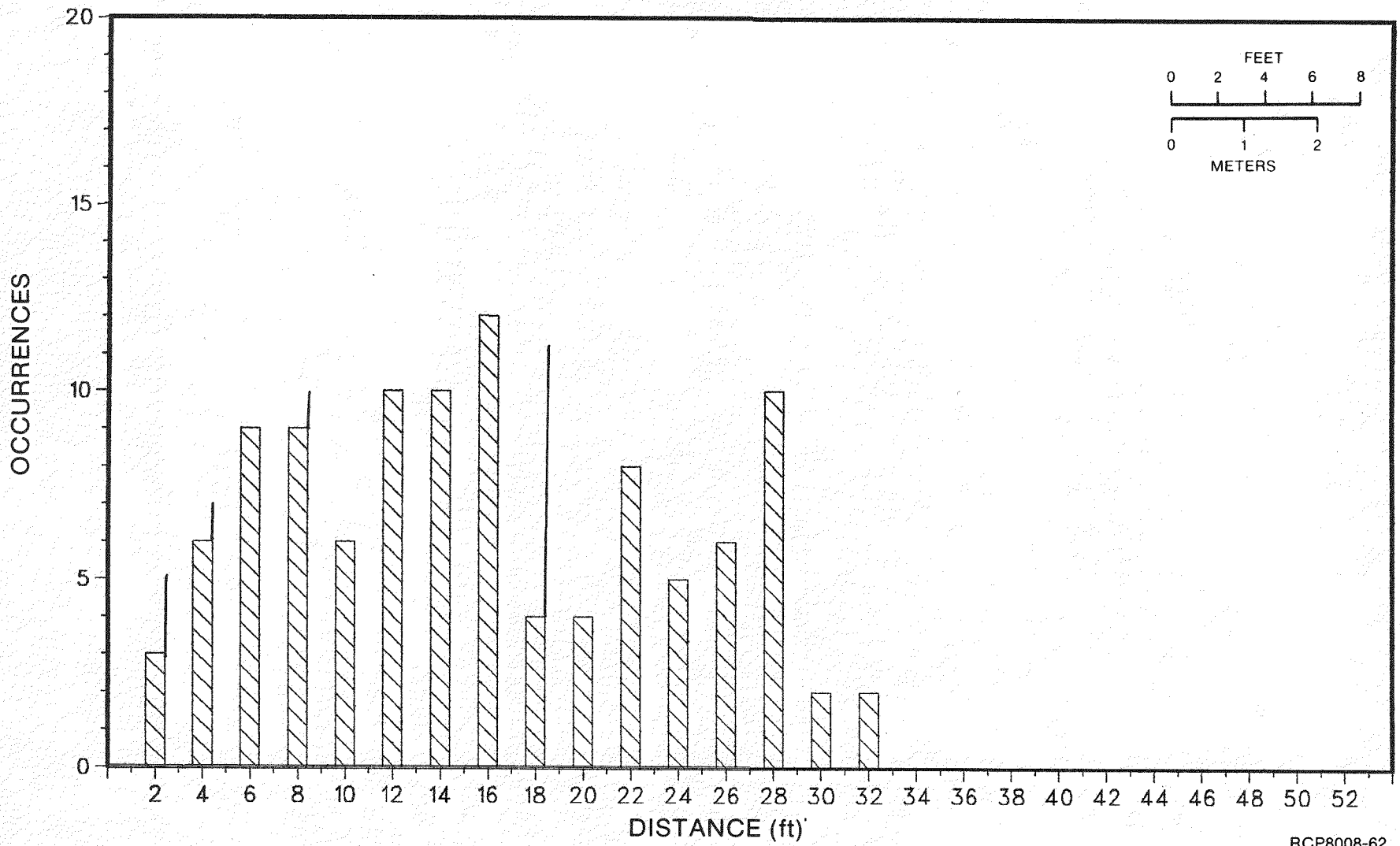


FIGURE 51. Core Hole 1E-3, Fracture Top Frequency.

RCP8008-62

RHO-BWI-ST-8

TABLE 12. Rock-Mass Classification Values.

Rock-Mass Quality (Q) (Barton)	
Exceptionally poor	0.001-0.01
Extremely poor	0.01-0.1
Very poor	0.1-1.0
Poor	1.0-4.0
Fair	4.0-10.0
Good	10.0-40.0
Very good	40.0-100.0
Extremely good	100.0-400.0
Exceptionally good	400.0-1000.0

Rock-Quality Designation (RQD) (Deere)	
Very poor	0-25
Poor	25-50
Fair	50-75
Good	75-90
Excellent	90-100

Rock-Mass Rating (RMR) (Bieniawski)	
Very poor	0-20
Poor	21-40
Fair	41-60
Good	61-80
Very Good	81-100

rating (Table 12) is lower, because it only considers one of the many parameters used in the other classifications. As previously stated, the rock was easily broken along healed joints due to weakening by the excavation and the borehole drilling; hence, fewer pieces were greater than 4 inches (10 centimeters) in length. However, RQD values are easy to compute and should be routinely recorded for all future boreholes, placing the values in their proper perspective.

The classifications indicate better overall ratings for the blocks of Full-Scale Heater Test #2. This most likely is attributed to the overall lower rock-quality designation values in Full-Scale Heater Test #1 caused by inconsistent excavation and drilling procedures. It is not believed that the overall competency is significantly different in Full-Scale Heater Test #1 than in Full-Scale Heater Test #2.

5.0 SUMMARY

The test rooms of the NSTF are located in the entablature of the Pomona Member of the Saddle Mountains Basalt, approximately 150 feet (45.7 meters) beneath the surface of Gable Mountain, an anticlinal outcrop on the Hanford Site. Tunnel excavations penetrated the Elephant Mountain Member, the Rattlesnake Ridge interbed, and into the entablature of the Pomona Member. Geotechnical input during construction, followed by detailed geologic characterization, provided the data for this report. This report was prepared as geologic documentation of the facility and will be used as baseline data for comparison to a post-test characterization report.

On the basis of the available data from the Pomona entablature, three joint sets have been identified by their angle of dip. The high-angle set from 66 to 90 degrees comprises 47% of the over 7,000 joints measured. These represent the faces of the polygonal cooling columns and some extend to 8 feet (2.4 meters) in length. The 37- to 65-degree set (23%) and the 0- to 37-degree set (30%) are generally discontinuous joints limited to the confines of an individual column. None of the joints were capable of being identified between boreholes or from the tunnel floor into the rock mass below.

No tectonically induced joints were recognized in the joint study. Joint in-filling was generally ≤ 0.3 millimeter and the filling was primarily a smectite clay with occasional calcite, pyrite, or silica.

Because of the preferential direction of the boreholes and tunnels, there was a bias in the strike direction of the joints sampled. Efforts to eliminate this bias were generally successful, but no preferred strike direction was seen in any of the three joint sets. It is presumed that the polygonal cooling pattern of the basalt results in a random orientation of the joints.

The rock, although highly jointed, may be classified as "good rock" using various engineering rock-mass classifications developed for an overall assessment of its constructability.

There were no anomalously jointed areas observed within the rock mass surrounding Full-Scale Heater Tests #1 or #2. Minimal oxidation was noted on few joints of the core from the instrument boreholes, although oxidized zones were seen elsewhere in the facility.

6.0 ACKNOWLEDGMENTS

We thank Mr. K. Ziegler for his assistance during the core drilling, Mr. L. G. Eriksson for his technical assistance, Mr. R. W. Cross and Mr. W. H. Crowley for their drafting, and those who reviewed this manuscript.

Foundation Sciences, Incorporated performed the overcoring tests; the hydrofracturing was performed under the direction of Lawrence Berkeley Laboratory; the cross-hole acoustic tests were done by Sigma Research, Incorporated; and the impression packer testing was performed by TAMS International.

APPENDIX A
DATA-GATHERING PROCEDURES

APPENDIX A
DATA-GATHERING PROCEDURES

The following is an explanation of three of the data-gathering techniques used in the NSTF geologic characterization: geomechanical logging, which describes individual fractures in oriented core samples; lithology and structure logging, which describes the lithology and general structural features and records rock-quality designation, core recovery percentage, and borehole location data; and detailed line mapping, which is a systematic sampling of joint and fracture data across a rock face or wall.

GEOMECHANICAL LOGGING (Figure A-1)

The codes entered on these logs for the NSTF differ slightly from those set up in the standard operating procedures used in the deep core holes on the Hanford Site and they are listed below.

Column 1 - Comment check; enter an identifying number for each line of comment if data from this line are to be listed, but not compiled.

Columns 2 to 6 - CORE HOLE; enter an identifying designation for the core hole, such as 1E1, 2M3, etc.

Columns 8 to 10 - RUN; enter run number for the individual core hole.

Columns 12 to 14 - FRAC NUM; enter fracture number for each run starting at 1 for the first fracture encountered at the top of a run.

Columns 16 to 21 - FRACTURE TOP (feet); enter the feet below the reference elevation for the top of the fracture. The reference elevation is normally ground surface; note that the entry should be to the nearest 0.01 foot. The decimal point is between Columns 19 and 20.

Columns 23 to 28 - FRACTURE BOTT (feet); enter feet below the reference elevation for the bottom of the fracture. The entry should be to the nearest 0.01 foot. The decimal point is between Columns 26 and 27.

Columns 30 to 32 and 34 to 35 - STRIKE and DIP; fracture planes are described in terms of strike and dip. STRIKE is the bearing of the plane projected to a horizontal ordinate scale of 0 to 360 degrees. DIP is the angle of the plane related to horizontal and normal to the strike. All attitudes of plane refer to the bottom or foot-wall portion of the fracture.

Columns 37 to 40 - WIDTH (mm); enter width in millimeters to the nearest 0.1 millimeter. Decimal point is between Columns 39 and 40.

Column 42 - TYPE; enter one number from the TYPE CODE.

FIGURE A-1. Geomechanical Core Log.

A-6400-069 (9-77)
RCP8007-100

Type Code

- 1 = Planar
- 2 = Irregular
- 3 = Curved
- 4 = Stepped
- 5 = Hairline (intact)
- 6 = Badly broken or rubble zone
- 9 = Drilling or hammer break

Columns 44 to 50 - TERMINATED; enter the fracture number within the same run if the fracture is terminated at the top (Columns 44 to 46) or bottom (Columns 48 to 50) by another fracture.

Columns 52 to 54 - CROSSES; enter the fracture number of a fracture within the same run if a fracture crosses another.

Columns 56 to 57 - FILL; enter an appearance description number from the APPEARANCE CODE in Column 56. Enter a letter from the MINERALOGY CODE in Column 57 if determinable (mineralogical evaluation may necessarily be done later or in a laboratory). If more than one type of in-filling or coating is encountered, list in COMMENTS.

Appearance Code

- 0 = Open fracture (no filling)
- 1 = Black filling
- 2 = White filling
- 3 = Light-green filling
- 4 = Dark-brown filling
- 5 = Light-brown filling
- 6 = Blue filling
- 7 = Dark-green filling
- 8 = Clear, amorphous filling
- 9 = Clear, crystalline filling

Mineralogy Code

- C = Clay
- N = Clay, nontronite
- M = Clay, montmorillonite
- Q = Quartz
- Z = Zeolite
- T = Calcite
- A = Volcanic ash or tuff
- P = Pyrite
- H = Hematite
- L = Limonite
- O = Other

Column 59 - ROUGHNESS; enter a number from the ROUGHNESS CODE.

Roughness Code

0 = Not Assigned

1 = Smooth

2 = Rough

3 = Polished

4 = Slickensided (Grooved)

5 = Pitted

Columns 60 to 73 - COMMENTS; enter any comments concerning unusual or noteworthy conditions encountered such as weathering or hydrothermal alteration. Note any vugs or amygdaloidal areas. Indicate if the vugs are partially or completely filled. If additional space is needed for comments, enter a "1" in Column 1 of the next line. Any information entered in this line will be listed, but not compiled. The entry should be identified by entering the core hole designation, run, and interval described in the FRACTURE TOP and FRACTURE BOTT columns. All other columns may be used for comments. If more than one line of additional comments is needed, enter a "2," "3," etc. and proceed as above.

Columns 74 to 80 - STRAT UNIT; enter a standard abbreviation for the stratigraphic unit encountered. This must be uniform for all entries for computer sorting.

Stratigraphic Unit Abbreviations

IHAR B = Ice Harbor Member

EL MT B = Elephant Mountain Member

RTL T I = Rattlesnake Ridge Interbed

POM B = Pomona Member

SEL I = Selah Interbed

ESQ B = Esquatzel Unit

CLD C I = Cold Creek Interbed

HUNT B = Huntzinger Member

UMAT B = Umatilla Member

MAB I = Mabton Interbed
PR B = Priest Rapids Member
ROZA B = Roza Member
FR SP B = Frenchman Springs Member
VAN SS = Vantage Sandstone
WAN FM = Wanapum Basalt
GR FM = Grande Ronde Basalt
UU = Umtanum Unit

NOTE: Entries in any column may be duplicated by extending a line down the page through the desired column.

Due to the sinuousness of many high-angle fractures, it was obvious that an individual fracture could exist along the core for up to 3 feet (1 meter), but have a varying strike. The average strike for a section of the fracture was recorded and another strike was recorded for an obvious change of strike direction. It was recorded as two separate fractures, with the uppermost fracture terminated at the bottom by the top of the remaining portion. The lower portion was recorded as terminated at the top by the lower part of the upper section. This is consistent with the detailed line mapping procedures used to map the fractures in the tunnel ribs.

Columns 37 to 40 measure the "width" of the fracture. Many of the fractures were broken along the in-filling material. The "width" of the fracture was measured or closely estimated as the summation of the amount of in-filling material on both pieces of the fracture. With the exception of fractures induced by a drilling or hammer break across solid rock, all fractures appeared to be totally filled with clay or other material. Therefore, the measurement of the in-filling material appears to be a valid or at least consistent way to measure the fracture width. The greater the fracture in-filling, the more accurate the recorded measurement.

All of the geomechanical logs prepared for this report were done by the authors. Use of the terms "planar," "rough," "smooth," etc. should, therefore, be consistent and relative throughout the report.

The following are the procedures that were to be used by the drilling contractor in handling the NSTF core and the logging procedures used by the geologists.

1. The drilling crew shall carefully open the split tube core barrel and remove the core run under the supervision of a drilling specialist or foreman. Proper continuity and

orientation of the core shall be maintained as it is placed into a core trough.

2. Each core run in the trough shall be identified by a wooden block showing the hole number and footage drilled, measured to the nearest one-tenth of a foot. This block shall be labeled by a member of the drilling crew or a geologist. Extreme care shall be taken to ensure proper measurement and labeling of each core run and to maintain the proper relationship and orientation of all cored pieces.
3. The driller or helper shall then place the core in a properly assembled manner into core boxes which shall be identified with a wooden block at the upper left of each box. This block shall show the hole number, box number, and footage of core contained within the box.
4. Unusual features, selected core intervals, or selected fractures and their filling may be preserved by wrapping them in aluminum foil and sealing with melted paraffin.
5. The geologist shall log the core as described in NSTF Core Logging in this Appendix.
6. The core shall be transported by the transportation services to the 2101-M Building, 200 East Area, Hanford Site and photographed by Pacific Northwest Laboratory's Photography Group. These photographs shall be stored in the project library and/or supplement the final NSTF report.

NEAR-SURFACE TEST FACILITY CORE LOGGING

The geologic log shall be prepared and completed as follows. Enter hole number, location, size, angle, elevation, and bearing. The geologist shall initial and date the log in the assigned spaces. Footage for each described zone shall precede descriptions. Descriptions shall follow the order in Geologic Core Log Definitions in this Appendix.

Each lithologic division is separated by semicolons and listings within the divisions are separated by commas. Repetition of descriptions are often omitted by simply listing the changes noted for a particular interval and not relisting obvious data. Noteworthy joints and their characteristics are listed beneath the bulk of the geologic description.

The rock-mass quality can be described in a number of quantitative ways. The simplest index of rock-mass quality and the one used here is the RQD (Deere, 1963). This designation, which varies from 0 to 100 is the percentage of pieces of core over 4 inches (100 millimeters) in a diamond drill core run. This index does not consider the rock strength; therefore, it should be used in conjunction with the uniaxial compressive

strength of the intact rock to describe the rock quality. The RQD should only be used as a general index, since it is sensitive to the drilling method, core size, water, and stress conditions at the depth of coring.

The core recovery is expressed as a percentage and is given for each core run. Each run is measured to the nearest one-tenth of a foot and that number is divided by the contractor's recorded depth. Often, a small portion of the core run remains at the bottom of the hole during retrieval of the core barrel. If this portion was obviously recovered at the start of the next run, it was considered as recovered in the run in which it was drilled.

No zones of soft material or anomalous voids were seen in the core. Because of this and the inability of the drill to grind away core, core recovery exceeded 98%.

The graphic log is used to visually show noteworthy features in the core. Established nomenclature and symbols are used. Hash marks indicating intensive jointing are not necessarily marked to a scale or degree of jointing. Likewise, individual joints, graphically depicted, do not reflect their aperture, strike, dip, or terminations; these are given in the geomechanical core logs. Only the apparent joint length and actual location are shown in the graphic log. Vugs and amygdalules are shown as to location and not necessarily to scale.

Geologic Core Log Definitions

Lithology Divisions

Rock Name

Weathering/Alteration State

Structure

Color

Texture

Hardness or Strength

1. Rock Name - Include the rock type most commonly encountered at Hanford:

Basalt	Scoria
Basalt (Flow Breccia)	Tuff
Palagonite	Vitric Tuff
Palagonite Tuff	Sandstone

Pillow Breccia	Clay
Pumice	Combinations of Above

2. Weathering/Alteration State -

Unaltered; no visible sign of weathering

Slightly Weathered/Altered; weathering developed on open discontinuity surfaces, but only slight weathering/alteration of rock material

Moderately Weathered/Altered; weathering extends throughout the rock mass, but the rock is not friable

Highly Weathered/Altered; weathering extends throughout the rock mass and the rock material is partly friable

Completely Weathered/Altered; rock is wholly decomposed and in a friable condition, but the rock texture and structure are preserved.

3. Structure -

Massive; brecciated (include description of fragments and matrix)

Faults; spacing of fractures, joints (both intact and closed)

Very wide	10 feet (3 meters) between fractures
Wide	3 to 10 feet (1 to 3 meters) between fractures
Moderately close	1 to 3 feet (0.3 to 1.0 meter) between fractures
Close	0.2 to 1.0 foot (6.1 to 30.5 centimeters) between fractures
Very close	0.2 foot (6.1 centimeters) between fractures

Predominant angle of fracturing

High angle (45 to 90 degrees)
Low angle (0 to 45 degrees)

Predominant type of fractures encountered

- Planar
- Irregular
- Curved
- Stepped
- Hairline
- Drilling Induced

Predominant fracture fillings

<u>Appearance</u>	<u>Mineralogy</u>
Open	Clay
Black	Quartz
White	Zeolite
Light Green	Calcite
Dark Green	Ash or Tuff
Brown	Pyrite
Blue	Other
Clear Amorphous	
Clear Crystalline	

If fractures are filled with clay or contain mineralization, give average fracture thickness and/or unusual thickness

Predominant fracture roughness

Smooth
Rough
Polished
Slickensided

4. Color - note on cover sheet stating all core is dark gray or black, unless otherwise noted.

5. Texture -

Aphanitic; individual crystals not visible to the unaided eye

Phaneritic; composed of grains individually visible to the unaided eye

Fine grained - <1 millimeter
 Medium grained - 1 to 5 millimeters
 Coarse grained - >5 millimeters

Porphyritic; describe percent, size, and mineral type of the phenocrysts

Vesicular; describe percent, size, and shape of vesicles

Amygdaloidal; describe percent, size, shape, and filling material of vesicles

Other terms as applicable

6. Hardness or Strength - note on cover sheet that all core is hard, unless otherwise noted.

The procedures used for the detailed line mapping at the NSTF are an adaptation of those developed by the consulting firm of Pincock, Allen, and Holt (Call and Others, 1976) (Figure A-2). It was used originally for the probabilistic joint analysis in evaluating slope stability, but was utilized here to characterize the jointing of the Pomona II flow. The parameters recorded are:

1. The distance is measured where the joint or its projection intersect the tape. For fractures parallel to the line, the distance where the observation is made is recorded.
2. The rock type in which the mapping is being conducted is recorded under Rock Type A.
3. Identification of the geologic structure is recorded.
4. Strike and dip are recorded as azimuth using a right-hand convention where the dip is always 90 degrees clockwise to strike. This method defines the orientation by a two-number designation. For wavy features, an average dip is recorded. A minimum dip on the flattest observable portion of the joint surface should be recorded to compare with the average dip. This deviation in dip is a quantitative measure of the waviness of the joint surface.
5. Waviness on a scale of 4 inches (10 centimeters) or more is given a qualitative rating consisting of three categories of waviness: planar; wavy; and irregular.
6. Length of the feature is the maximum traceable distance observed. This measurement often extends beyond the mapping zone and is limited by tunnel dimensions and support systems.
7. The overlap measurement is made along the maximum trace length of the joint. The length is recorded from the bottom termination to the line. If the fracture terminates below the line, a minus distance is recorded. When the bottom of the joint is above the line, a plus distance is recorded. A measurement is not recorded for joints with traces parallel to the line (Figure A-3).
8. The manner in which a joint terminates is described according to five classes: in rock; none; en echelon; high-angle against another fracture (720 degrees); and low-angle against another fracture (<20 degrees). The termination of both ends of the fracture is described (Figure A-4).
9. Roughness is a qualitative rating of small irregularities on the fracture surface. Two categories are considered; smooth and rough.

DATA SHEET FOR DETAIL LINE MAPPING

PAGE 1 OF 1

BY _____

BEARING PLUNGE STRIKE DIP LINE NO. ELEV. LOCATION DATE BY

EXAMPLE

ROCK TYPE ABBREVIATIONS		STRUCTURE TYPE		GEOMETRY	
		SJ	SINGLE JOINT	P=PLANARITY-P.W.I	R=ROUGHNESS-S.R
		FT	FAULT	M=MINIMUM DIP	
		CT	CONTACT		TERMINATION
				H >20°	R IN ROCK
				L <20°	N NONE
					E EN ECHELON
WATER D=DRY W=WET F=FLOWING S=SQUIRTING		OVERLAP			
FILLING ABBREVIATIONS		MEASURED FROM TAPE ALONG TRACE			
N	NONE	OR PROJECTED TRACE TO BOTTOM			
		OF JOINT			
		+ ABOVE TAPE - BELOW TAPE			

BCP8007-99

FIGURE A-2. Data Sheet for Detail Line Mapping.

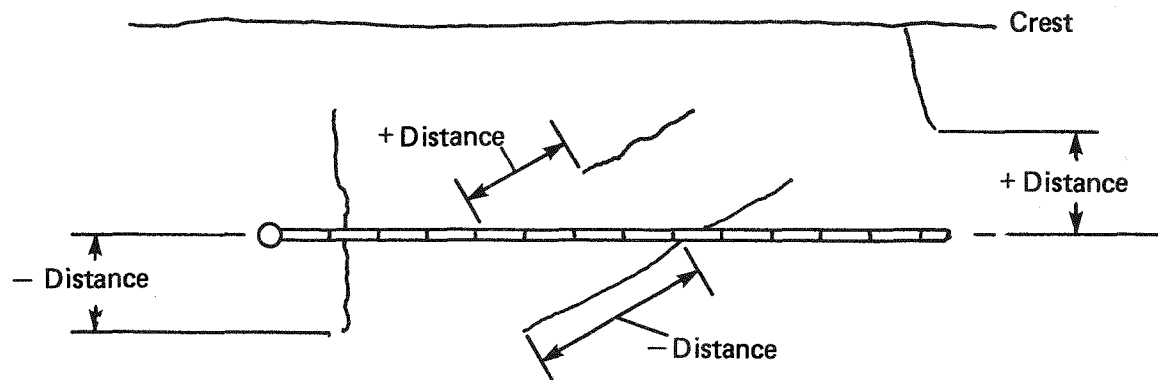


FIGURE A-3. Distance Measurements.

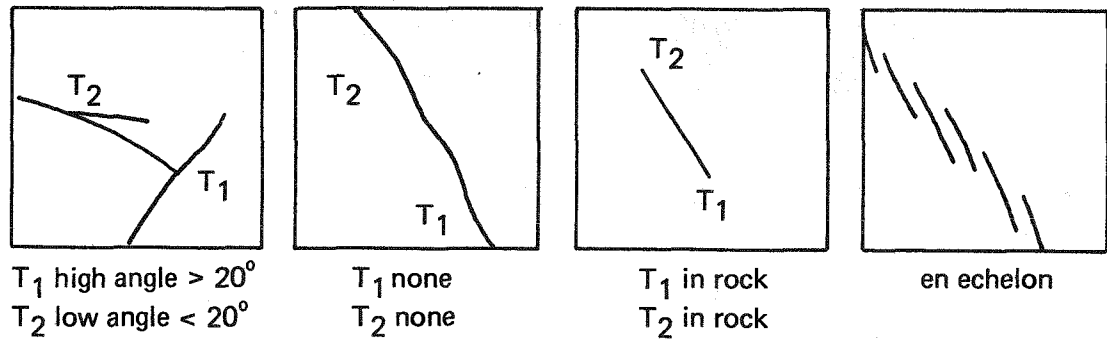


FIGURE A-4. Joint Terminations.

10. The fracture thickness is recorded as the width of in-filling material between the joint surfaces.
11. The filling material is recorded using a code appropriate to the material being observed.
12. Water conditions are recorded using the designations moist, wet, or flowing.

RHO-BWI-ST-8

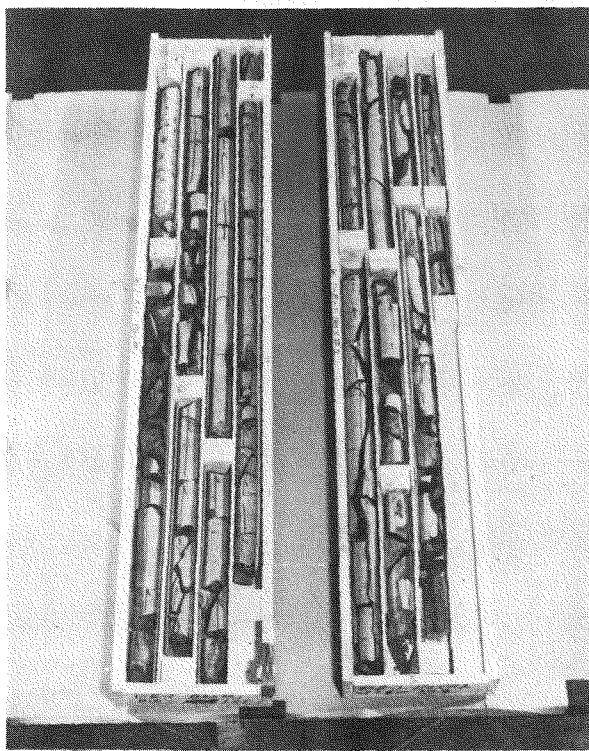
APPENDIX B
PHOTOGRAPHS OF INSTRUMENT BOREHOLE CORE

APPENDIX B

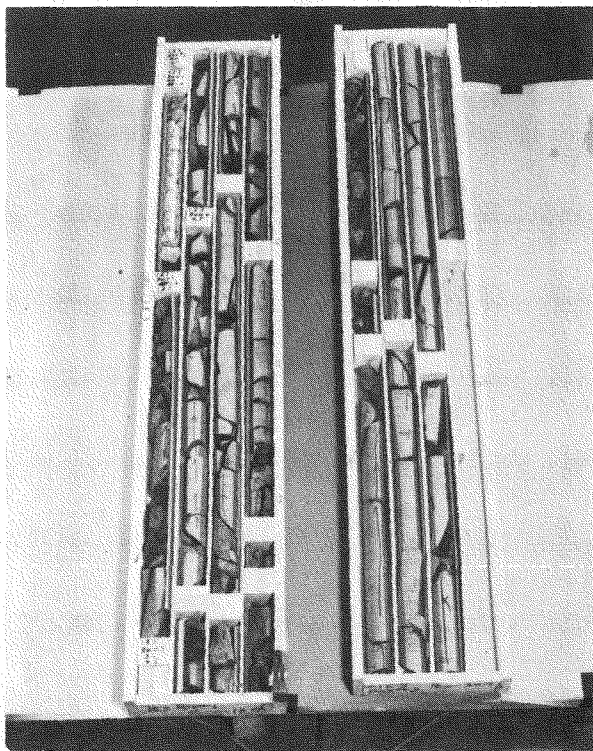
PHOTOGRAPHS OF INSTRUMENT BOREHOLE CORE

The following are photographs of the principal boreholes used for the data analysis. The remaining borehole photographs and photographs of the walls of the main heater holes in Full-Scale Heater Tests #1 and #2 are located in the Basalt Waste Isolation Project Library.

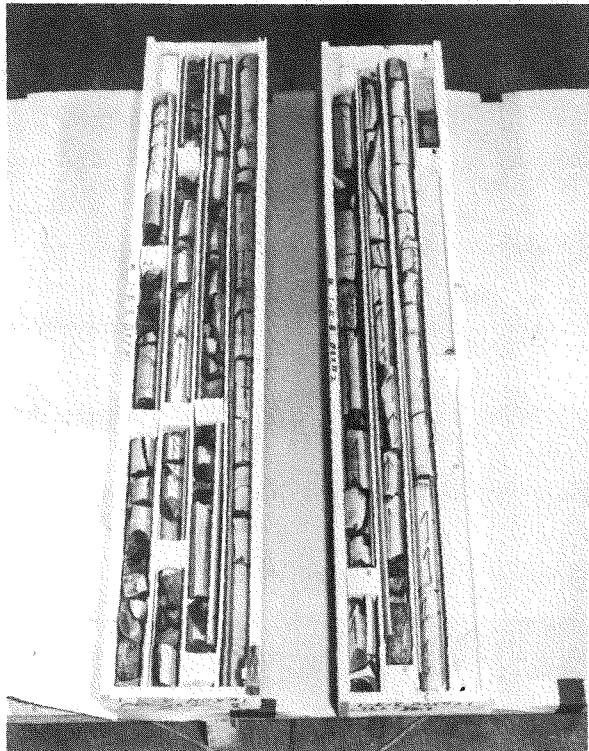
RHO-BWI-ST-8



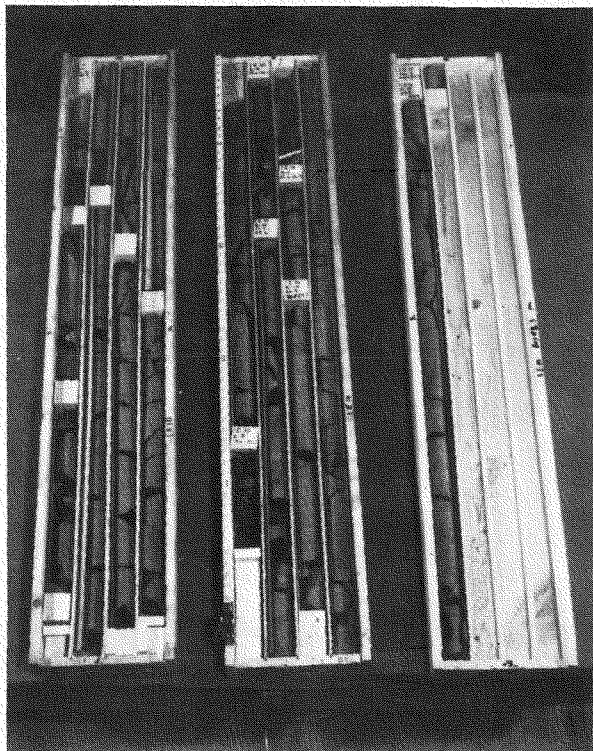
1E1



1E3



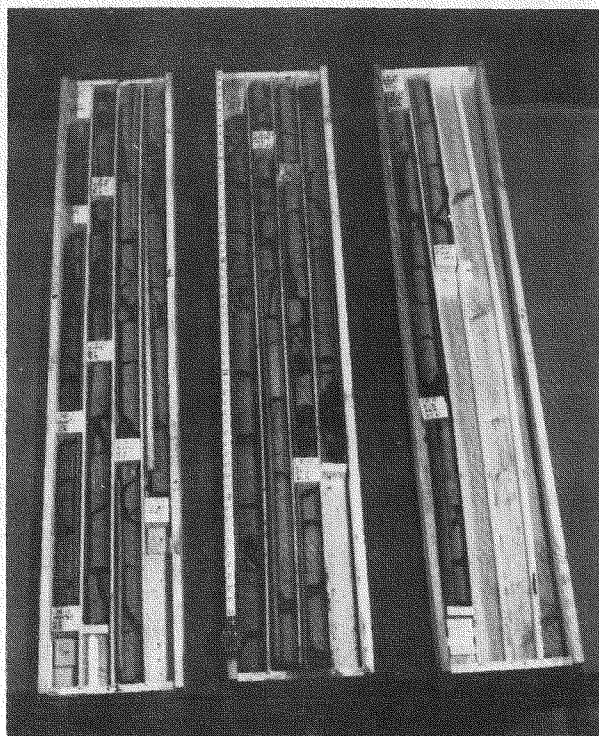
1E8



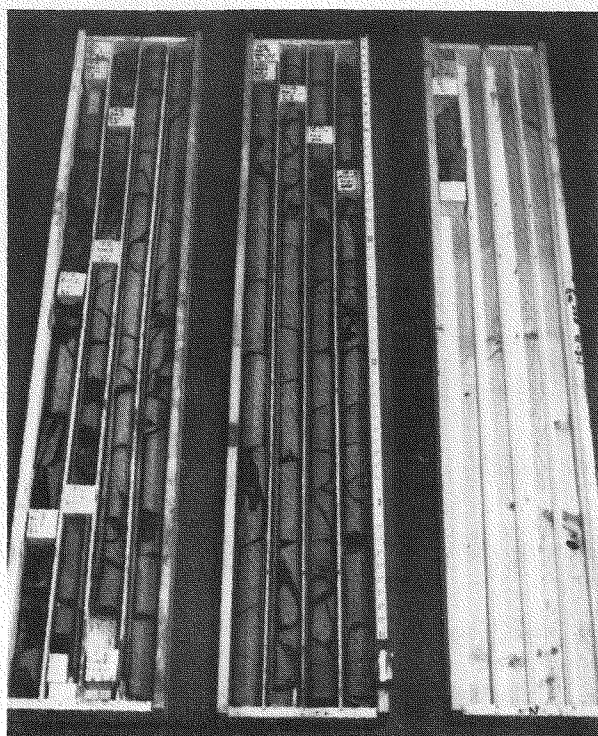
1E10

RCP8007-163

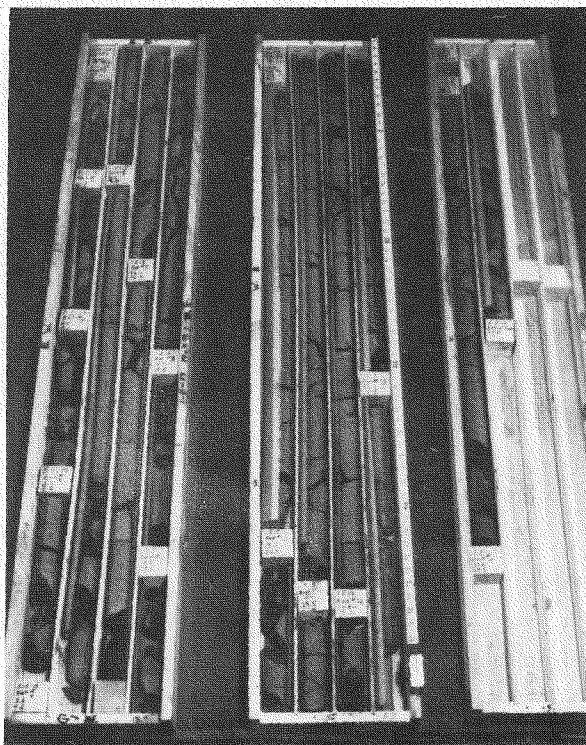
B-3



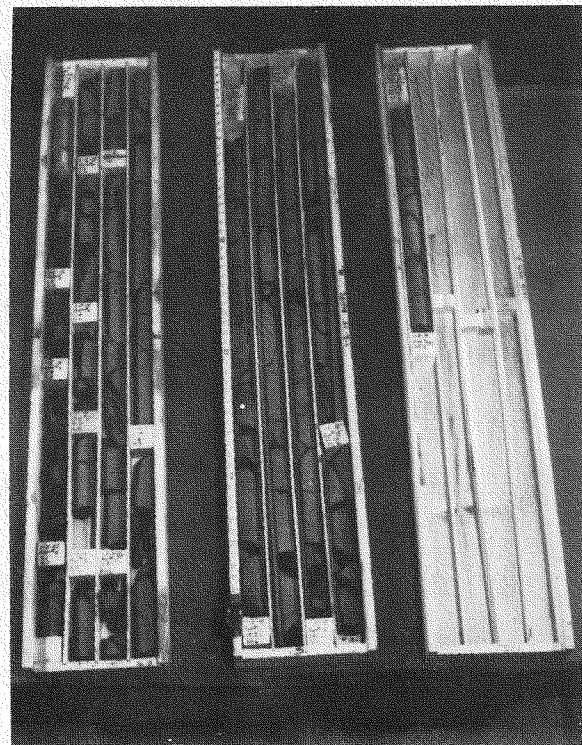
1E11



1E12



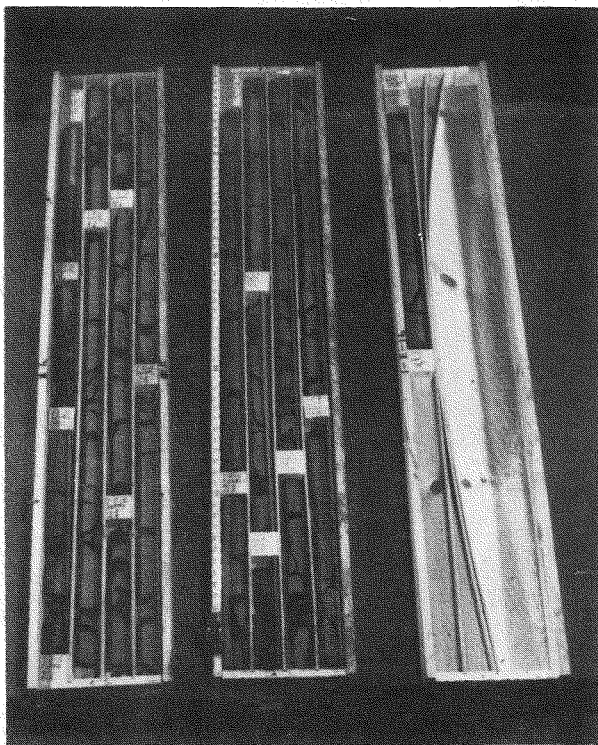
1E13



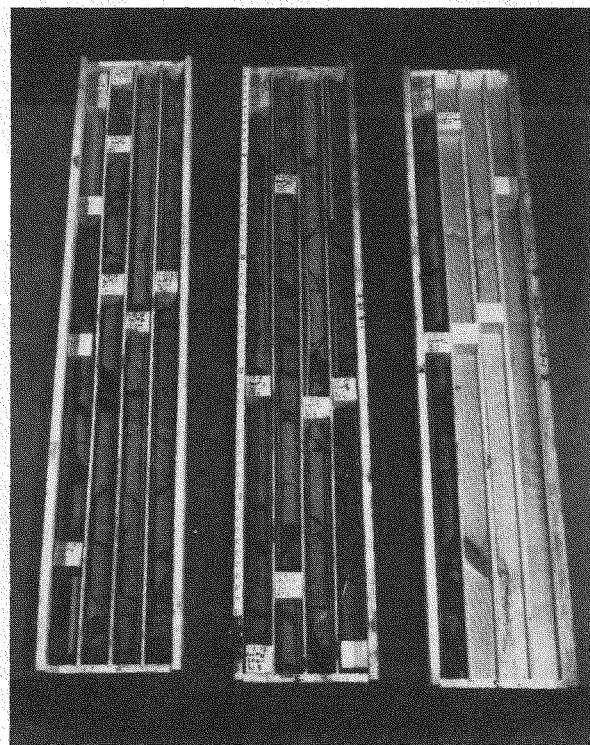
1E15

RCP8007-164

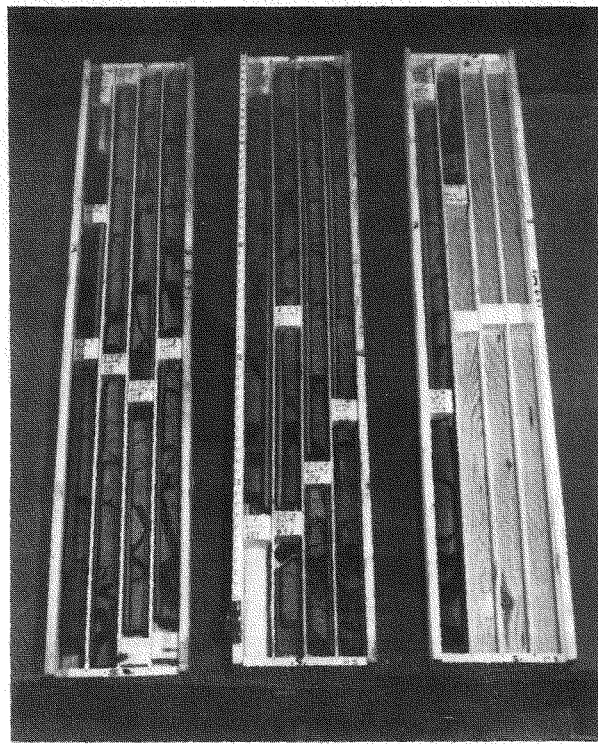
RHO-BWI-ST-8



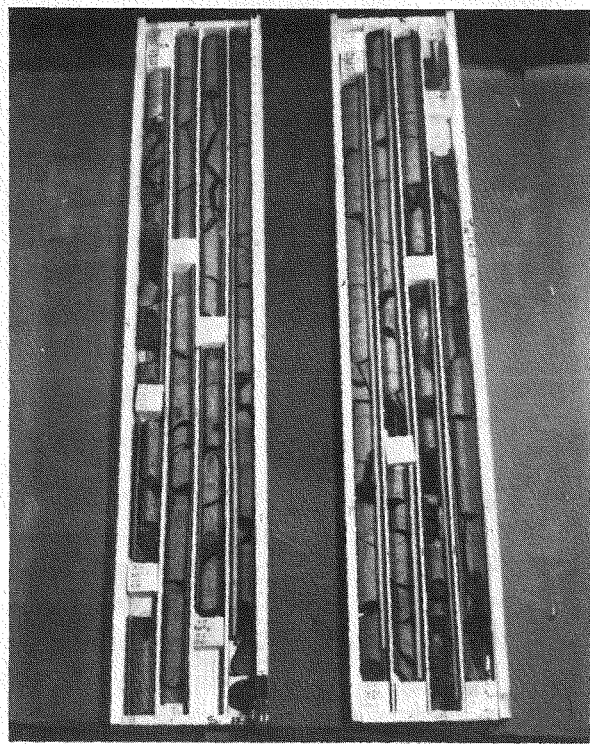
1E16



1E17



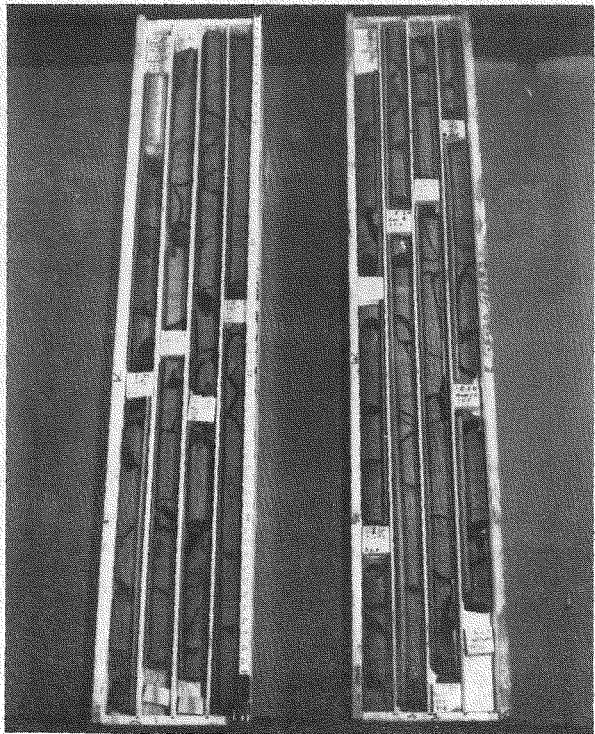
1E18



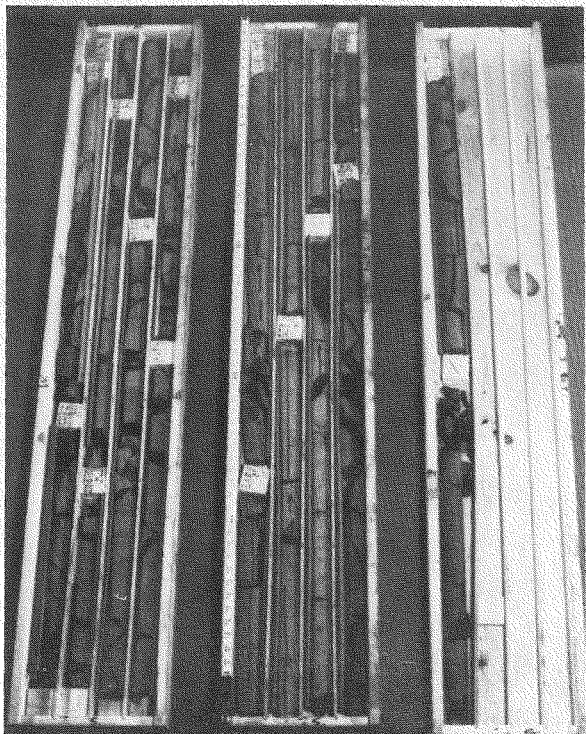
1E19

RCP8007-165

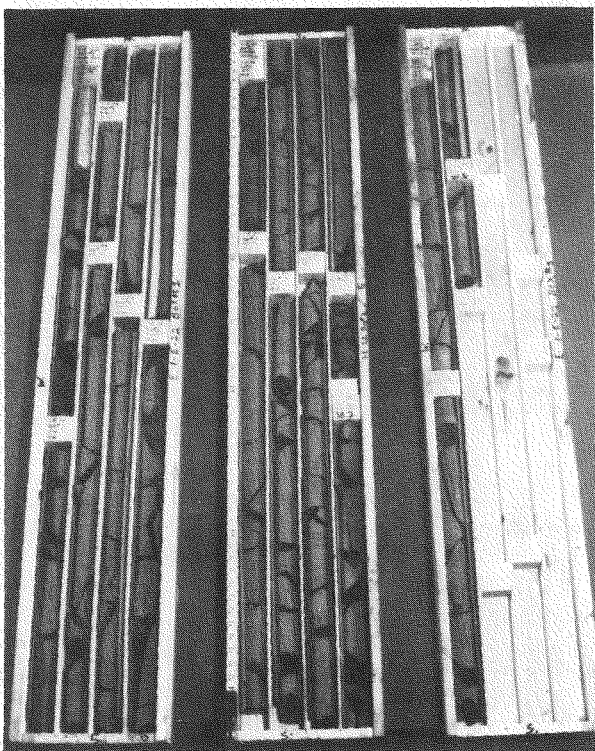
B-5



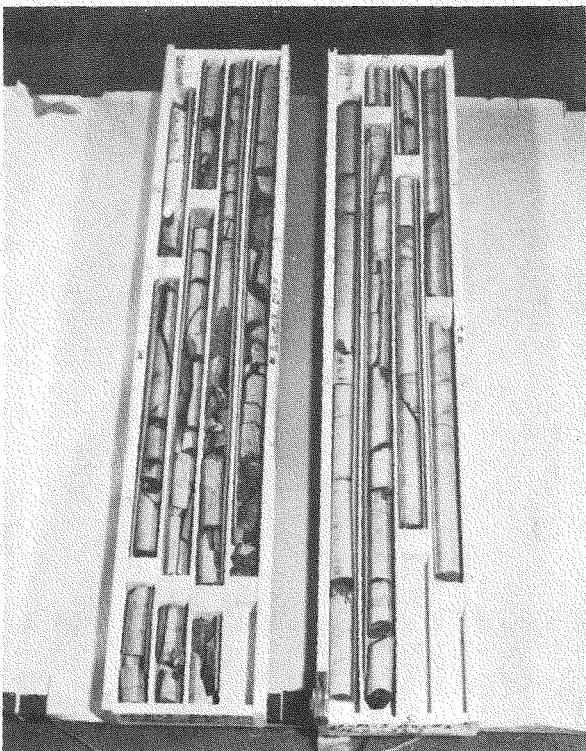
1E20



1E21



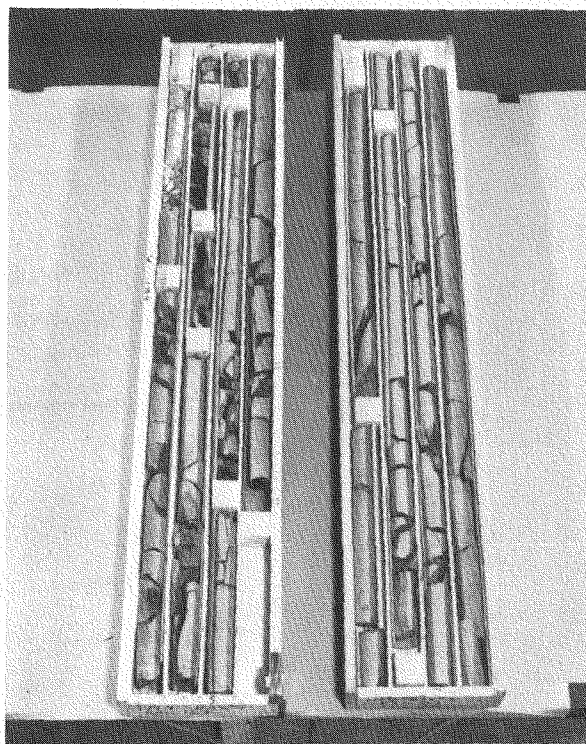
1E22



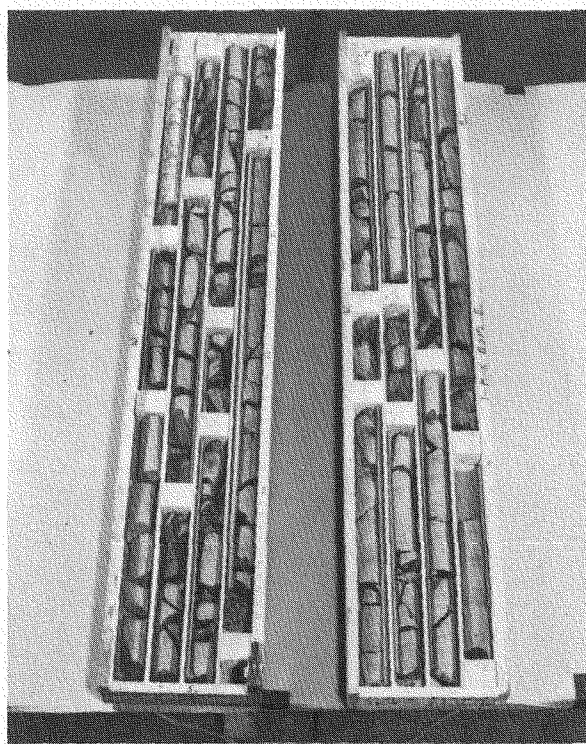
1M3

RCP8007-166

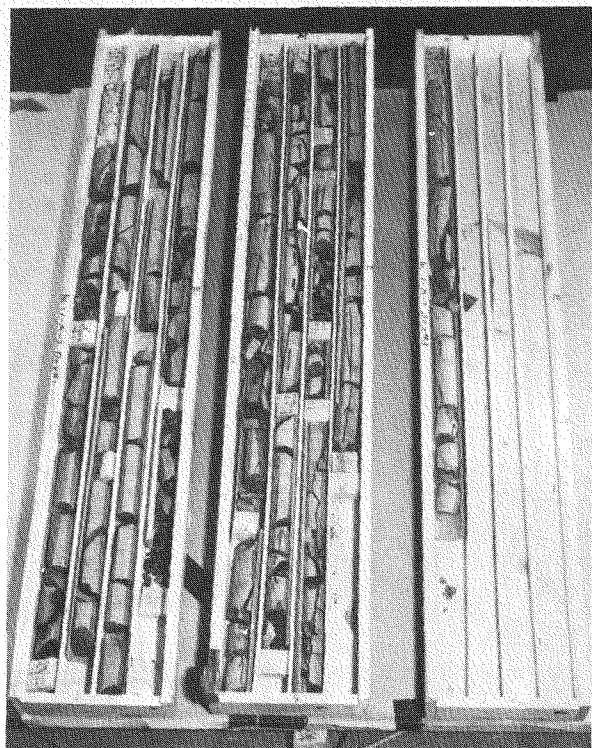
RHO-BWI-ST-8



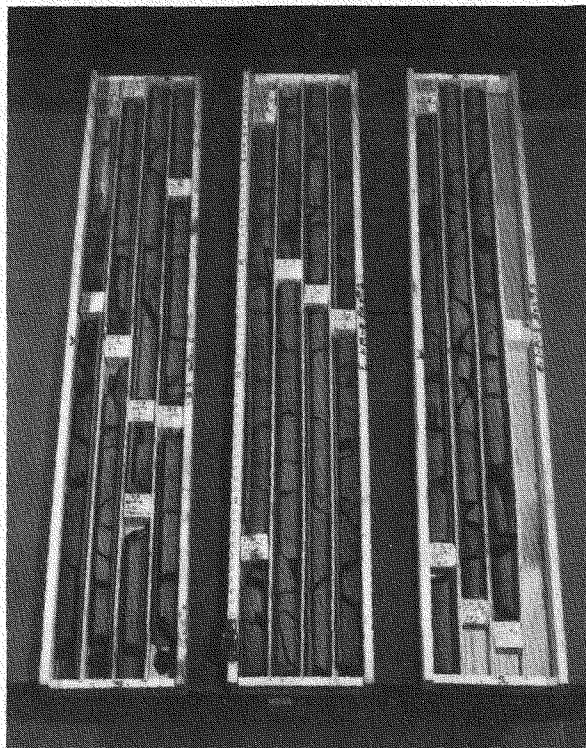
1M4



1M5



1M7

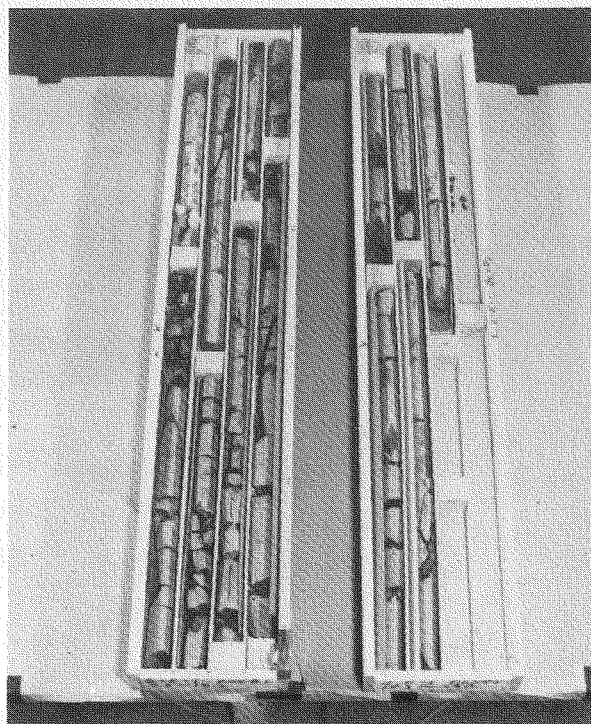


1M8

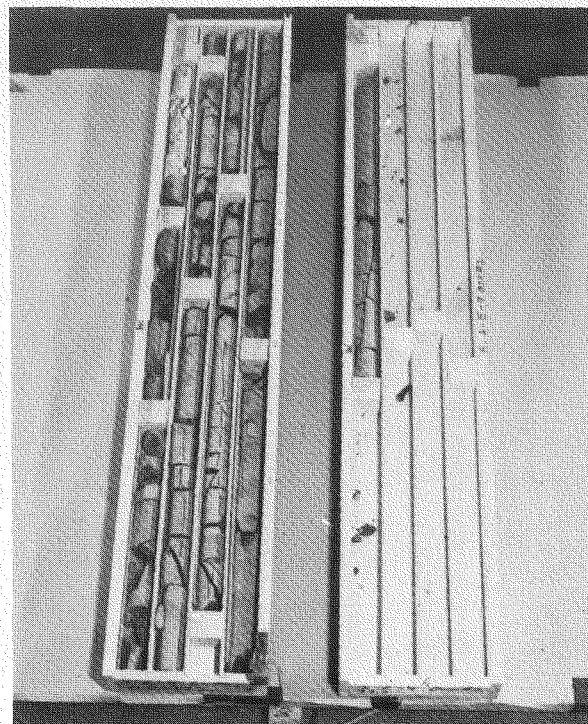
RCP8007-167

B-7

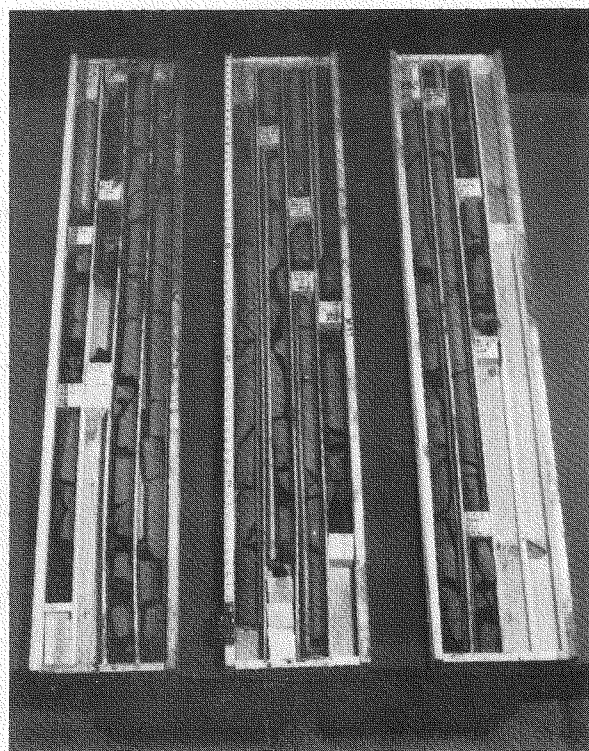
RHO-BWI-ST-8



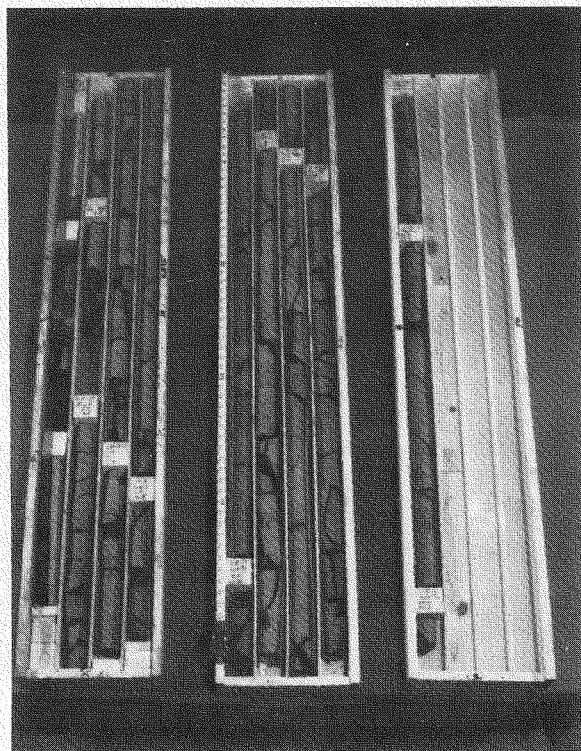
2E1



2E9



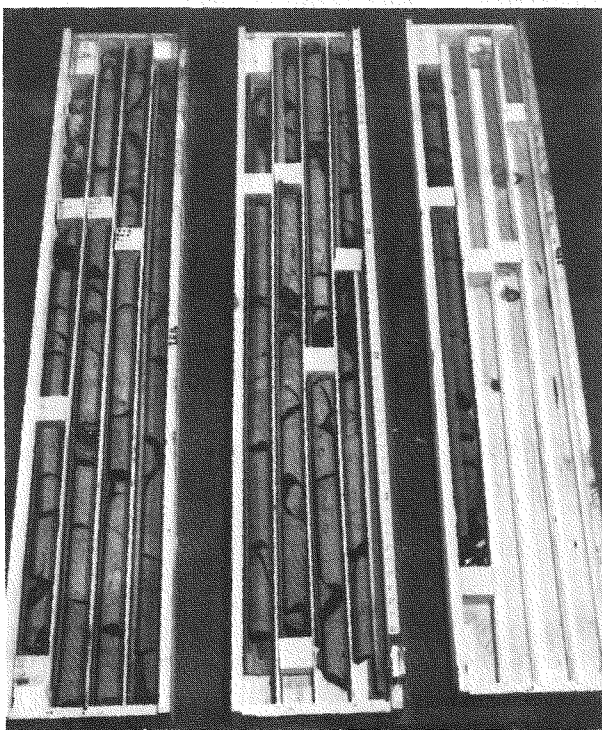
2E14



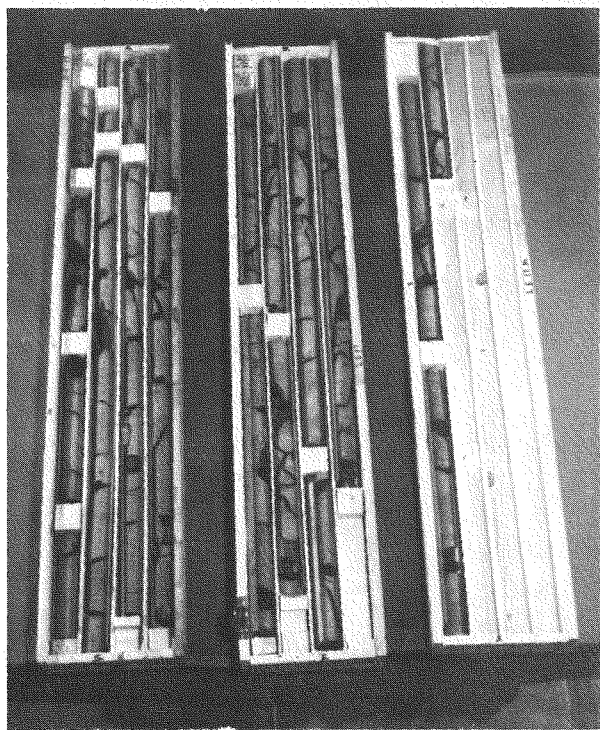
2E15

RCP8007-168

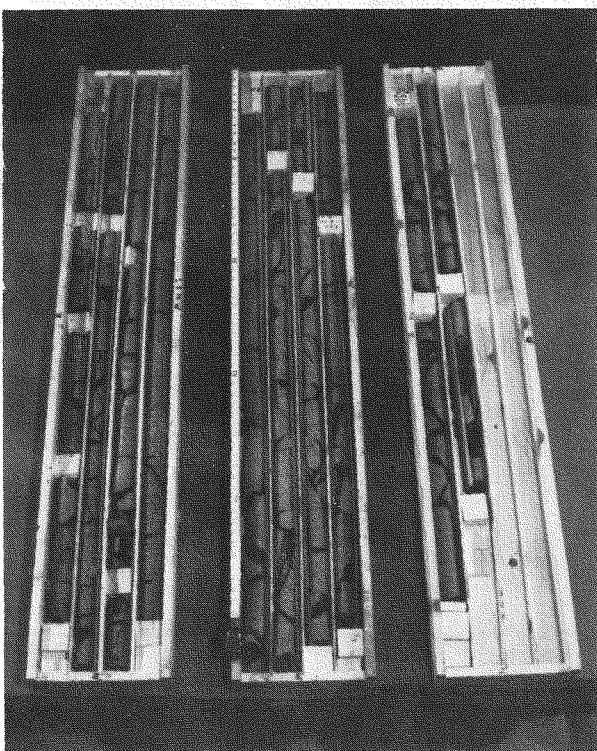
RHO-BWI-ST-8



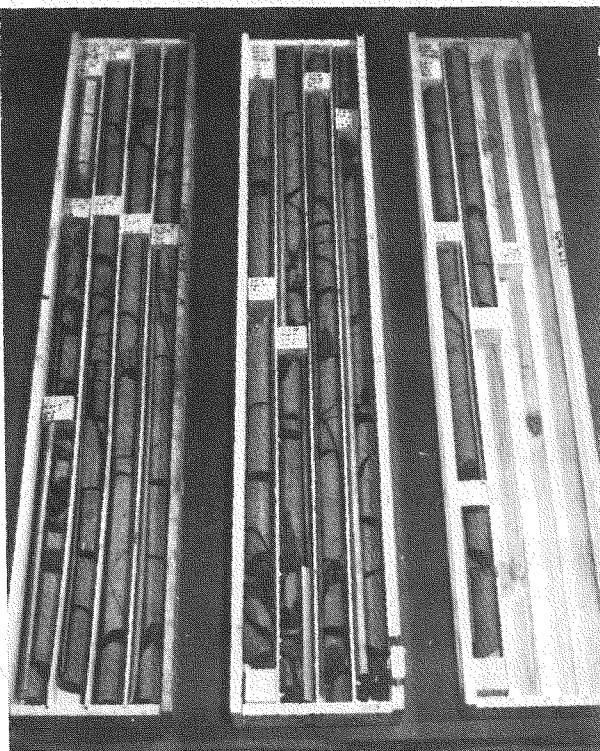
2E16



2E17



2E18

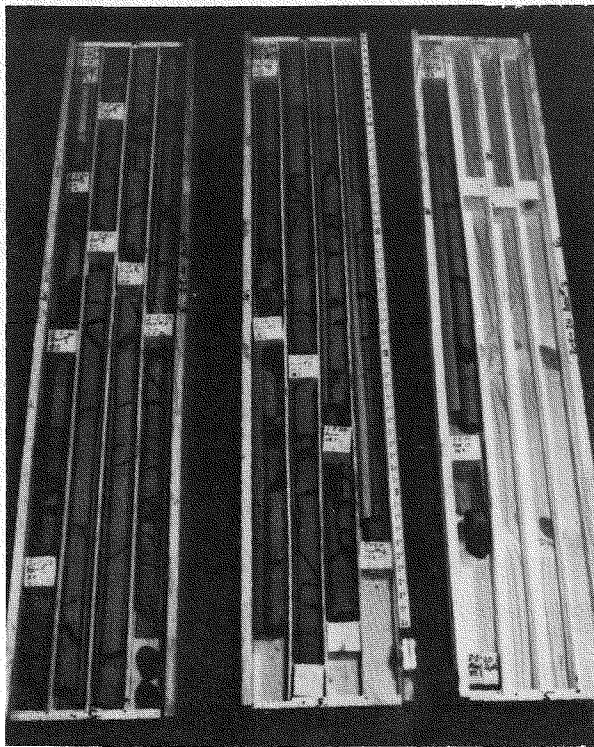


2E19

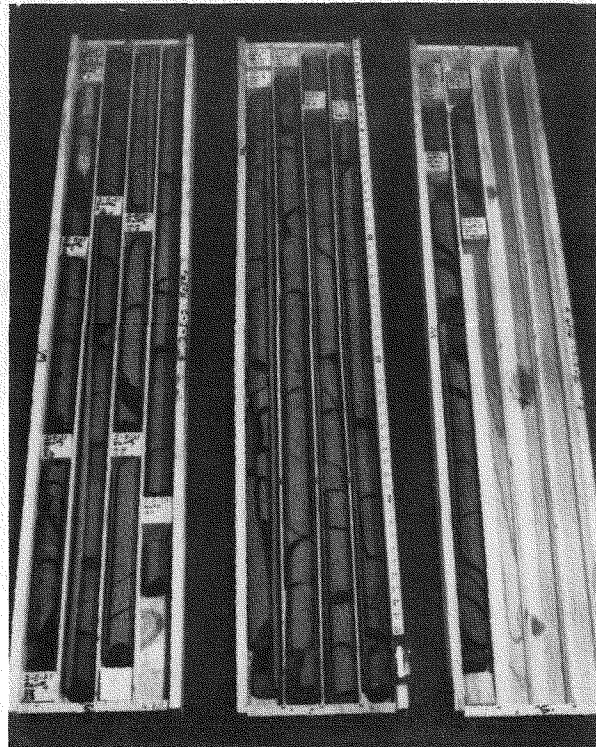
RCP8007-169

B-9

RHO-BWI-ST-8



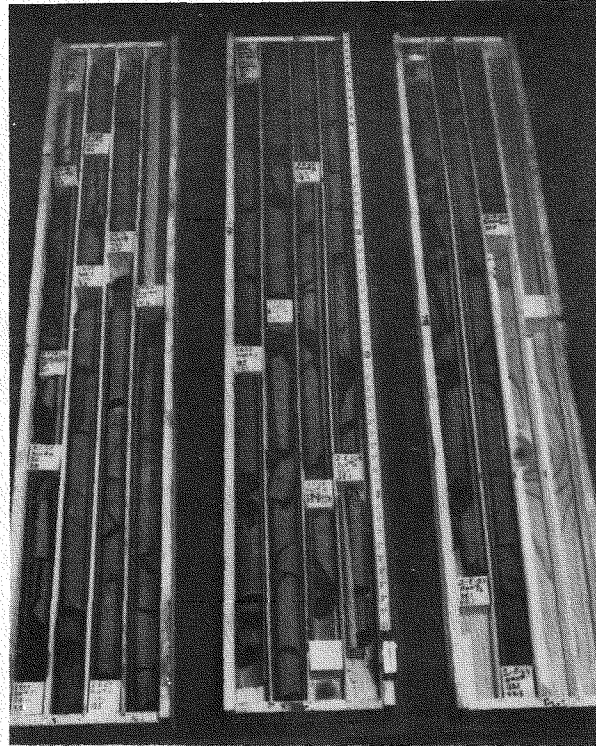
2E20



2E21



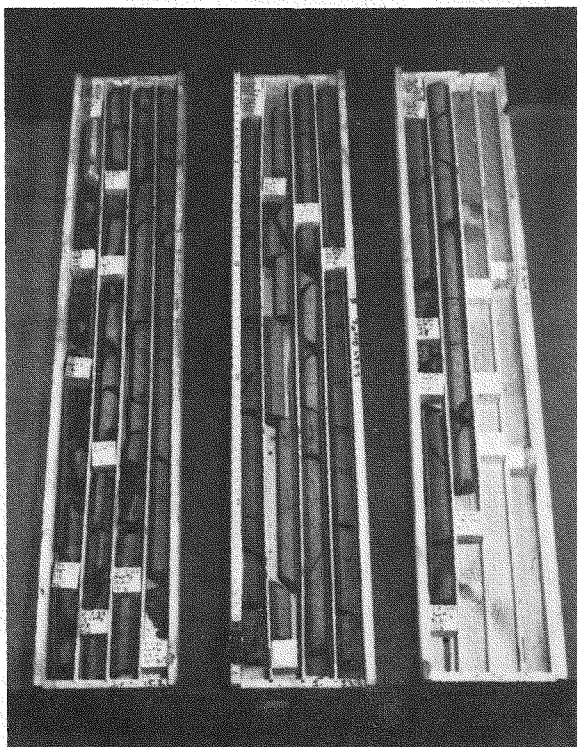
2E22



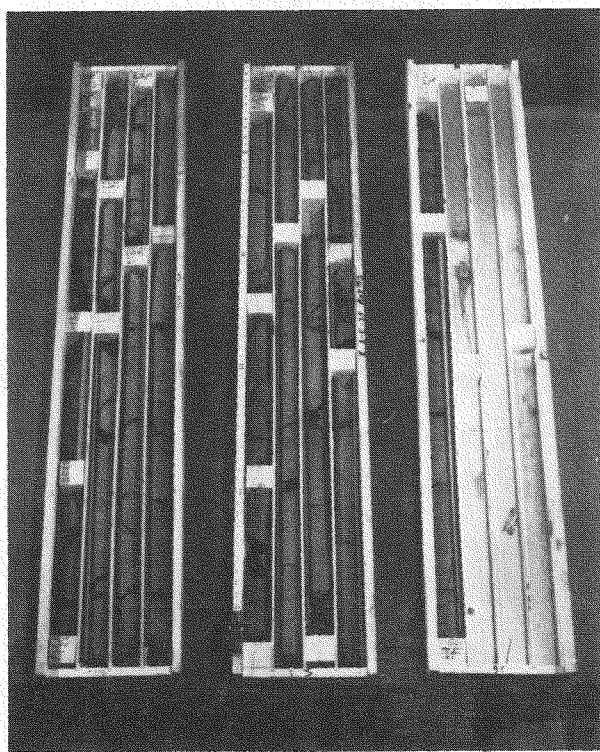
2E23

RCP8007-170

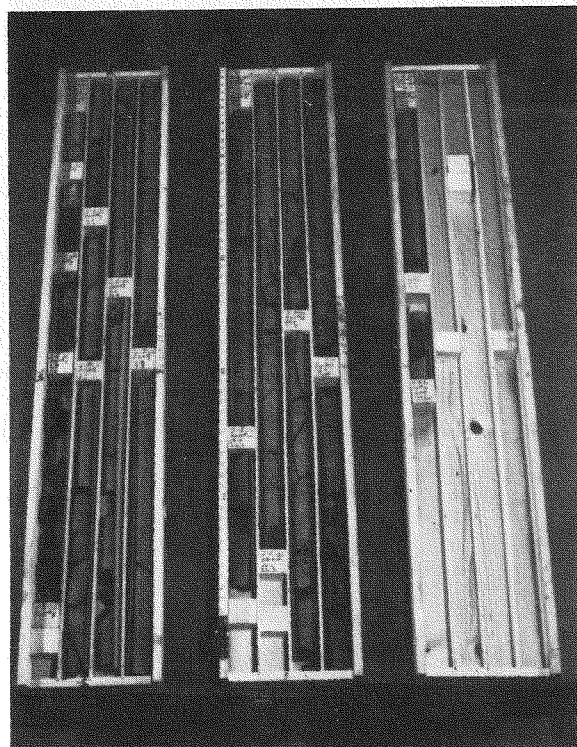
RHO-BWI-ST-8



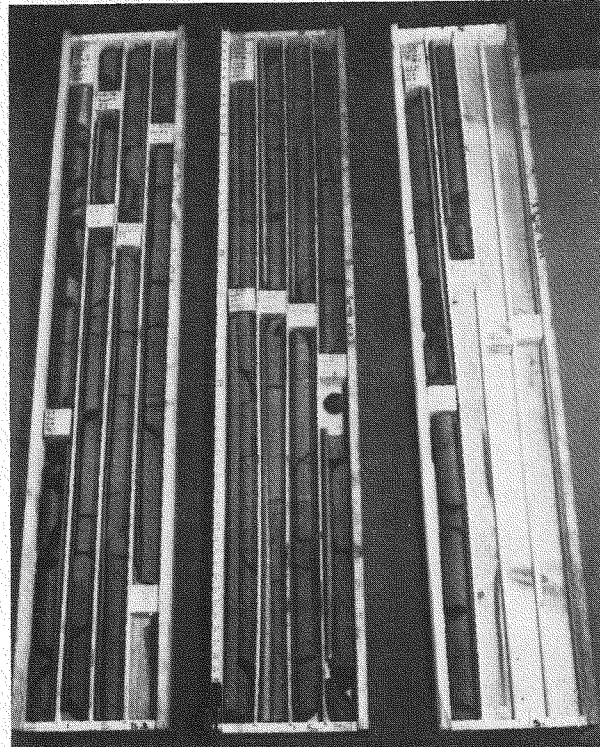
2E24



2E25



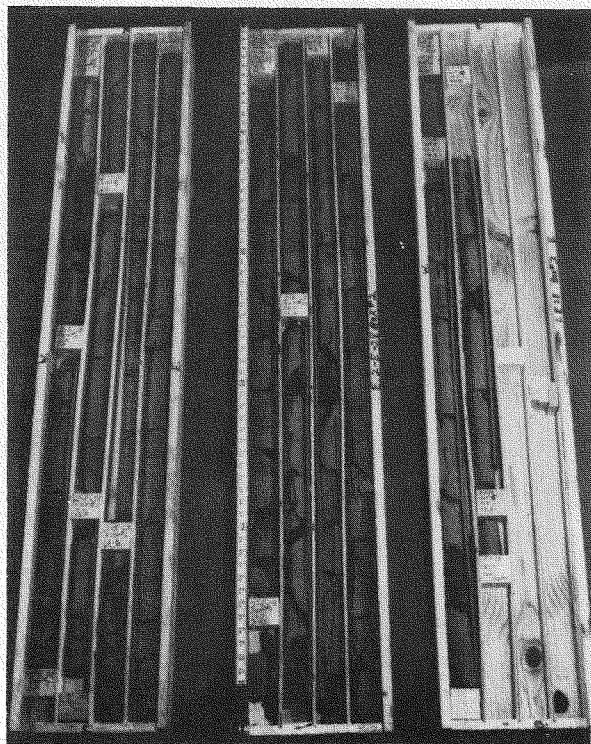
2E26



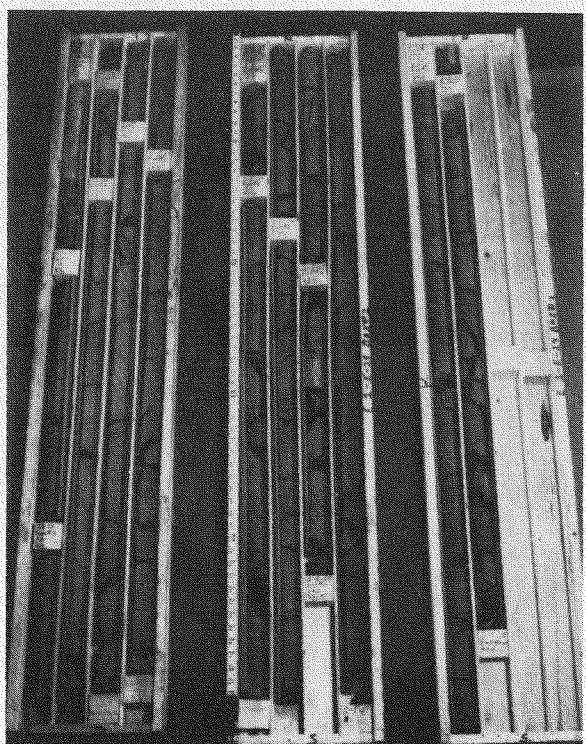
2E27

RCP8007-171

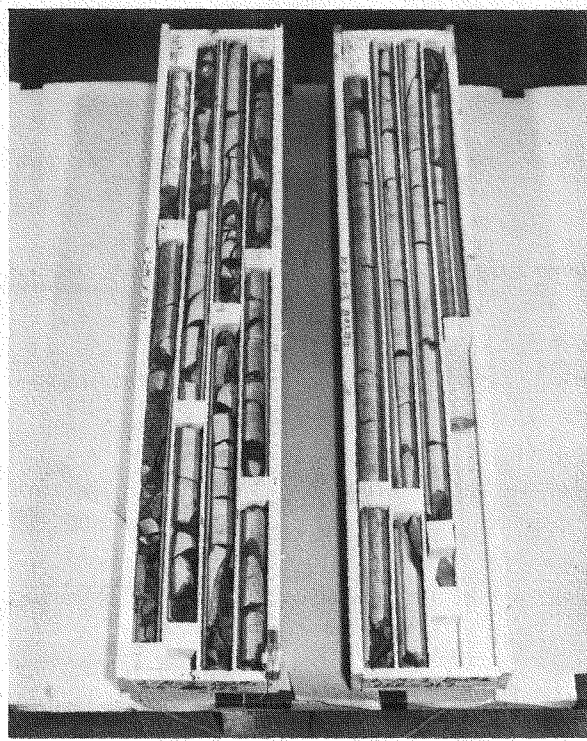
RHO-BWI-ST-8



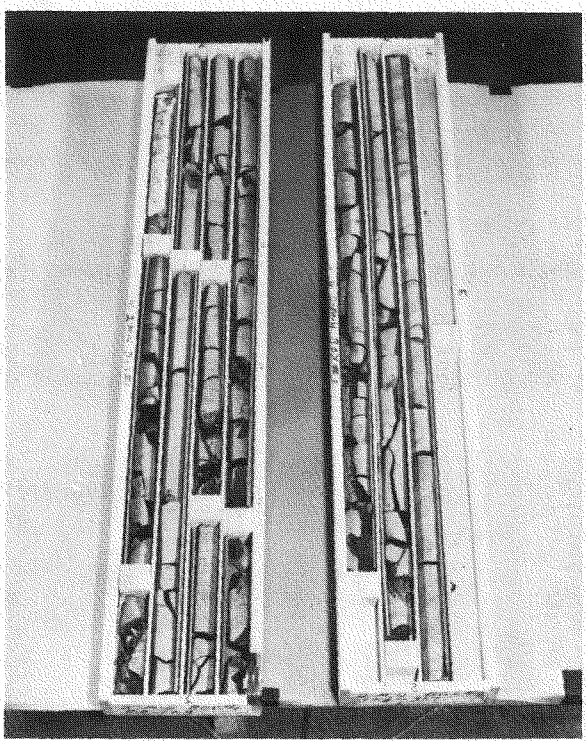
2E28



2E29



2M3

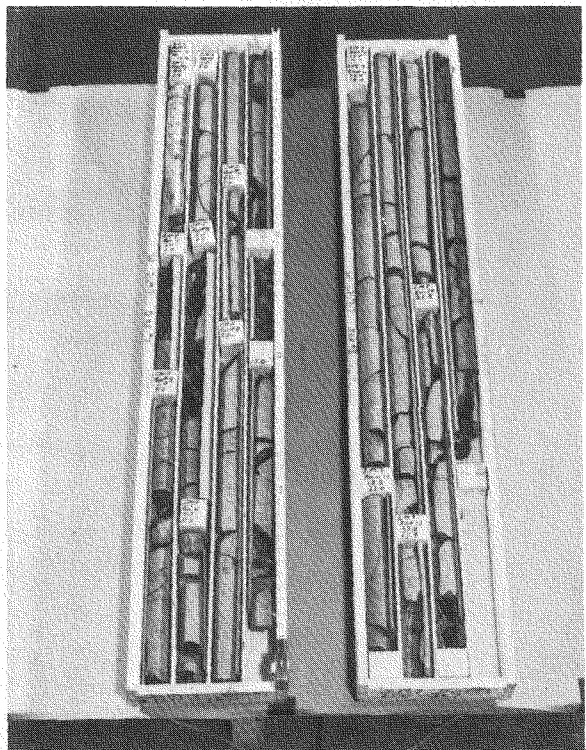


2M4

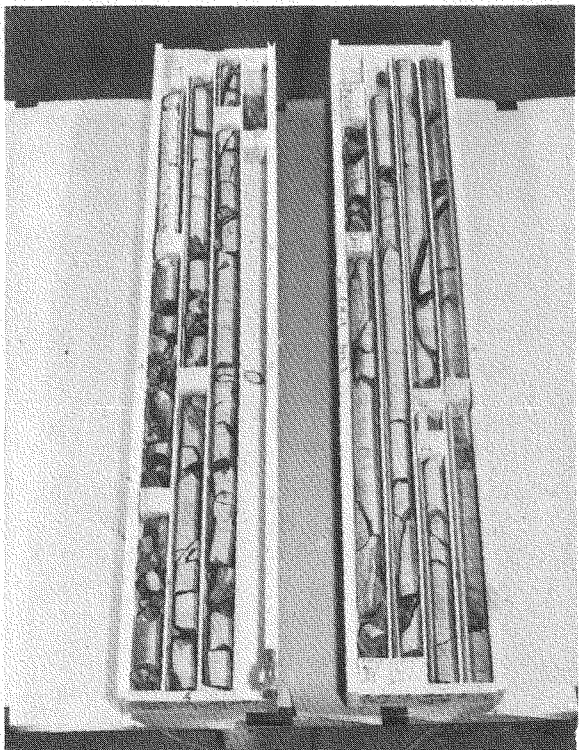
RCP8007-172

B-12

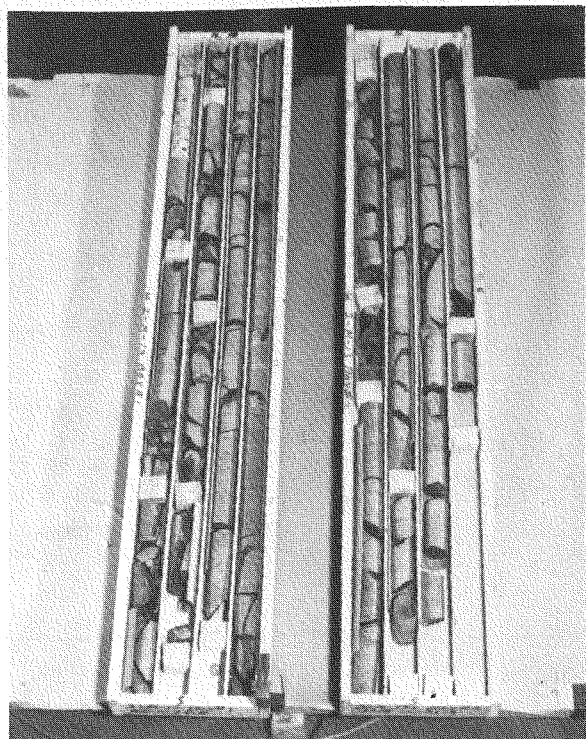
RHO-BWI-ST-8



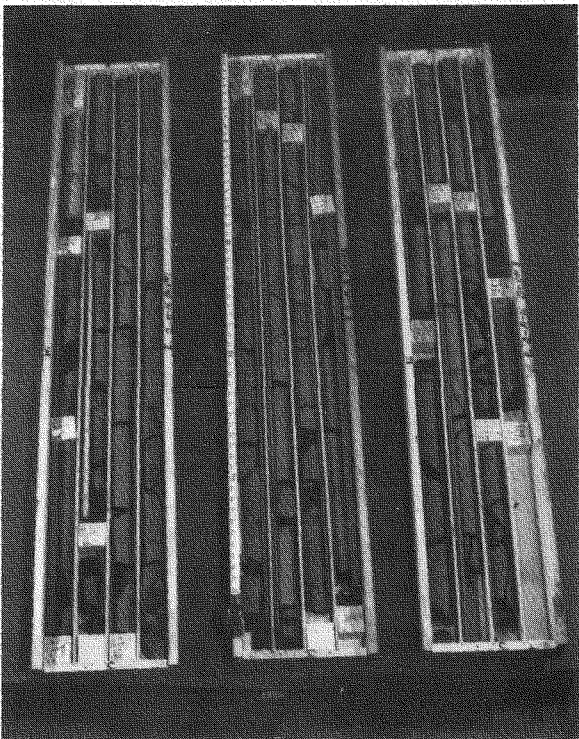
2M7



2M12



2M13



2M16

RCP8007-173

B-13

APPENDIX C

GRAPHS AND TABLES OF JOINT CHARACTERISTICS

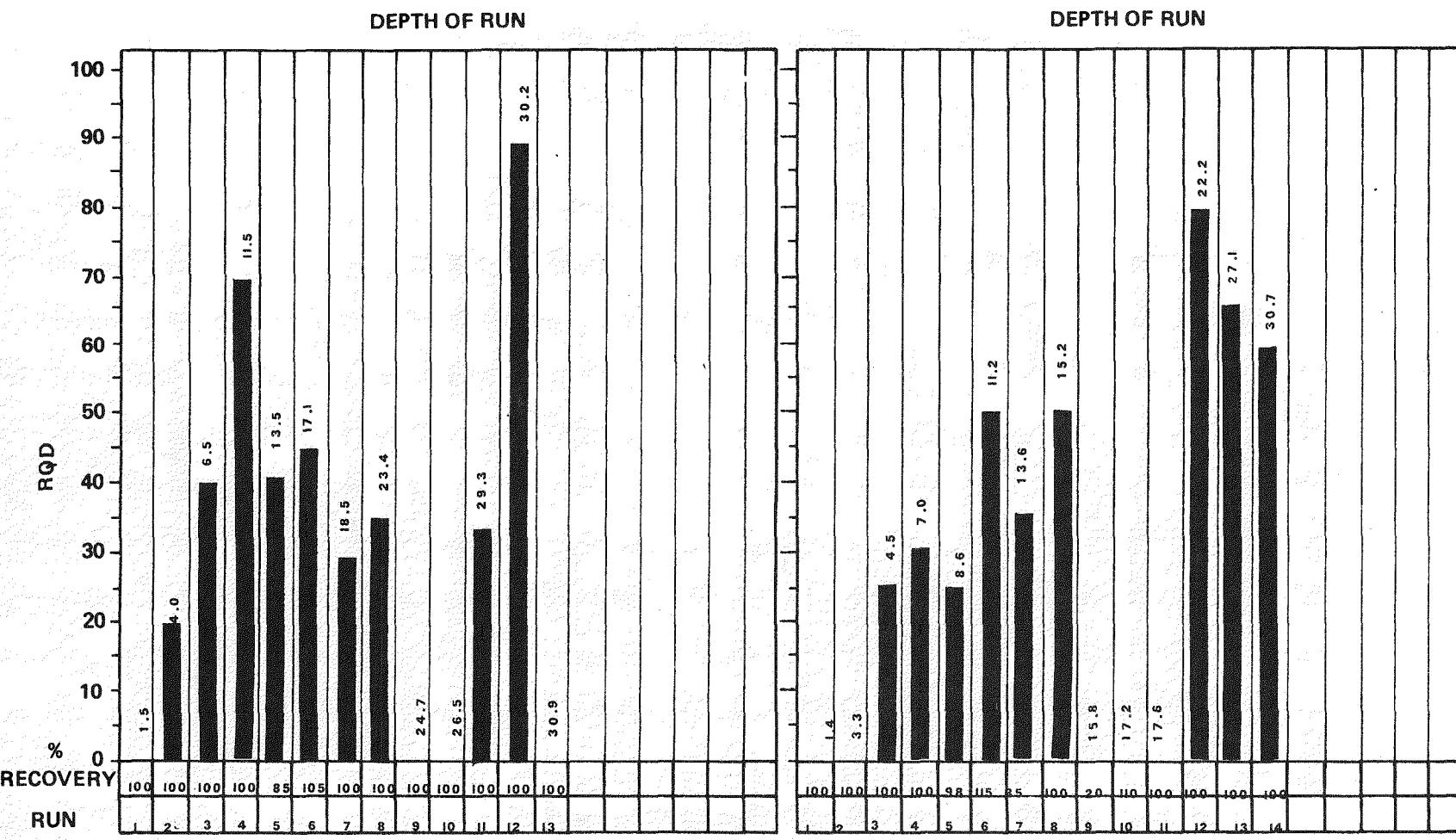
APPENDIX C

GRAPHS AND TABLES OF JOINT CHARACTERISTICS

The following histograms present the rock-quality designation values and core recovery of each core run for the boreholes of Section A-2-1. The number at the end of each bar is the borehole depth (in feet) for the end of each run.

These boreholes are the principal holes used in the data analysis of the 12 blocks in each of the Full-Scale Heater Tests.

C-3



HOLE IE1
DEPTH 30.6

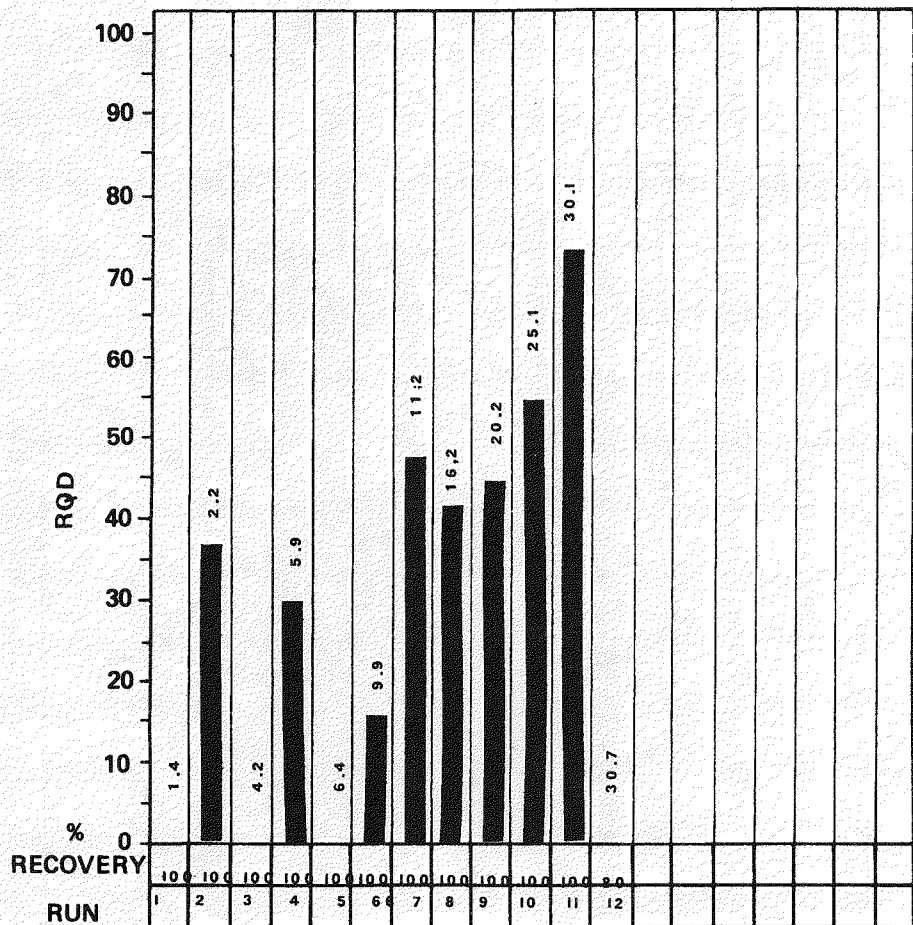
HOLE IE3
DEPTH 30.7

RCP8007-72

RHO-BWI-ST-8

C-4

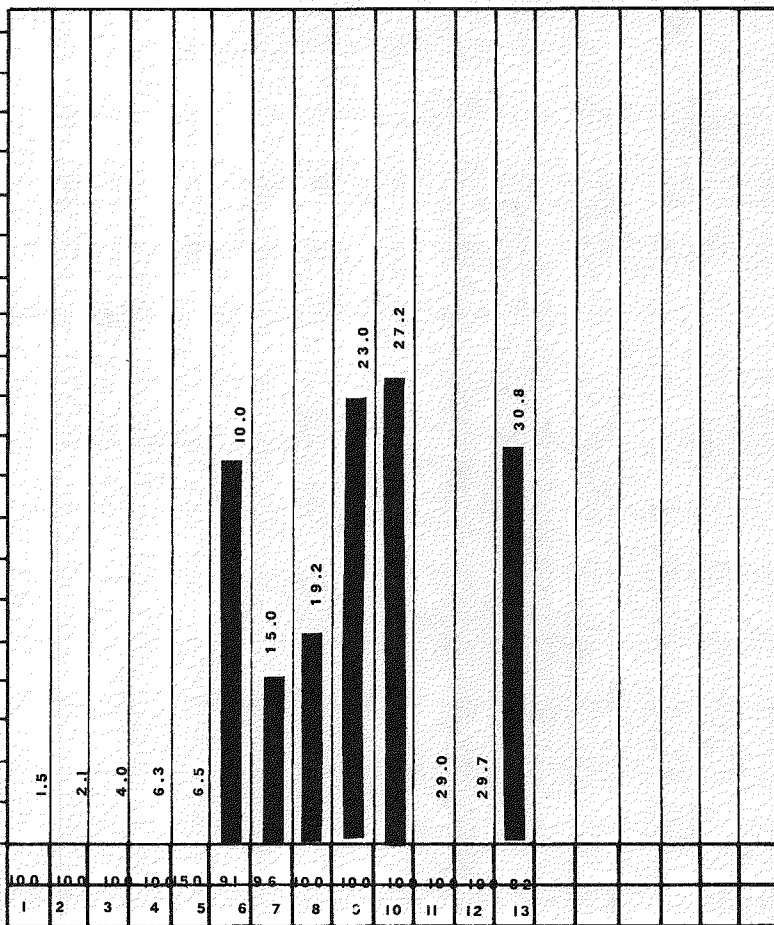
DEPTH OF RUN



HOLE IE8

DEPTH 30.7

DEPTH OF RUN



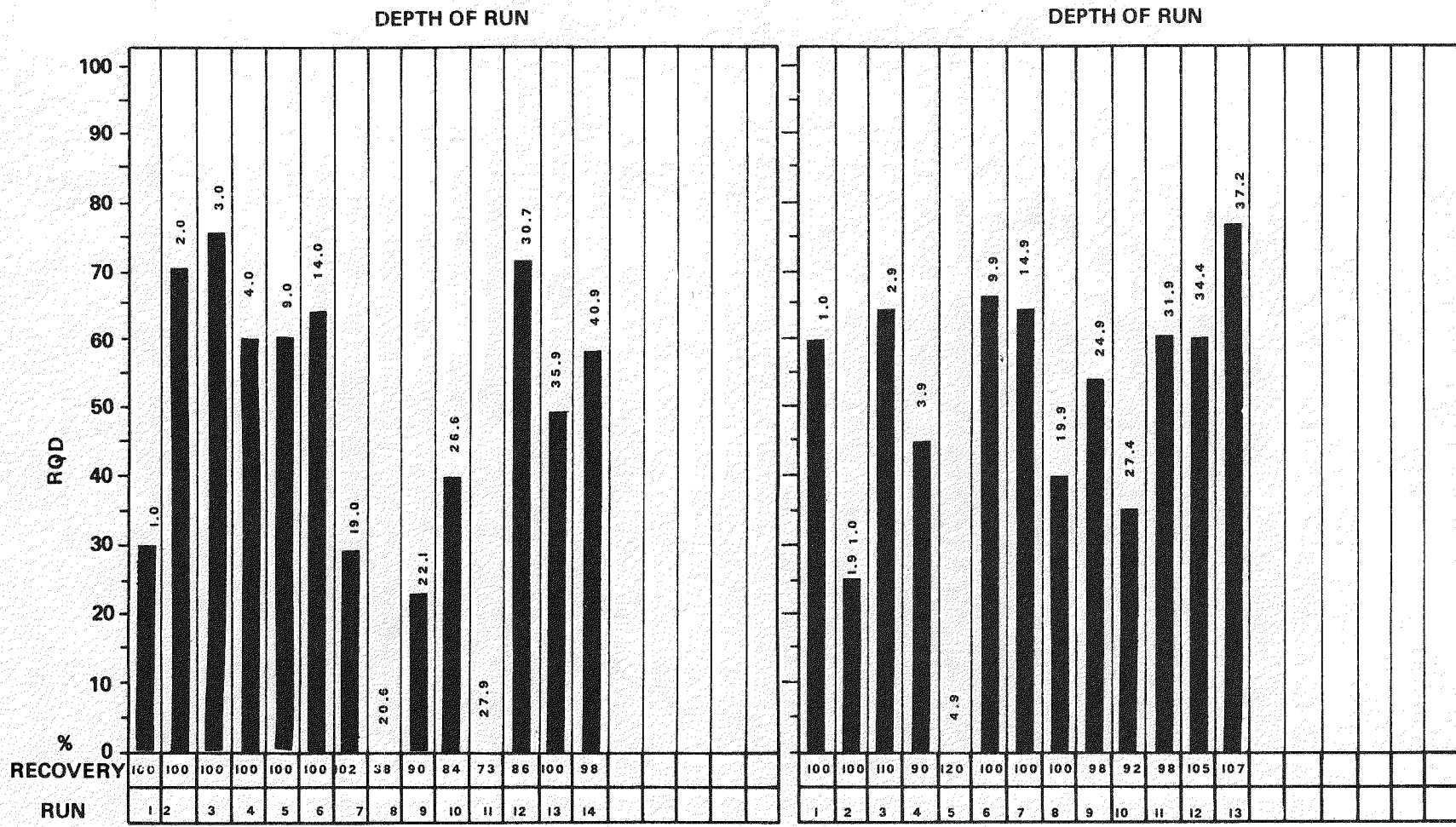
HOLE IE9

DEPTH 30.8

RCP8007-73

RHO-BMI-ST-8

C-5



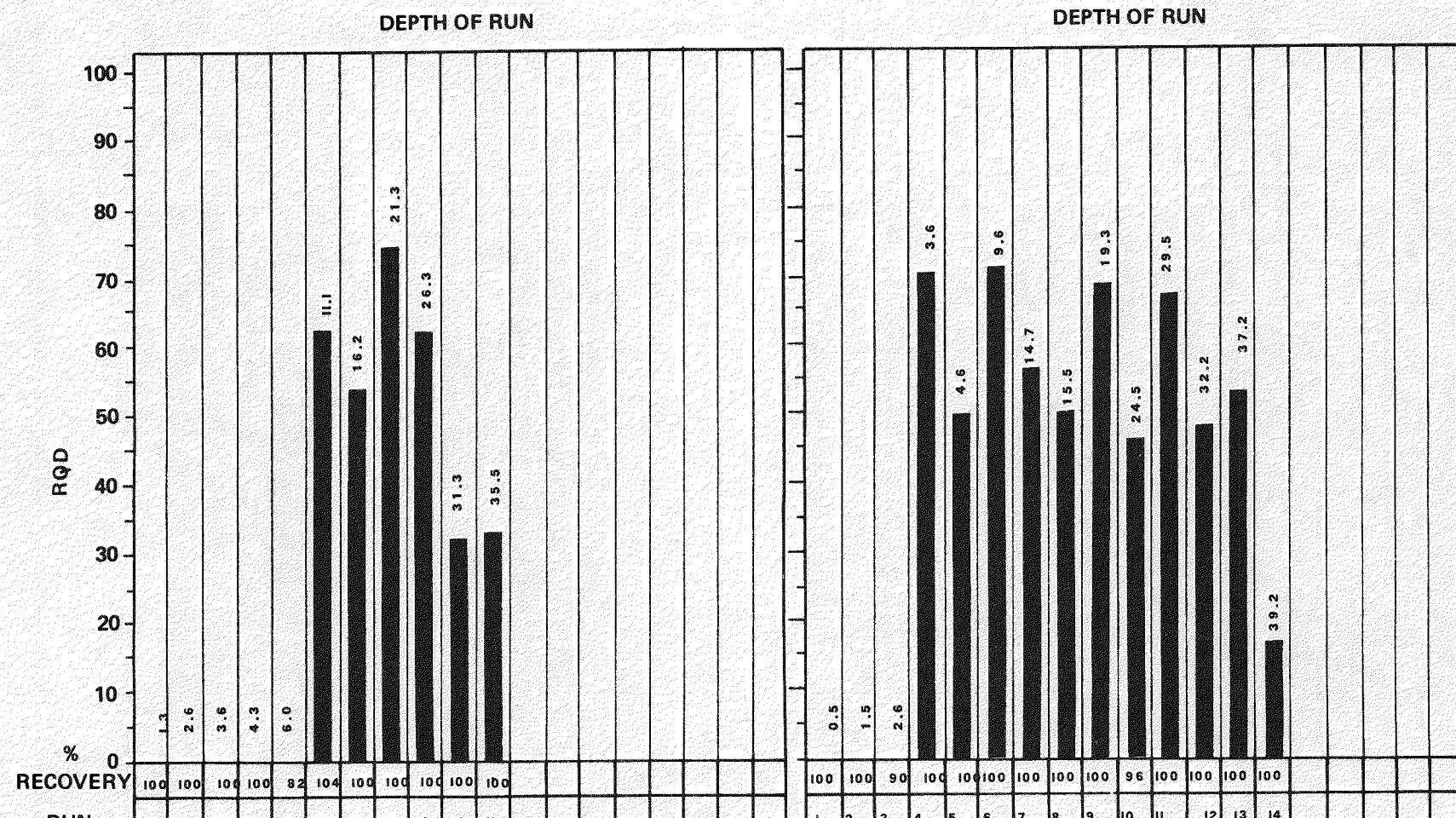
HOLE IE10
DEPTH 40.9

HOLE IE11
DEPTH 37.2

RCP8007-74

RHO-BWI-ST-8

9-C



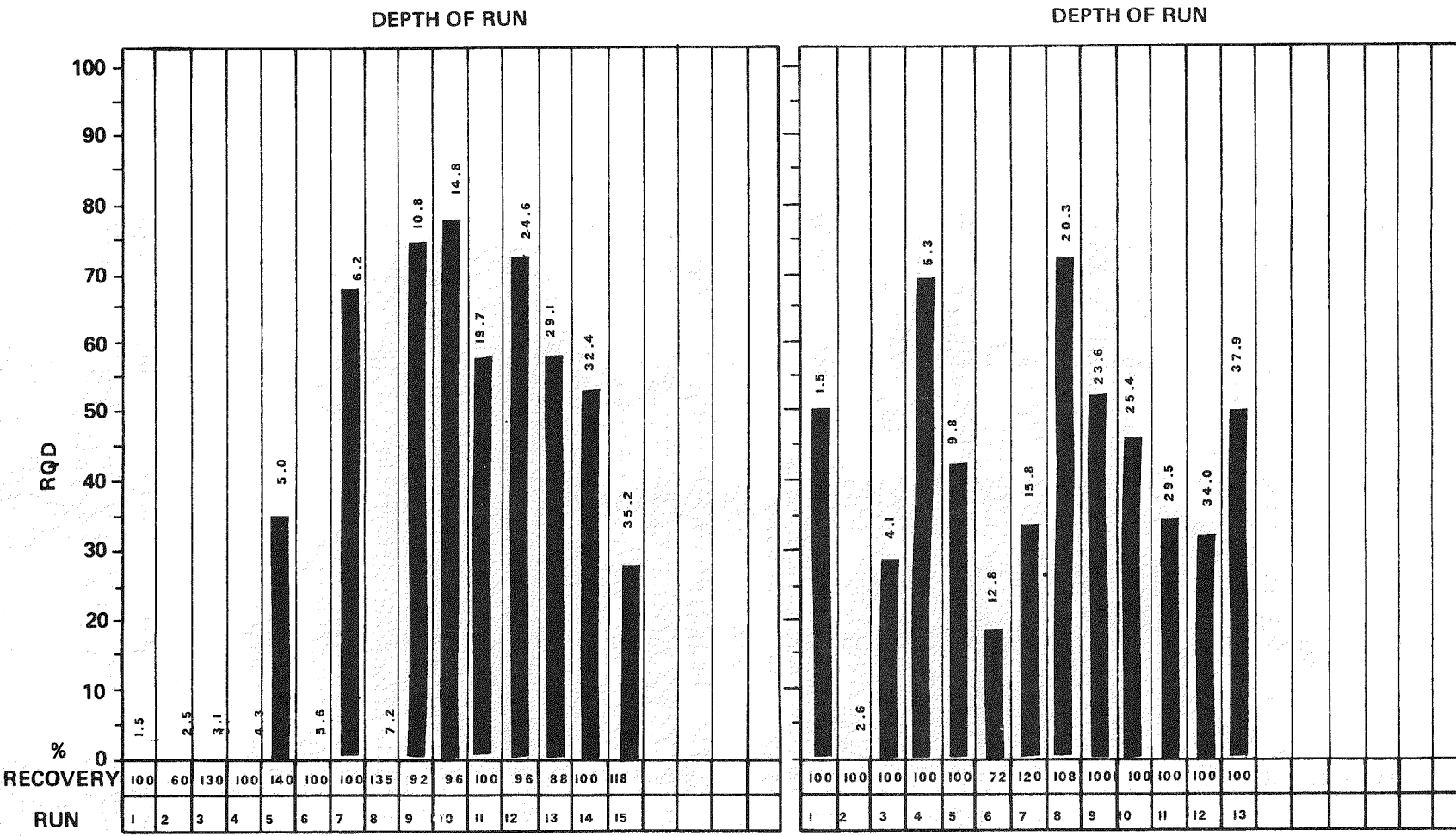
HOLE IE12
DEPTH 35.5

HOLE IE13
DEPTH 39.2

RCP8007-75

RHO-BMI-ST-8

C-7

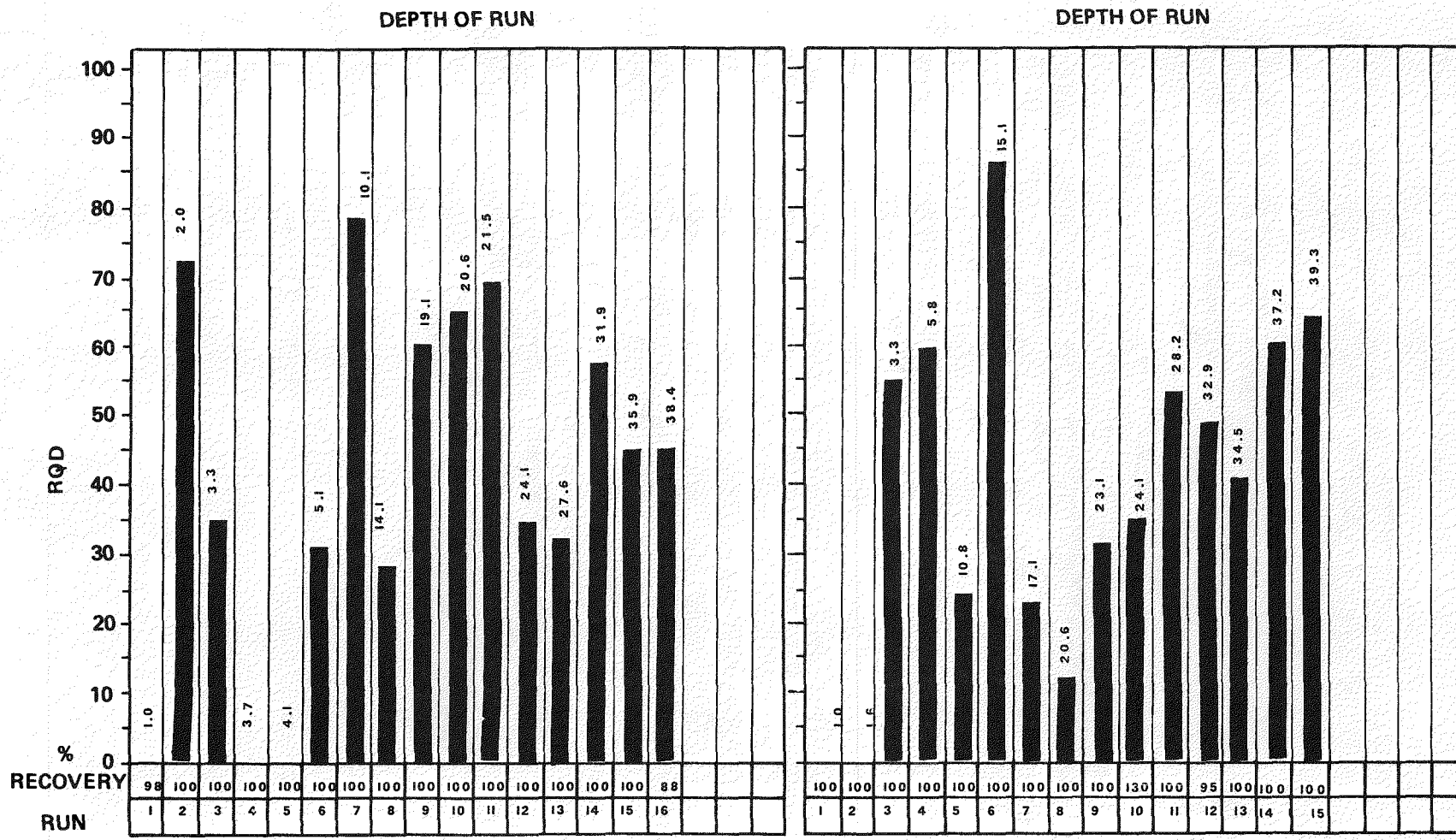


HOLE IE15
DEPTH 35.2

HOLE IE16
DEPTH 37.9

RCP8007-76

RHO-BWI-ST-8

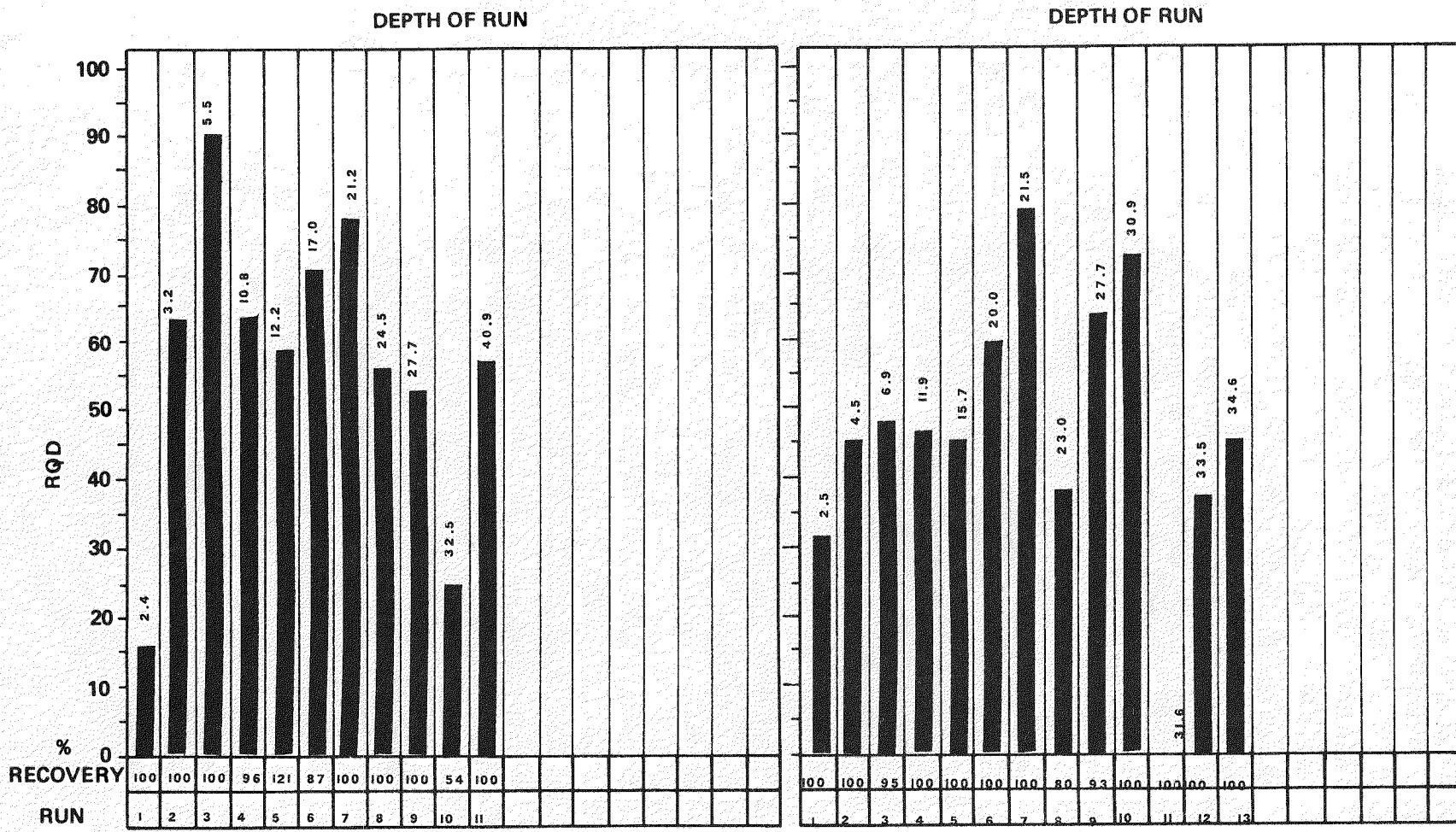


HOLE IE17
DEPTH 38.4

HOLE IE18
DEPTH 39.3

RCP8007-77

6-C



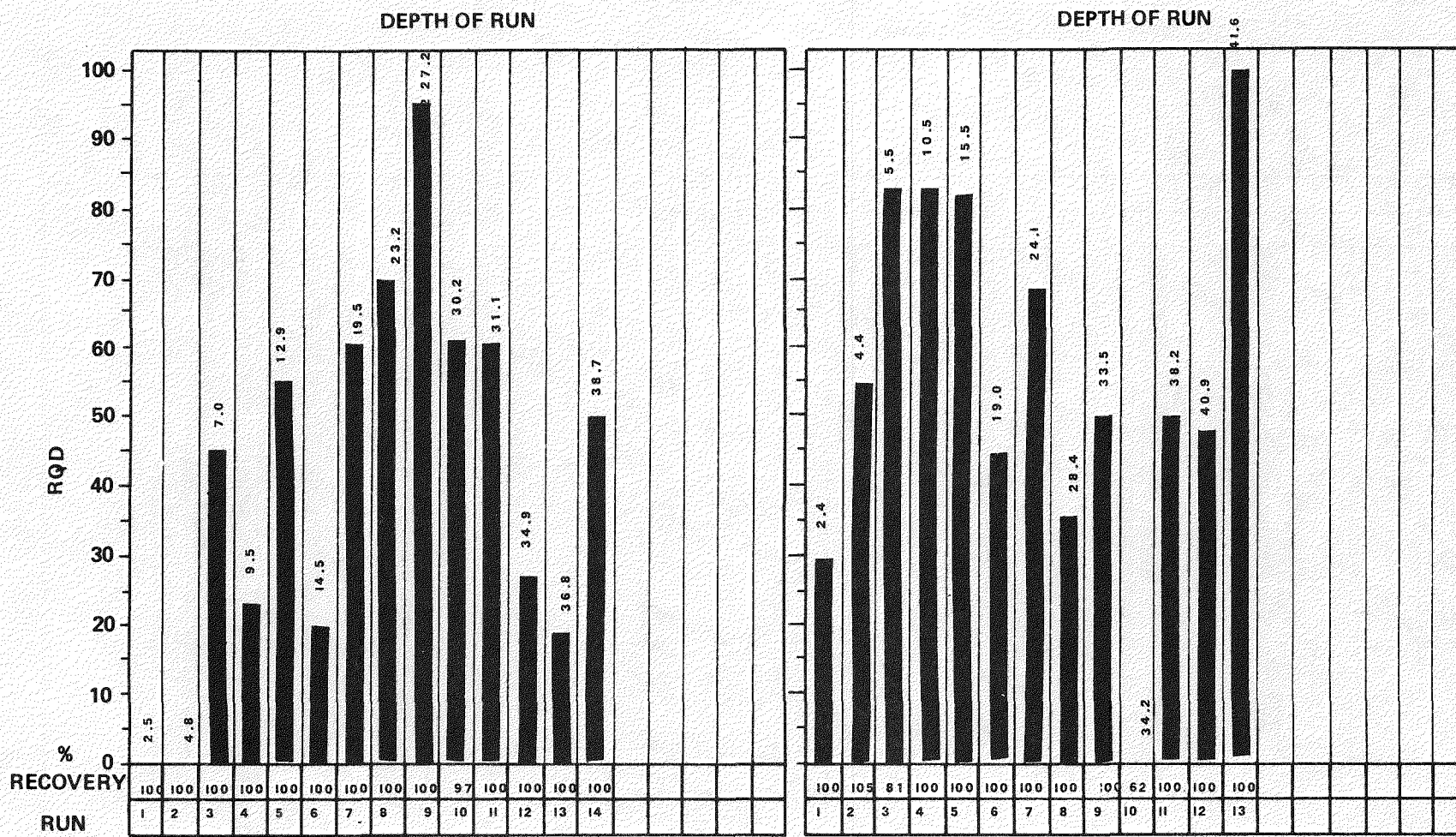
HOLE 1E19
DEPTH 34.6

HOLE 1E20
DEPTH 36.2

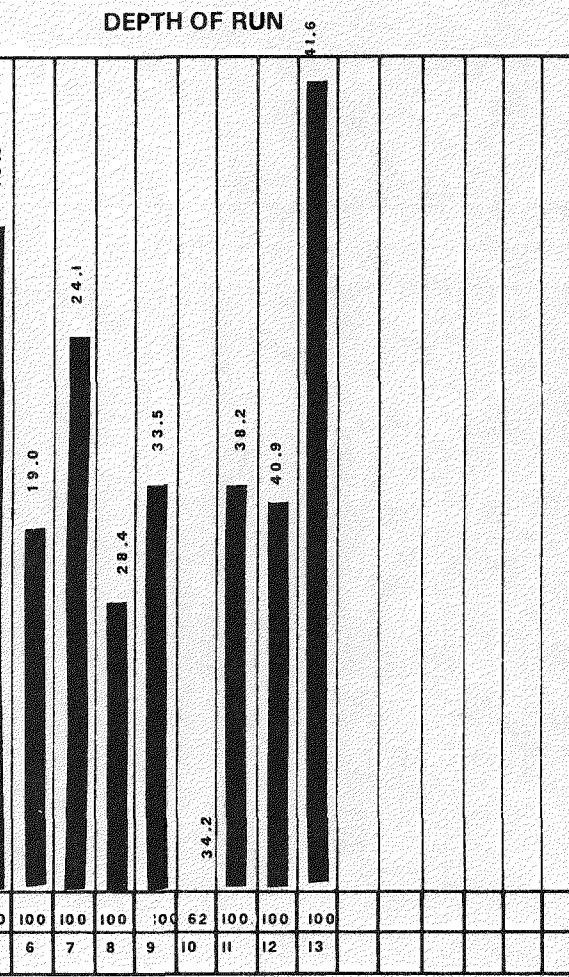
RCP8007-78

RHO-BWI-ST-8

C-10



HOLE IE21
DEPTH 38.7

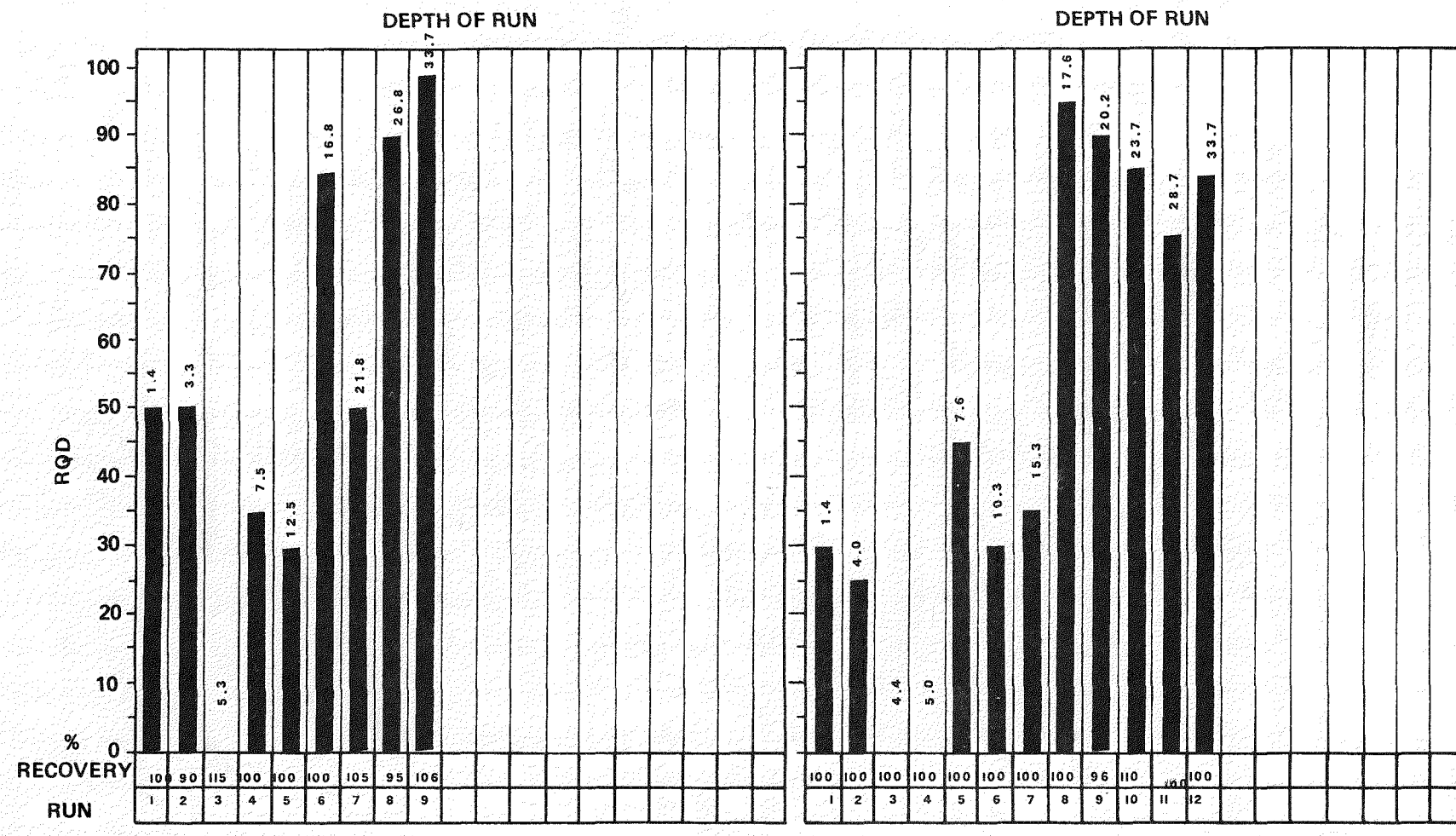


HOLE IE22
DEPTH 41.6

RHO-BMI-ST-8

RCP8007-79

C-11



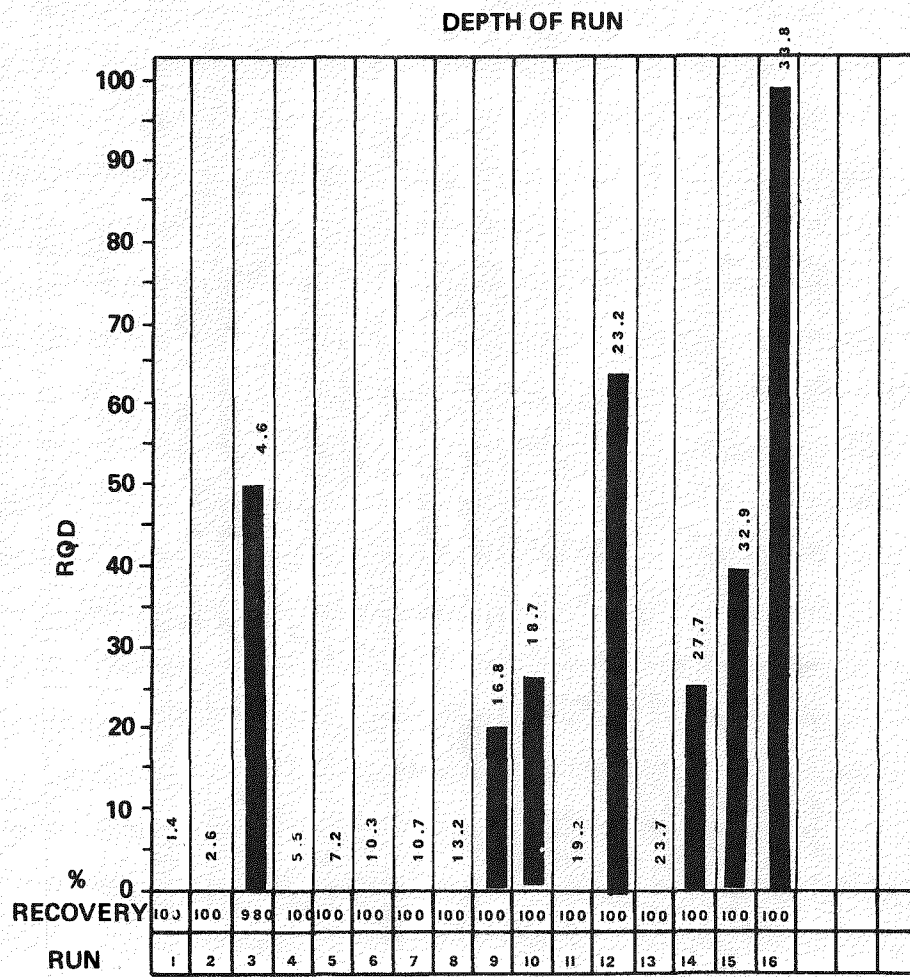
HOLE IM3
DEPTH 33.7

HOLE IM4
DEPTH 33.7

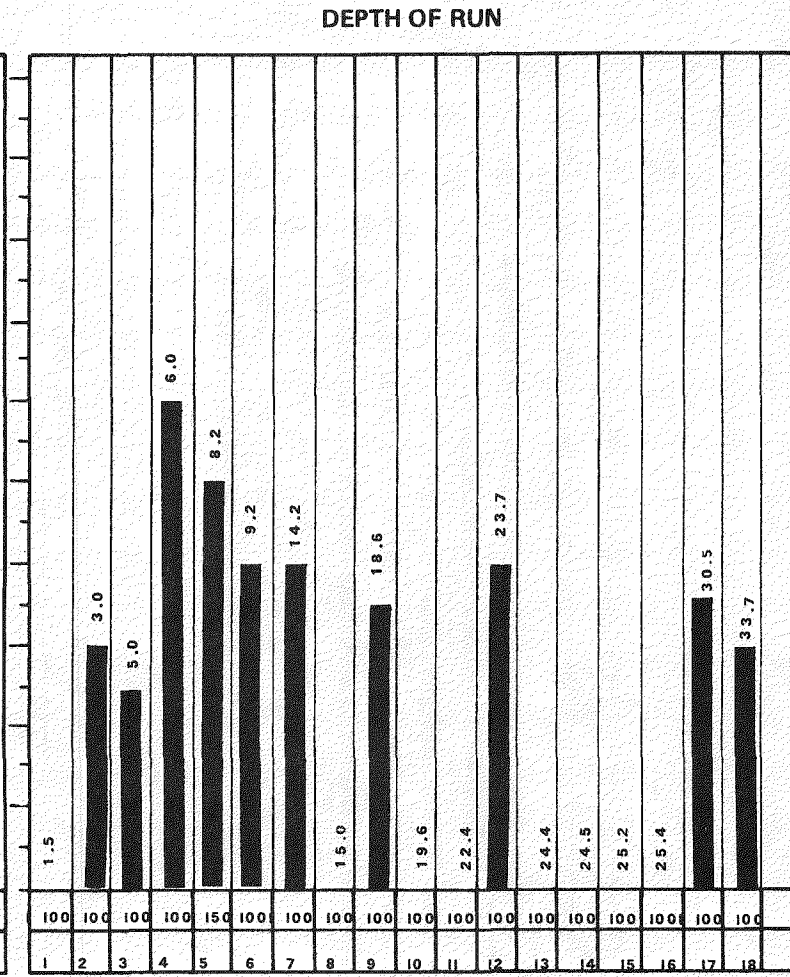
RCP8007-80

RHO-BWI-ST-8

C-12



HOLE IM5
DEPTH 33.8

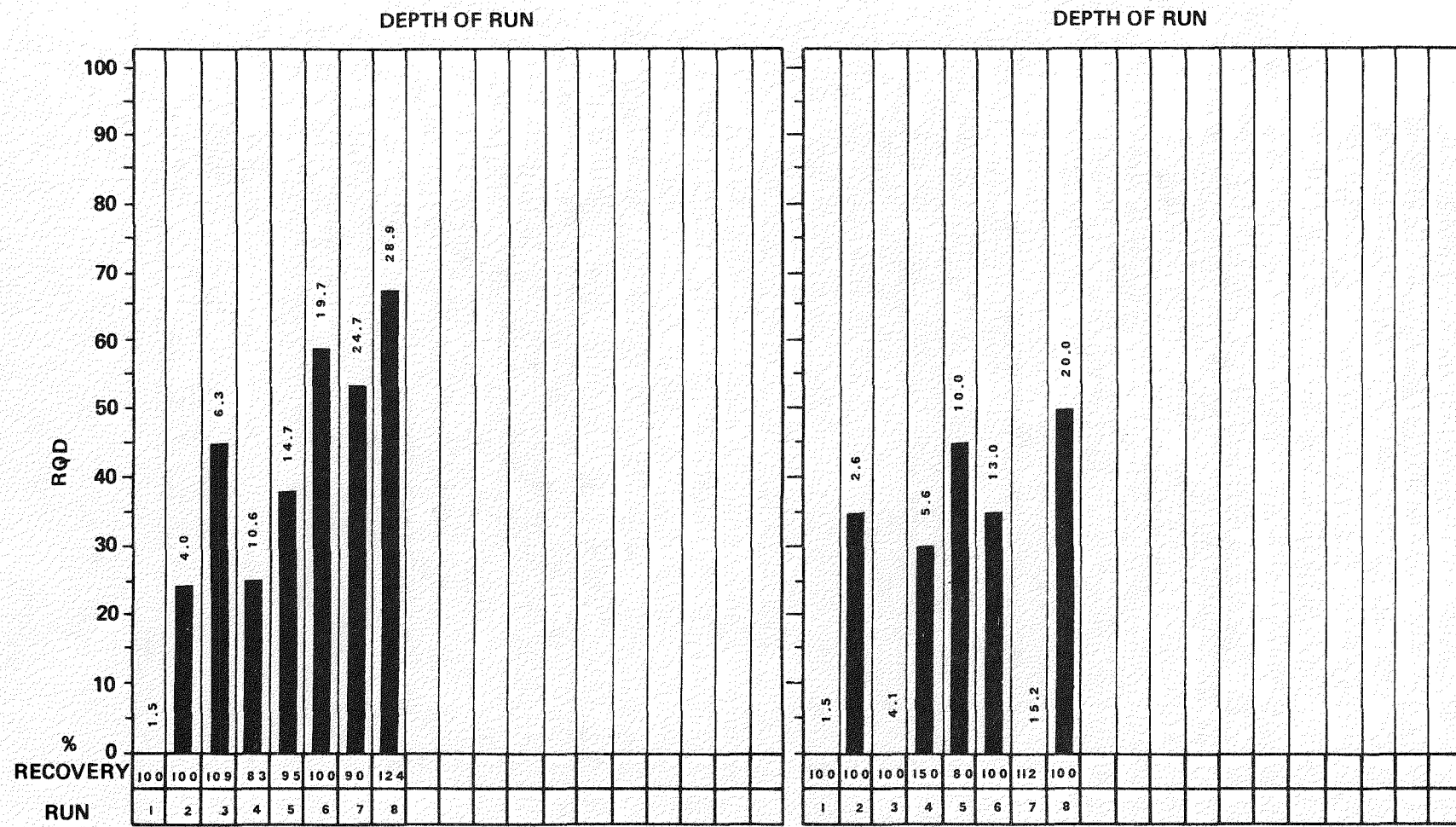


HOLE IM7
DEPTH 33.7

RCP8007-81

RHO-BMI-ST-8

C-13



HOLE 2E1

DEPTH 28.9

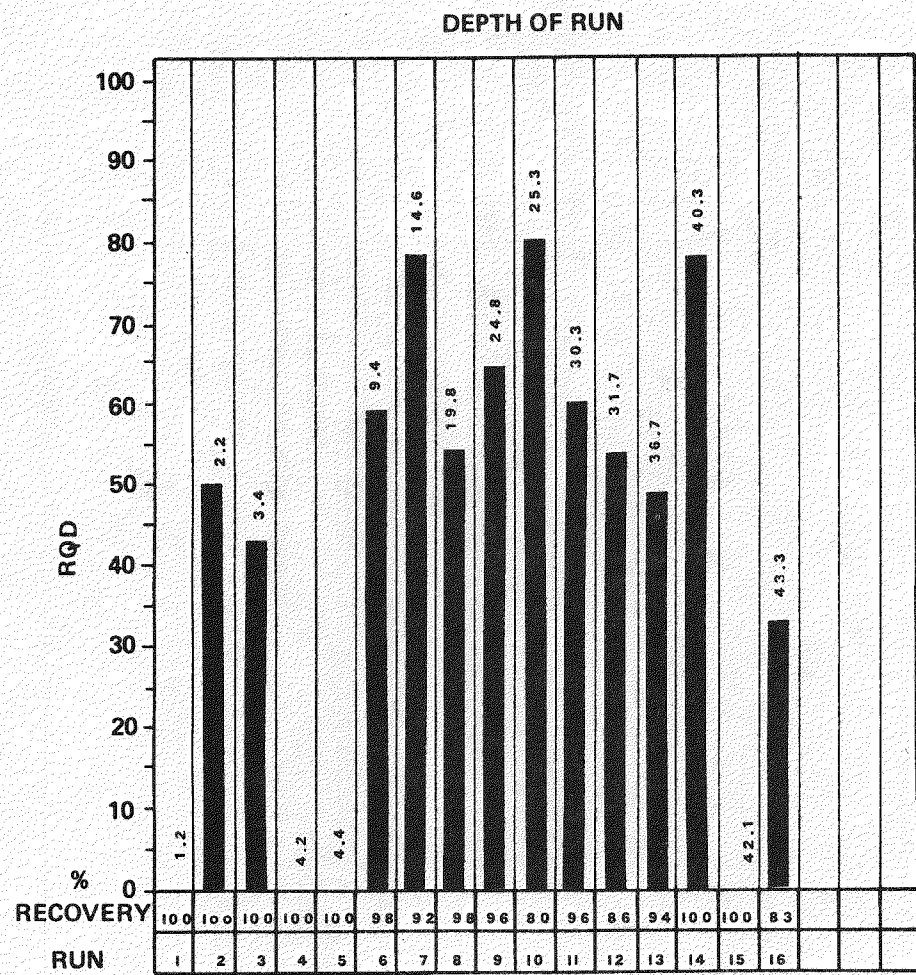
HOLE 2E9

DEPTH 20.0

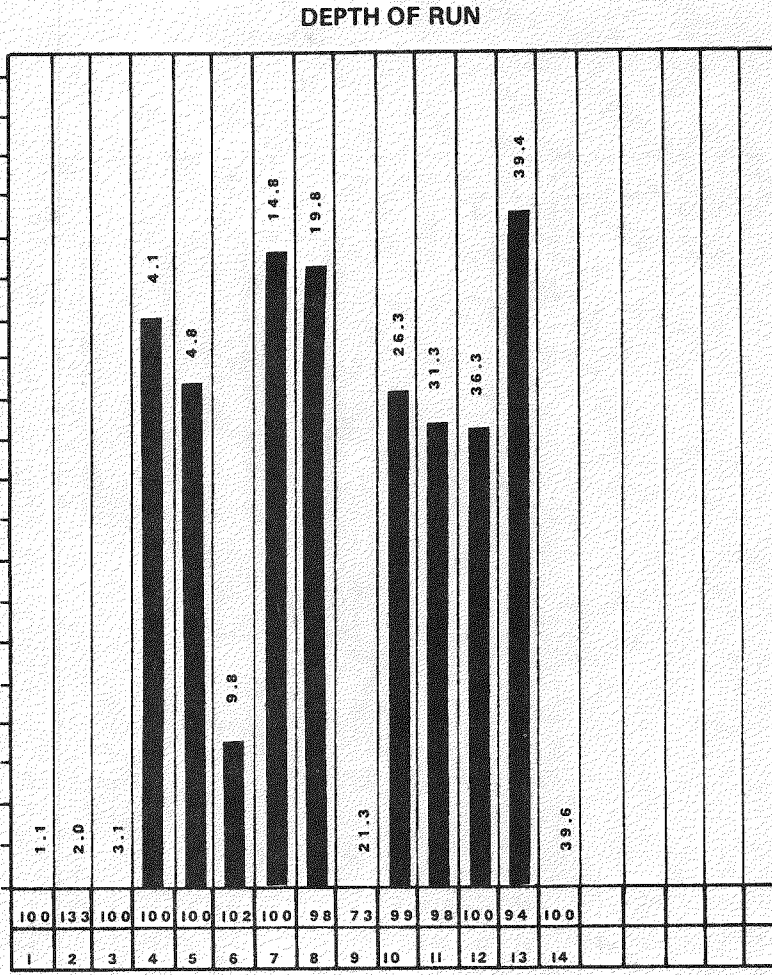
RCP8007-82

RHO-BWI-ST-8

C-11



HOLE 2E14
DEPTH 43.3

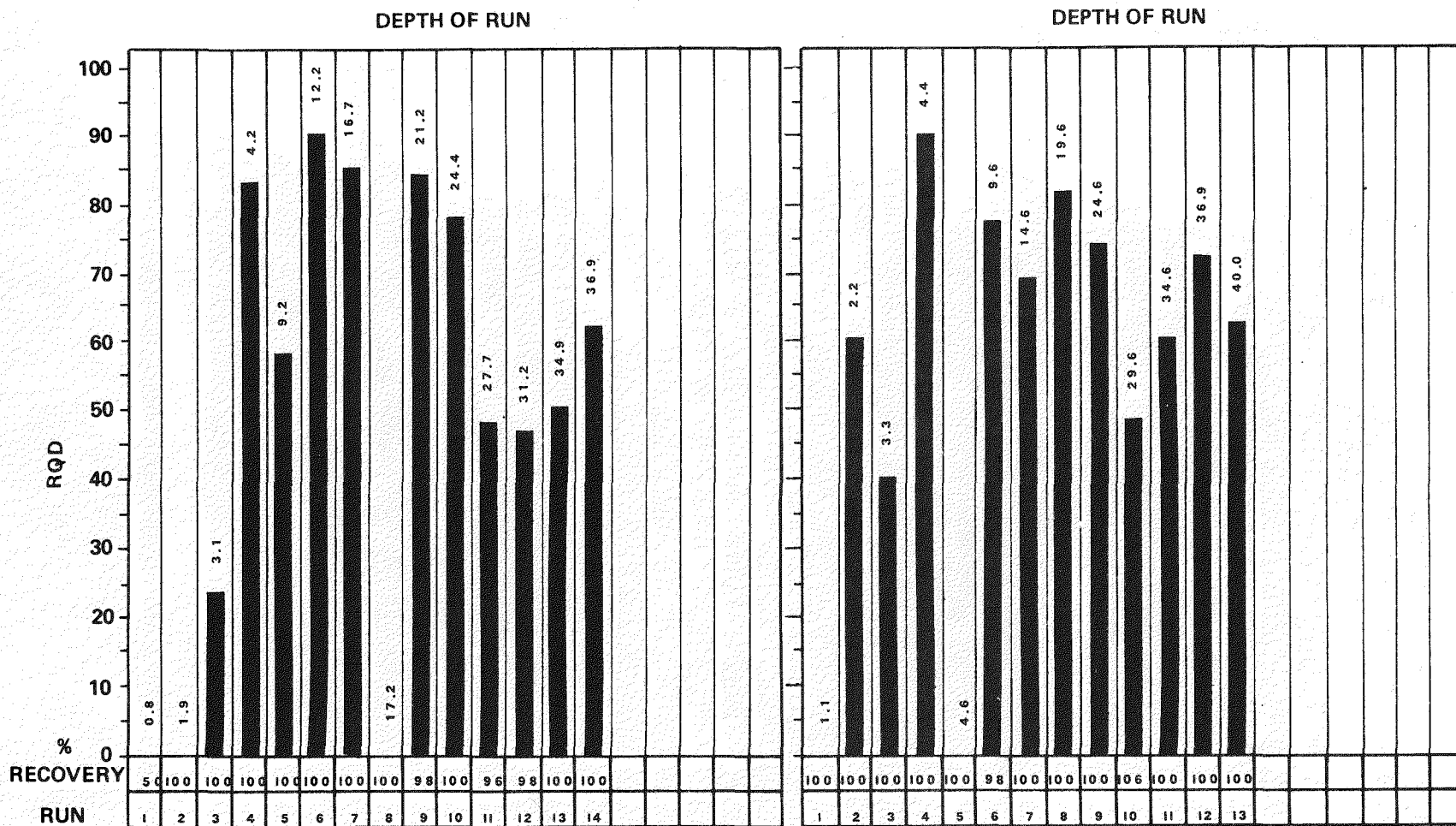


HOLE 2E15
DEPTH 39.6

RCP8007-83

RHO-BMI-ST-8

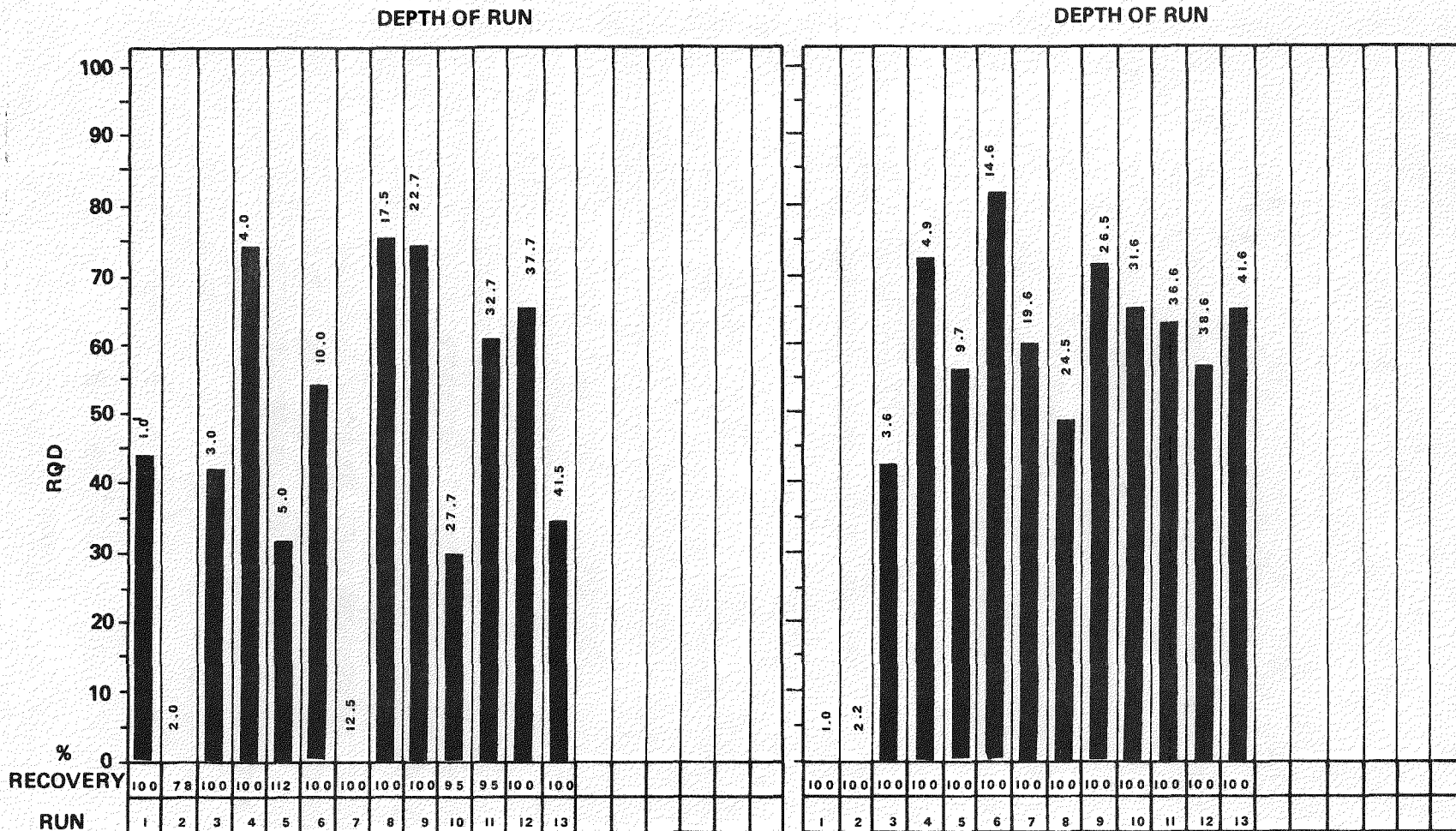
C-15

HOLE 2E16DEPTH 36.9HOLE 2E17DEPTH 40.0

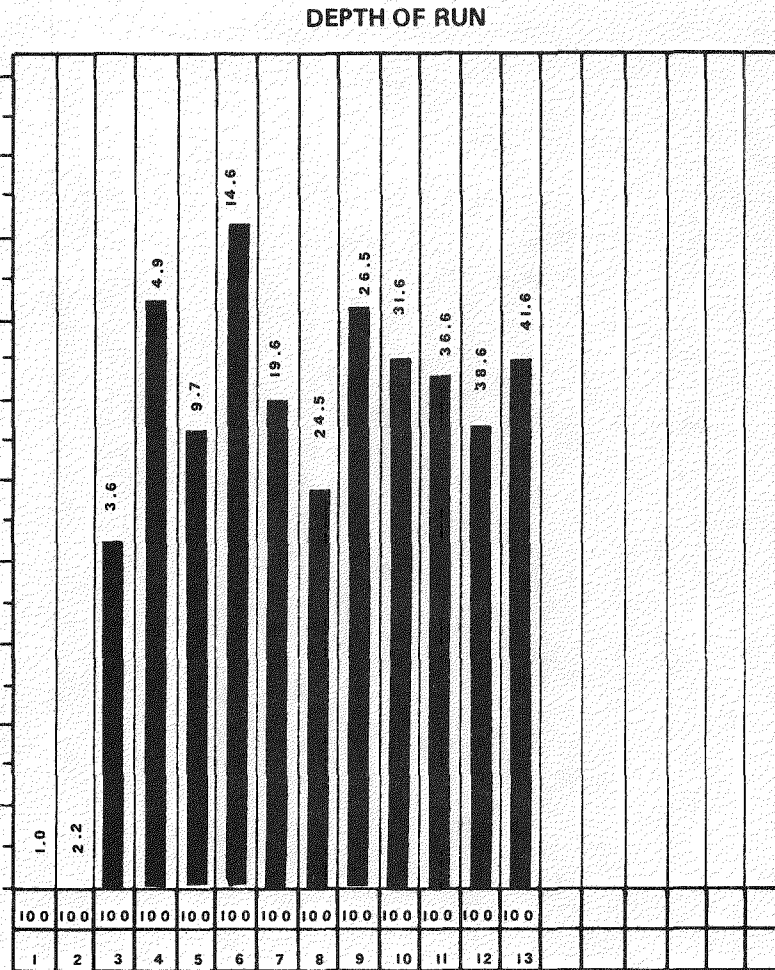
RCP8007-84

RHO-BWI-ST-8

C-16



HOLE 2E18
DEPTH 42.7

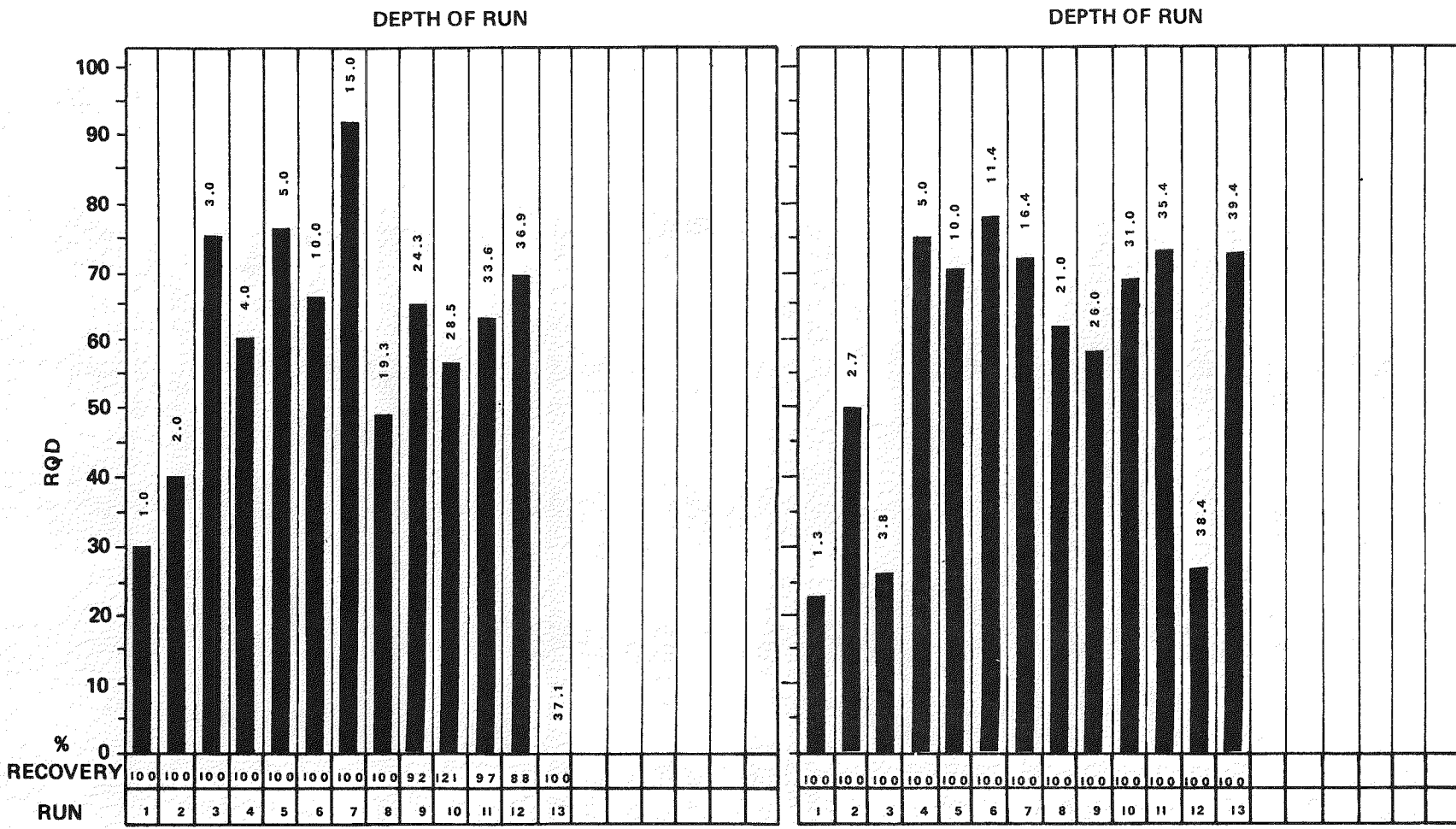


HOLE 2E19
DEPTH 41.6

RCP8007-85

RHO-BWI-ST-8

C-17



HOLE 2E20

DEPTH 37.1

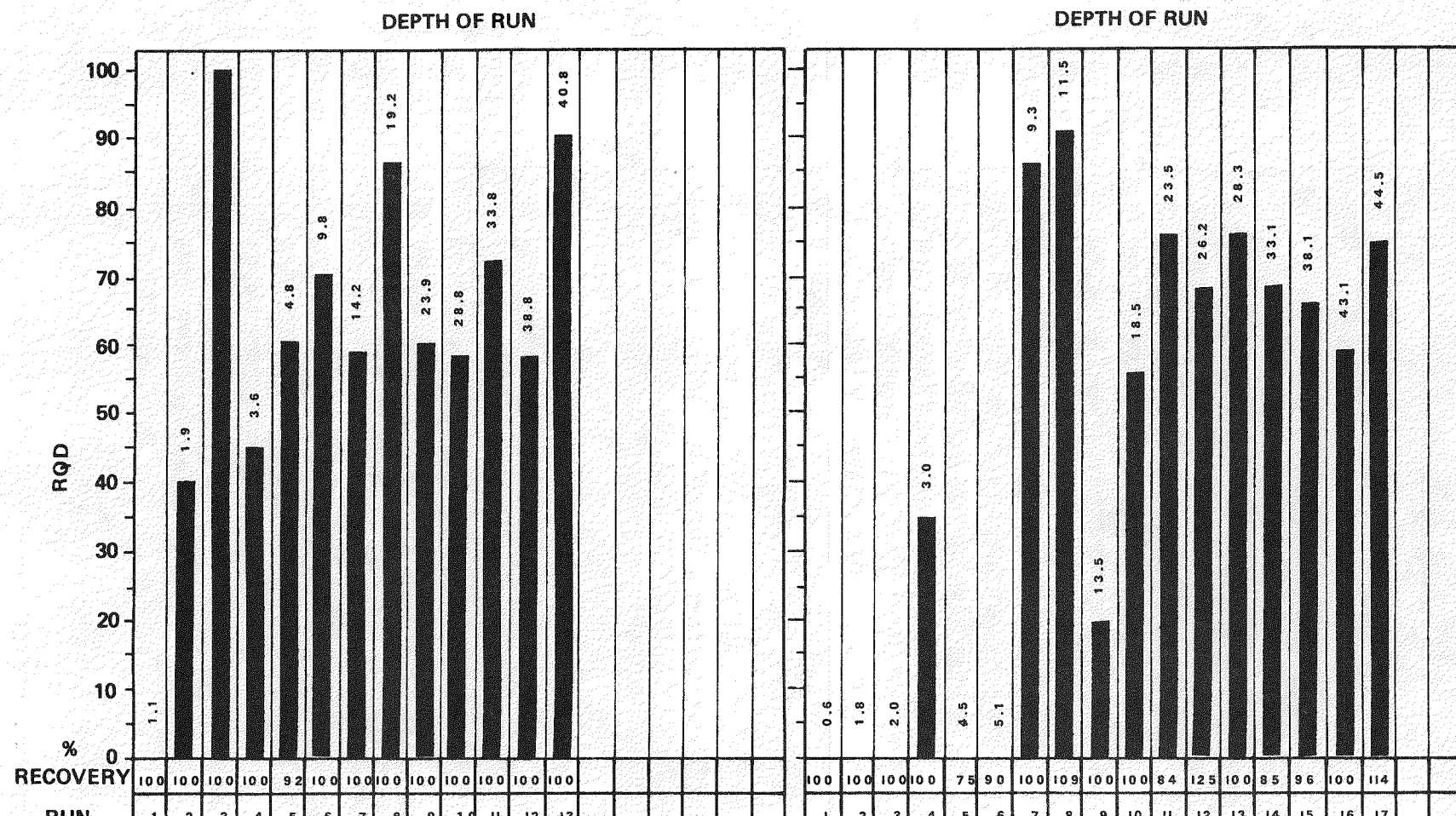
HOLE 2E21

DEPTH 39.4

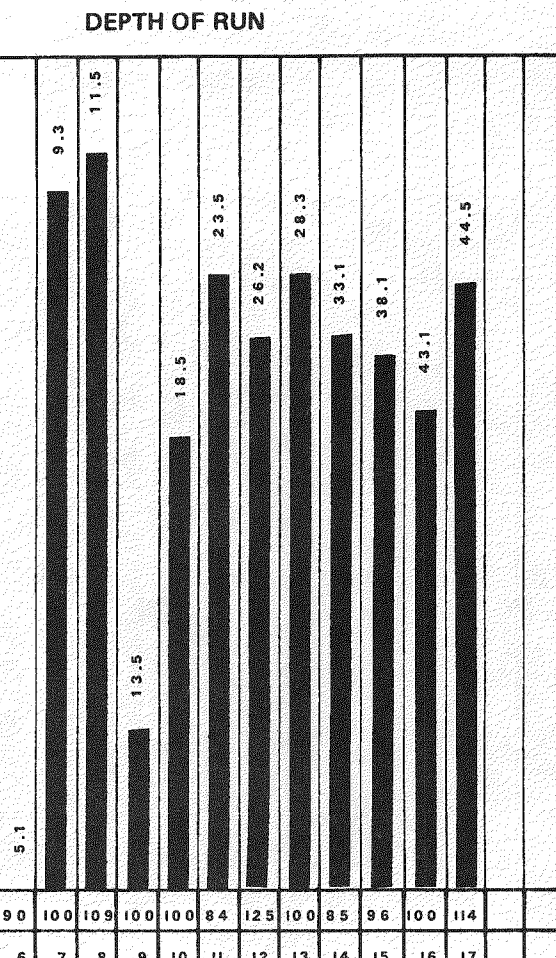
RCP8007-86

RHO-BMI-ST-8

C-18



HOLE 2E22
DEPTH 40.8

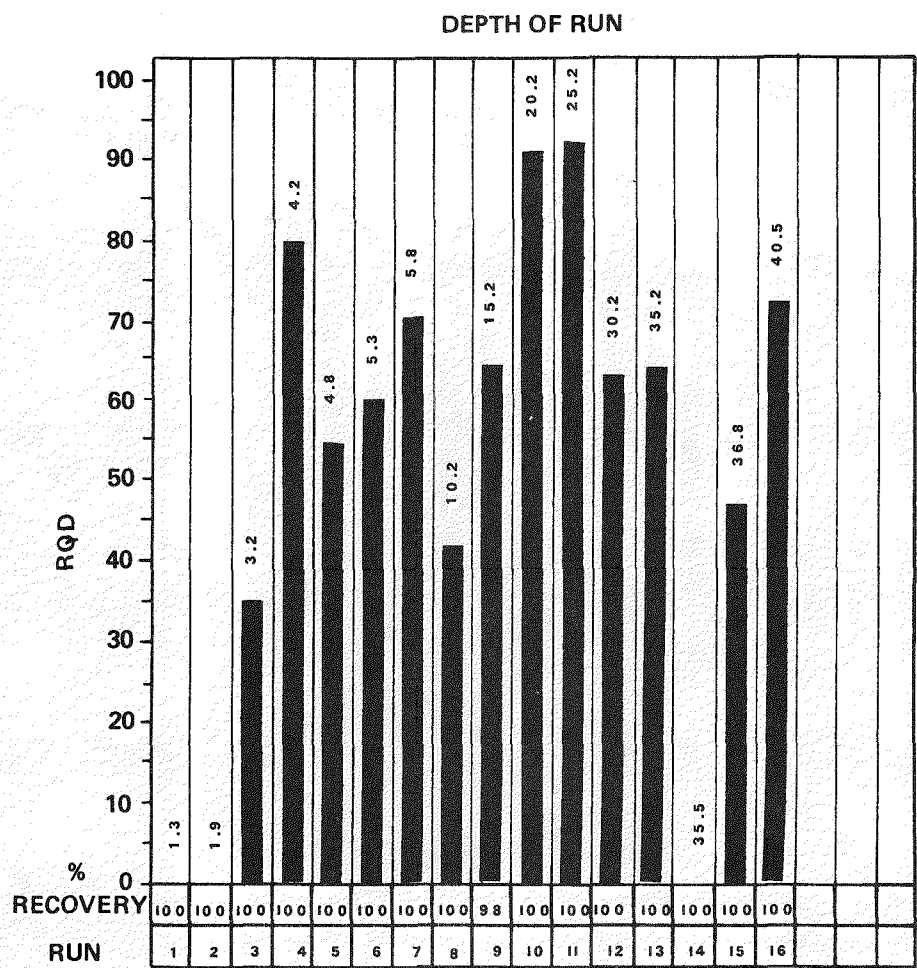
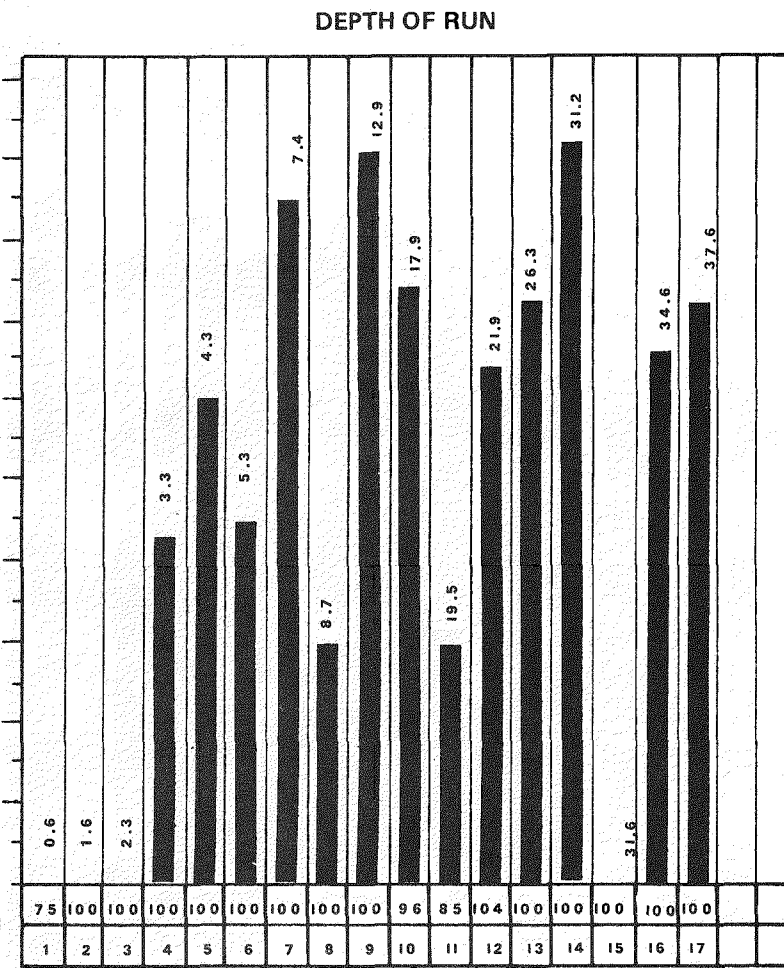


HOLE 2E23
DEPTH 44.5

RCP8007-87

RHO-BMI-ST-8

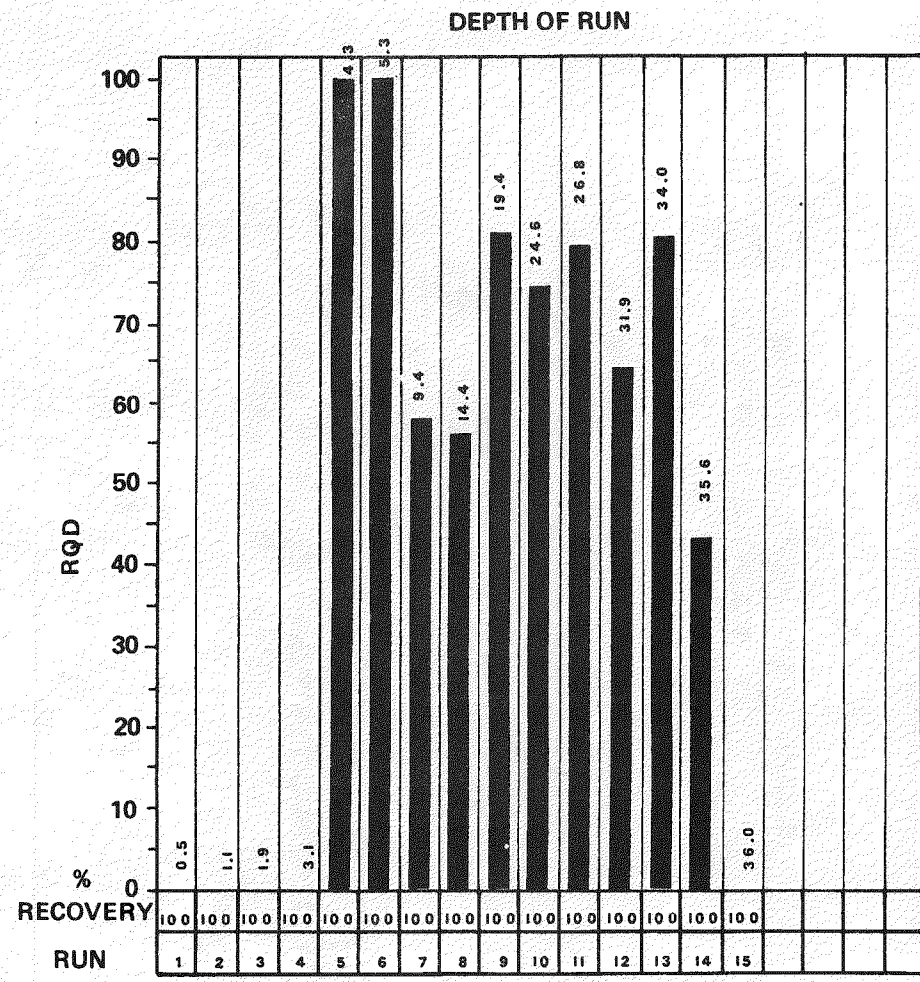
C-19

HOLE 2E24DEPTH 40.5HOLE 2E25DEPTH 37.6

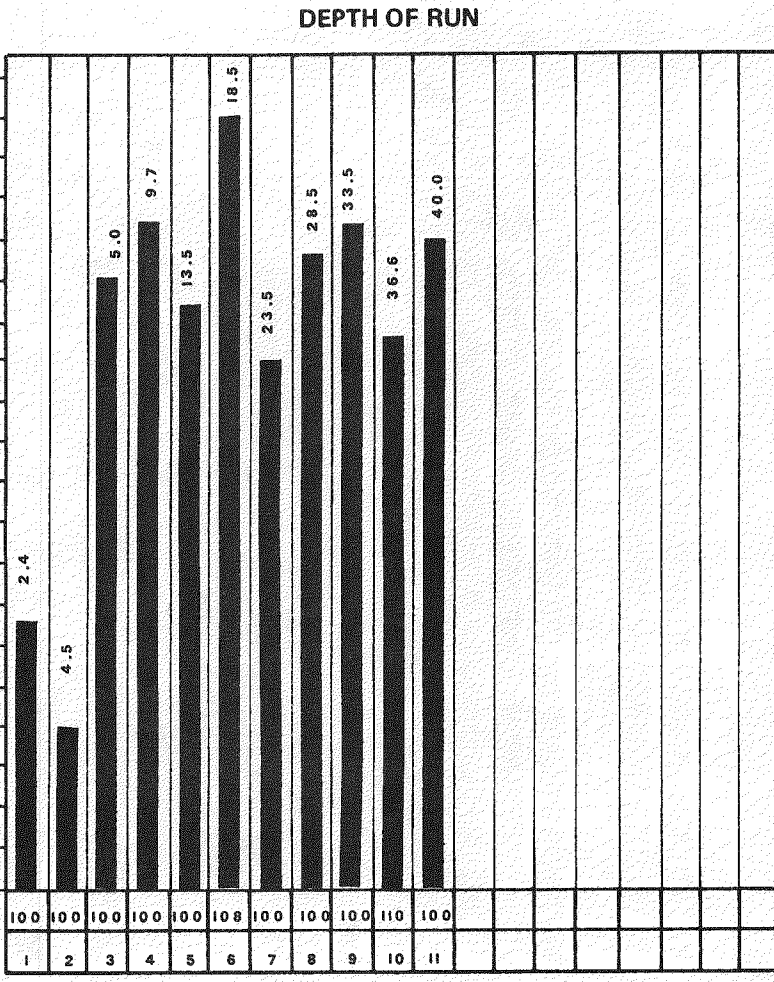
RCP8007-88

RHO-BWI-ST-8

C-20



HOLE 2E26
DEPTH 36.0

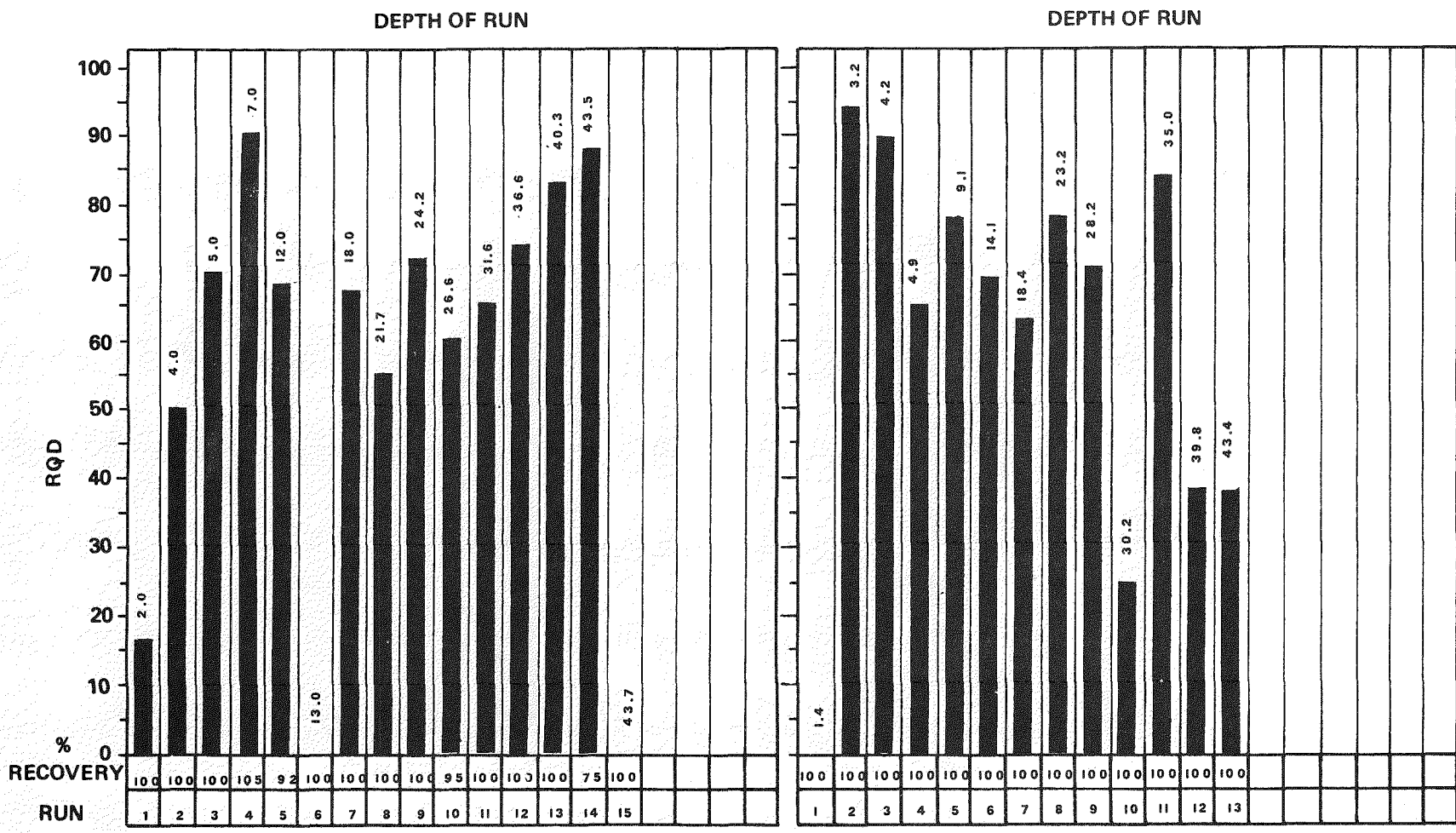


HOLE 2E27
DEPTH 40.0

RCP8007-89

RHO-BWI-ST-8

C-21



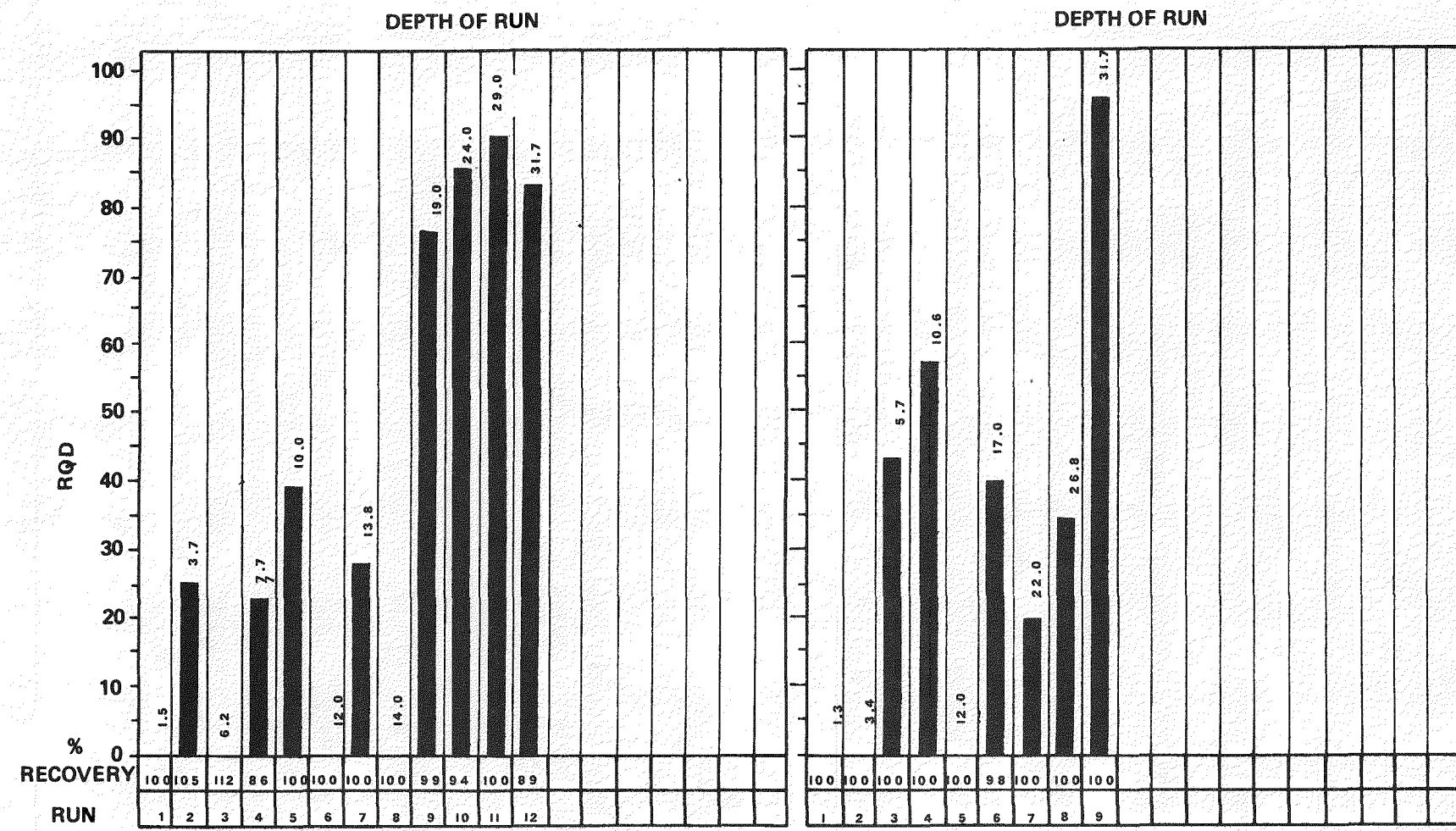
HOLE 2E28
DEPTH 43.7

HOLE 2E29
DEPTH 43.4

RCP8007-90

RHO-BWI-ST-8

C-22



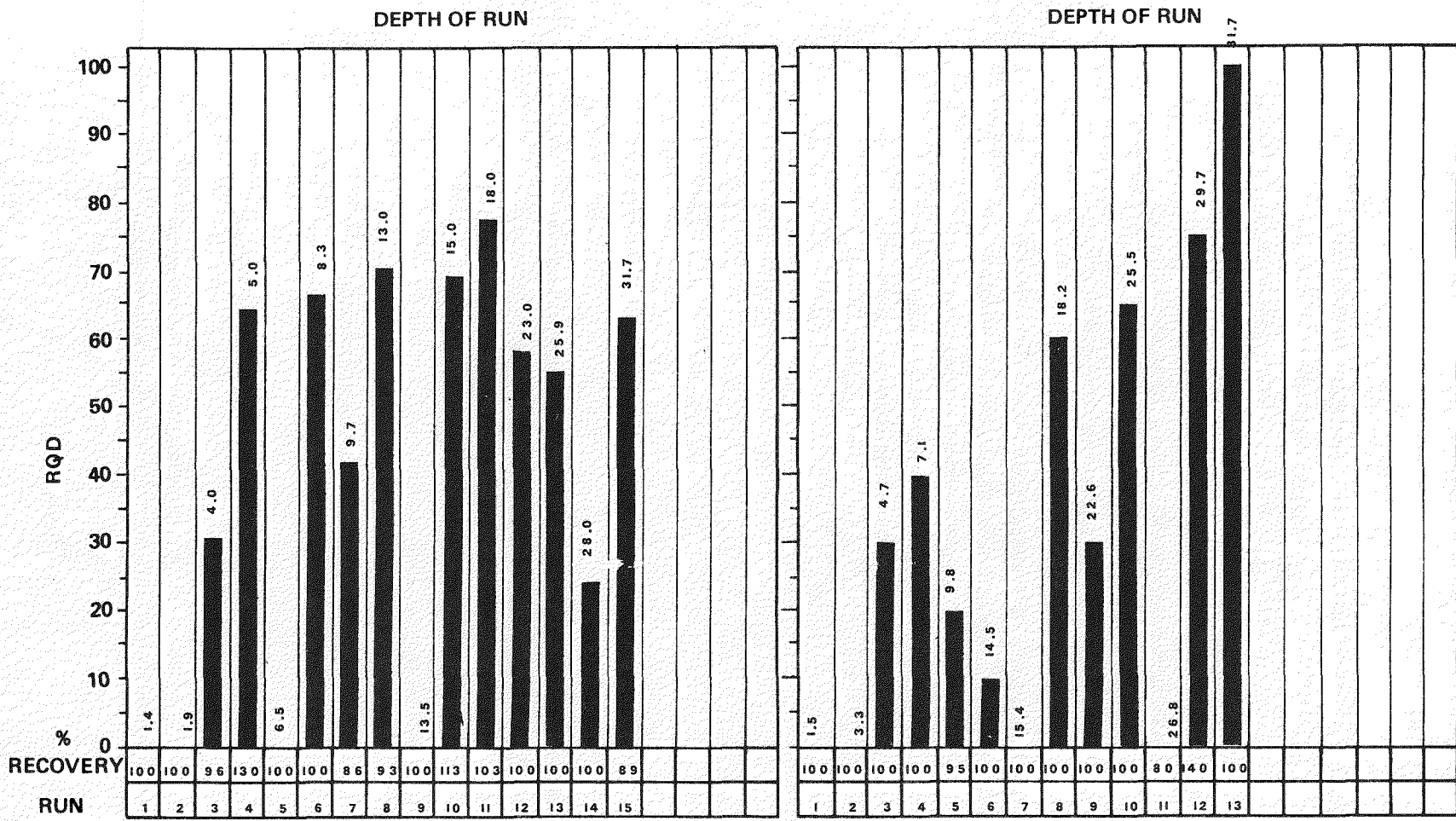
HOLE 2M3
DEPTH 31.7

HOLE 2M4
DEPTH 31.7

RCP8007-91

RHO-BWI-ST-8

C-23



HOLE 2M7

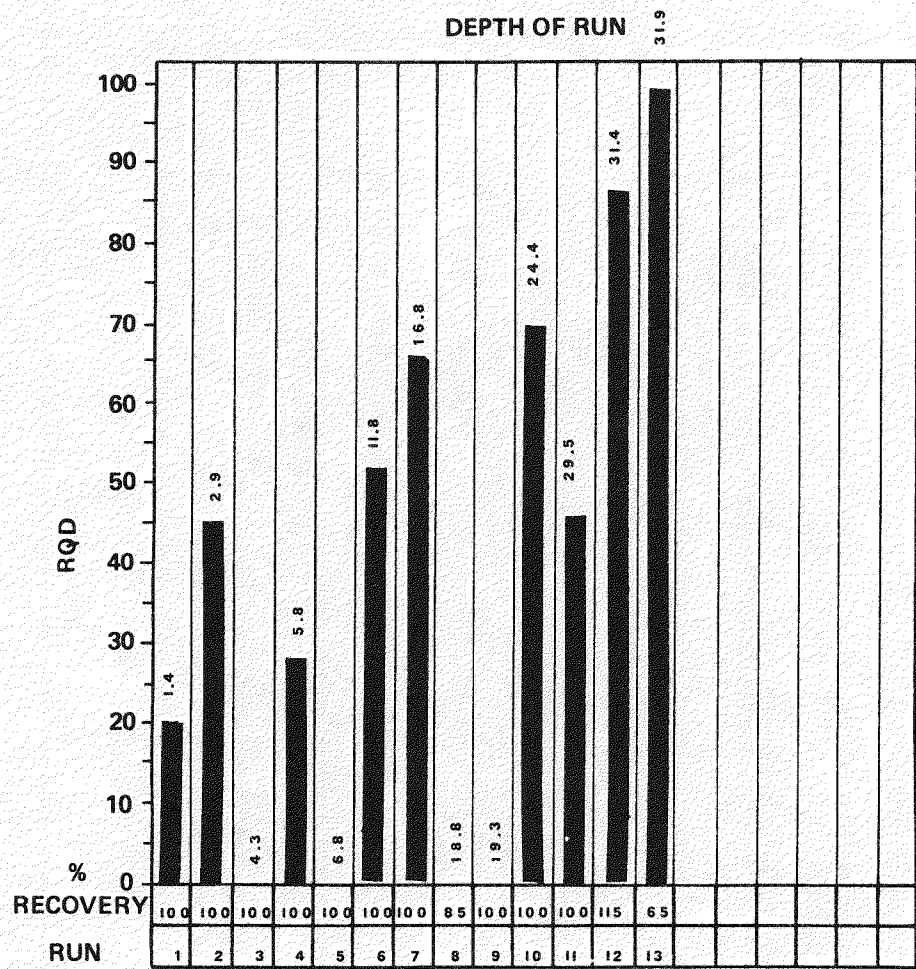
DEPTH 31.7

HOLE 2M12

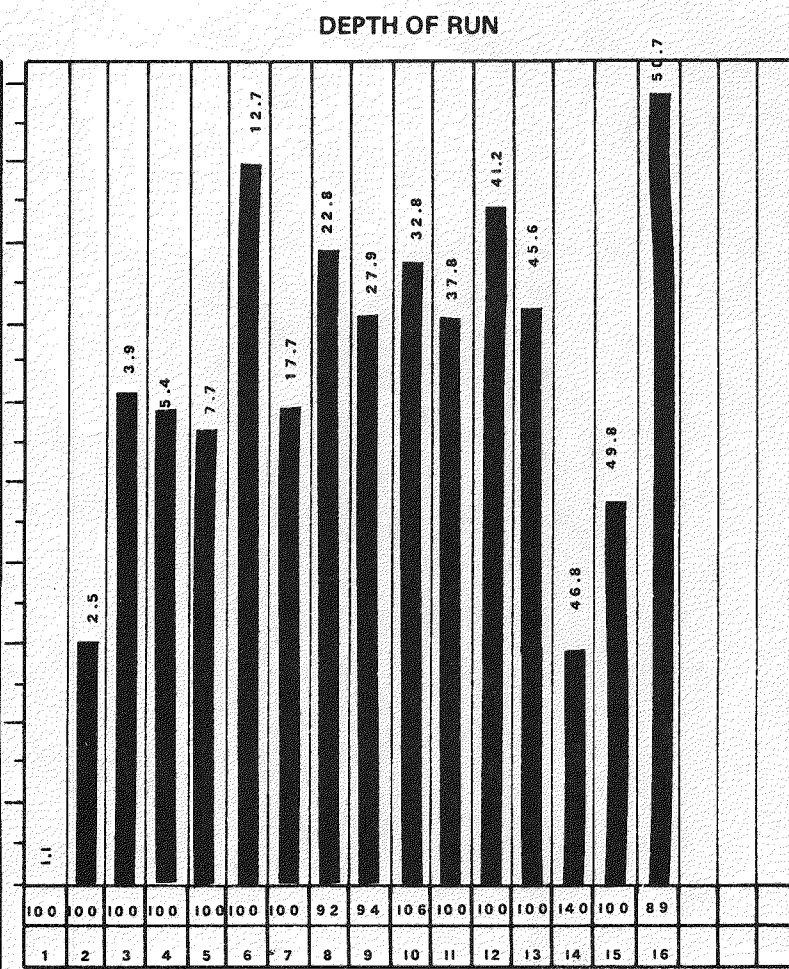
DEPTH 31.7

RCP8007-92

C-24



HOLE 2 M 13
DEPTH 31.9

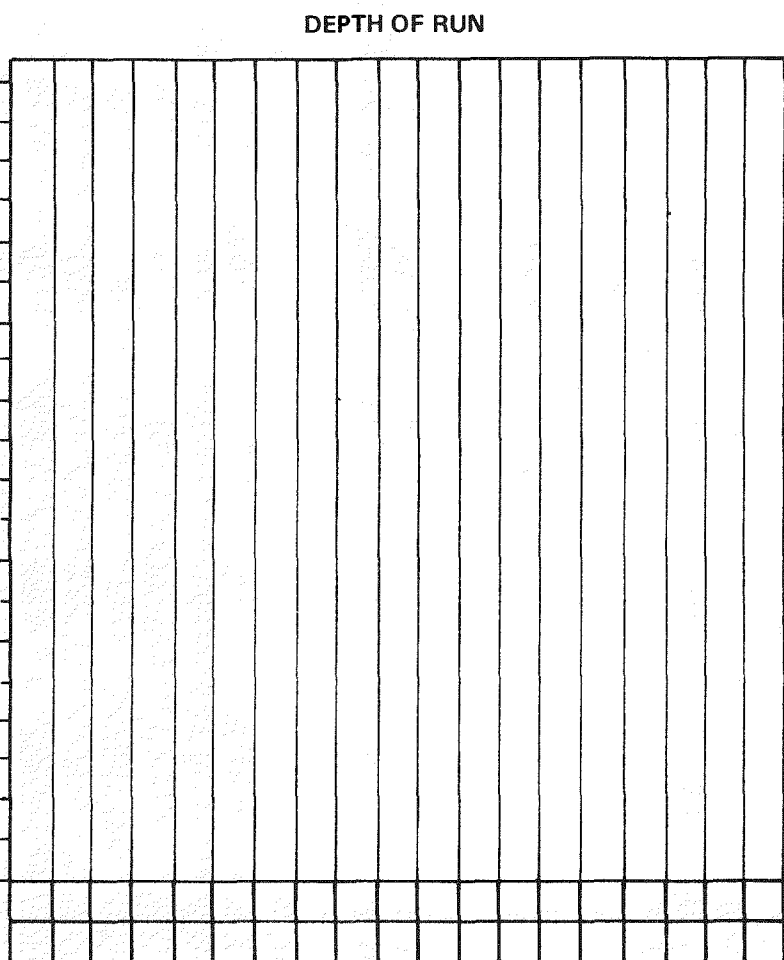
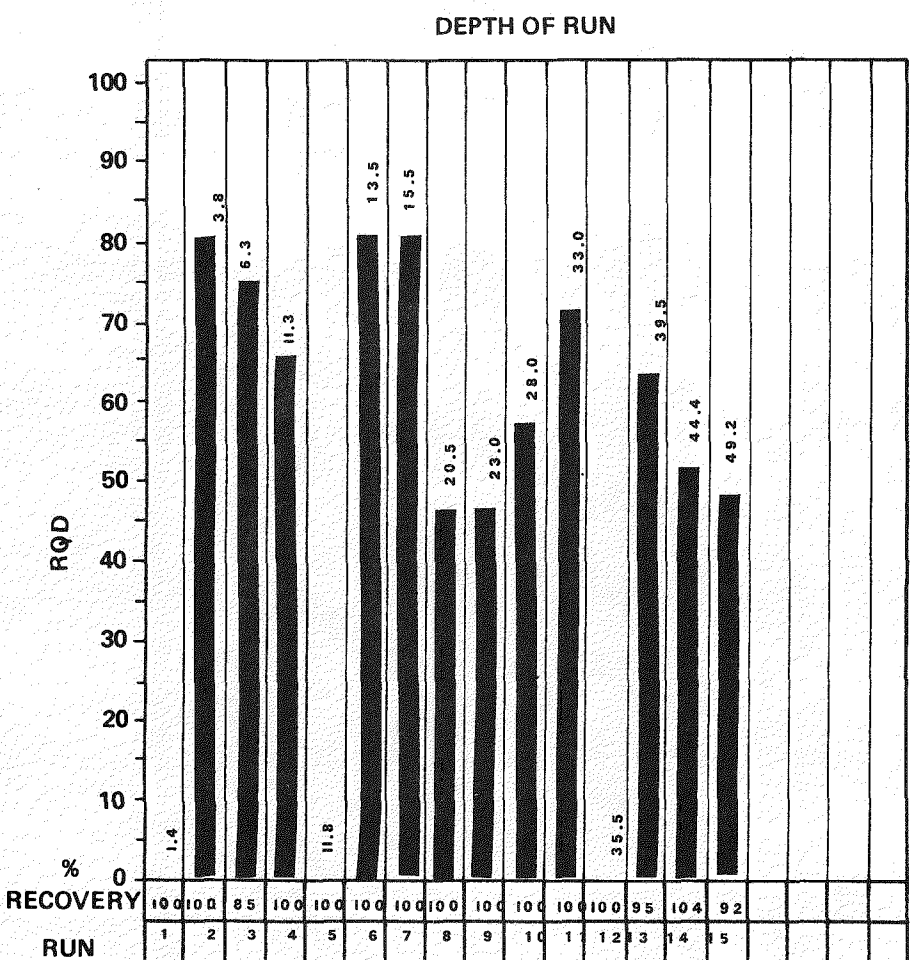


HOLE 2 M 16
DEPTH

RCP8007-93

RHO-BMI-ST-8

RHO-BWI-ST-8



HOLE IM 8
DEPTH 49.2

HOLE
DEPTH

RCP8007-94

The following tables are a summarization of the joint densities and RQD values of each of the twelve blocks in Full-Scale Heater Tests #1 and #2.

TABLE C-1. Joint Density of Block 1-1.

Location	Horizontal Hole	Footage* (meters)	Joints**	Vertical Hole	Footage* (meters)	Joints**
1-1-A	1E-13	23-32 (7.0- 9.8)	43	1E-3	0-10 (0.0-3.0)	43
	1E-12	23-32 (7.0- 9.8)	49	1M-4	0-10 (0.0-3.0)	51
Total		18 (5.5)	92		30 (9.1)	140
1-1-B	1E-16	23-32 (7.0- 9.8)	40	1M-4	10-18 (3.0-5.5)	25
	1E-17	23-32 (7.0- 9.8)	47	1M-5	10-18 (3.0-5.5)	47
	1M-8	23-32 (7.0- 9.8)	33	1E-3	10-18 (3.0-5.5)	46
Total		27 (8.2)	120		24 (7.3)	118
1-1-C	1E-20	24-33 (7.3-10.1)	39	1M-4	18-26 (5.5-7.9)	23
	1E-21	24-33 (7.3-10.1)	37	1M-5	18-26 (5.5-7.9)	43
	1E-22	24-33 (7.3-10.1)	37	1E-3	18-26 (5.5-7.9)	24
Total		36 (11.0)	146			90
Block Subtotal		81 (24.7)	358		78 (23.8)	348
				4.42 joints/foot (14.5 joints/meter)	4.46 joints/foot (14.6 joints/meter)	
				4.44 joints/foot (14.6 joints/meter)		

*Measured from actual collar location.

**Includes rubble zones (6 joints/foot [20 joints/meter] factor).

C-27

RHO-BWI-ST-8

TABLE C-2. Joint Density of Block 1-2.

Location	Horizontal Hole	Footage* (meters)	Joints**	Vertical Hole	Footage* (meters)	Joints**
1-2-A	1E-10	22-31 (6.7- 9.4)	51	1M-3	0-10 (0.0-3.0)	46
	1E-11	22-31 (6.7- 9.4)	37	1E-1	0-10 (0.0-3.0)	42
	Total	18 (5.5)	88		20 (6.1)	88
1-2-B	1E-15	22-31 (6.7- 9.4)	36	1M-3	10-18 (3.0-5.5)	39
				1E-1	10-18 (3.0-5.5)	32
	Total	9 (2.7)	36		18 (5.5)	71
1-2-C	1E-18	23-32 (7.0- 9.8)	50	1M-3	18-26 (5.5-7.9)	19
	1E-19	23-32 (7.0- 9.8)	46	1E-1	18-26 (5.5-7.9)	32
	1E-20	24-33 (7.3-10.1)	39			
Total		27 (8.2)	135		16 (4.9)	51
Block Subtotal		54 (16.5)	259		52 (15.8)	210
		4.80 joints/foot (15.7 joints/meter)			4.04 joints/foot (13.3 joints/meter)	
TOTAL				4.42 joints/foot (14.5 joints/meter)		

*Measured from actual collar location.

**Includes rubble zones (6 joints/foot [20 joints/meter] factor).

TABLE C-3. Joint Density of Block 1-3.

Location	Horizontal Hole	Footage* (meters)	Joints**	Vertical Hole	Footage* (meters)	Joints**
1-3-A	1E-13	32-39 (9.8-11.9)	35	1E-3	0-10 (0.0-3.0)	43
	1E-12	32-36 (9.8-11.0)	20	1M-7	0-10 (0.0-3.0)	43
	Total	11 (3.4)	55		20 (6.1)	86
1-3-B	1E-16	32-38 (9.8-11.6)	26	1E-3	10-18 (3.0-5.5)	46
	1E-17	32-39 (9.8-11.9)	26	1M-7	10-18 (3.0-5.5)	45
	1M-8	32-41 (9.8-12.5)	52			
	Total	17 (5.2)	104		16 (4.9)	91
1-3-C	1E-20	33-35 (10.1-10.7)	10	1E-3	18-26 (5.5-7.9)	24
	1E-21	33-41 (10.1-12.5)	32	1M-7	18-26 (5.5-7.9)	49
	1E-22	33-41 (10.1-12.5)	42			
	1M-8	33-41 (10.1-12.5)	52			
	Total	26 (7.9)	136		16 (4.9)	73
Block Subtotal		60 (18.3)	295		52 (15.8)	250
				4.92 joints/foot (16.1 joints/meter)		
				4.81 joints/foot (15.7 joints/meter)		
TOTAL				4.87 joints/foot (16.0 joints/meter)		

*Measured from actual collar location.

**Includes rubble zones (6 joints/foot [20 joints/meter] factor).

TABLE C-4. Joint Density of Block 1-4.

Location	Horizontal Hole	Footage* (meters)	Joints**	Vertical Hole	Footage* (meters)	Joints**
1-4-A	1E-10	31-40 (9.4-12.2)	36	1E-1	0-10 (0.0-3.0)	42
	1E-11	31-37 (9.4-11.3)	29	1E-8	0-10 (0.0-3.0)	50
				1E-9	0-10 (0.0-3.0)	55
Total		15 (4.6)	65		30 (9.1)	147
1-4-B	1E-15	31-35 (9.4-10.7)	19	1E-1	10-18 (3.0-5.5)	32
				1E-8	10-18 (3.0-5.5)	35
				1E-9	10-18 (3.0-5.5)	48
Total		4 (1.2)	19		24 (7.3)	115
1-4-C	1E-18	32-39 (9.8-11.9)	35	1E-1	18-26 (5.5-7.9)	32
	1E-19	32-36 (9.8-11.0)	23	1E-8	18-26 (5.5-7.9)	33
	1E-20	33-35 (10.1-10.7)	6	1E-9	18-26 (5.5-7.9)	29
Total		13 (4.0)	61		24 (7.3)	94
Block Subtotal		32 (9.8)	148		78 (23.8)	356
				4.63 joints/foot (15.2 joints/meter)		4.56 joints/foot (15.0 joints/meter)
TOTAL				4.60 joints/foot (15.1 joints/meter)		

*Measured from actual collar location.

**Includes rubble zones (6 joints/foot [20 joints/meter] factor).

TABLE C-5. Joint Density of Block 2-1.

Location	Horizontal Hole	Footage* (meters)	Joints**	Vertical Hole	Footage* (meters)	Joints**
2-1-A	2E-16	24-33 (7.3-10.1)	45	2M-7	0-10 (0.0-3.0)	53
	2E-17	24-33 (7.3-10.1)	53			
	2E-18	24-33 (7.3-10.1)	43			
Total		27 (8.2)	141		10 (3.0)	53
2-1-B	2E-21	24-33 (7.3-10.1)	34	2M-7	10-18 (3.0-5.5)	29
	2E-22	25-34 (7.6-10.4)	37			
	2E-23	25-34 (7.6-10.4)	38			
	2M-16	25-34 (7.6-10.4)	35			
Total		36 (11.0)	144		8 (2.4)	29
2-1-C	2E-27	25-34 (7.6-10.4)	32	2M-7	18-26 (5.5-7.9)	25
	2E-28	25-34 (7.6-10.4)	29			
	2E-29	25-34 (7.6-10.4)	31			
	2M-16	25-34 (7.6-10.4)	35			
Total		36 (11.0)	127		8 (2.4)	25
Block Subtotal		99 (30.2)	412		26 (7.9)	107
				4.16 joints/foot (13.6 joints/meter)		4.12 joints/foot (13.5 joints/meter)
TOTAL				4.14 joints/foot (13.6 joints/meter)		

*Measured from actual collar location.

**Includes rubble zones (6 joints/foot [20 joints/meter] factor).

TABLE C-6. Joint Density of Block 2-2.

Location	Horizontal Hole	Footage* (meters)	Joints**	Vertical Hole	Footage* (meters)	Joints**	
2-2-A	2E-14	24-33 (7.3-10.1)	46	2M-3	0-10 (0.0-3.0)	46	
	2E-15	24-33 (7.3-10.1)	36	2M-4	0-10 (0.0-3.0)	47	
Total		18 (5.5)	82			20 (6.1)	
2-2-B	2E-19	24-33 (7.3-10.1)	47	2M-3	10-18 (3.0-5.5)	40	
	2E-20	24-33 (7.3-10.1)	45	2M-4	10-18 (3.0-5.5)	41	
Total		18 (5.5)	92			16 (4.9)	
2-2-C	2E-24	25-34 (7.6-10.4)	26	2M-3	18-26 (5.5-7.9)	35	
	2E-25	25-34 (7.6-10.4)	32	2M-4	18-26 (5.5-7.9)	22	
	2E-26	25-34 (7.6-10.4)	32				
Total		27 (8.2)	90			16 (4.9)	
Block Subtotal		63 (19.2)	264			52 (15.8)	
				4.19 joints/foot (13.7 joints/meter)		4.44 joints/foot (14.6 joints/meter)	
TOTAL				4.32 joints/foot (14.2 joints/meter)			

*Measured from actual collar location.

**Includes rubble zones (6 joints/foot [20 joints/meter] factor).

TABLE C-7. Joint Density of Block 2-3.

Location	Horizontal Hole	Footage* (meters)	Joints**	Vertical Hole	Footage* (meters)	Joints**
2-3-A	2E-16	33-37 (10.1-11.3)	16	2M-12	0-10 (0.0-3.0)	50
	2E-17	33-40 (10.1-12.2)	29	2M-13	0-10 (0.0-3.0)	56
	2E-18	33-42.5 (10.1-13.0)	43	2E-9	0-10 (0.0-3.0)	55
Total		20.5 (6.2)	88		30 (9.1)	161
2-3-B	2E-21	33-39.5 (10.1-12.0)	25	2M-12	10-18 (3.0-5.5)	41
	2E-22	34-41 (10.4-12.5)	26	2M-13	10-18 (3.0-5.5)	39
	2E-23	34-43 (10.4-13.1)	36	2E-9	10-18 (3.0-5.5)	38
	2M-16	34-43 (10.4-13.1)	26			
Total		31.5 (9.6)	113		24 (7.3)	118
2-3-C	2E-27	34-40 (10.4-12.2)	21	2M-12	18-26 (5.5-7.9)	27
	2E-28	34-43 (10.4-13.1)	27	2M-13	18-26 (5.5-7.9)	30
	2E-29	34-43 (10.4-13.1)	38	2E-19	18-20 (5.5-6.1)	8
	2M-16	34-43 (10.4-13.1)	26			
Total		33 (10.1)	112		18 (5.5)	65
Block Subtotal		85 (25.9)	313		72 (21.9)	344
				3.68 joints/foot (12.1 joints/meter)		
				4.78 joints/foot (15.7 joints/meter)		
TOTAL				4.23 joints/foot (13.9 joints/meter)		

*Measured from actual collar location.

**Includes rubble zones (6 joints/foot [20 joints/meter] factor).

TABLE C-8. Joint Density of Block 2-4.

Location	Horizontal Hole	Footage* (meters)	Joints**	Vertical Hole	Footage* (meters)	Joints**
2-4-A	2E-14	33-42 (10.1-12.8)	42	2E-1	0-10 (0.0-3.0)	48
	2E-15	33-39 (10.1-11.9)	24	2E-9	0-10 (0.0-3.0)	55
Total		15 (4.6)	66	20 (6.1)		103
2-4-B	2E-19	33-42 (10.1-12.8)	36	2E-1	10-18 (3.0-5.5)	37
	2E-20	33-37 (10.1-11.3)	15	2E-9	10-18 (3.0-5.5)	37
Total		13 (4.0)	51	16 (4.9)		74
2-4-C	2E-24	34-41 (10.4-12.5)	28	2E-1	18-26 (5.5-7.9)	24
	2E-25	34-38 (10.4-11.6)	10	2E-9	18-20 (5.5-6.1)	8
	2E-26	34-36 (10.4-11.0)	10			
Total		13 (4.0)	48	10 (3.0)		32
Block Subtotal		41 (12.5)	165	46 (14.0)		209
				4.02 joints/foot (13.2 joints/meter)		
				4.54 joints/foot (14.9 joints/meter)		
TOTAL				4.30 joints/foot (14.1 joints/meter)		

*Measured from actual collar location.

**Includes rubble zones (6 joints/foot [20 joints/meter] factor).

TABLE C-9. Rock-Quality Designation Values of Block 1-1.

Location	Horizontal Hole	Depth Feet (meters)	RQD	Vertical Hole	Depth Feet (meters)	RQD
1-1-A	1E-13	23-32 (7.0- 9.8)	67	1M-4	0-10 (0.0-3.0)	30
	1E-12	23-32 (7.0- 9.8)	47	1M-5	0-10 (0.0-3.0)	10
				1E-3	0-10 (0.0-3.0)	25
			57			22
Total RQD	35					
1-1-B	1E-16	23-32 (7.0- 9.8)	33	1M-4	10-18 (3.0-5.5)	54
	1E-17	23-32 (7.0- 9.8)	45	1M-5	10-18 (3.0-5.5)	23
	1M-8	23-32 (7.0- 9.8)	64	1E-3	10-18 (3.0-5.5)	34
			47			37
Total RQD	42					
1-1-C	1E-20	24-33 (7.3-10.1)	57	1M-4	18-26 (5.5-7.9)	23
	1E-21	24-33 (7.3-10.1)	62	1M-5	18-26 (5.5-7.9)	43
	1E-22	24-33 (7.3-10.1)	43	1E-3	18-26 (5.5-7.9)	24
	1M-8	23-32 (7.3- 9.8)	64			
Subtotal			56			30
Total RQD	45					

C-35

RHO-BWI-ST-8

TABLE C-10. Rock-Quality Designation Values of Block 1-2.

Location	Horizontal Hole	Depth Feet (meters)	RQD	Vertical Hole	Depth Feet (meters)	RQD
1-2-A	1E-10	22-31 (6.7- 9.4)	44	1M-3	0-10 (0.0-3.0)	46
	1E-11	22-31 (6.7- 9.4)	51	1E-1	0-10 (0.0-3.0)	42
	Subtotal		47			44
Total RQD		45				
1-2-B	1E-15	22-31 (6.7- 9.4)	65	1M-3	10-18 (3.0-5.5)	39
				1E-1	10-18 (3.0-5.5)	32
	Subtotal		65			35
Total RQD		46				
1-2-C	1E-18	23-32 (7.0- 9.8)	48	1M-3	18-26 (5.5-7.9)	19
	1E-19	23-32 (7.0- 9.8)	36	1E-1	18-26 (5.5-7.9)	32
	1E-20	24-33 (7.3-10.1)	57			
	Subtotal		47			25
Total RQD		31				

TABLE C-11. Rock-Quality Designation Values of Block 1-3.

Location	Horizontal Hole	Depth Feet (meters)	RQD	Vertical Hole	Depth Feet (meters)	RQD
1-3-A	1E-12	32-36 (9.8-11.0)	33	1E-3	0-10 (0.0-3.0)	43
	1E-13	32-39 (9.8-11.9)	44	1M-7	0-10 (0.0-3.0)	43
Subtotal			40			43
Total RQD	42					
1-3-B	1E-16	32-38 (9.8-11.6)	44	1E-3	10-18 (3.0-5.5)	34
	1E-17	32-39 (9.8-11.9)	45	1M-7	10-18 (3.0-5.5)	38
Subtotal	1M-8	32-41 (9.8-12.5)	39			36
Total RQD	39		42			
1-3-C	1E-20	33-35 (10.1-10.7)	45	1E-3	18-26 (5.5-7.9)	22
	1E-21	33-41 (10.1-12.5)	33	1M-7	18-26 (5.5-7.9)	10
Subtotal	1E-22	33-41 (10.1-12.5)	33			
Total RQD	1M-8	33-41 (10.1-12.5)	39			16

TABLE C-12. Rock-Quality Designation Values of Block 1-4.

Location	Horizontal Hole	Depth Feet (meters)	RQD	Vertical Hole	Depth Feet (meters)	RQD
1-4-A	1E-10	31-40 (9.4-12.2)	51	1E-1	0-10 (0.0-3.0)	44
	1E-11	31-37 (9.4-11.3)	69	1E-8	0-10 (0.0-3.0)	13
				1E-9	0-10 (0.0-3.0)	16
	Subtotal		58			24
Total RQD	35					
1-4-B	1E-15	31-35 (9.4-10.7)	41	1E-1	10-18 (3.0-5.5)	41
				1E-8	10-18 (3.0-5.5)	42
				1E-9	10-18 (3.0-5.5)	22
	Subtotal		41			35
Total RQD	36					
1-4-C	1E-18	32-39 (9.8-11.9)	58	1E-1	18-26 (5.5-7.9)	21
	1E-19	32-36 (9.8-11.0)	57	1E-8	18-26 (5.5-7.9)	58
	1E-20	33-35 (10.1-10.7)	45	1E-9	18-26 (5.5-7.9)	56
	Subtotal		56			45
Total RQD	49					

C-38

RHO-BWI-ST-8

TABLE C-13. Rock-Quality Designation Values of Block 2-1.

Location	Horizontal Hole	Depth Feet (meters)	RQD	Vertical Hole	Depth Feet (meters)	RQD
2-1-A	2E-16	24-33 (7.3-10.1)	48	2M-7	0-10 (0.0-3.0)	32
	2E-17	24-33 (7.3-10.1)	54			
	2E-18	24-33 (7.3-10.1)	45			
	Subtotal		49			32
	Total RQD	44				
2-1-B	2E-21	24-33 (7.3-10.1)	53	2M-7	10-18 (3.0-5.5)	68
	2E-22	25-34 (7.6-10.4)	64			
	2E-23	25-34 (7.6-10.4)	67			
	2M-16	25-34 (7.6-10.4)	74			
	Subtotal		61			68
	Total RQD	62				
2-1-C	2E-27	25-34 (7.6-10.4)	58	2M-7	18-26 (5.5-7.9)	57
	2E-28	25-34 (7.6-10.4)	65			
	2E-29	25-34 (7.6-10.4)	68			
	2M-16	25-34 (7.6-10.4)	74			
	Subtotal		72			57
	Total RQD	69				

C-39

RHO-BWI-ST-8

TABLE C-14. Rock-Quality Designation Values of Block 2-2.

Location	Horizontal Hole	Depth Feet (meters)	RQD	Vertical Hole	Depth Feet (meters)	RQD
2-2-A	2E-14	24-33 (7.3-10.1)	54	2M-3	0-10 (0.0-3.0)	18
	2E-15	24-33 (7.3-10.1)	56		0-10 (0.0-3.0)	36
	Subtotal		55			27
Total RQD		40				
2-2-B	2E-19	24-33 (7.3-10.1)	67	2M-3	10-18 (3.0-5.5)	47
	2E-20	24-33 (7.3-10.1)	60		10-18 (3.0-5.5)	40
	Subtotal		63			43
Total RQD		54				
2-2-C	2E-24	25-34 (7.6-10.4)	63	2M-3	18-26 (5.5-7.9)	86
	2E-25	25-34 (7.6-10.4)	76		18-26 (5.5-7.9)	28
	2E-26	25-34 (7.6-10.4)	71			
Subtotal		70				57
Total RQD		65				

C-40

RHO-BWI-ST-8

TABLE C-15. Rock-Quality Designation Values of Block 2-3.

Location	Horizontal Hole	Depth Feet (meters)	RQD	Vertical Hole	Depth Feet (meters)	RQD
2-3-A	2E-16	33-37 (10.1-11.3)	54	2M-12	0-10 (0.0-3.0)	19
	2E-17	33-40 (10.1-12.2)	67	2M-13	0-10 (0.0-3.0)	34
	2E-18	33-42.5 (10.1-13.0)	52	2E-9	0-10 (0.0-3.0)	29
	Subtotal		58			27
Total RQD	39					
2-3-B	2E-21	33-39.5 (10.1-12.0)	56	2M-12	10-18 (3.0-5.5)	26
	2E-22	34-41 (10.4-12.5)	67	2M-13	10-18 (3.0-5.5)	47
	2E-23	34-43 (10.4-13.1)	64	2E-9	10-18 (3.0-5.5)	34
	2M-16	34-43 (10.4-13.1)	69			36
Subtotal			64			
Total RQD	52					
2-3-C	2E-27	34-40 (10.4-12.2)	75	2M-12	18-26 (5.5-7.9)	37
	2E-28	34-43 (10.4-13.1)	82	2M-13	18-26 (5.5-7.9)	57
	2E-29	34-43 (10.4-13.1)	38	2E-9	18-26 (5.5-7.9)	50
	2M-16	34-43 (10.4-13.1)	69			48
Subtotal			65			
Total RQD	58					

C-41

RHO-BWI-ST-8

TABLE C-16. Rock-Quality Designation Values of Block 2-4.

Location	Horizontal Hole	Depth Feet (meters)	RQD	Vertical Hole	Depth Feet (meters)	RQD	
2-4-A	2E-14	33-42 (10.1-12.8)	55	2E-1	0-10 (0.0-3.0)	26	
	2E-15	33-39 (10.1-11.9)		2E-9	0-10 (0.0-3.0)	29	
Subtotal						27	
Total RQD		39					
2-4-B	2E-19	33-42 (10.1-12.8)	64	2E-1	10-18 (3.0-5.5)	49	
	2E-20	33-37 (10.1-11.3)		2E-9	10-18 (3.0-5.5)	34	
Subtotal						41	
Total RQD		51					
2-4-C	2E-24	34-41 (10.4-12.5)	60	2E-1	18-26 (5.5-7.9)	59	
	2E-25	34-48 (10.4-14.6)		2E-9	18-26 (5.5-7.9)	50	
	2E-26	34-36 (10.4-11.0)					
Subtotal						54	
Total RQD		57					

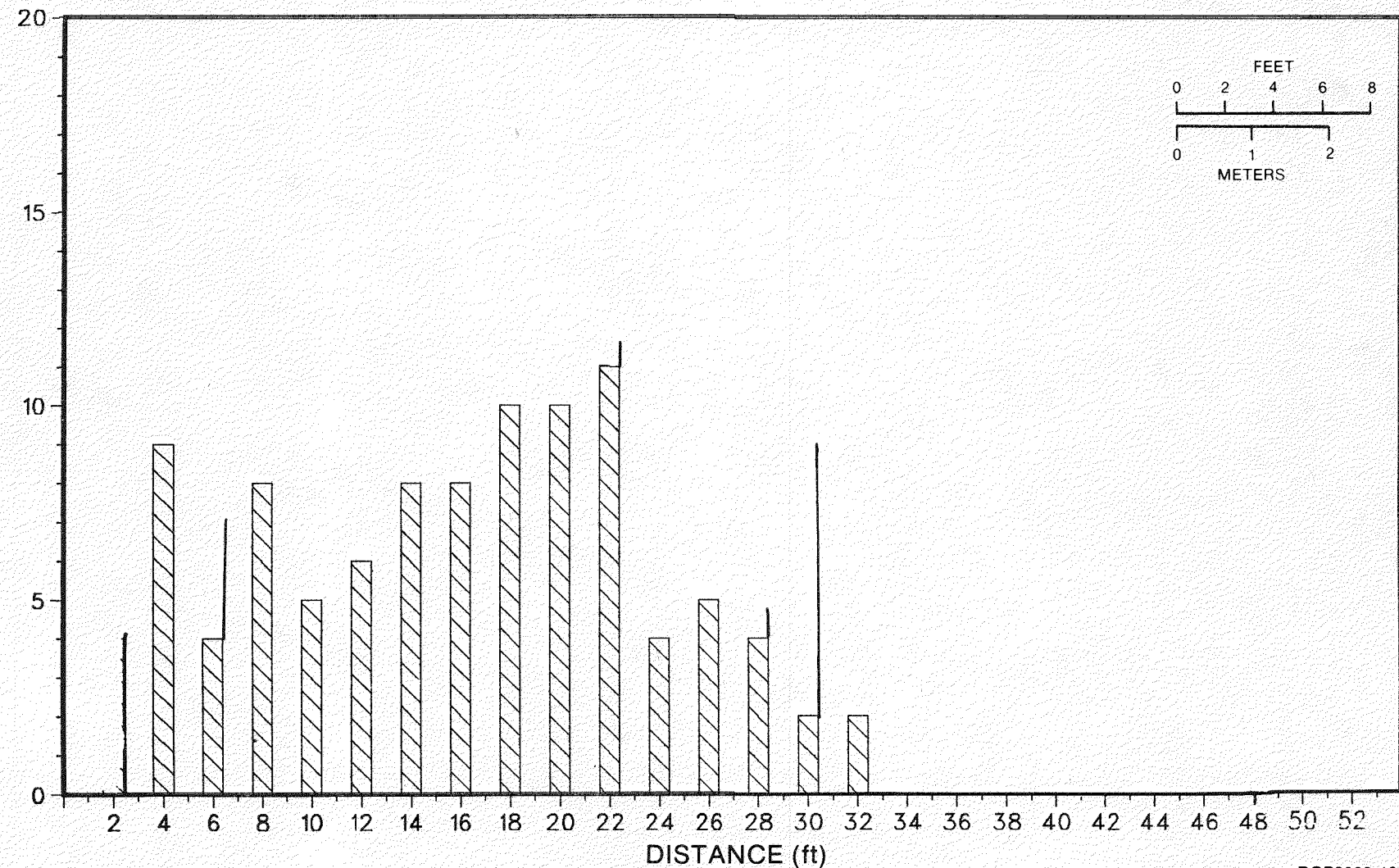
C-42

RHO-BWI-ST-8

The following histograms are a depiction of the joint frequency of each of the principal boreholes in 2-foot (6-centimeter) intervals. The solid line represents rubble zones, using a factor of 6 joints per foot (30 centimeters).

BASALT CORE GEO-MECHANICAL DATA

CORE HOLE 1E1
FRACTURE TOP FREQUENCY

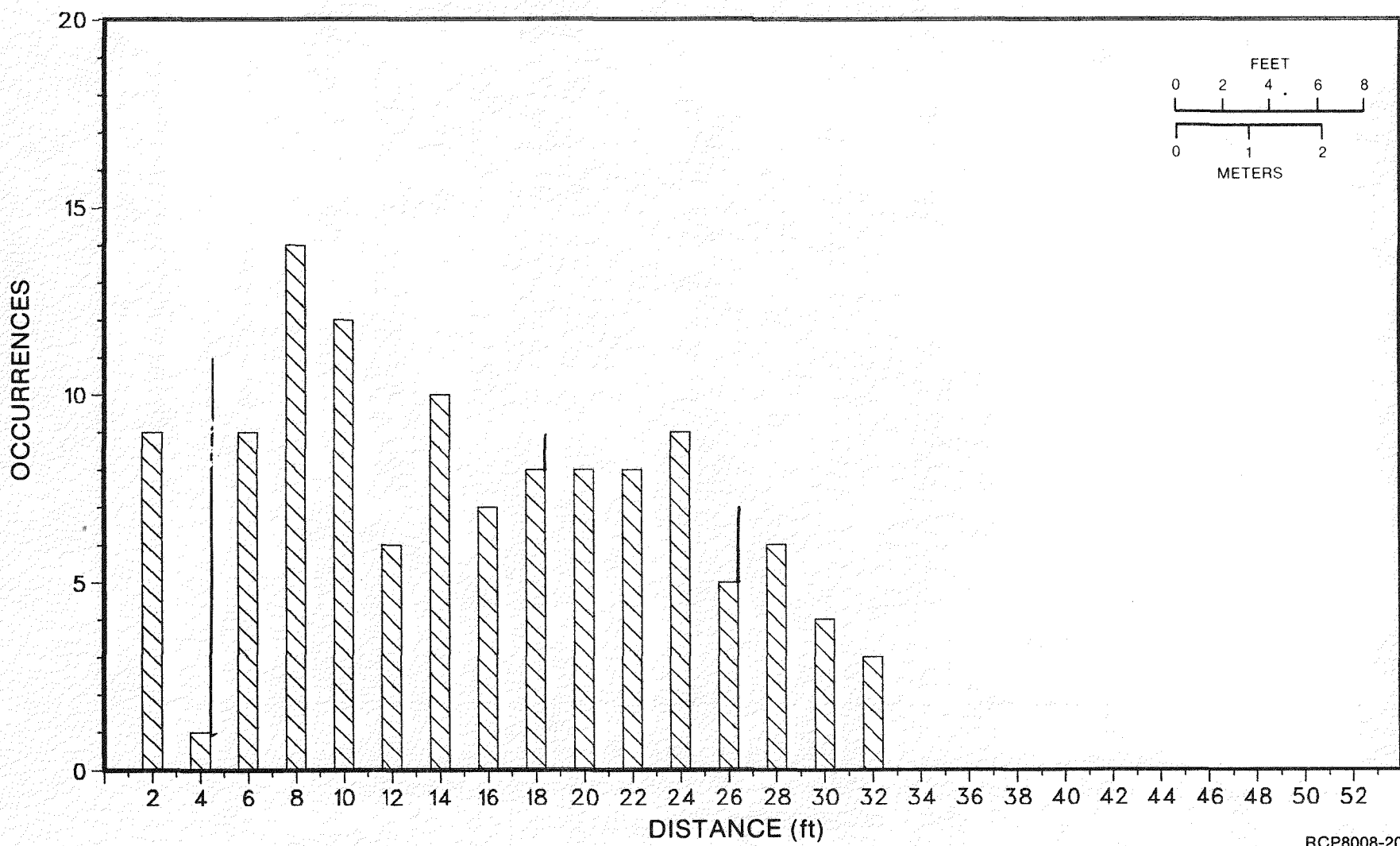


RHO-BWI-ST-8

RCP8008-19

BASALT CORE GEO-MECHANICAL DATA

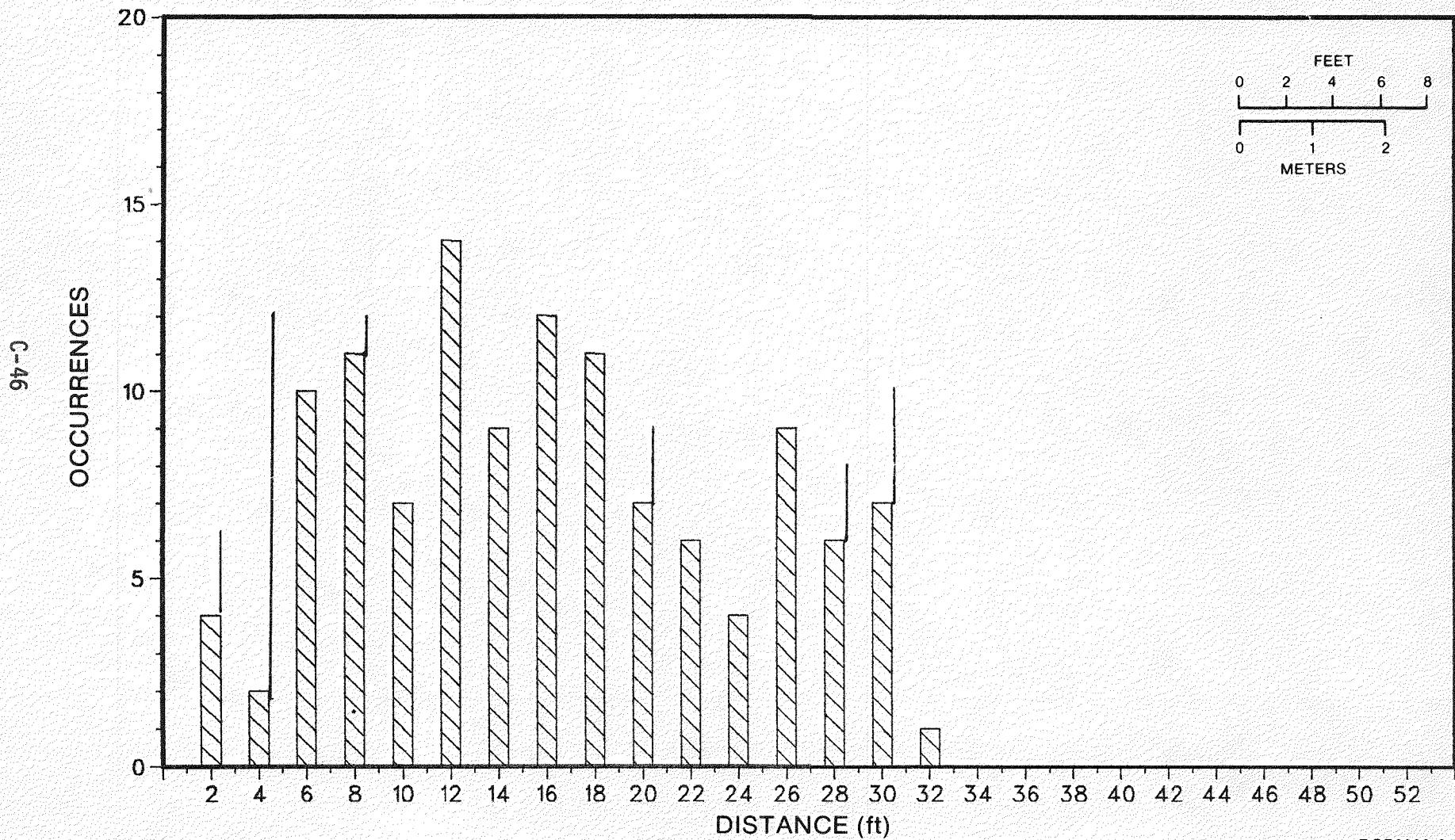
CORE HOLE 1E8
FRACTURE TOP FREQUENCY



RCP8008-20

RHO-BWI-ST-8

BASALT CORE GEO-MECHANICAL DATA
CORE HOLE 1E9
FRACTURE TOP FREQUENCY

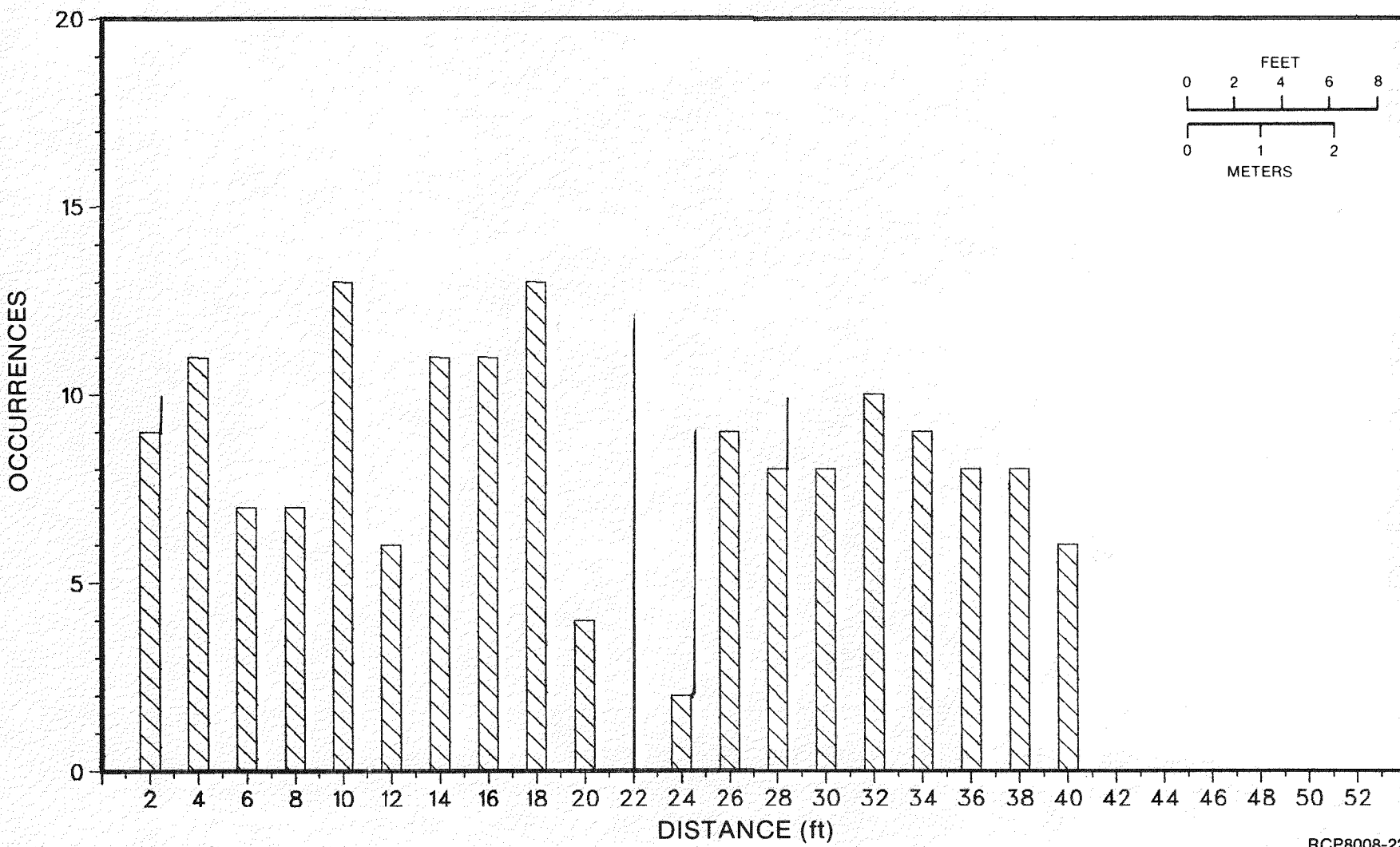


RHO-BMI-ST-8

RCP8008-21

BASALT CORE GEO-MECHANICAL DATA

CORE HOLE 1E10
FRACTURE TOP FREQUENCY

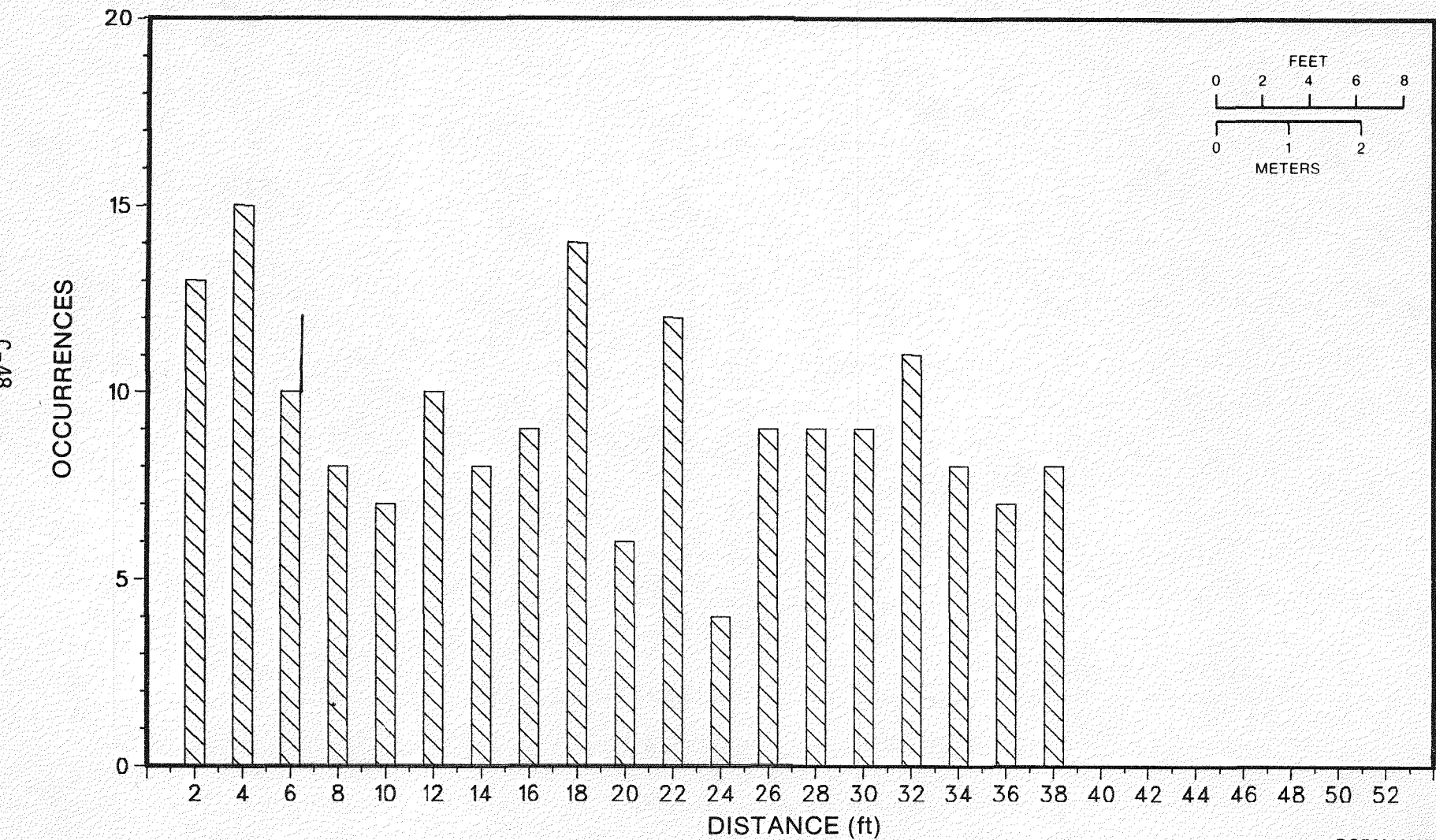


C-47

RHO-BWI-ST-8

RCP8008-22

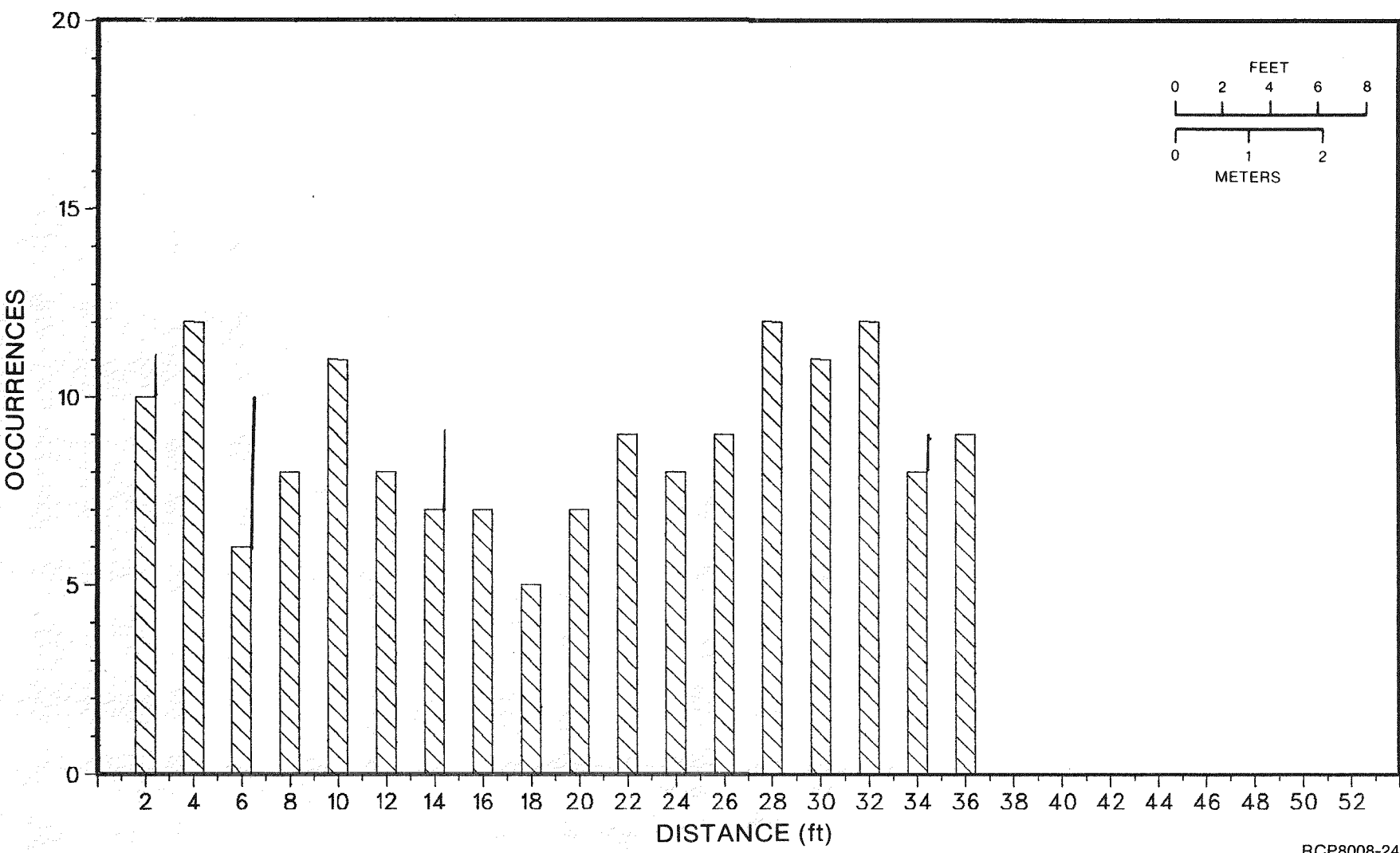
BASALT CORE GEO-MECHANICAL DATA
CORE HOLE 1E11
FRACTURE TOP FREQUENCY



RHO-BWI-ST-8

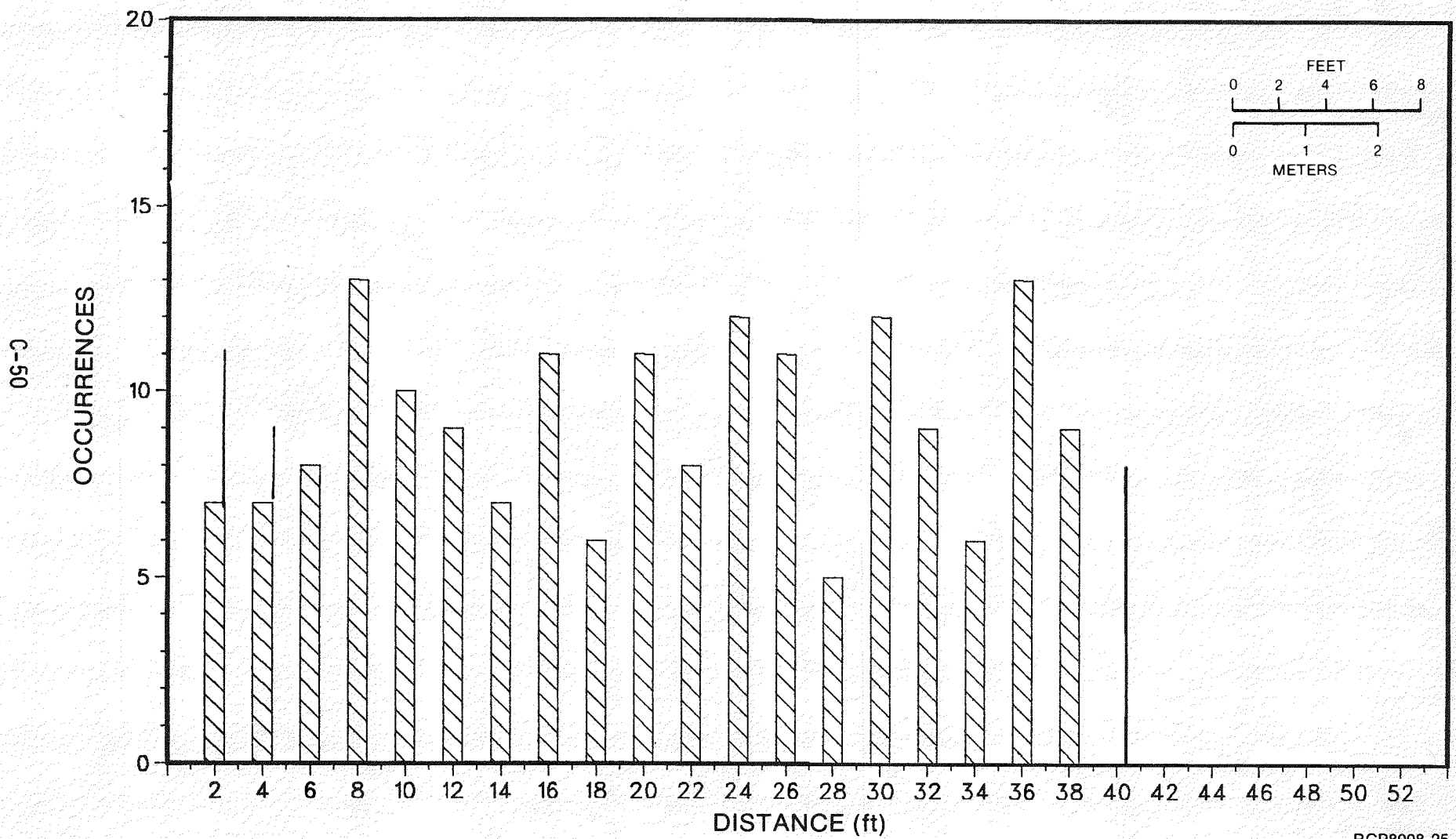
RCP8008-23

BASALT CORE GEO-MECHANICAL DATA
CORE HOLE 1E12
FRACTURE TOP FREQUENCY



BASALT CORE GEO-MECHANICAL DATA

CORE HOLE 1E13
FRACTURE TOP FREQUENCY

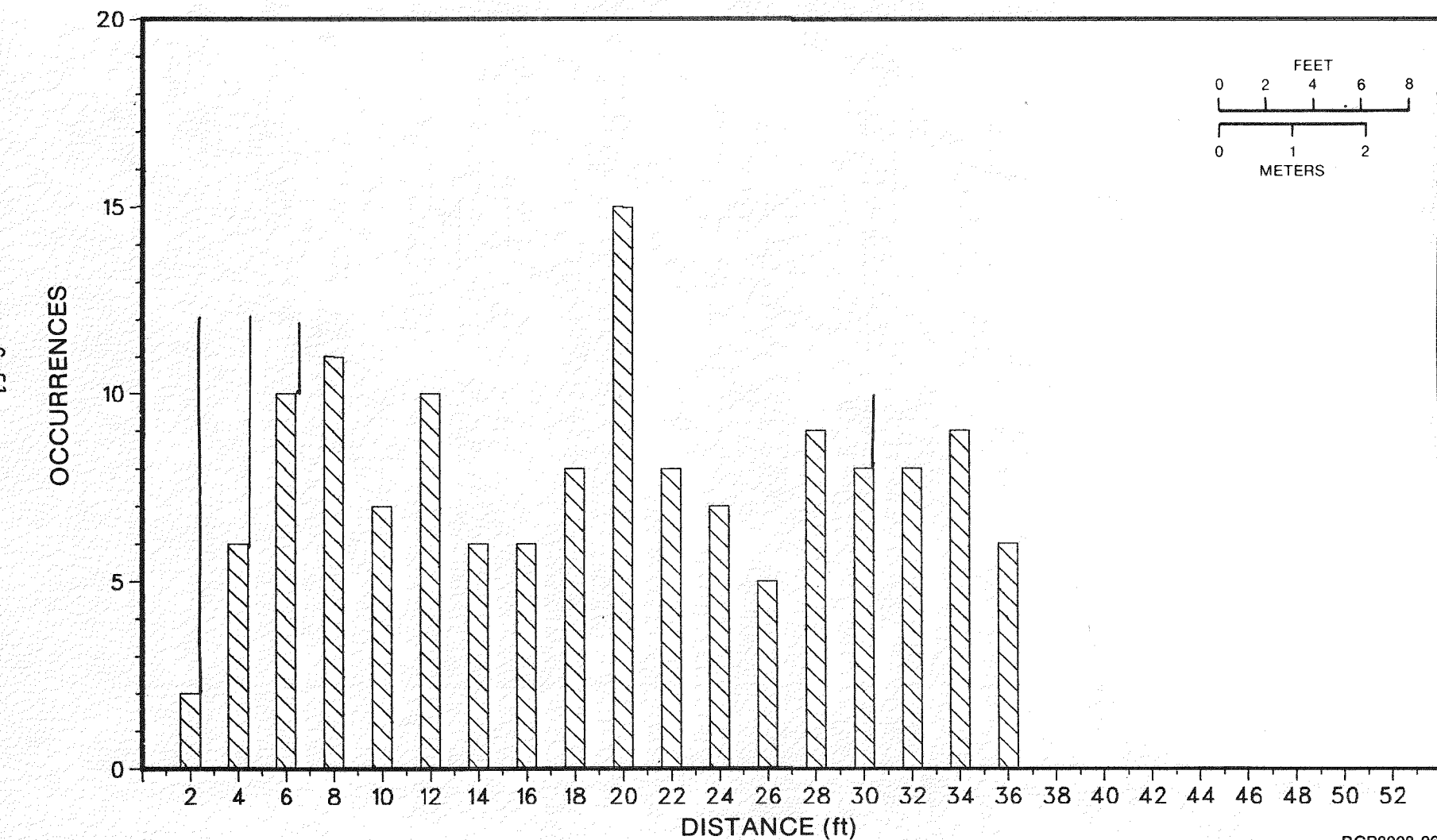


RHO-BWI-ST-8

RCP8008-25

BASALT CORE GEO-MECHANICAL DATA

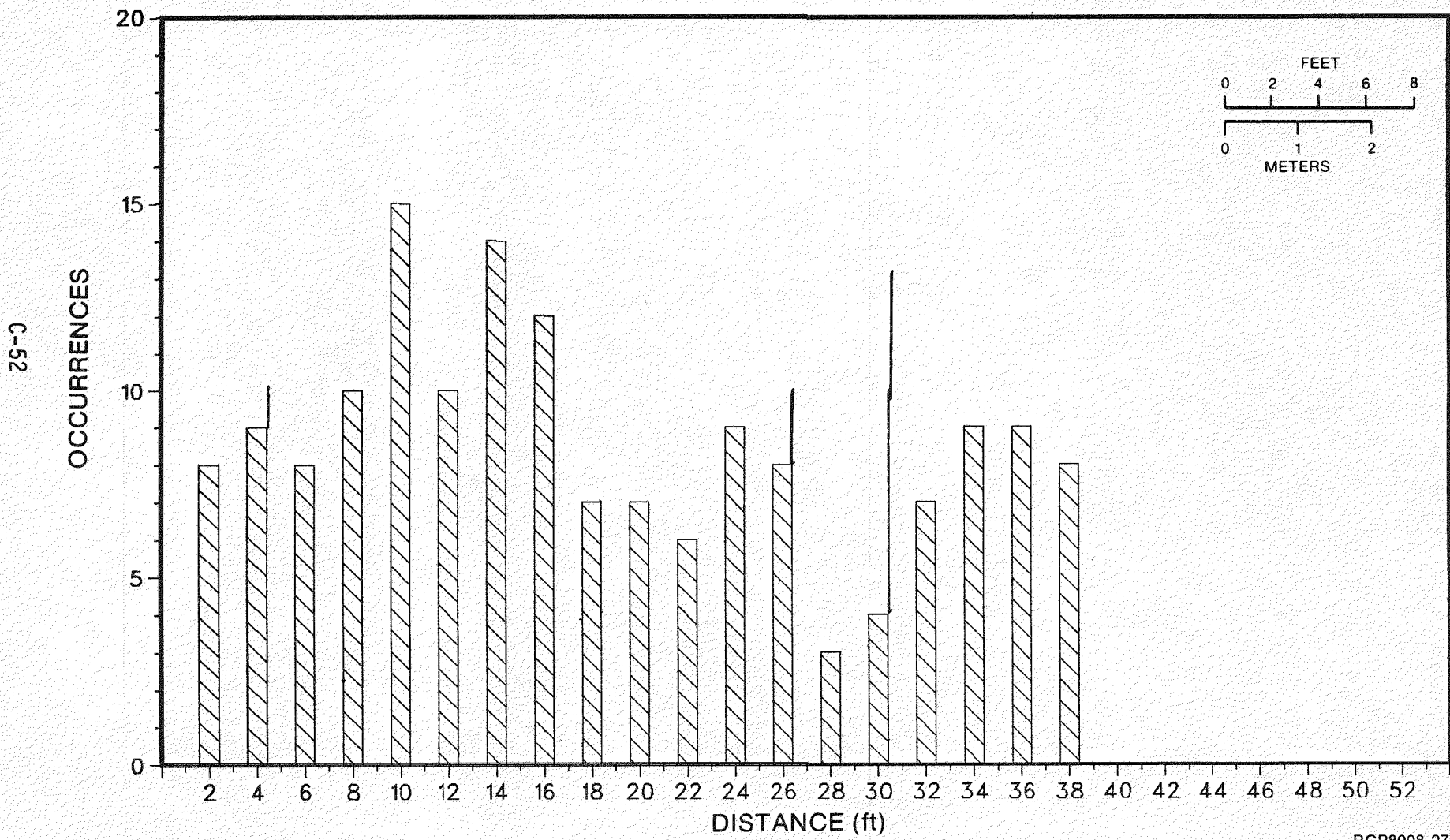
CORE HOLE 1E15
FRACTURE TOP FREQUENCY



RCP8008-26

RHO-BWI-ST-8

BASALT CORE GEO-MECHANICAL DATA
CORE HOLE 1E16
FRACTURE TOP FREQUENCY

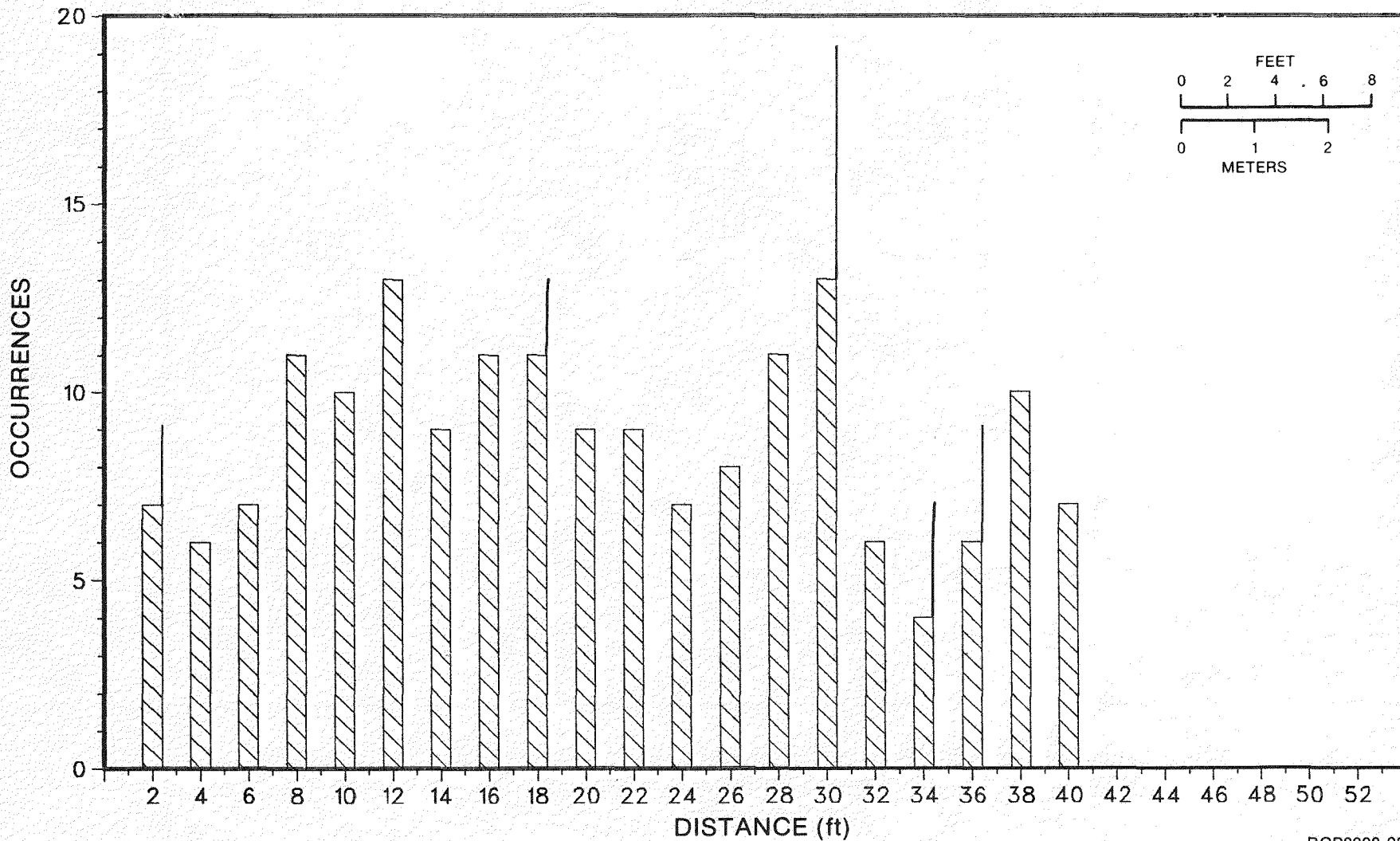


RHO-BMI-ST-8

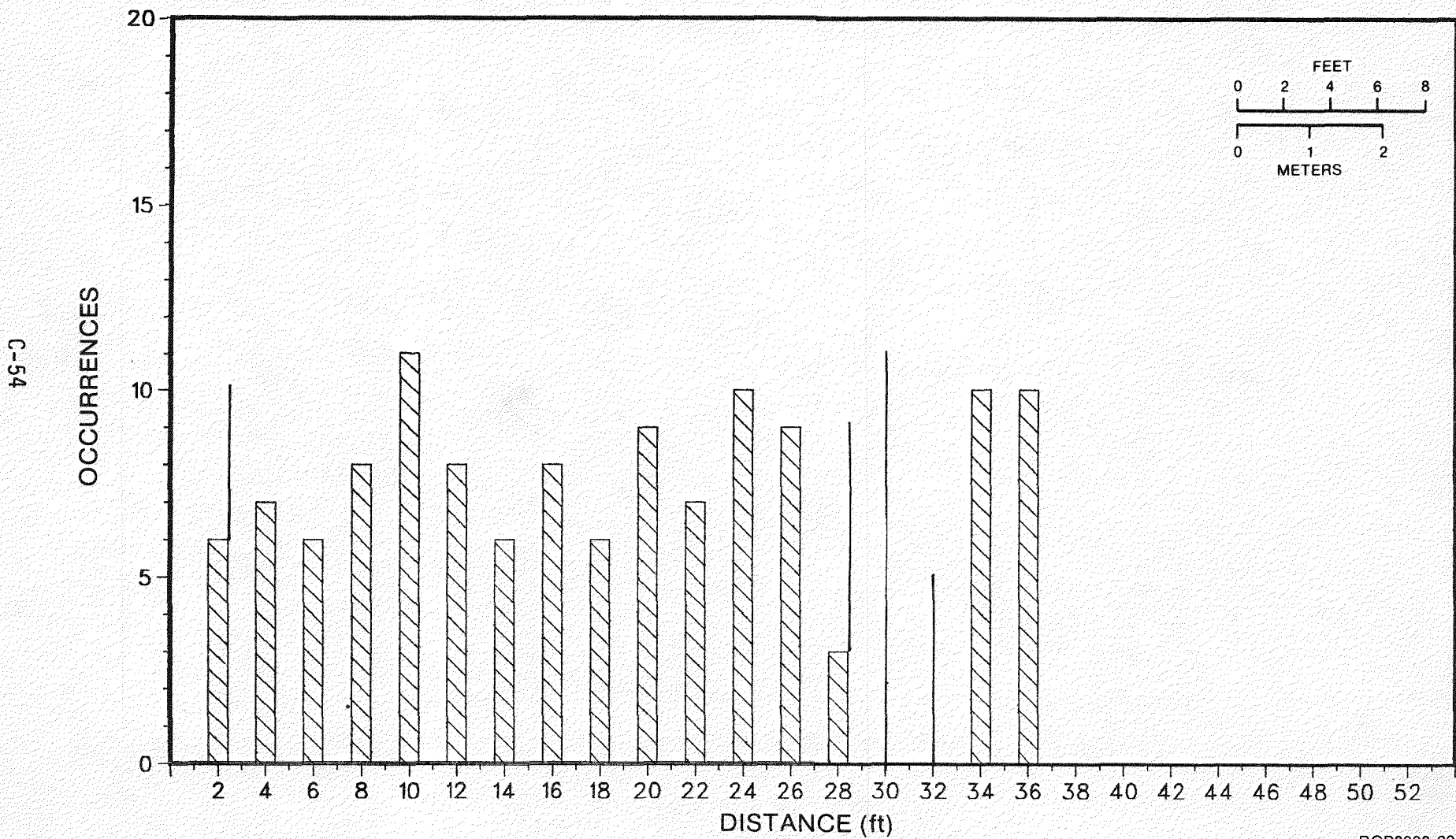
RCP8008-27

BASALT CORE GEO-MECHANICAL DATA

CORE HOLE 1E18
FRACTURE TOP FREQUENCY



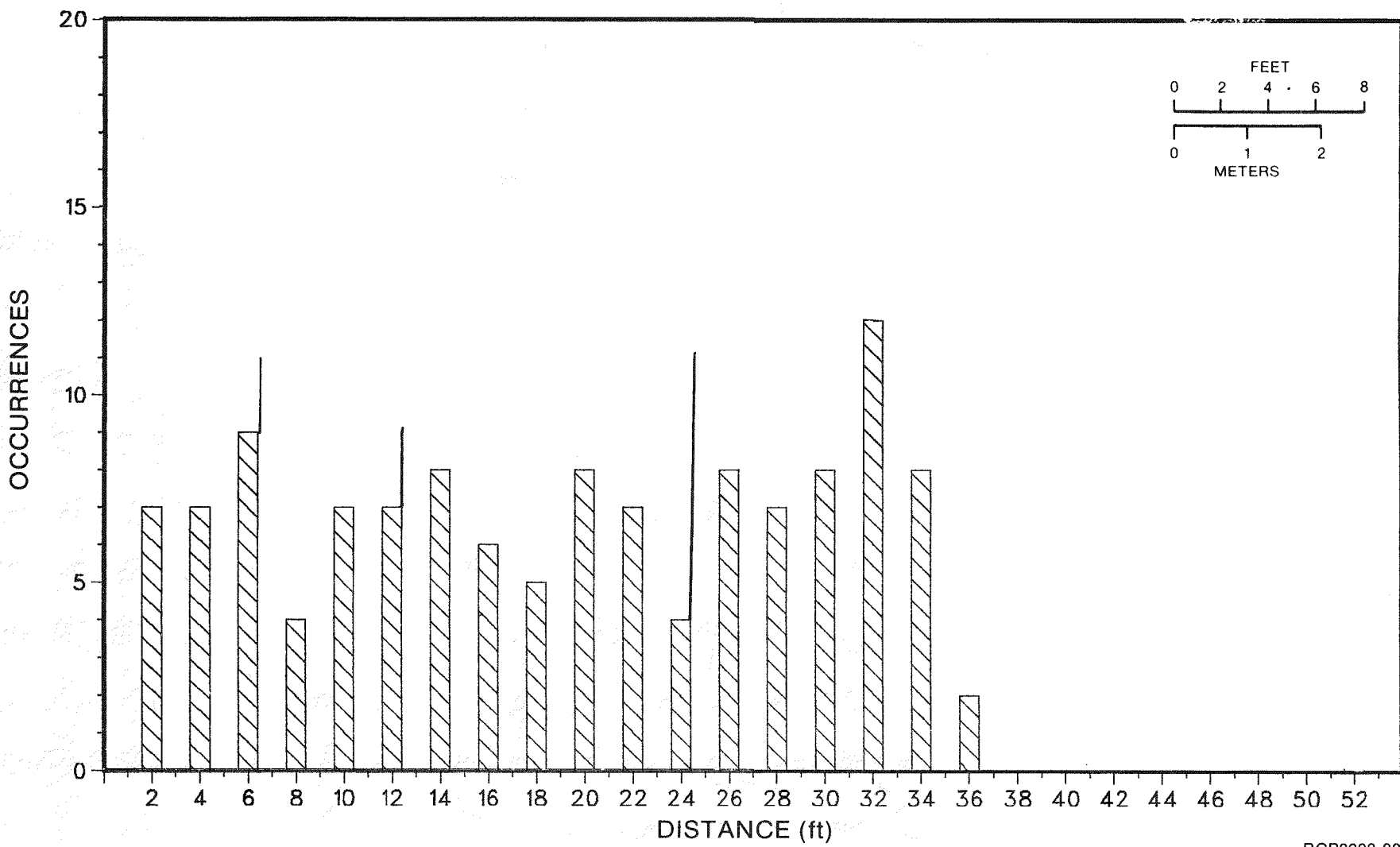
BASALT CORE GEO-MECHANICAL DATA
CORE HOLE 1E19
FRACTURE TOP FREQUENCY



RCP8008-29

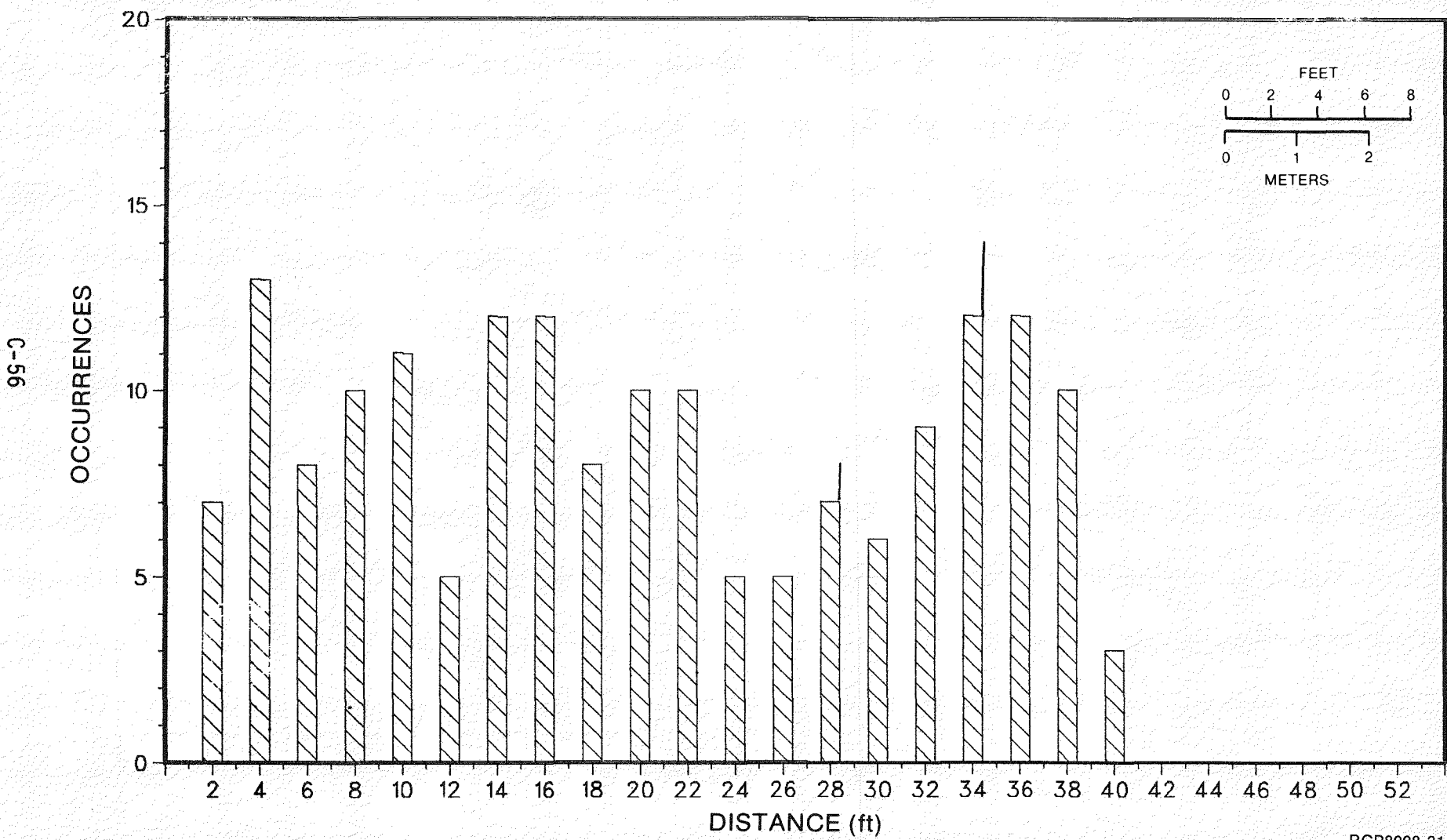
RHO-BWI-ST-8

BASALT CORE GEO-MECHANICAL DATA
CORE HOLE 1E20
FRACTURE TOP FREQUENCY



RHO-BWI-ST-8

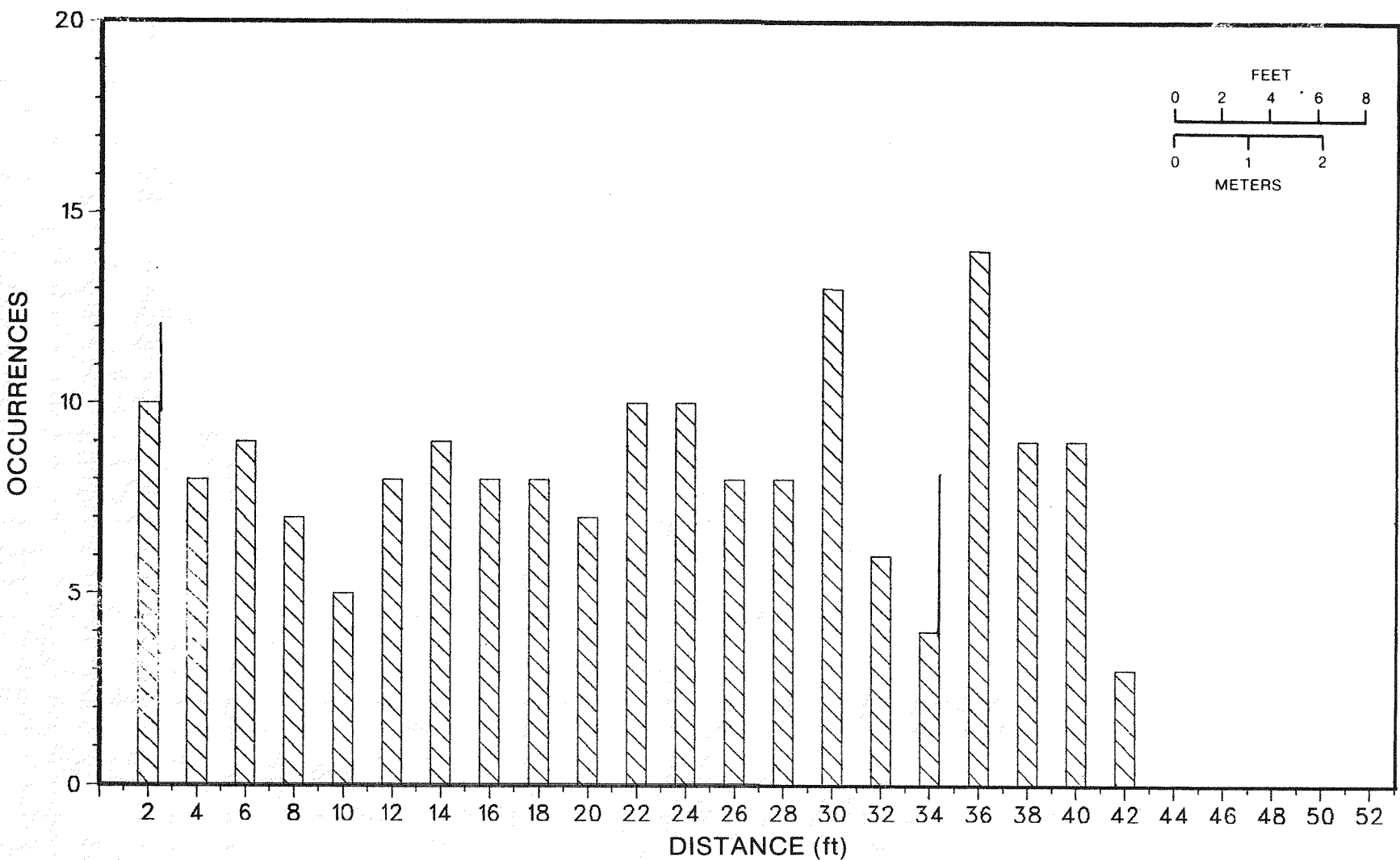
BASALT CORE GEO-MECHANICAL DATA
CORE HOLE 1E21
FRACTURE TOP FREQUENCY



RCP8008-31

RHO-BMI-ST-8

BASALT CORE GEO-MECHANICAL DATA
CORE HOLE 1E22
FRACTURE TOP FREQUENCY

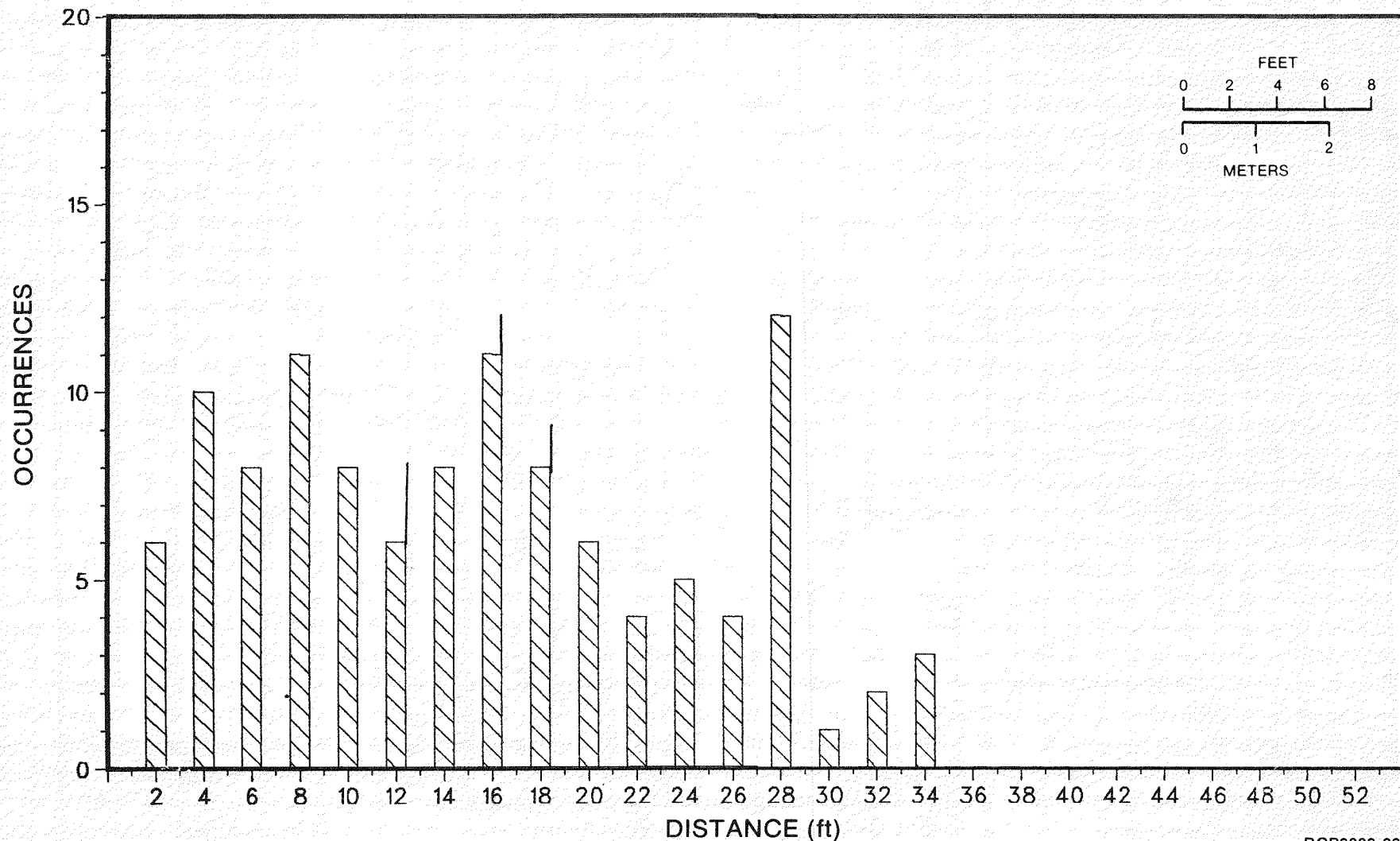


RHO-BWI-ST-8

RCP8008-32

BASALT CORE GEO-MECHANICAL DATA

CORE HOLE 1M3
FRACTURE TOP FREQUENCY

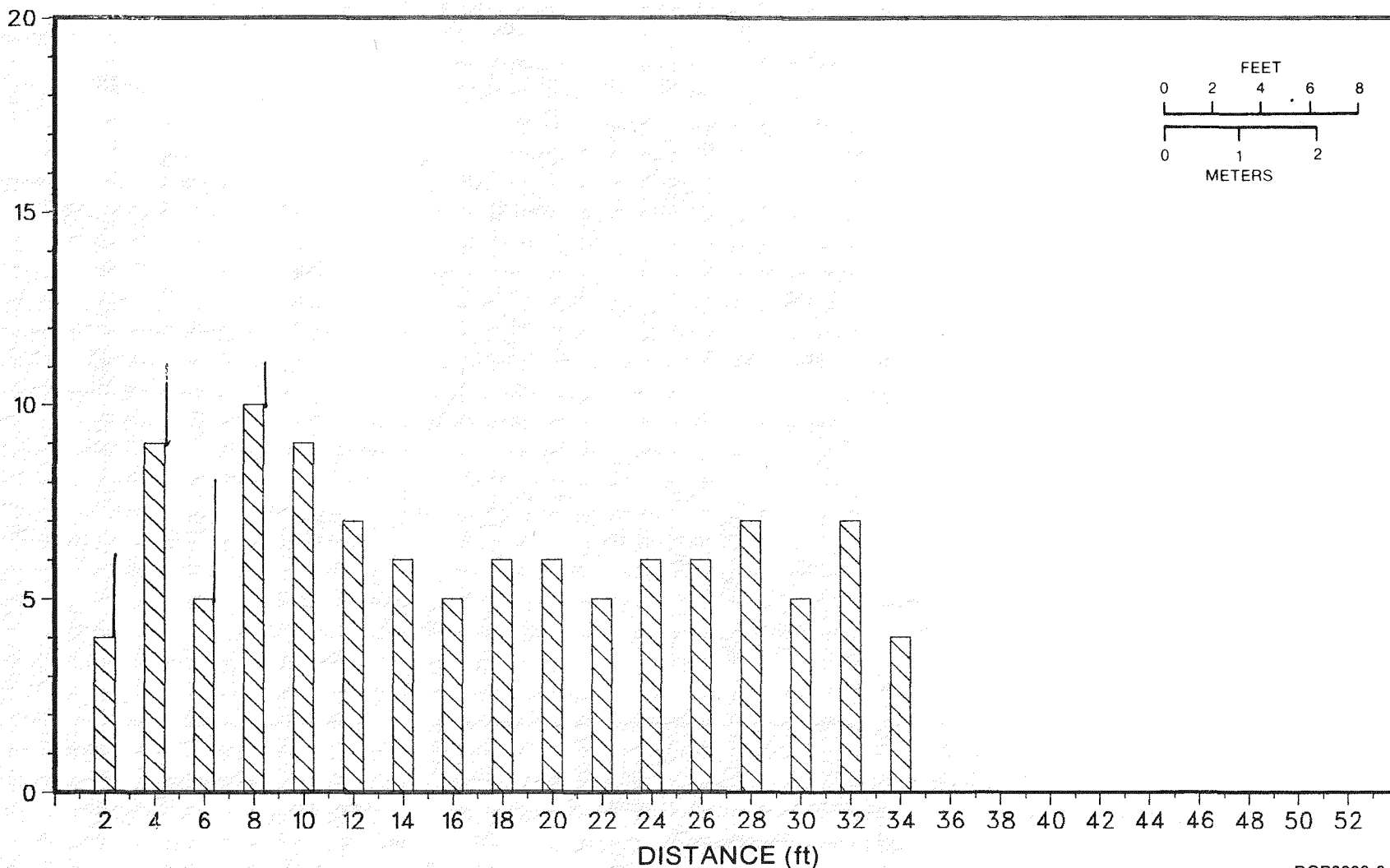


RCP8008-33

RHO-BWI-ST-8

BASALT CORE GEO-MECHANICAL DATA
CORE HOLE 1M4
FRACTURE TOP FREQUENCY

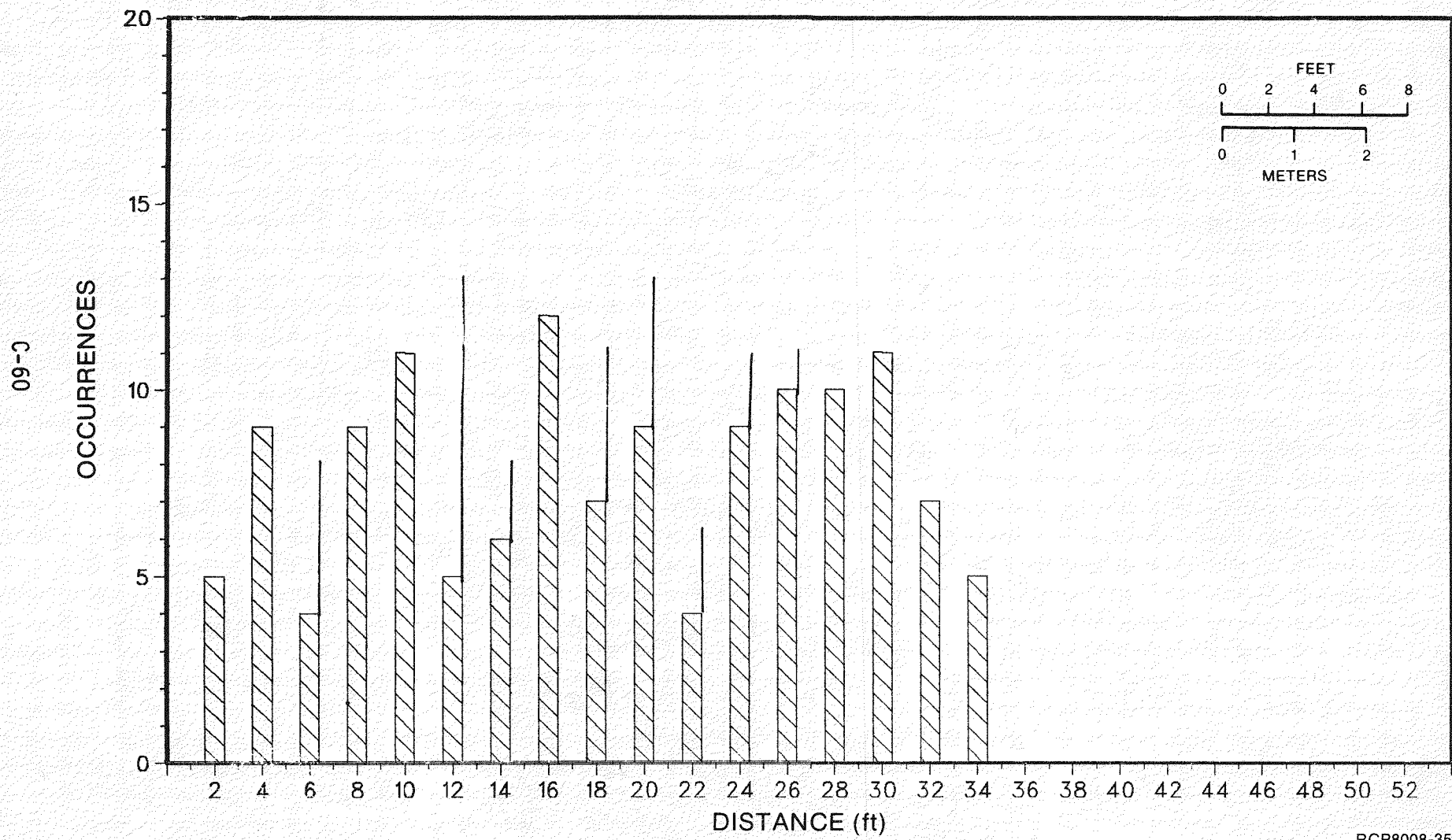
69-J



RHO-BWI-ST-8

RCP8008-34

BASALT CORE GEO-MECHANICAL DATA
CORE HOLE 1M5
FRACTURE TOP FREQUENCY

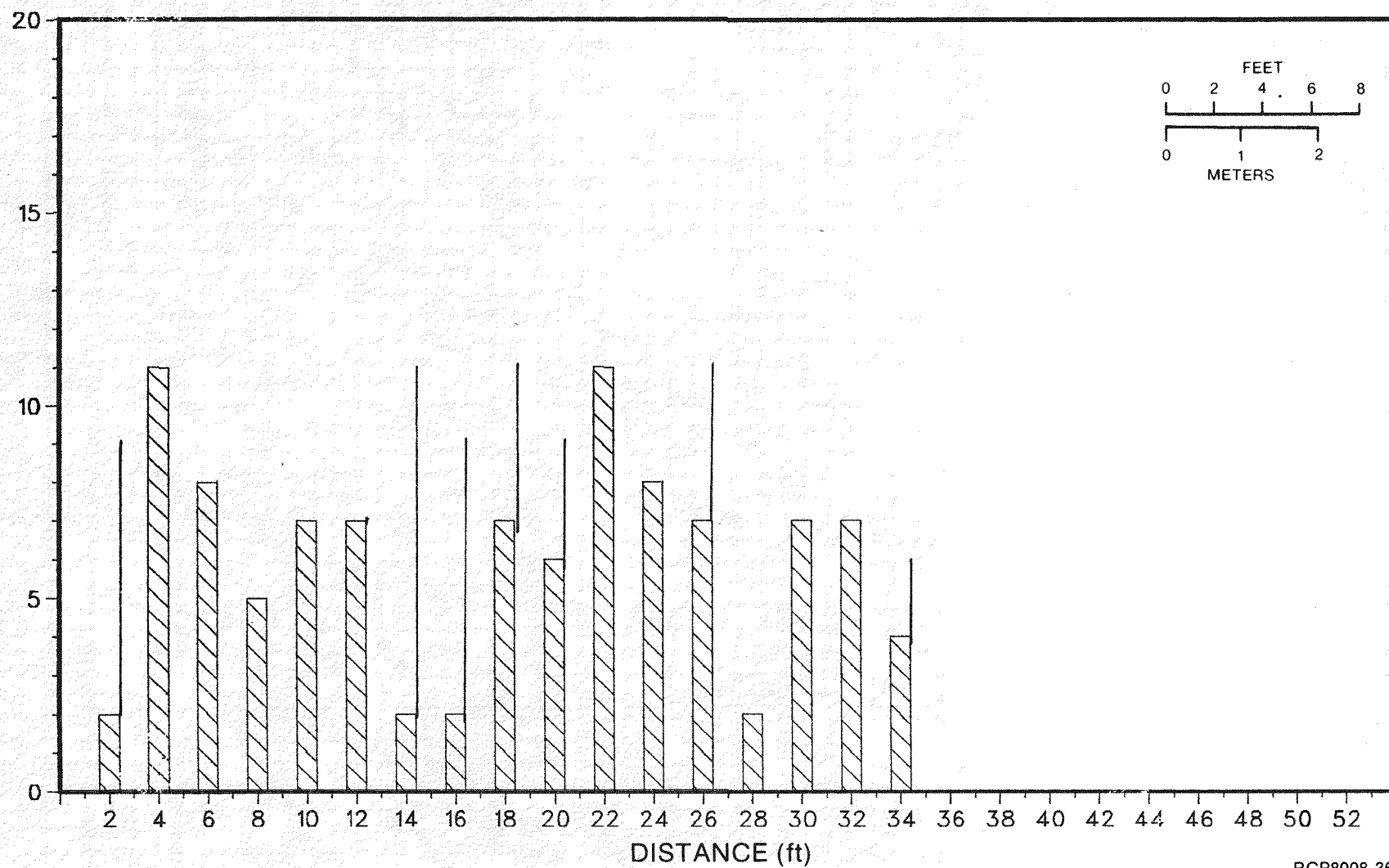


RHO-BWI-ST-8

RCP8008-35

BASALT CORE GEO-MECHANICAL DATA
CORE HOLE 1M7
FRACTURE TOP FREQUENCY

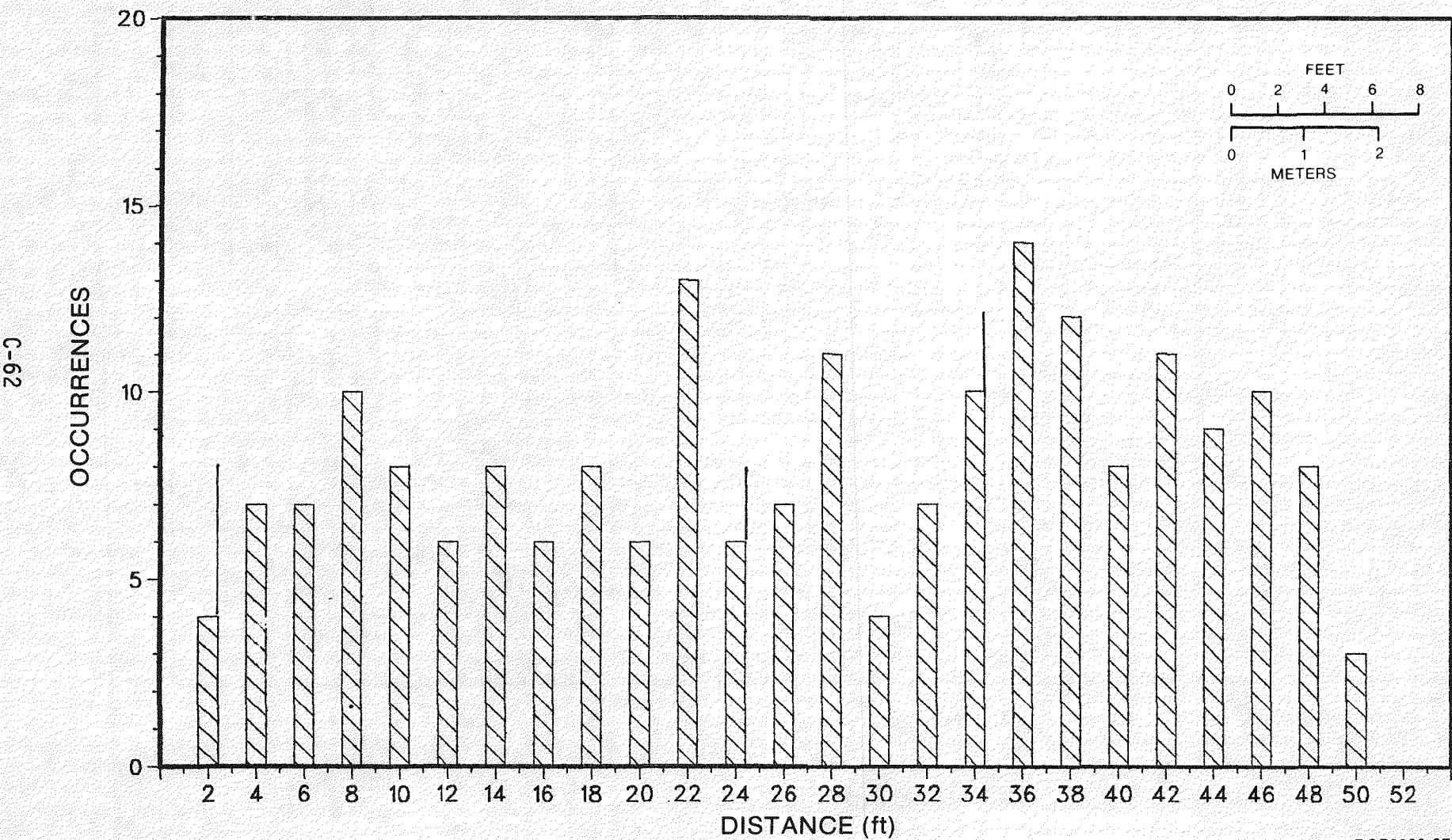
C-61



RCP8008-36

RHO-BWI-ST-8

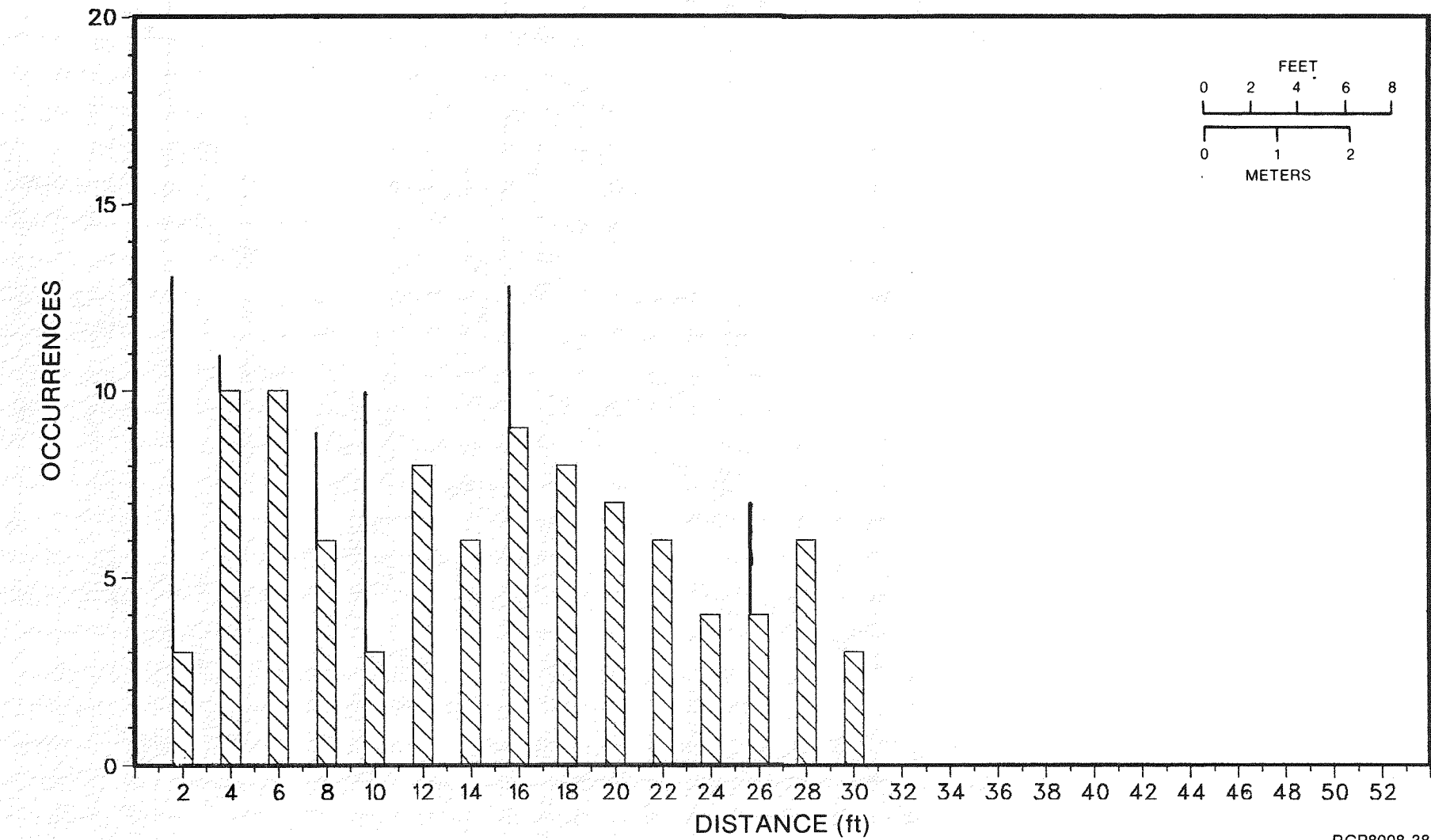
BASALT CORE GEO-MECHANICAL DATA
CORE HOLE 1M8
FRACTURE TOP FREQUENCY



RCP8008-37

RHO-BWI-ST-8

BASALT CORE GEO-MECHANICAL DATA
CORE HOLE 2E1
FRACTURE TOP FREQUENCY

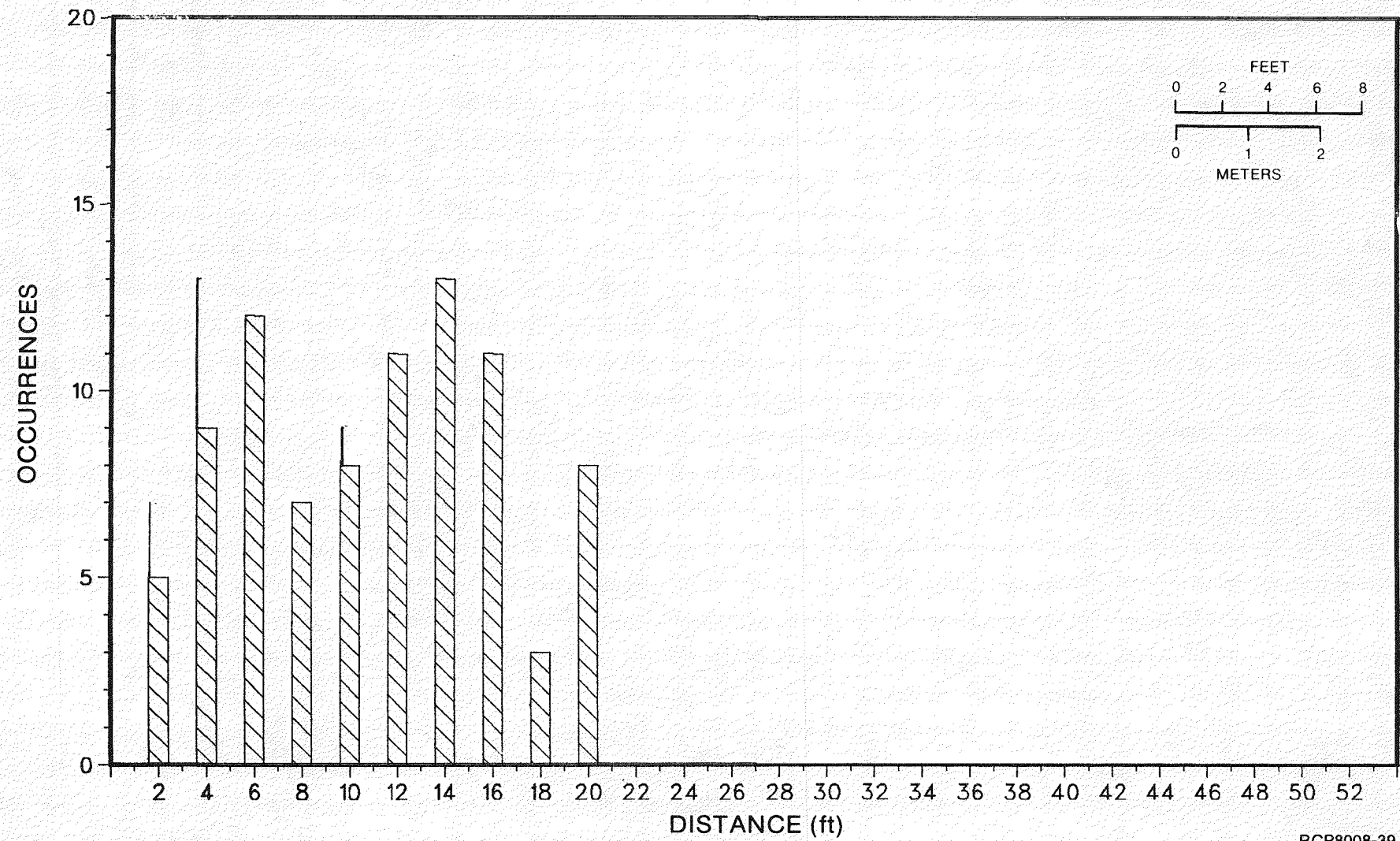


RCP8008-38

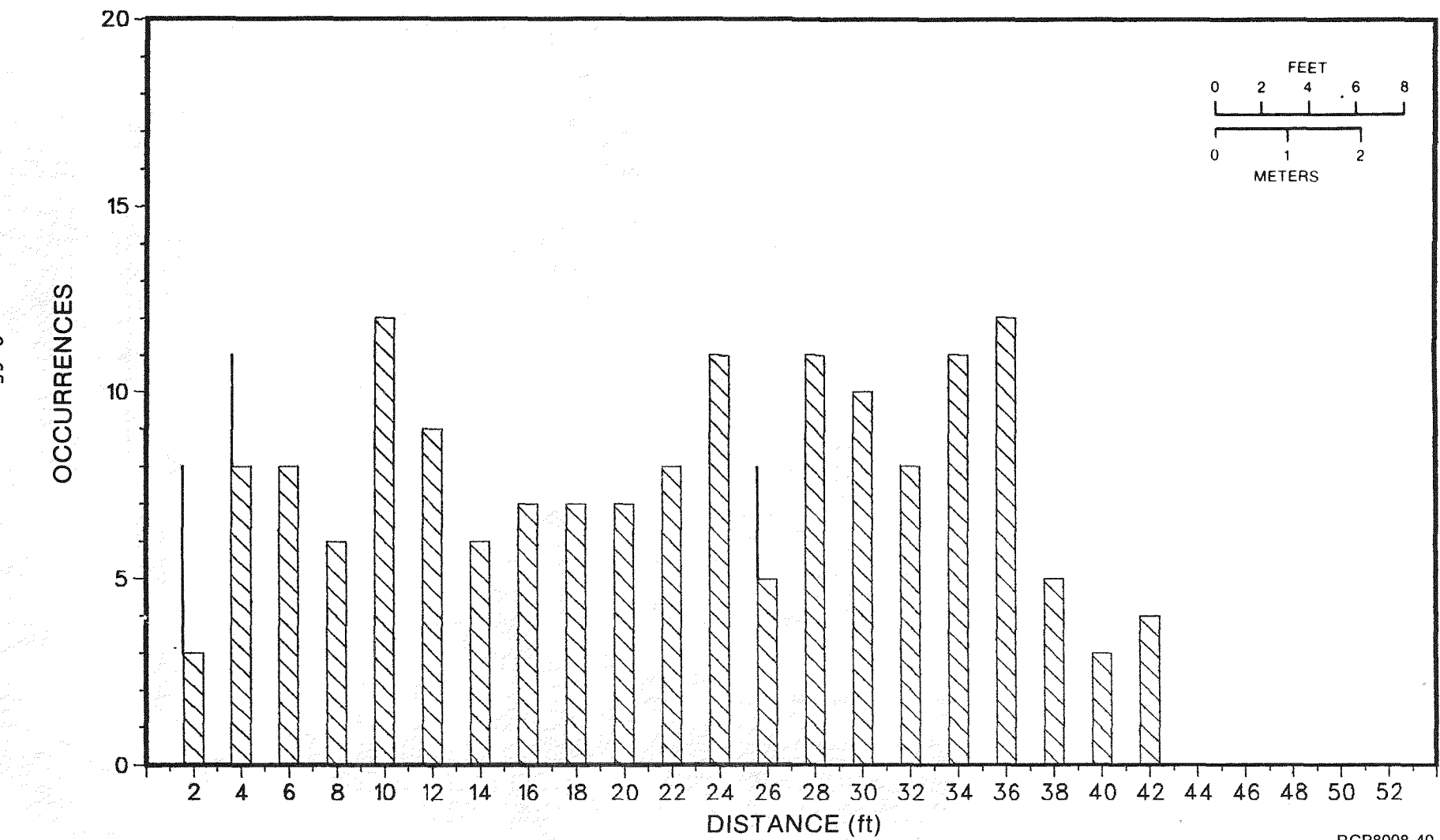
RHO-BWI-ST-8

BASALT CORE GEO-MECHANICAL DATA

CORE HOLE 2E9
FRACTURE TOP FREQUENCY



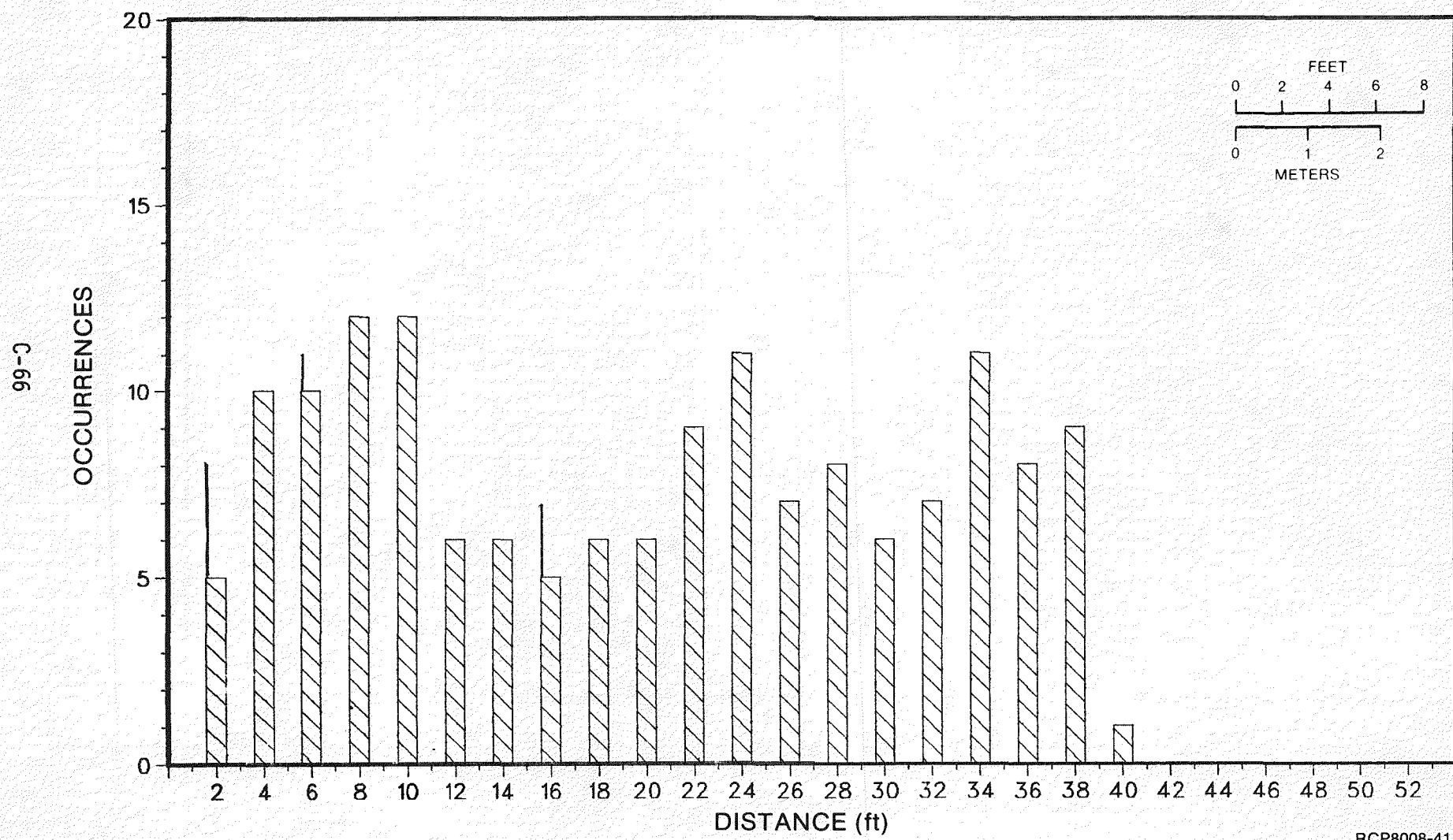
BASALT CORE GEO-MECHANICAL DATA
CORE HOLE 2E14
FRACTURE TOP FREQUENCY



RHO-BWI-ST-8

RCP8008-40

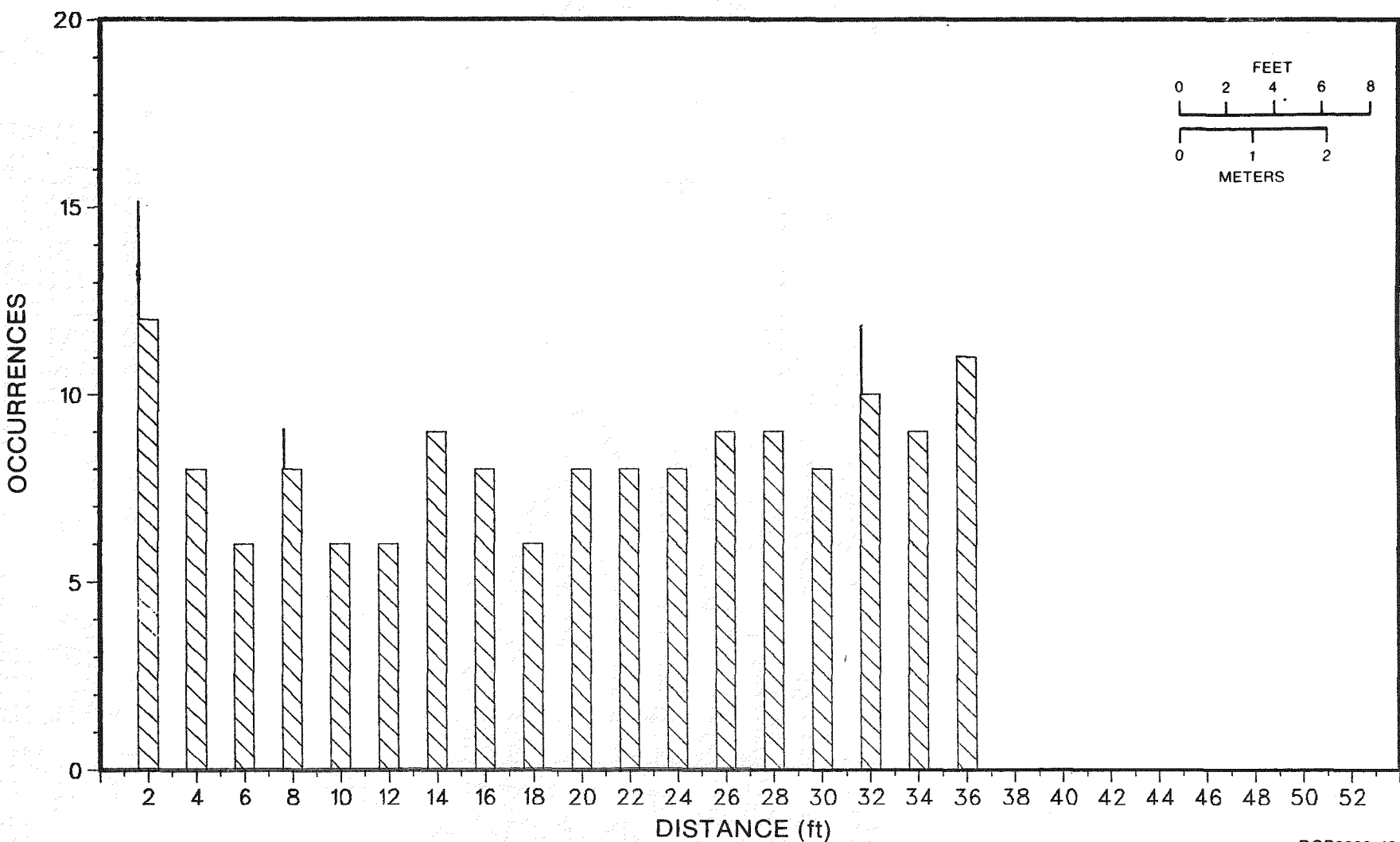
BASALT CORE GEO-MECHANICAL DATA
CORE HOLE 2E15
FRACTURE TOP FREQUENCY



RCP8008-41

RHO-BMI-ST-8

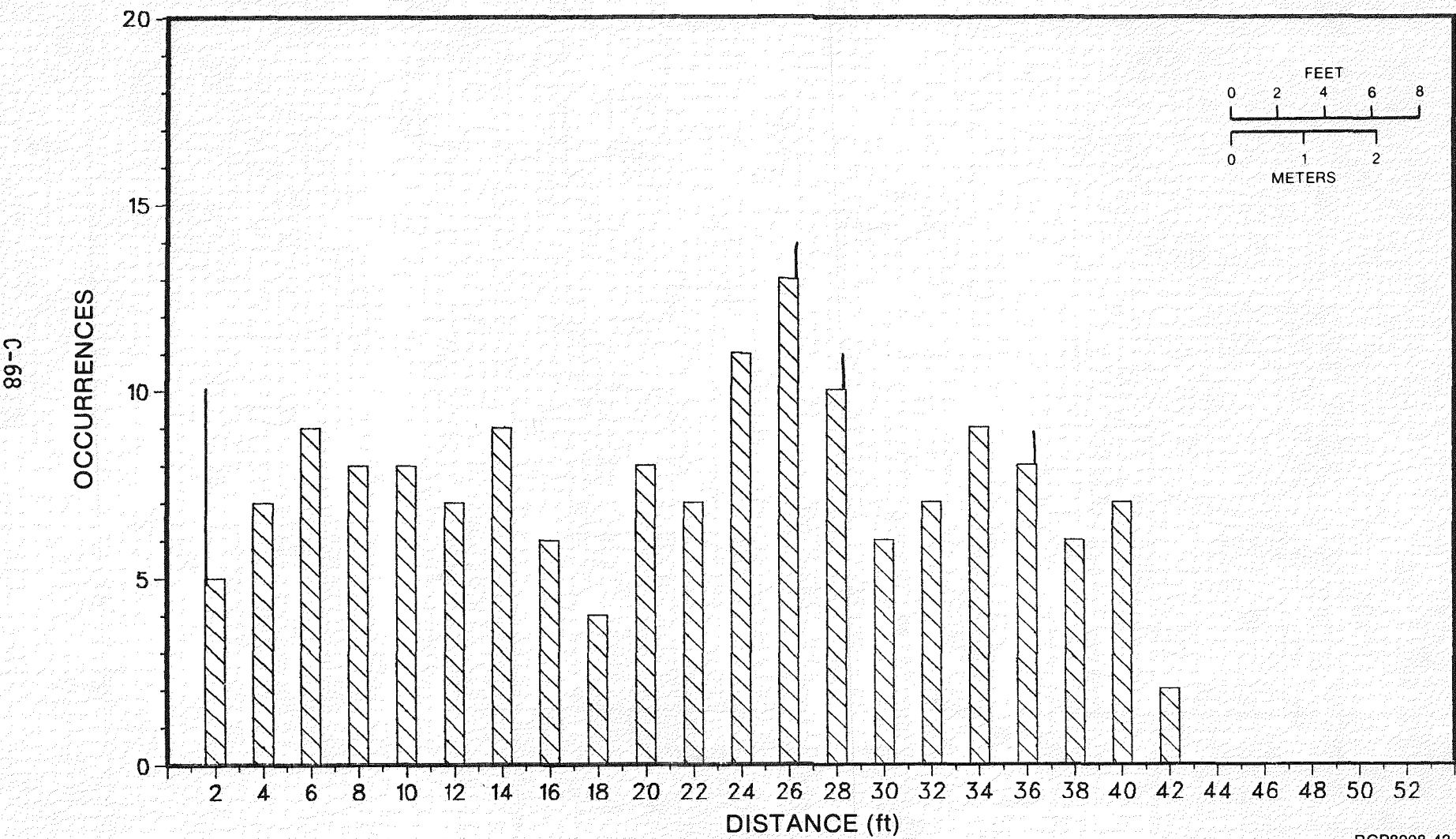
BASALT CORE GEO-MECHANICAL DATA
CORE HOLE 2E16
FRACTURE TOP FREQUENCY



RCP8008-42

RHO-BWI-ST-8

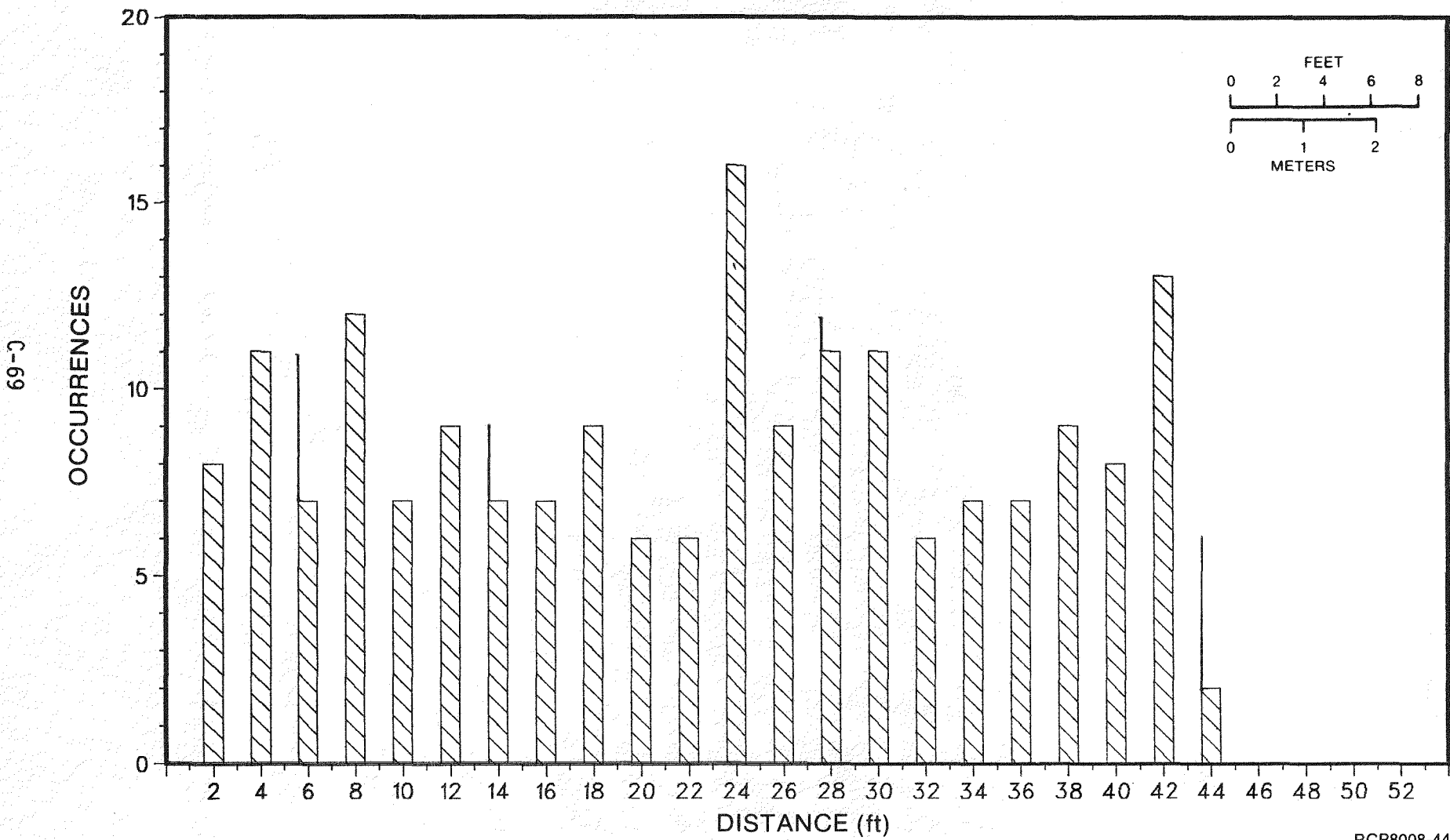
BASALT CORE GEO-MECHANICAL DATA
CORE HOLE 2E17
FRACTURE TOP FREQUENCY



RHO-BWI-ST-8

RCP8008-43

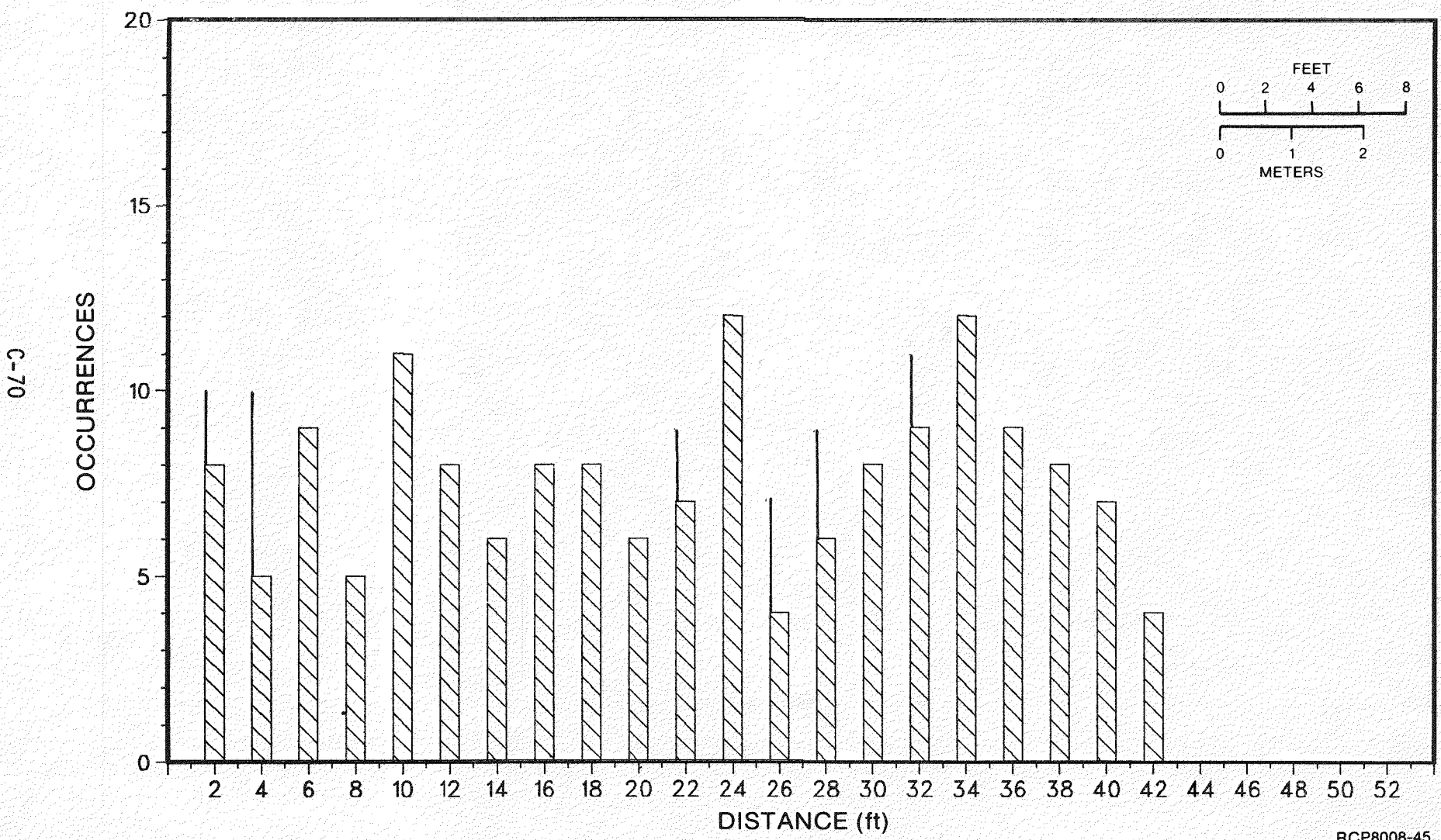
BASALT CORE GEO-MECHANICAL DATA
CORE HOLE 2E18
FRACTURE TOP FREQUENCY



RHO-BWI-ST-8

RCP8008-44

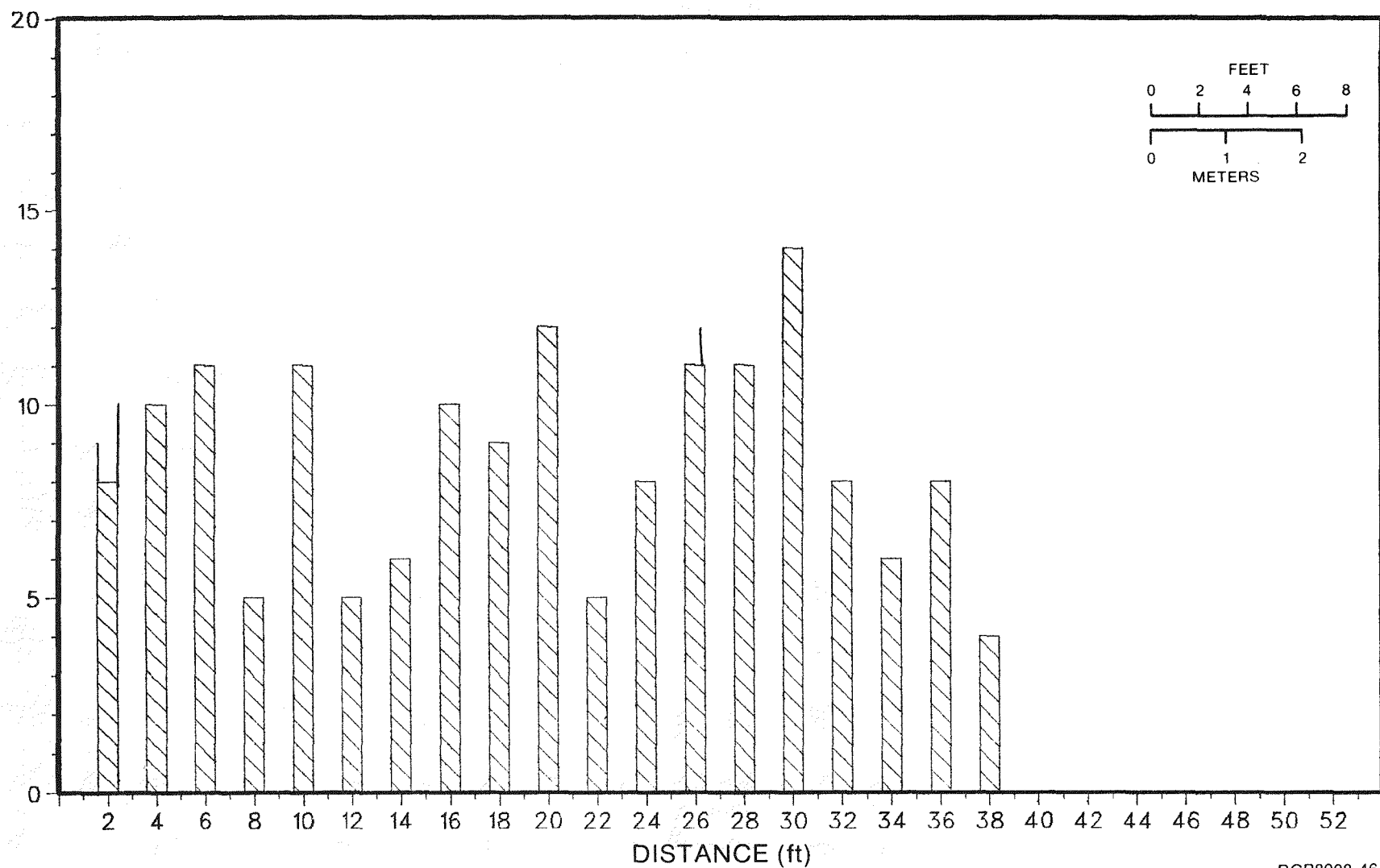
BASALT CORE GEO-MECHANICAL DATA
CORE HOLE 2E19
FRACTURE TOP FREQUENCY



RCP8008-45

RHO-BWI-ST-8

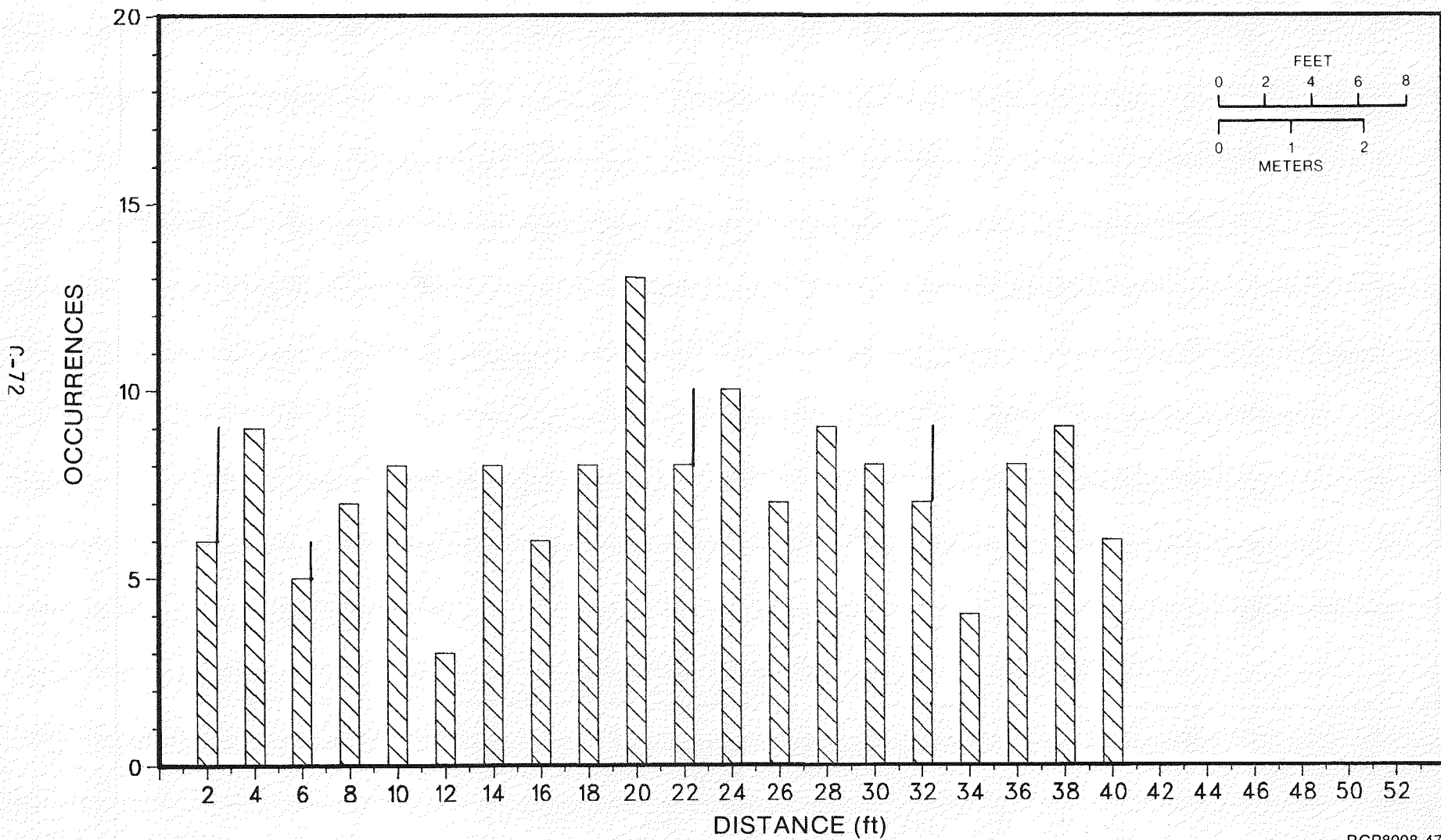
BASALT CORE GEO-MECHANICAL DATA
CORE HOLE 2E20
FRACTURE TOP FREQUENCY



RCP8008-46

RHO-BWI-ST-8

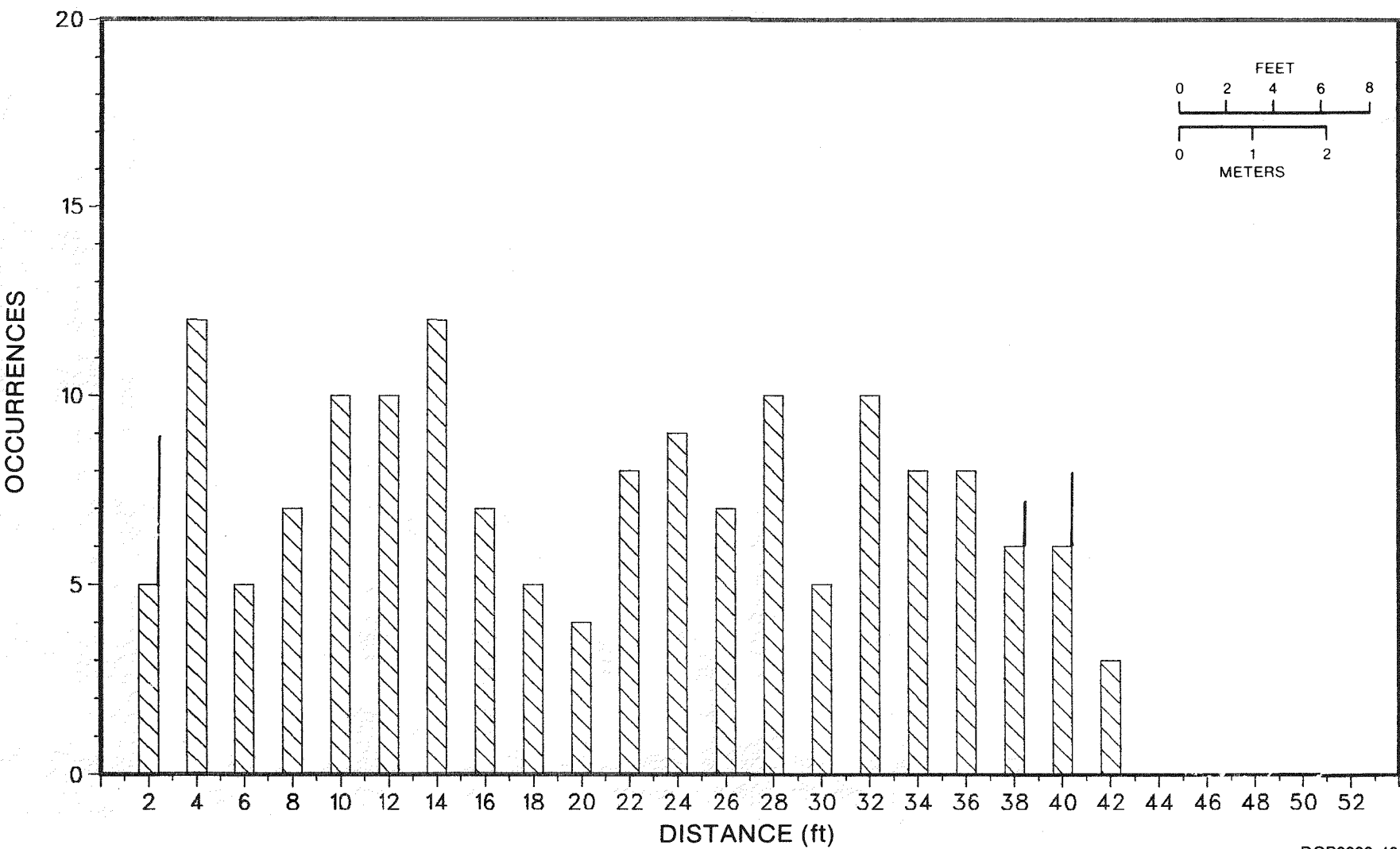
BASALT CORE GEO-MECHANICAL DATA
CORE HOLE 2E21
FRACTURE TOP FREQUENCY



RCP8008-47

RHO-BWI-ST-8

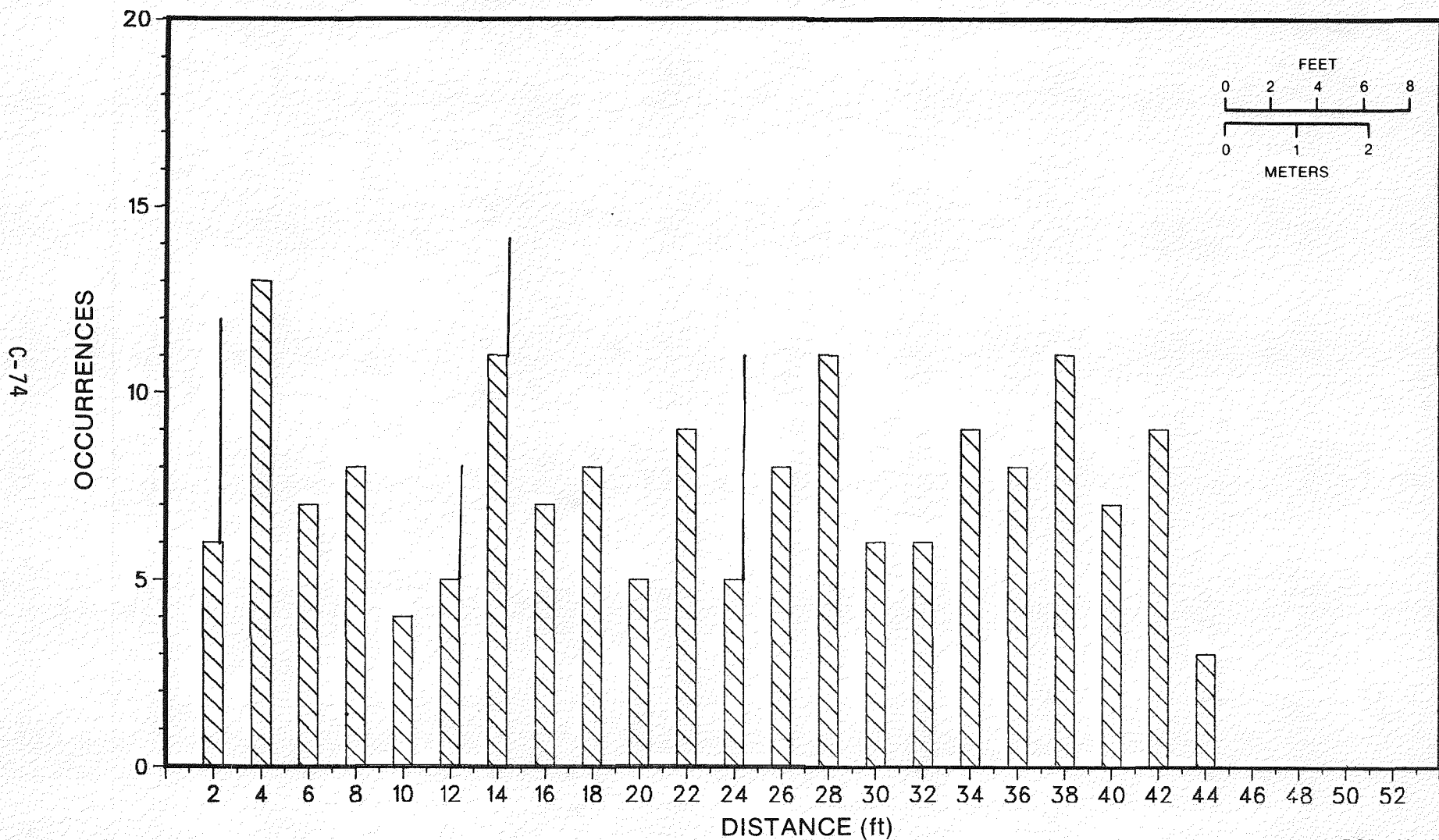
BASALT CORE GEO-MECHANICAL DATA
CORE HOLE 2E22
FRACTURE TOP FREQUENCY



RHO-BWI-ST-8

RCP8008-48

BASALT CORE GEO-MECHANICAL DATA
CORE HOLE 2E23
FRACTURE TOP FREQUENCY

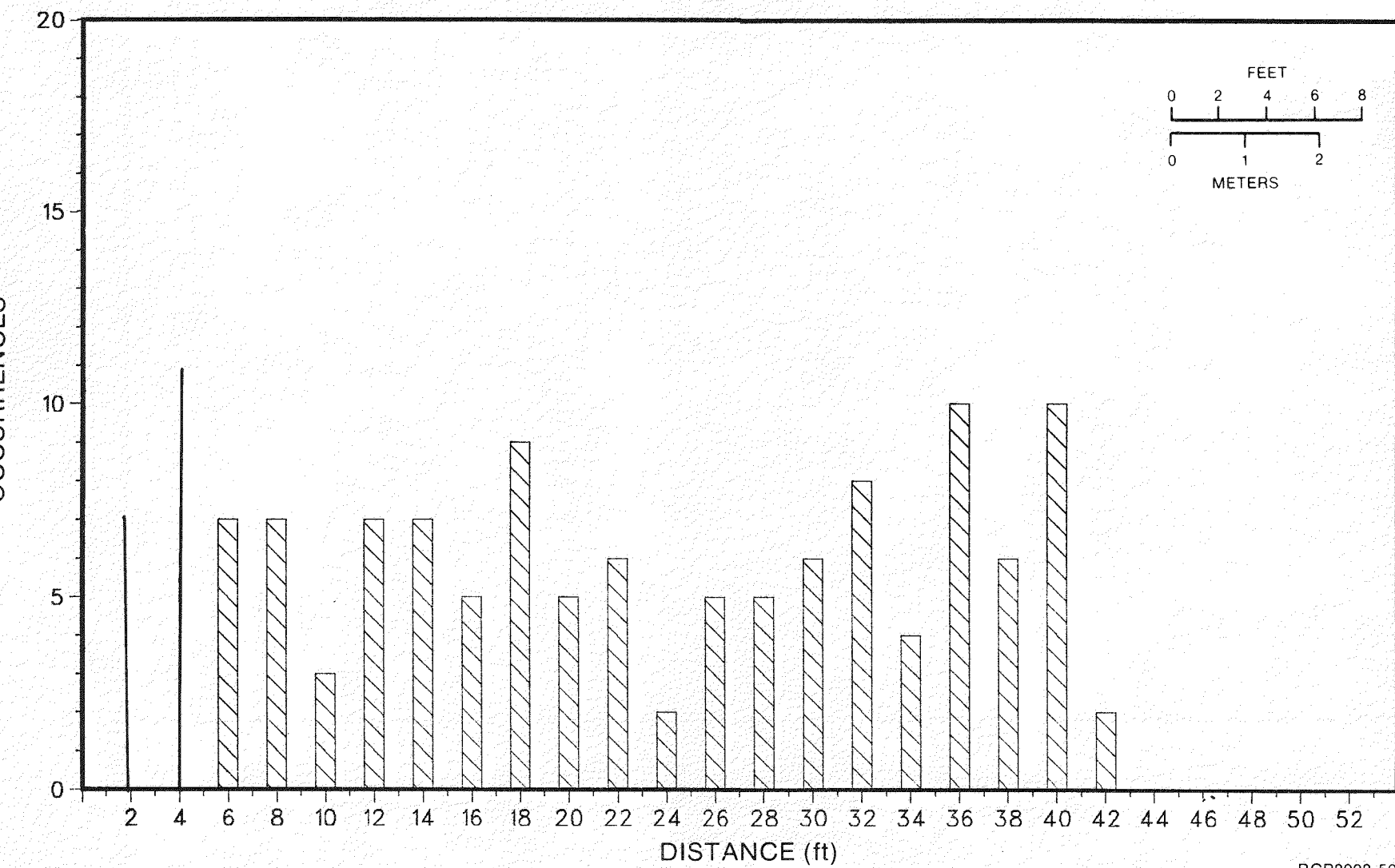


RHO-BWI-ST-8

RCP8008-49

BASALT CORE GEO-MECHANICAL DATA
CORE HOLE 2E24
FRACTURE TOP FREQUENCY

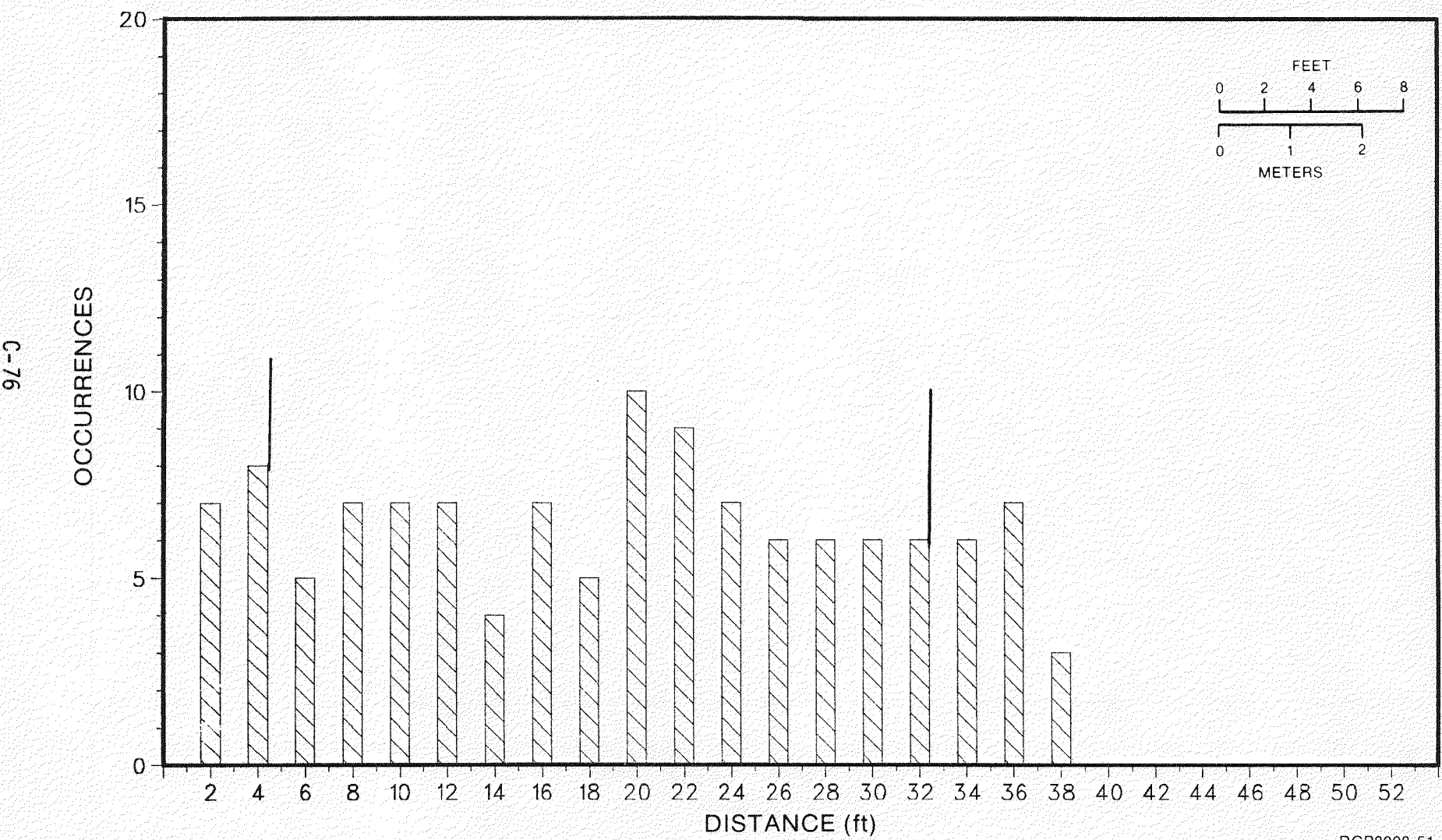
C-75



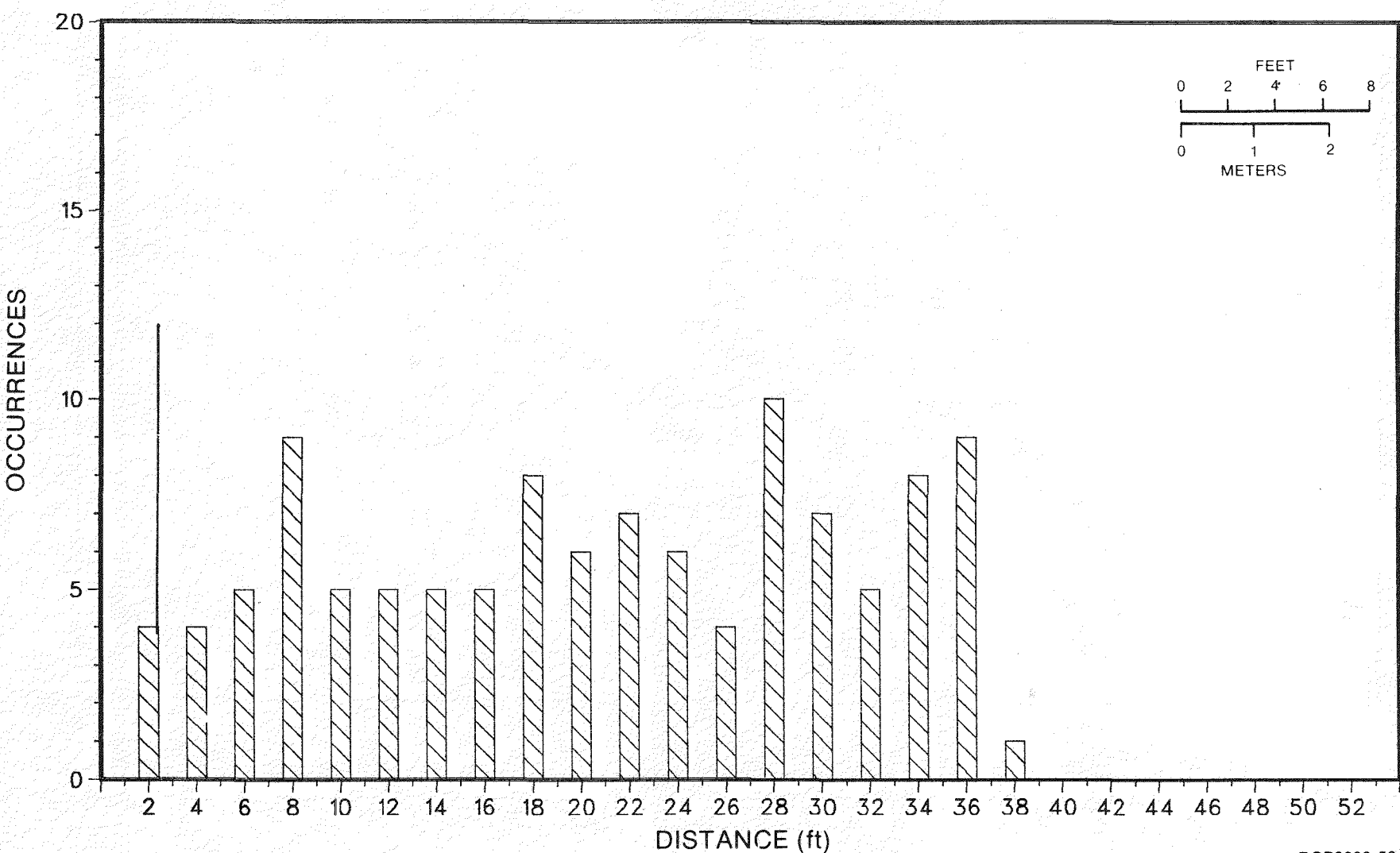
RCP8008-50

RHO-BWI-ST-8

BASALT CORE GEO-MECHANICAL DATA
CORE HOLE 2E25
FRACTURE TOP FREQUENCY



BASALT CORE GEO-MECHANICAL DATA
CORE HOLE 2E26
FRACTURE TOP FREQUENCY



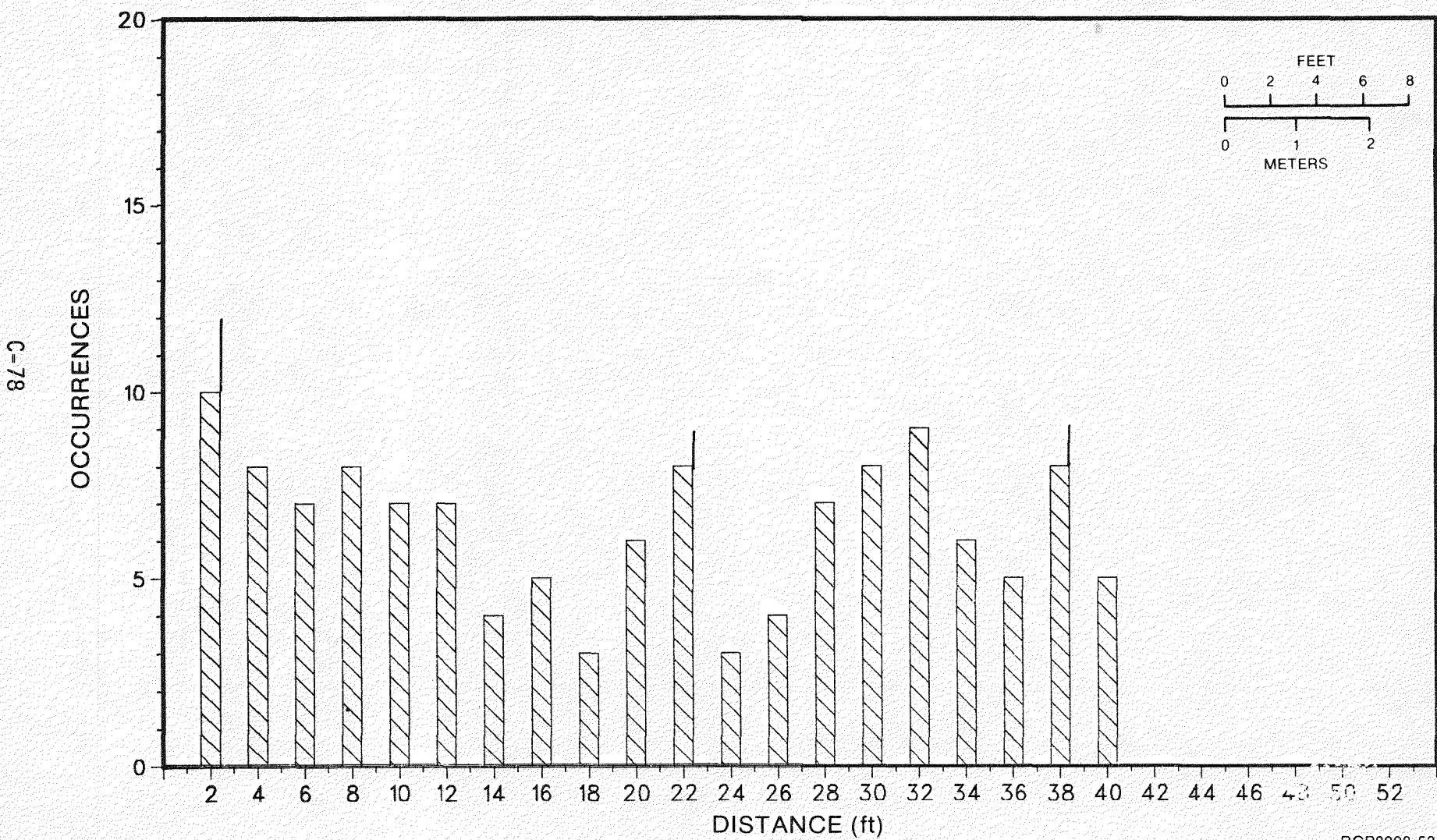
C-77

RHO-BWI-ST-8

RCP8008-52

BASALT CORE GEO-MECHANICAL DATA

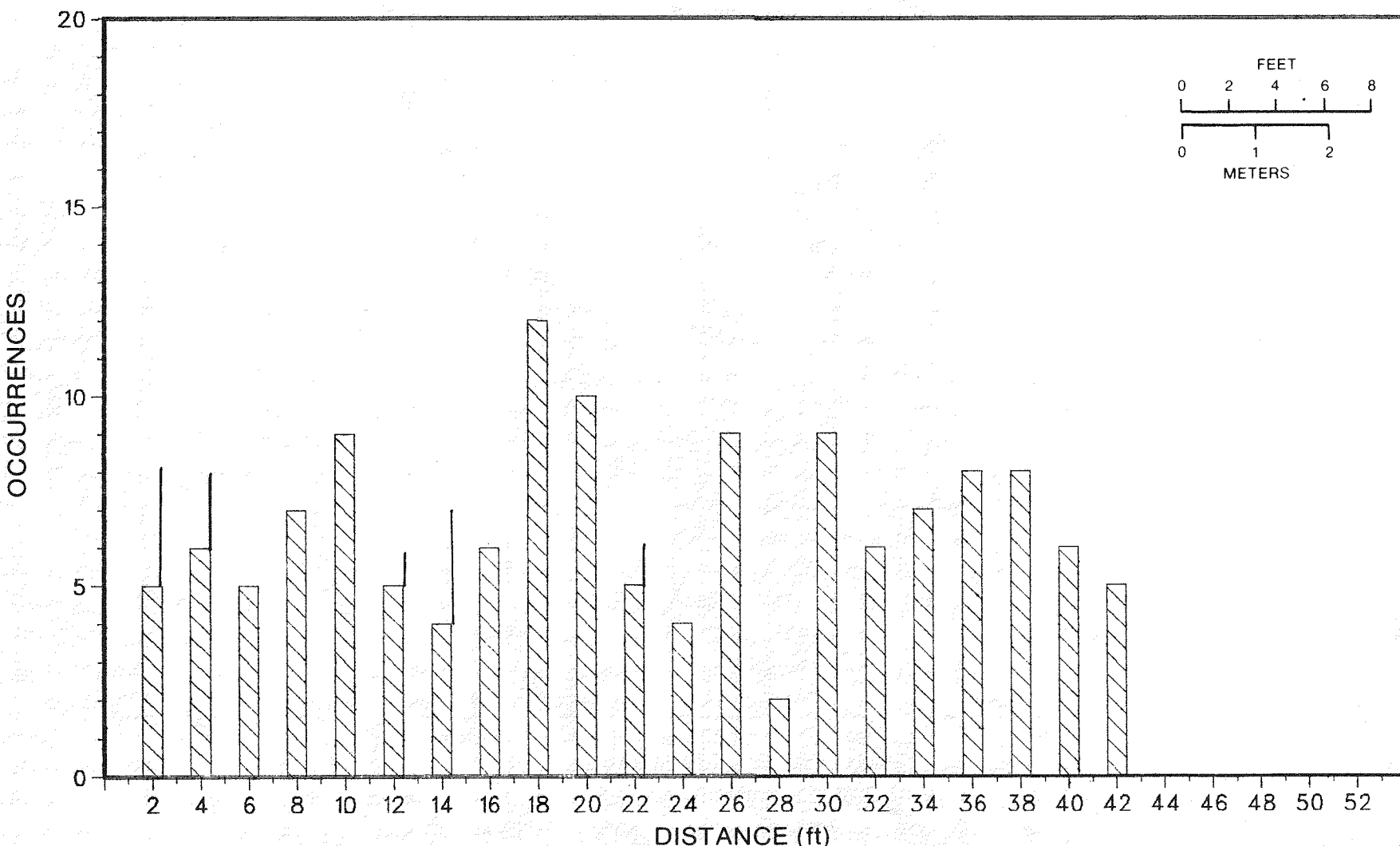
CORE HOLE 2E27
FRACTURE TOP FREQUENCY



RCP8008-53

RHO-BWI-ST-8

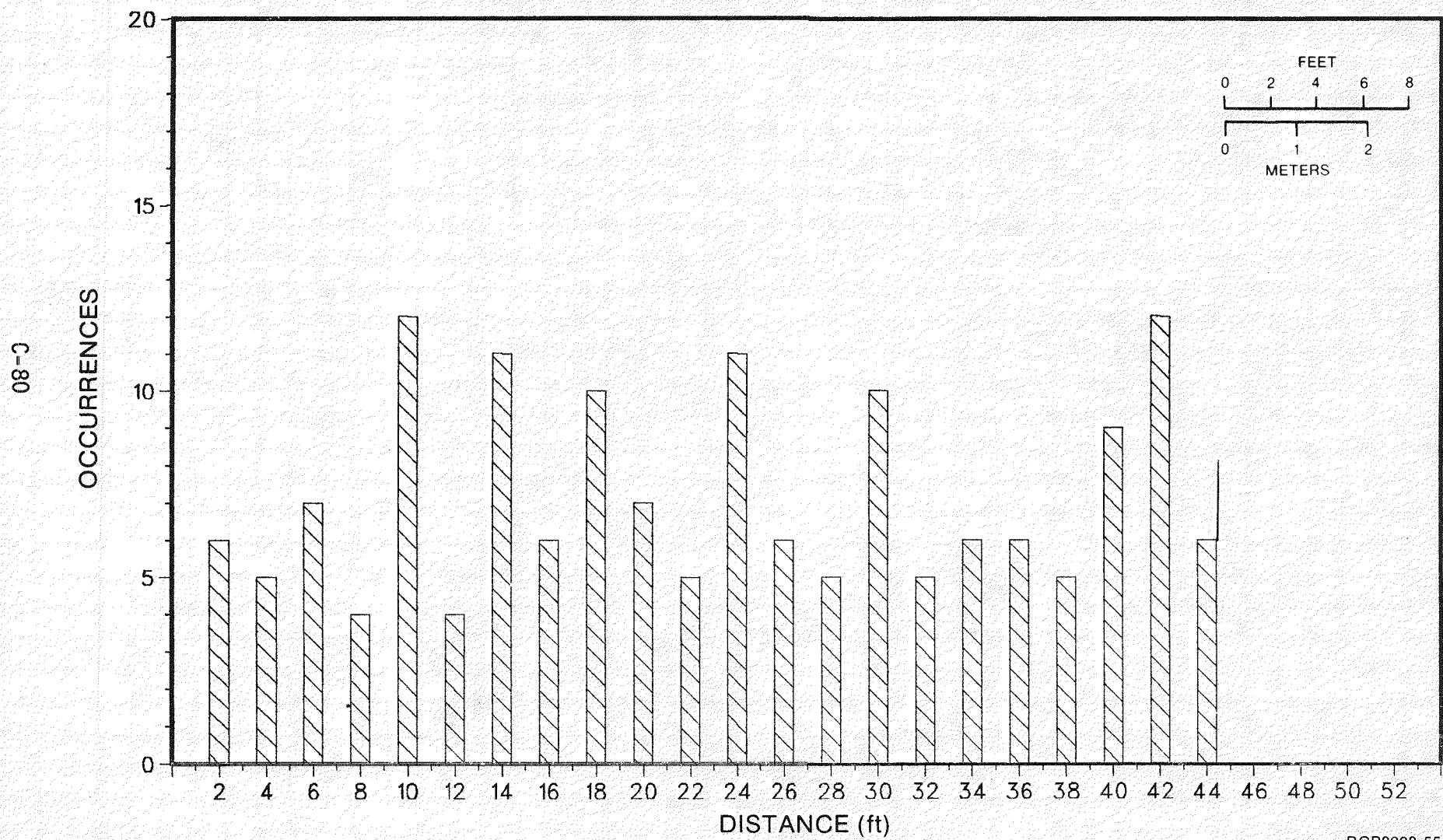
BASALT CORE GEO-MECHANICAL DATA
CORE HOLE 2E28
FRACTURE TOP FREQUENCY



RCP8008-54

RHO-BWI-ST-8

BASALT CORE GEO-MECHANICAL DATA
CORE HOLE 2E29
FRACTURE TOP FREQUENCY

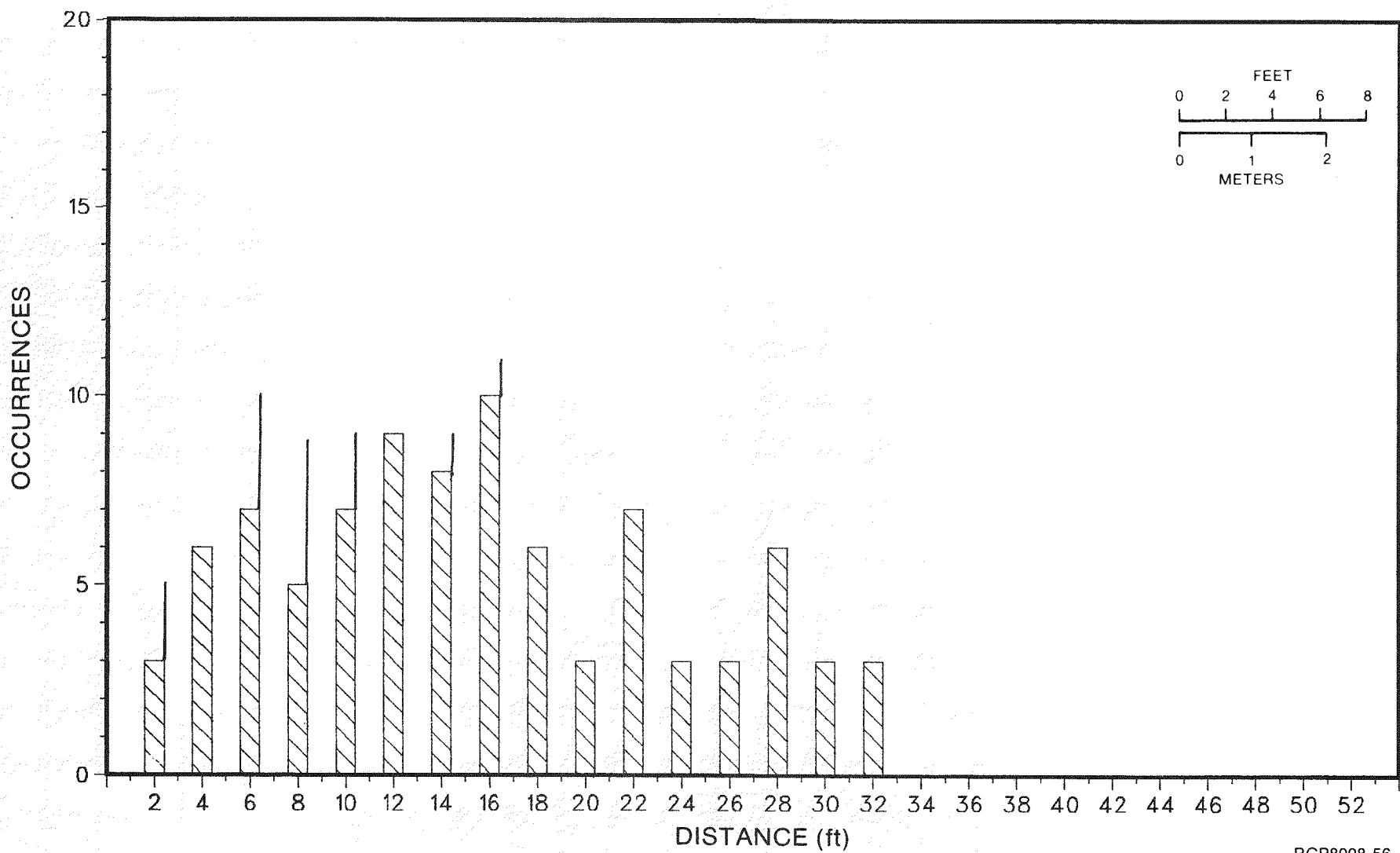


RHO-BWI-ST-8

RCP8008-55

BASALT CORE GEO-MECHANICAL DATA

CORE HOLE 2M3
FRACTURE TOP FREQUENCY



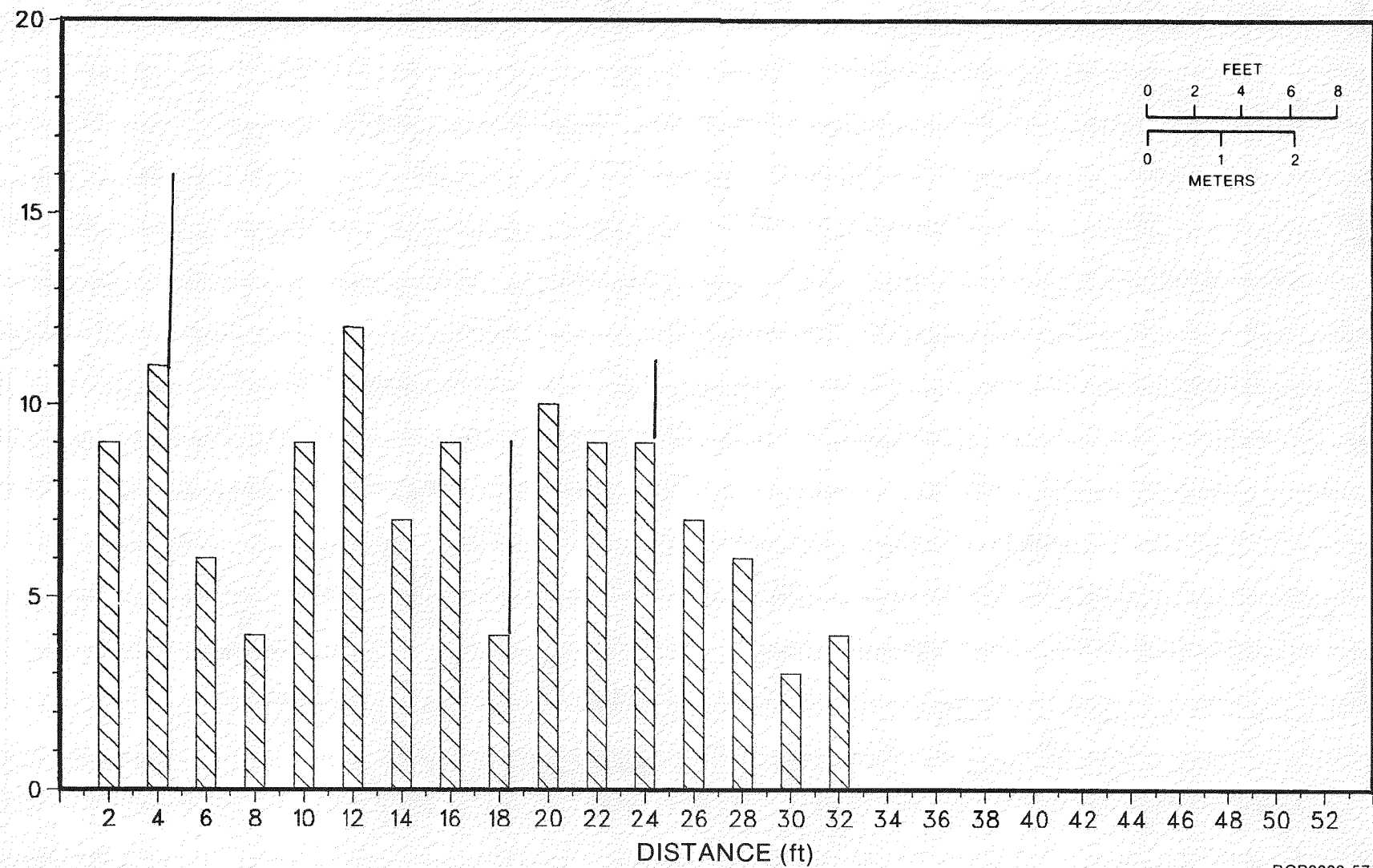
C-81

RHO-BWI-ST-8

RCP8008-56

BASALT CORE GEO-MECHANICAL DATA

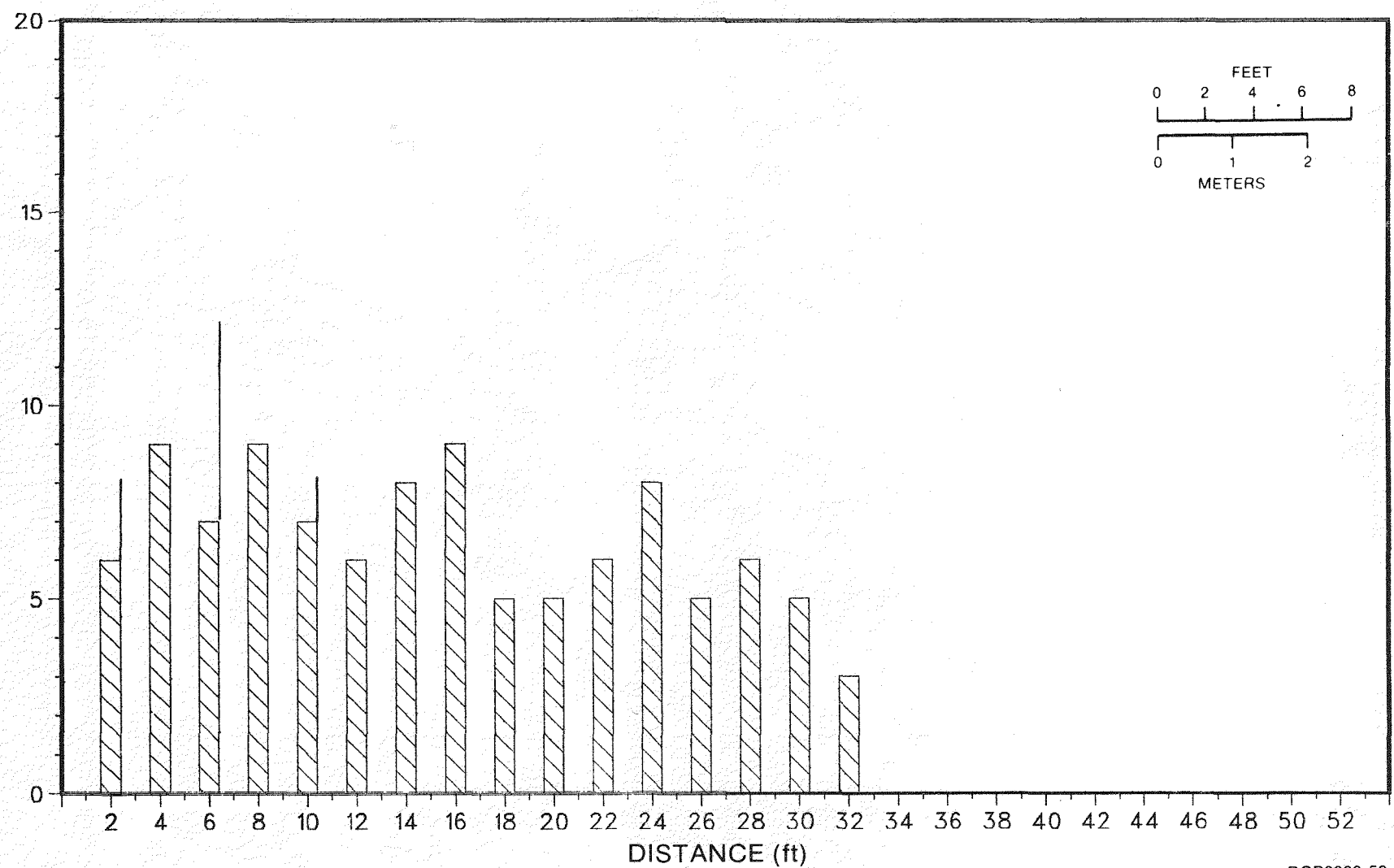
CORE HOLE 2M4
FRACTURE TOP FREQUENCY



RCP8008-57

RHO-BWI-ST-8

BASALT CORE GEO-MECHANICAL DATA
CORE HOLE 2M7
FRACTURE TOP FREQUENCY



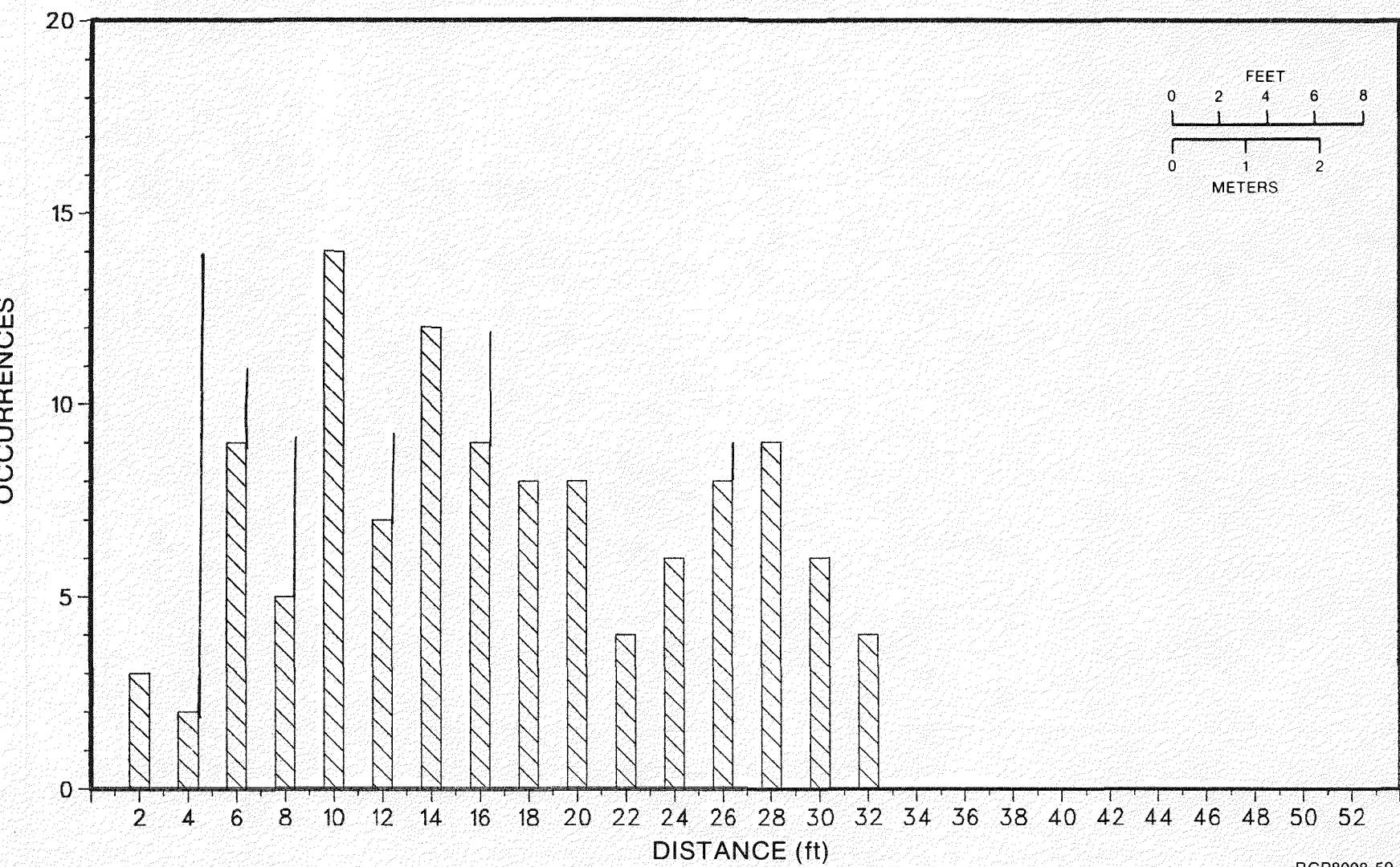
C-83

RHO-BMI-ST-8

RCP8008-58

BASALT CORE GEO-MECHANICAL DATA
CORE HOLE 2M12
FRACTURE TOP FREQUENCY

C-84

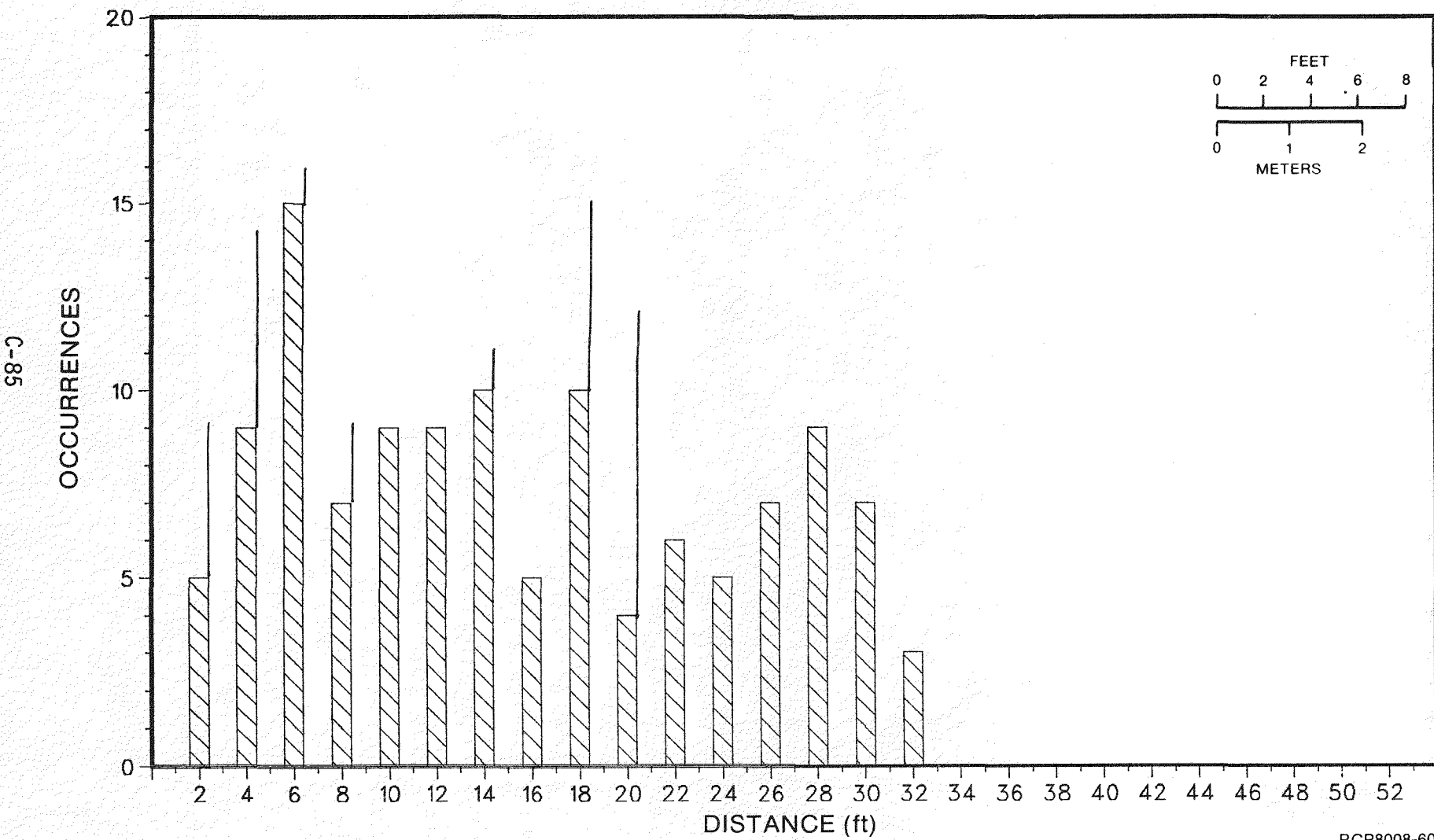


RCP8008-59

RHO-BWI-ST-8

BASALT CORE GEO-MECHANICAL DATA

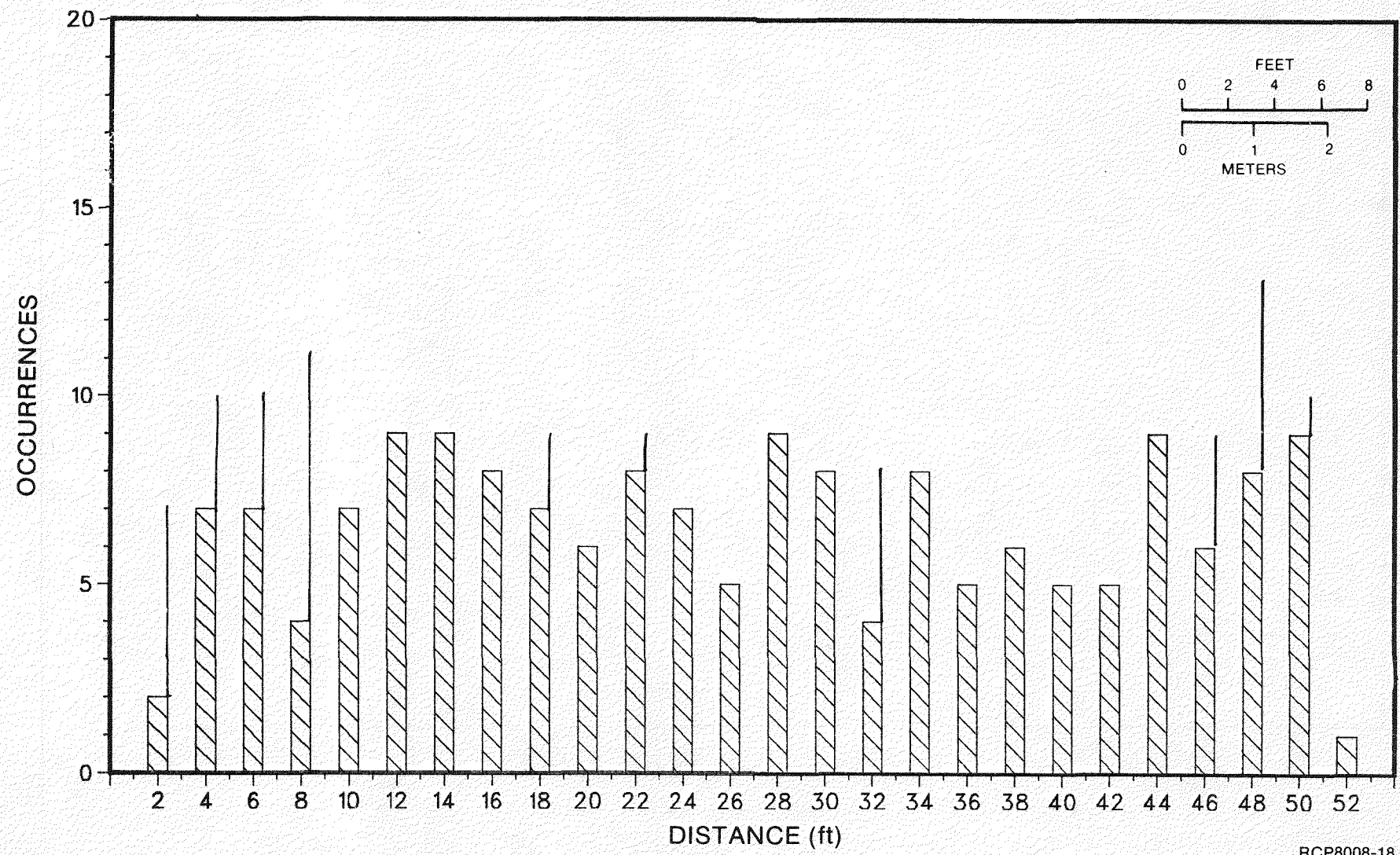
CORE HOLE 2M13
FRACTURE TOP FREQUENCY



RHO-BNI-ST-8

RCP8008-60

RHO-BMI-ST-8



RCP8008-18

The following table is a random sampling of joint in-filling colors and joint roughness. There are 100 points each from the vertical and horizontal holes. It is apparent that neither the joint in-filling color nor the joint roughness can be used to determine or characterize joint sets.

TABLE C-17. Joint Set Characteristics.

Dip Range (degrees)	Infilling Color			
	Black	Light Green	Blue	Dark Green
0-37	60	38	30	76
38-56	68	8	58	66
67-90	52	22	48	78

	Roughness	
	Smooth	Rough
0-37	90	110
38-66	60	140
67-90	57	143

The following equal area stereonet plots represent an equal number of data points from the horizontal and vertical holes. Both Full-Scale Heater Tests #1 and #2 show extreme scatter, making the definition of joint sets with stereographic plots very difficult.

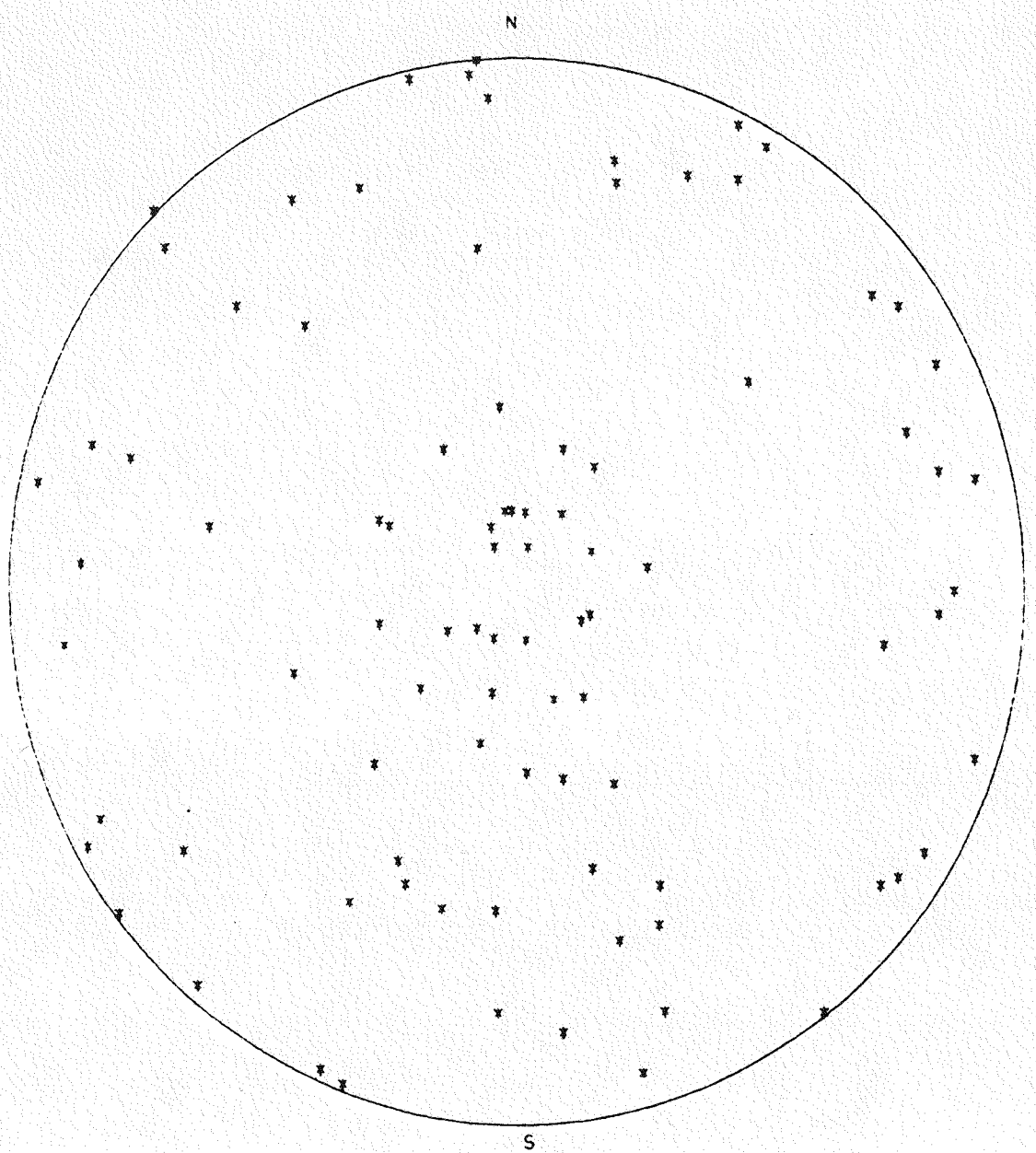


FIGURE C-1. Stereonet Plot of Joints in Full-Scale Heater Test #1.

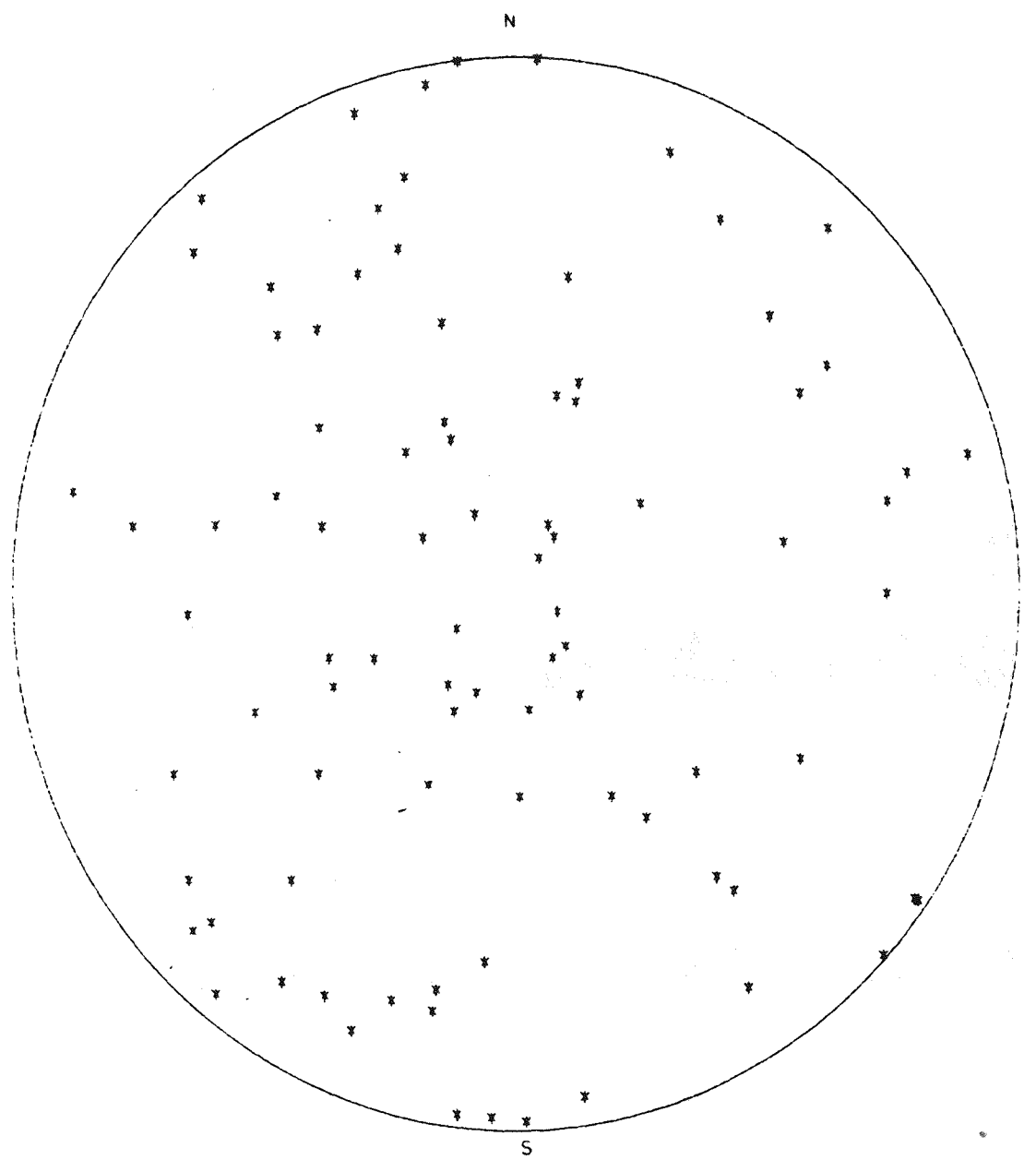


FIGURE C-2. Stereonet Plot of Joints in Full-Scale Heater Test #2.

The following data are available in the Basalt Waste Isolation Project Library:

- Core logs of each borehole
- Geomechanical logs
- Core photographs
- Photographs of the NSTF construction and geology
- Detailed line maps
- Photographs of the borehole walls in the main heater holes of Full-Scale Heater Tests #1 and #2
- Additional histogram plots.

The following are available for inspection in the Basalt Waste Isolation Project Core Library:

- All borehole core
- Impression packer sleeves.

REFERENCES

Barton, N., Lien, R., and Lunde, T., 1974, Engineering Classification of Rock Masses for the Design of Tunnel Support, Norwegian Geotechnical Institute No. 106, Oslo, Norway.

Bieniawski, Z. T., 1979, The Geomechanics Classification in Rock Engineering Applications.

Bingham, J. W., Lundquist, C. J., and Baltz, E. H., 1970, Geologic Investigations of Faulting in the Hanford Region, Washington (with a section on the occurrence of microearthquakes), U.S. Geological Survey Open-File Report, 104 p.

Call, R. D., Savel, J. P., and Nicholas, D. E., 1976, Estimation of Joint Set Characteristics from Surface Mapping Data, Pincock, Allen, and Holt, Inc., Tucson, Arizona.

Deere, D. U., 1963, "Technical Description of Rock Cores for Engineering Purposes," Felsmechanik und Ingenieurgeologie, 1 (1), p. 16-22.

Duvall, W. I., Miller, R. J., and Wang, F. D., 1978, Preliminary Report on Physical and Thermal Properties of Basalt; Drill Hole DC-10; Pomona Flow-Gable Mountain, RHO-BWI-C-11, Rockwell Hanford Operations, Richland, Washington.

Fecht, K. R., 1978a, Geology of Gable Mountain-Gable Butte Area, RHO-BWI-LD-5, Rockwell Hanford Operations, Richland, Washington.

Fecht, K. R., 1978b, Geology along Topographic Profile for the Near-Surface Test Facility, RHO-BWI-LD-16, Rockwell Hanford Operations, Richland, Washington.

Newcomb, R. C., Strand, J. R., and Frank, F. J., 1972, Geology and Groundwater Characteristics of the Hanford Reservation of the U.S. Atomic Energy Commission, Washington, U.S. Geological Survey Professional Paper 717.

Schmincke, H. U., 1964, Petrology, Paleocurrents and Interbedded Yakima Basalt Flows, South Central Washington, Ph.D. Dissertation, The Johns Hopkins University, Baltimore, Maryland.

Sharpe, S. D., 1979, Site Selection Report, Basalt Waste Isolation Program, Near-Surface Test Facility, RHO-BWI-CD-20, Rockwell Hanford Operations, Richland, Washington.

Staff, 1979 Basalt Technology Unit, Design Engineering Department, and Hardy, M. P., University of Minnesota, Phase I Heater Test Plan for the Thermomechanical Response of Basalt, RHO-BWI-CD-15 REV 2, Rockwell Hanford Operations, Richland, Washington.

Thorpe, R., 1979, Characterization and Discontinuities in the Stripa Granite Time-Scale Heater Experiment, LBL-7083, Lawrence Berkeley Laboratory, Berkeley, California.